UNIVERSIDAD DE CASTILLA-LA MANCHA

E.T.S. INGENIEROS INDUSTRIALES DE ALBACETE

DEPARTAMENTO DE INGENIERÍA QUÍMICA

ELECTROCHEMICAL TECHNOLOGIES TO REDUCE THE ENVIRONMENTAL AND SANITARY IMPACT OF HOSPITAL URINES

Thesis submitted in fulfilment of the requirements for the degree of Doctor (international PhD) by the University of Castilla-La Mancha

MIGUEL HERRAIZ CARBONÉ

Advisors:

Dra. Cristina Sáez Jiménez

Dra. Engracia Lacasa Fernández

Albacete, 2021

Dra. D.ª Cristina Sáez Jiménez, Catedrática de Universidad de Ingeniería Química de la Universidad de Castilla-La Mancha, y

Dra. D.ª Engracia Lacasa Fernández, Profesora Contratado Doctor Interino de Ingeniería Química de la Universidad de Castilla-La Mancha

CERTIFICAN: Que el presente trabajo de investigación titulado: *"Electrochemical technologies to reduce the environmental and sanitary impact of hospital urines"* constituye la memoria que presenta D. MIGUEL HERRAIZ CARBONÉ para aspirar al grado de Doctor (Doctorado Internacional) por la Universidad de Castilla-La Mancha en el programa de doctorado de Ingeniería Química y Ambiental, y que ha sido realizado en los laboratorios del Departamento de Ingeniería Química de la Universidad de Castilla-La Mancha bajo su dirección.

Y para que conste a los efectos oportunos, firman el presente certificado en Albacete a 26 de octubre de dos mil veintiuno.

SAEZ JIMENEZ CRISTINA - 06257475A

Firmado digitalmente por SAEZ JIMENEZ CRISTINA - 06257475A
Fecha: 2021.10.26 08:57:30 +02'00'

LACASA FERNANDEZ ENGRACIA - 47080242R

Firmado digitalmente por LACASA FERNANDEZ ENGRACIA - 47080242R
Fecha: 2021.10.26 09:02:08 +02'00'

Dra. D.ª Cristina Sáez Jiménez

Dra. D.ª Engracia Lacasa Fernández

FUNDING

The present doctoral thesis was financially supported by Junta de Comunidades de Castilla-La Mancha (JCCM) and European Union through the grant SBPLY/18/180501/000009 and the project SBPLY/17/180501/000396 (UrinETech).

Additionally, it was obtained support through the project PID2019-110904RB-I00 (ETECHU) financed by the Ministry of Science and Innovation.

PUBLICATIONS RELATED TO THE THESIS

SCIENTIFIC PAPERS:

M. Herraiz-Carboné, S. Cotillas, E. Lacasa, P. Cañizares, M.A. Rodrigo, C. Sáez, *Removal of antibiotic resistant bacteria by electrolysis with diamond anodes: A pretreatment or a tertiary treatment?* Journal of Water Process Engineering, 38 (2020) 101557.

M. Herraiz-Carboné, S. Cotillas, E. Lacasa, A. Moratalla, P. Cañizares, M.A. Rodrigo, C. Sáez. *Improving the biodegradability of hospital urines polluted with chloramphenicol by the application of electrochemical oxidation,* Science of the Total Environment, 725 (2020) 138430.

M. Herraiz-Carboné, E. Lacasa, S. Cotillas, M. Vasileva, P. Cañizares, M.A. Rodrigo, C. Sáez, *The role of chloramines on the electrodisinfection of Klebsiella pneumoniae in hospital urines*, Chemical Engineering Journal, 409 (2021) 128253.

M. Herraiz-Carboné, S. Cotillas, E. Lacasa, P. Cañizares, M.A. Rodrigo, C. Sáez, *Enhancement of UV disinfection of urine matrixes by electrochemical oxidation*, Journal of Hazardous Materials, 410 (2021) 124548.

M. Herraiz-Carboné, S. Cotillas, E. Lacasa, P. Cañizares, M.A. Rodrigo, C. Sáez, *Disinfection of urines using an electro-ozonizer*, Electrochimica Acta, 382 (2021) 138343.

M. Herraiz-Carboné, S. Cotillas, E. Lacasa, C. Sainz de Baranda, E. Riquelme, P. Cañizares, M.A. Rodrigo, C. Sáez, *Are we correctly targeting the research on disinfection of antibiotic-resistant bacteria (ARB)?* Journal of Cleaner Production, 320 (2021) 128865.

M. Herraiz-Carboné, S. Cotillas, E. Lacasa, C. Sainz de Baranda, E. Riquelme, P. Cañizares, M.A. Rodrigo, C. Sáez, *A review on disinfection technologies for controlling the antibiotic resistance spread*, Science of The Total Environment, 797 (2021) 149150.

M. Herraiz-Carboné, S. Cotillas, E. Lacasa, M. Vasileva, C. Sainz de Baranda, E. Riquelme, C. Sáez, *Disinfection of polymicrobial urines by electrochemical oxidation: removal of antibiotic-resistant bacteria and genes*, Journal of Hazardous Materials, submitted.

CONTRIBUTIONS IN NATIONAL AND INTERNATIONAL CONGRESSES:

S. Cotillas, E. Lacasa, M. Herraiz-Carboné, C. Sáez. P. Cañizares, M.A. Rodrigo. Removal of antibiotic penicillin g by conductive-diamond electrochemical oxidation. *3rd e3 Mediterranean symposium: electrochemistry for environment and energy*. Oral communication. 2-5 July 2018, Madrid, (Spain).

M. Herraiz-Carboné, S. Cotillas, E. Lacasa, C. Sáez. P. Cañizares, M.A. Rodrigo. Disinfection of urine by electrolysis: a suitable choice? *25th annual meeting of the international society of electrochemistry*. Poster. May 2019, Toledo (Spain).

M. Herraiz-Carboné, S. Cotillas, E. Lacasa, C. Sáez. P. Cañizares, M.A. Rodrigo. The role of anode material in the selective oxidation of antibiotics in urine. *25th Annual meeting of the international society of electrochemistry*. Poster. May 2019, Toledo (Spain).

M. Herraiz-Carboné, S. Cotillas, E. Lacasa, C. Sáez. P. Cañizares, M.A. Rodrigo. Influence of reactor design on the electrodisinfection of hospital urines. *Congreso internacional de ingeniería química, 3ª edición (ANQUE-ICCE3)*. Oral communication. June 2019, Santander (Spain).

M. Herraiz-Carboné, S. Cotillas, E. Lacasa, C. Sáez. P. Cañizares, M.A. Rodrigo. Is it possible to improve the biodegradability of hospital effluents by electrochemical advanced oxidation processes? *6th European conference on environmental applications of advanced oxidation processes*. Oral communication. June 2019, Portoroz (Slovenia).

M. Herraiz-Carboné, S. Cotillas, E. Lacasa, C. Sáez. P. Cañizares, M.A. Rodrigo. Towards the reduction of environmental and sanitary impact of hospital urines using electrochemical technology. *XI Meeting of the electrochemistry group of Spanish royal*

society of chemistry. *XX Iberian meeting of electrochemistry*. Oral communication. July 2019, Huelva (Spain).

E. Lacasa, M. Herraiz-Carboné, S. Cotillas, C. Sáez. P. Cañizares, M.A. Rodrigo. Antibiotic-resistant bacteria abatement in hospital urines by electrochemical advanced oxidation technologies. *IV Iberoamerican conference on advanced oxidation technologies*. Oral communication. November 2019, Natal-RN (Brazil).

M. Herraiz-Carboné, S. Cotillas, E. Lacasa, C. Sainz de Baranda, E. Riquelme, P. Cañizares, M.A. Rodrigo, C. Sáez. The role of water matrix on the removal of antibiotic-resistant bacteria by electrochemical oxidation. *71st Annual Meeting of the International Society of Electrochemistry (ISE)*. Oral communication. September 2020, Belgrade Online (Serbia).

M. Herraiz-Carboné, M. Gómez, S. Cotillas, E. Lacasa, C. Sáez. P. Cañizares, M.A. Rodrigo. Application of MIKROZON® electrochemical technology to the disinfection of hospital urines. *International workshop on Advanced Electrchemical Oxidation for Water Reuse (ELO-WATER)*. Oral communication. September de 2020, Nancy online (France).

M. Herraiz-Carboné, S. Cotillas, E. Lacasa, C. Sainz de Baranda, E. Riquelme, P. Cañizares, M.A. Rodrigo, C. Sáez Reducción del impacto ambiental y sanitario de orinas hospitalarias mediante tecnologías electroquímicas. *V Workshop de la Red E3TECH / I Workshop Iberoamericano a Distancia (Aplicaciones Medioambientales y Energéticas de la Tecnología Electroquímica, V E3TECH)*. Poster. October 2020, online (Spain).

M. Herraiz-Carboné, S. Cotillas, E. Lacasa, C. Sainz de Baranda, E. Riquelme, P. Cañizares, M.A. Rodrigo, C. Sáez. Influencia de las variables de operación en la eliminación de bacterias resistentes a los antibióticos mediante oxidación electroquímica. *XXIV Congreso de la Sociedad Iberoamericana de Electroquímica (SIBAE 2020)*. Poster. December 2020, Montevideo online (Uruguay).

M. Herraiz-Carboné, S. Cotillas, E. Lacasa, C. Sainz de Baranda, E. Riquelme, P. Cañizares, M.A. Rodrigo, C. Sáez. Influencia de las variables de operación en la

eliminación de bacterias resistentes a los antibióticos mediante oxidación electroquímica. *IV Seminario UPMWater*. Oral communication. January 2021, Madrid online (Spain).

M. Herraiz-Carboné, S. Cotillas, E. Lacasa, C. Sainz de Baranda, E. Riquelme, P. Cañizares, M.A. Rodrigo, C. Sáez. Towards the removal of antibiotic-resistant bacteria in polymicrobial urines by electrochemical oxidation. *29th Annual Meeting of the International Society of Electrochemistry*. Oral communication. April 2021, Mikulov online (Czech Republic).

M. Herraiz-Carboné, S. Cotillas, E. Lacasa, C. Sainz de Baranda, E. Riquelme, P. Cañizares, M.A. Rodrigo, C. Sáez. Photo-assisted electrochemical disinfection of hospital urines using a novel flow-through reactor. *12th European Symposium On Electrochemical Engineering*. Oral communication. June 2021, Leeuwarden online (The Netherlands).

M. Herraiz-Carboné, A. Moratalla, V. Pertegal, S. Cotillas, E. Lacasa, C. Sainz de Baranda, E. Riquelme, P. Cañizares, M.A. Rodrigo, C. Sáez. Electrochemical technology as a key tool to reduce the hazardousness of hospital urines. *72nd Annual Meeting of the International Society of Electrochemistry*. Poster. Augost-September 2021, Jeju Island online (Korea).

M. Herraiz-Carboné, A. Moratalla, S. Cotillas, E. Lacasa, A. Valladolid, S. Ruiz, P. Cañizares, M.A. Rodrigo, C. Sáez. Removal of iodinated radiocontrast iopamidol in hospital urines by electrochemical technologies: electrolysis vs. electrocoagulation. *72nd Annual Meeting of the International Society of Electrochemistry*. Oral communication. Augost-September 2021, Jeju Island online (Korea).

M. Herraiz-Carboné, S. Cotillas, E. Lacasa, P. Cañizares, M.A. Rodrigo, C. Sáez. Reducing the spread of antibiotic-resistant bacteria (ARB) in complex urines with electrochemical technology. *Symposium of the Spanish Royal Society of Chemistry*. Poster. September 2021, Online conference (Spain).

INDEX

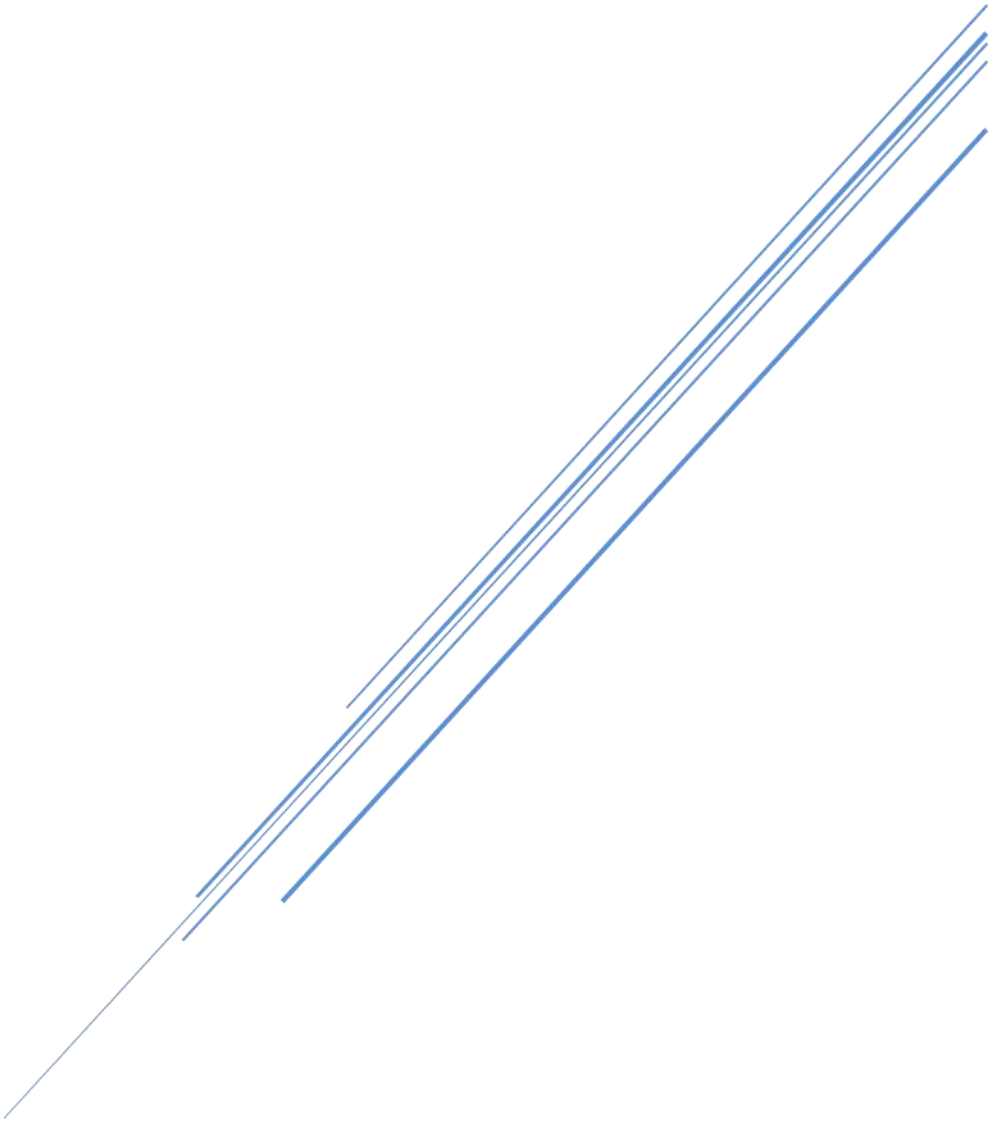

CHAPTER 1:

SUMMARY

In last years, the occurrence of bacteria with the capacity of survive and multiply in the presence of the antibiotics specifically designed to kill them, the so-called Antibiotic-Resistant Bacteria (ARB) has become a global concern because of the potential threats they can pose to human health. Diseases produced by these ARB cannot be effectively treated with antibiotics, being responsible for more than 700,000 human deaths per year. ARB can transfer their antibiotic resistance genes (ARGs) from one bacterium to another, favouring the spread of antibiotic resistance in the environment. The World Health Organization (WHO) has considered ARB as one of the three main threats of the 21st century due to the large number of infections and deaths they cause worldwide each year.

One of the most concentrated sources of ARB are hospital effluents and, specifically, urine from immunocompromised patients where simultaneously coexist bacteria causing urinary tract infections with excreted pharmaceuticals. Currently, hospital urines are typically merged with other hospital effluents and then, discharged into the municipal sewer system and treated together with urban effluents in municipal wastewater treatment facilities (WWTPs). The inefficiency of biological treatments from WWTPs to treat hospital effluents leads the spread of ARB and ARGs in the environmental water sources, negatively affecting aquatic organisms and human health. This makes urine treatment a key objective for reducing the environmental and health impact of hospital effluents. For this reason, the priority of this project is to face the problem directly in the pollution source, within the framework of the regional and national projects “Electrochemical technologies for the treatment of hospital urines: reduction of environmental and health impact (SBPLY/17/180501/000396) and “Electrochemical technologies facing the challenge of hospital urine treatment (PID2019-110904RB-I00), respectively.

In this context, electrochemical oxidation (EO) has aroused great interest among disinfection processes since EO has been reported to attain complete disinfection in urban wastewaters thanks to the in-situ generation of disinfectant species from the electrooxidation of the ions naturally contained in the effluent treated. This PhD Thesis is focused on the removal of bacteria from hospital urines based on our previous works

related to the disinfection of urban treated wastewater, facing the challenge of the reactor layout. Specifically, the main objective of the present PhD Thesis is to assess the technical feasibility of different electrochemical processes including electrolysis and photoelectrolysis, to reduce the environmental and health impact of ARB from hospital urines, avoiding the formation of undesired disinfection by-products. To meet this general objective, results presented in Chapter 5 have been divided in the following five different sections, which correspond to the five partial objectives of this work.

In section 5.1, a prospective study of pathogens causing Urinary Tract Infections (UTIs) was carried out within the period 2014 to 2018. This study was accomplished in collaboration with the University Hospital Complex of Albacete, Spain (CHUA) as model of sanitary facility. This allows to evaluate the occurrence and fate of ARB in a real environment as well as the problematic associated with ARB in a hospital complex. The study proved that *E. coli* was the most significant bacteria found in Positive Urines (PUs) and that gram-negative bacteria (*E. coli*, *K. pneumoniae*, *P. aeruginosa* and *P. mirabilis*) predominated over gram-positive bacteria (*E. faecalis*) and yeasts (*C. albicans*). *K. pneumoniae* showed the highest percentages of antibiotic resistance. However, the research carried out on the disinfection processes of ARB was mainly related to the removal of *E. coli*, which confirms that the importance given to *K. pneumoniae* as ARB from a sanitary viewpoint does not correspond to the research carried out on the disinfection processes. Hence, it was pointed out the need to search and develop novel technologies that allow to remove *K. pneumoniae* for decreasing the sanitary and environmental impact of the effluents infected with this bacterium.

In section 5.2, a preliminary study of the electrochemical technology as an alternative for the removal of bacteria in two different treatment scenarios (synthetic urban wastewater and synthetic hospital urines) was conducted using a parallel flow reactor with BDD anodes at 10 A m^{-2}. This study proved that even the bacterial removal efficiency was lower in hospital urines (competitive oxidation reactions), the occurrence of hazardous disinfection by-products was avoided in this matrix since the production of hypochlorite and the subsequent formation of inorganic chloramines were favoured. Subsequently, a preliminary evaluation of electrolysis for the reduction of the potential

chemical risk of hospital urines was also conducted. Chloramphenicol (CAP) was selected as a model of antibiotic and the influence of anodic material (BDD and MMO) and current density (50, 25, 12.5 A m^{-2}) was evaluated. This study concluded that the electrochemical oxidation with BDD anodes applying 12.5 A m^{-2} (8 Ah dm^{-3}) allows to degrade CAP from hospital urines, increasing their biodegradability up to 40 % follows the Zahn-Wellens method. However, this study also pointed out that the electrical charges required for the removal of antibiotics were much higher than those required for disinfection (8 Ah dm^{-3} *vs.* < 0.15 Ah dm^{-3}) and then, other parallel studies out of this thesis were carried out on this topic.

In this regard, the development of suitable disinfection technologies as a pre-treatment to remove *K. pneumoniae* from hospital urines was evaluated in section 5.3. The main objective of this section was to gain insight into the role of the electro-generated oxidants on the disinfection process. Firstly, the contribution of chloramines on the electrochemical disinfection process was evaluated testing two concepts of electrochemical cell design with MMO anodes: a conventional parallel flow reactor and a microfluidic flow-through reactor. The influence of current density (5-50 A m^{-2}) was also studied, and results were compared with other simpler "urine" matrices and with chemical disinfection tests. Results showed that the disinfection process of *K. pneumoniae* from hospital urines relies on the current density and the reactor layouts. The presence of chlorides in hospital urines contributed to the generation of hypochlorite and chloramines. The formation of chloramines was enhanced using the flow-through reactor layout. Additionally, chemical disinfection tests proved a stronger bactericidal effect of hypochlorite in comparison with chloramines. However, chloramines played a key role in the disinfection process since they contribute not only as disinfectants but avoiding the generation of chlorine derived by-products.

Additionally, the contribution of ozone on the electrochemical disinfection process was also evaluated testing a PEM-electrolyzer (MIKROZON® cell) especially designed to produce ozone in low-conductivity water. The influence of current intensity and hospital urine composition was studied. Results showed that the MIKROZON® cell reached total disinfection from current intensities higher than 0.5 A. The combined

effect of ozone and chlorine disinfectants attained higher disinfection rates than the values obtained when single ozone was the main disinfectant electrogenerated (urine without chlorides) at current intensities lower than 0.5 A. At values of 1.0 A, the disinfection rates were quite similar which revealed that large amounts of ozone were electrogenerated. The crystal violet assay showed that the combined effect of all disinfectants promoted higher cell damages, increasing the cell wall permeability. Ozone was proved to attack DNA to a greater extent from current intensities higher than 0.5 A. Finally, during the treatment of diluted urines at 1.0 A, higher disinfection rates were obtained due to the minimization of competitive reactions.

Electrochemical oxidation can promote the formation of hydroxyl radicals and disinfectant species from water electrolysis which may be activated by the irradiation of UV light, increasing the quantity of free radicals available for disinfection purposes. In section 5.4, the assessment of coupling of electrochemical oxidation with UV light was developed using a microfluidic flow-through reactor for the removal of *K. pneumoniae* in hospital urines. The influence of the current density (5-50 A m^{-2}) and the anode material (BDD and MMO) was tested on the production of disinfectants not only of hypochlorite but also monochloramine, dichloramine and trichloramine. Results showed that UV disinfection could not reach the complete disinfection of *K. pneumoniae.* However, electrochemical oxidation with BDD and MMO anodes led to complete removal of ARB from urine when applying 50 A m^{-2}. The disinfection rate was higher when working with MMO anodes since BDD anodes favoured competitive oxidation reactions between bacteria and the organics contained in urine. Finally, photoelectrolysis was proved to enhance single UV disinfection and electrolysis performances. A marked synergistic effect was found when UV disinfection was enhanced by electrolysis at 5 A m^{-2} with BDD and MMO anodes.

In section 5.5, the validation of electrochemical technology for the treatment of complex synthetic urine matrices (polymicrobial urines) was carried out. The polymicrobial hospital urines simulates real hospital urines since the pandemic caused by the coronavirus SARS-CoV-2 did not allow us to validate the electrochemical technology in a real environment due to the sanitary restrictions. Firstly, the

simultaneous occurrence of more than one pathogen causing UTIs in real hospital urines was analysed based on data supplied by the Microbiology and Parasitology Service from CHUA. From this study, the most prevalent combinations of bacteria presented in real urines from hospitalized patients were: 1) *E. faecalis* and *K. pneumoniae*, 2) *E. coli* and *E. faecalis*, and 3) *K. pneumoniae* and *E. coli*. Subsequently, the microfluidic flow-through reactor and the MIKROZON® cell were evaluated for the abatement of ARB pairs working under the most suitable operating conditions reported in previous sections. Hence, the microfluidic flow-through reactor was tested with MMO anodes at 50 A m^{-2} and the MIKROZON® cell worked at 1 A. Results showed that the microfluidic flow-through reactor achieved removal rates between 5 and 6 logs after 180 min whereas the MIKROZON® cell reached the total disinfection (7 logs) after 60 min. Additionally, the denaturation of DNA and ARGs in polymicrobial hospital urines was also considered. While no noticeable changes in the ARGs concentration were observed with the flow-through reactor, the MIKROZON® cell reached a mean decrease in ARGs ranked as follows: bla_{KPC} (4.18-logs) > bla_{TEM} (3.96-logs) > *erm*B (3.23-logs), offering a mean depletion of 3.77-logs for all ARGs tested. Finally, Scanning Electron Microscope (SEM) images confirmed the complete disinfection attained using the MIKROZON® cell where severe damages were induced in the cell walls, resulting in the integrity loss of bacterial structures.

CAPÍTULO 1:

RESUMEN

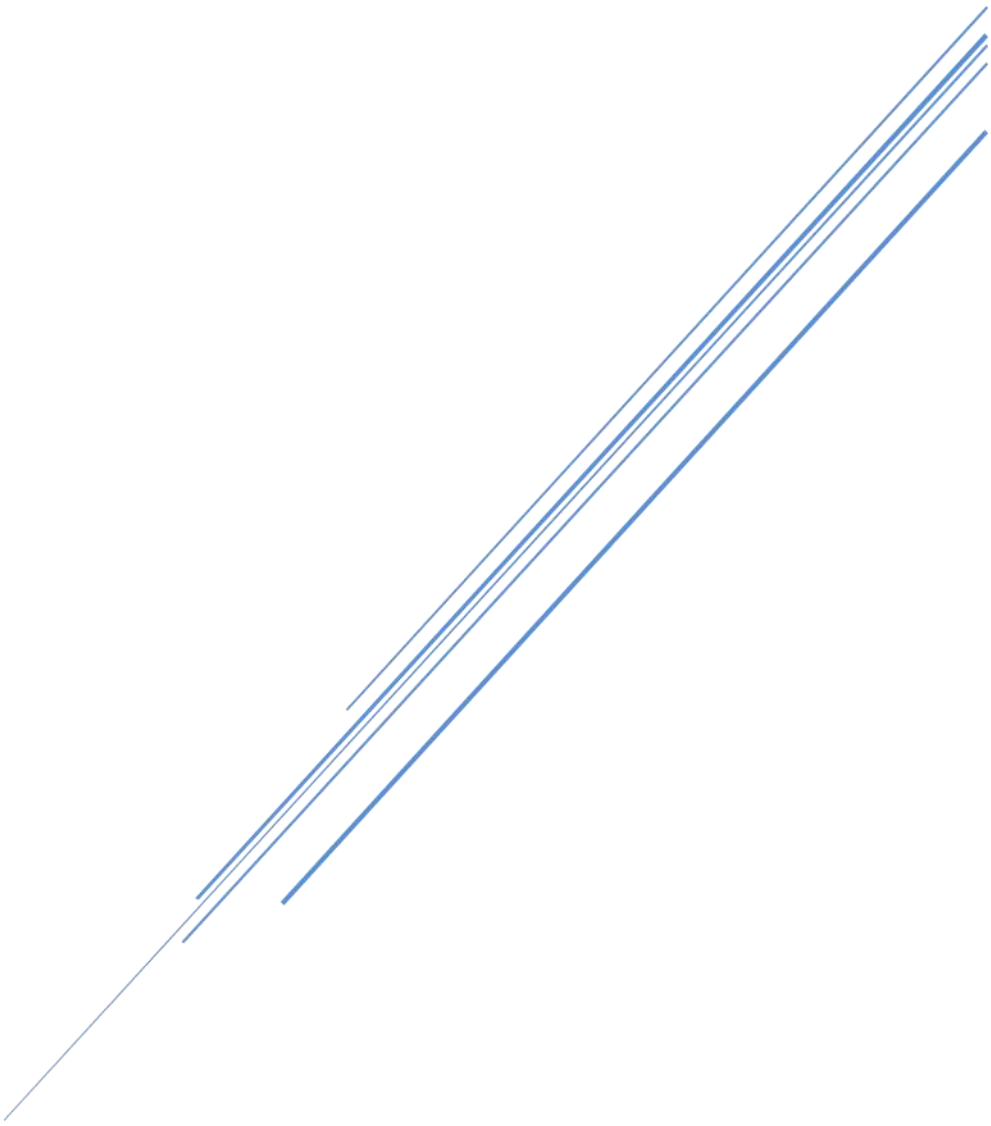

En los últimos años, la aparición de las denominadas bacterias resistentes a los antibióticos (*Antibiotic-Resistant Bacteria*, ARB) con capacidad de sobrevivir y multiplicarse en presencia de antibióticos específicamente diseñados para matarlas, se ha convertido en una preocupación mundial por las potenciales amenazas que pueden suponer para la salud humana. Las enfermedades producidas por estas ARB no pueden ser tratadas eficazmente con antibióticos, siendo responsables de más de 700.000 muertes al año de personas. Las ARB pueden transferir sus genes de resistencia antibiótica (*Antibiotic Resistance Genes*, ARGs) de una bacteria a otra, favoreciendo la propagación de la resistencia a los antibióticos en el medio ambiente. La Organización Mundial de la Salud ha considerado las ARB como una de las tres principales amenazas del siglo XXI debido al gran número de infecciones y muertes que causan cada año en todo el mundo.

Uno de los efluentes con mayor concentración de ARB son los efluentes hospitalarios y, en concreto, la orina de los pacientes inmunodeprimidos donde coexisten simultáneamente las bacterias que causan las infecciones del tracto urinario con los productos farmacéuticos excretados. En la actualidad, las orinas hospitalarias suelen mezclarse con otros efluentes hospitalarios y, posteriormente, se vierten en el sistema de alcantarillado municipal y se tratan junto con los efluentes urbanos en las instalaciones municipales de tratamiento de aguas residuales (EDAR). La ineficacia de los tratamientos biológicos de las EDAR para tratar los efluentes hospitalarios conduce a la propagación de ARB y ARGs en el medio ambiente, afectando negativamente a los organismos acuáticos y a la salud humana. Esto hace del tratamiento de la orina un objetivo clave para reducir el impacto ambiental y sanitario de los efluentes hospitalarios. Por ello, la prioridad de este proyecto es abordar el problema directamente en la fuente de contaminación, dentro del marco de los proyectos regionales y nacionales "Tecnologías electroquímicas para el tratamiento de orinas hospitalarias: reducción del impacto ambiental y sanitario (SBPLY/17/180501/000396) y "Tecnologías electroquímicas ante el reto del tratamiento de orinas hospitalarias (PID2019-110904RB-I00), respectivamente En este contexto, la oxidación electroquímica (EO) ha despertado un gran interés entre los procesos de desinfección, ya que se ha

comprobado que la EO es capaz de conseguir una desinfección completa en aguas residuales urbanas, gracias a la generación *in situ* de especies desinfectantes a partir de la electrooxidación de los iones naturalmente contenidos en el efluente tratado.

Por tanto, esta Tesis Doctoral se centra en la eliminación de bacterias de las orinas hospitalarias, basándose en nuestros trabajos anteriores relacionados con la desinfección de aguas residuales urbanas depuradas teniendo en cuenta la influencia del diseño del reactor electroquímico. En concreto, el objetivo principal de la presente Tesis Doctoral es evaluar la viabilidad técnica de diferentes procesos electroquímicos, incluyendo la electrólisis y la fotoelectrolisis, para reducir el impacto ambiental y sanitario de las bacterias resistentes a los antibióticos en orinas hospitalarias, evitando la formación de subproductos de desinfección no deseados. Para cumplir con este objetivo general, se plantean 5 objetivos parciales a los que se les da respuesta en los apartados en los que se ha subdivido el Capítulo 5 de resultados.

En la sección 5.1 se realizó un estudio prospectivo de los patógenos causantes de las infecciones del tracto urinario (UTIs) en el período 2014 a 2018. Este estudio se realizó en colaboración con el Complejo Hospitalario Universitario de Albacete (CHUA) como modelo de instalación sanitaria. Esto permite evaluar la presencia de ARB en un entorno real, así como la problemática asociada a las ARB en un complejo hospitalario. El estudio demostró que *E. coli* fue la bacteria más significativa encontrada en las orinas positivas (PUs) y que las bacterias gram-negativas (*E. coli*, *K. pneumoniae*, *P. aeruginosa* y *P. mirabilis*) predominan sobre las bacterias gram-positivas (*E. faecalis*) y los hongos (*C. albicans*). La *K. pneumoniae* mostró los porcentajes más altos de resistencia a los antibióticos. Sin embargo, las investigaciones realizadas sobre los procesos de desinfección estaban relacionadas principalmente con la eliminación de *E. coli*, lo que confirma que la importancia que se da a la *K. pneumoniae* como ARB desde el punto de vista sanitario no se corresponde con las investigaciones realizadas sobre los procesos de desinfección. Por lo tanto, se señaló la necesidad de buscar y desarrollar tecnologías novedosas que permitan eliminar cepas resistentes de *K. pneumoniae* para disminuir el impacto sanitario y ambiental de los efluentes infectados con esta bacteria.

En la sección 5.2, se realizó un estudio preliminar de la tecnología electroquímica como alternativa para la eliminación de bacterias en dos escenarios de tratamiento diferentes (aguas residuales urbanas sintéticas y orinas hospitalarias sintéticas) utilizando un reactor convencional de flujo paralelo con ánodos DDB a 10 A m^{-2}. Este estudio demostró que, aunque la eficiencia de eliminación de bacterias era menor en las orinas hospitalarias (debido a reacciones de oxidación competitivas), se evitaba la aparición de subproductos de desinfección peligrosos en esta matriz, ya que se favorecía la producción de hipoclorito y la posterior formación de cloraminas inorgánicas. Posteriormente, se realizó una evaluación preliminar de la electrólisis para la reducción del potencial riesgo químico de la orina hospitalaria. Se seleccionó el cloranfenicol (CAP) como modelo de antibiótico y se evaluó la influencia del material anódico (BDD y MMO) y la densidad de corriente (50, 25 y 12,5 A m^{-2}). Este estudio demostró que la oxidación electroquímica con ánodos BDD aplicando 12,5 A m^{-2} (8 Ah dm^{-3}) permite degradar el CAP de las orinas hospitalarias, aumentando su biodegradabilidad hasta un 40 % según el método de Zahn-Wellens. Sin embargo, este estudio también mostró que las cargas eléctricas requeridas para la eliminación de los antibióticos eran mucho mayores que las requeridas para la desinfección (8 Ah dm^{-3} *vs.* < 0,15 Ah dm^{-3}) y por este motivo, se iniciaron otros estudios paralelos que quedan fuera del objetivo de esta tesis.

En este sentido, en la sección 5.3 se evaluó el desarrollo de tecnologías electroquímicas de desinfección como pretratamiento para eliminar *K. pneumoniae* de las orinas hospitalarias. El objetivo principal de esta sección era conocer el rol de los oxidantes electrogenerados en el proceso de desinfección. En primer lugar, se evaluó la contribución de las cloraminas probando dos conceptos de diseño de celdas electroquímicas con ánodos MMO: un reactor convencional de flujo paralelo y un reactor microfluídico de flujo a través. También se estudió la influencia de la densidad de corriente (5-50 A m^{-2}) y se compararon los resultados con otras matrices de "orina" más sencillas y con ensayos de desinfección química. Los resultados mostraron que el proceso de desinfección de *K. pneumoniae* a partir de orina hospitalaria depende de la densidad de corriente y de la disposición del reactor. La presencia de cloruros en las

orinas hospitalarias contribuyó a la generación de hipoclorito y cloraminas. La formación de cloraminas se potenciaba en el reactor microfluídico de flujo a través gracias a su mayor tiempo de residencia hidráulico. Además, las pruebas de desinfección química demostraron el mayor efecto bactericida del hipoclorito en comparación con las cloraminas. Sin embargo, las cloraminas desempeñan un papel clave en el proceso de desinfección, ya que contribuyen no sólo como agentes desinfectantes sino evitando la generación de subproductos de desinfección clorados.

Además, se evaluó la contribución del ozono en el proceso de desinfección electroquímica probando un electrolizador tipo PEM (*Polymer Electrolyte Membrane*) (celda MIKROZON®) especialmente diseñado para producir ozono en aguas de baja conductividad. Se estudió la influencia de la densidad de corriente y la composición de la orina hospitalaria. Los resultados mostraron que la celda MIKROZON® alcanzaba la desinfección total a partir de intensidades de corriente superiores a 0,5 A. El efecto combinado de los desinfectantes ozono y cloro alcanzó tasas de desinfección superiores a los valores obtenidos cuando el ozono era el principal desinfectante electrogenerado (orina sin cloruros) a intensidades de corriente inferiores a 0,5 A. A valores de 1,0 A, las tasas de desinfección fueron similares, lo que reveló que grandes cantidades de ozono fueron electrogeneradas. El ensayo de cristal violeta demostró que el efecto combinado de todos los desinfectantes promovía mayores daños celulares, aumentando la permeabilidad de la pared celular. Se demostró que el ozono atacaba el ADN en mayor medida a partir de intensidades de corriente superiores a 0,5 A. Finalmente, durante el tratamiento de orinas diluidas a 1,0 A, se obtuvieron mayores tasas de desinfección debido a la minimización de las reacciones competitivas.

La oxidación electroquímica genera la formación de radicales hidroxilos y especies desinfectantes a partir de la electrólisis del agua, que pueden ser activados mediante irradiación con luz UV. En la sección 5.4, se evalúa el acoplamiento de la oxidación electroquímica con la desinfección UV en el reactor microfluídico de flujo a través para la eliminación de *K. pneumoniae* en orinas hospitalarias. Se estudió la influencia de la densidad de corriente (5-50 A m^{-2}) y del material del anódico (BDD y MMO) en la producción de desinfectantes no sólo de hipoclorito sino también de

monocloramina, dicloramina y tricloramina. Los resultados mostraron que la desinfección UV alcanzaba la desinfección completa de *K. pneumoniae*. Sin embargo, la oxidación electroquímica con ánodos BDD y MMO permitía la eliminación total de *K. pneumoniae* en la orina al aplicar 50 A m^{-2}. La tasa de desinfección fue mayor cuando se trabajó con ánodos MMO, ya que los ánodos BDD favorecen las reacciones de oxidación competitivas entre las bacterias y los compuestos orgánicos de la orina. Por último, se demostró que la fotoelectrolisis mejoraba el rendimiento de la desinfección en la fotolisis y en la electrólisis. Se observó que al acoplar la irradiación por luz UV al proceso de electrólisis, se obtenía un marcado efecto sinérgico en la desinfección a 5 A m^{-2} con ánodos BDD y MMO.

En la sección 5.5, se llevó a cabo la validación de la tecnología electroquímica para el tratamiento de matrices complejas de orina sintética (orinas polimicrobianas). Las orinas hospitalarias polimicrobianas simulan las orinas hospitalarias reales, ya que la pandemia causada por el coronavirus SARS-CoV-2 no nos permitió validar la tecnología electroquímica en un entorno real debido a las restricciones sanitarias. En primer lugar, se analizó la ocurrencia simultánea de más de un patógeno causante de infecciones urinarias en orinas hospitalarias reales, a partir de los datos suministrados por el Servicio de Microbiología y Parasitología del CHUA. A partir de este estudio, se conocen las combinaciones de bacterias más prevalentes que se presentan en las orinas reales de pacientes hospitalizados, y se seleccionan las parejas bacterianas para las pruebas electroquímicas: 1) *E. faecalis* y *K. pneumoniae*, 2) *E. coli* y *E. faecalis*, y 3) *K. pneumoniae* y *E. coli*. A continuación, se evaluó la influencia del reactor microfluídico de flujo a través y la celda MIKROZON® para la desinfección de orinas polimicrobianas trabajando bajo las condiciones de operación más adecuadas reportadas en las secciones anteriores. Así, el reactor microfluídico de flujo a través se utilizó con ánodos MMO a 50 A m^{-2} y la celda MIKROZON® trabajó a 1 A. Los resultados mostraron que el reactor microfluídico de flujo a través alcanzó tasas de eliminación de entre 5 y 6 logs después de 180 minutos, mientras que la celda MIKROZON® logró la desinfección total (7 logs) después de 60 minutos. Además, se observó la desnaturalización del ADN y de los ARGs en las orinas hospitalarias polimicrobianas.

Mientras que no se observaron cambios notables en la concentración de ARGs con el reactor microfluídico de flujo a través, la celda MIKROZON® alcanzó una disminución media de ARGs clasificada en el orden: *bla*$_{KPC}$ (4,18-logs) > *bla*$_{TEM}$ (3,96-logs) > *erm*B (3,23-logs), logrando una disminución media de 3,77-logs para todos los ARGs probados. Por último, las imágenes del microscopio electrónico de barrido (*Scanning Electron Microscope*, SEM) confirmaron la completa desinfección alcanzada con la celda MIKROZON® donde se indujeron graves daños en las paredes celulares, lo que provocó la pérdida de integridad de las estructuras bacterianas.

CHAPTER 2:

INTRODUCTION

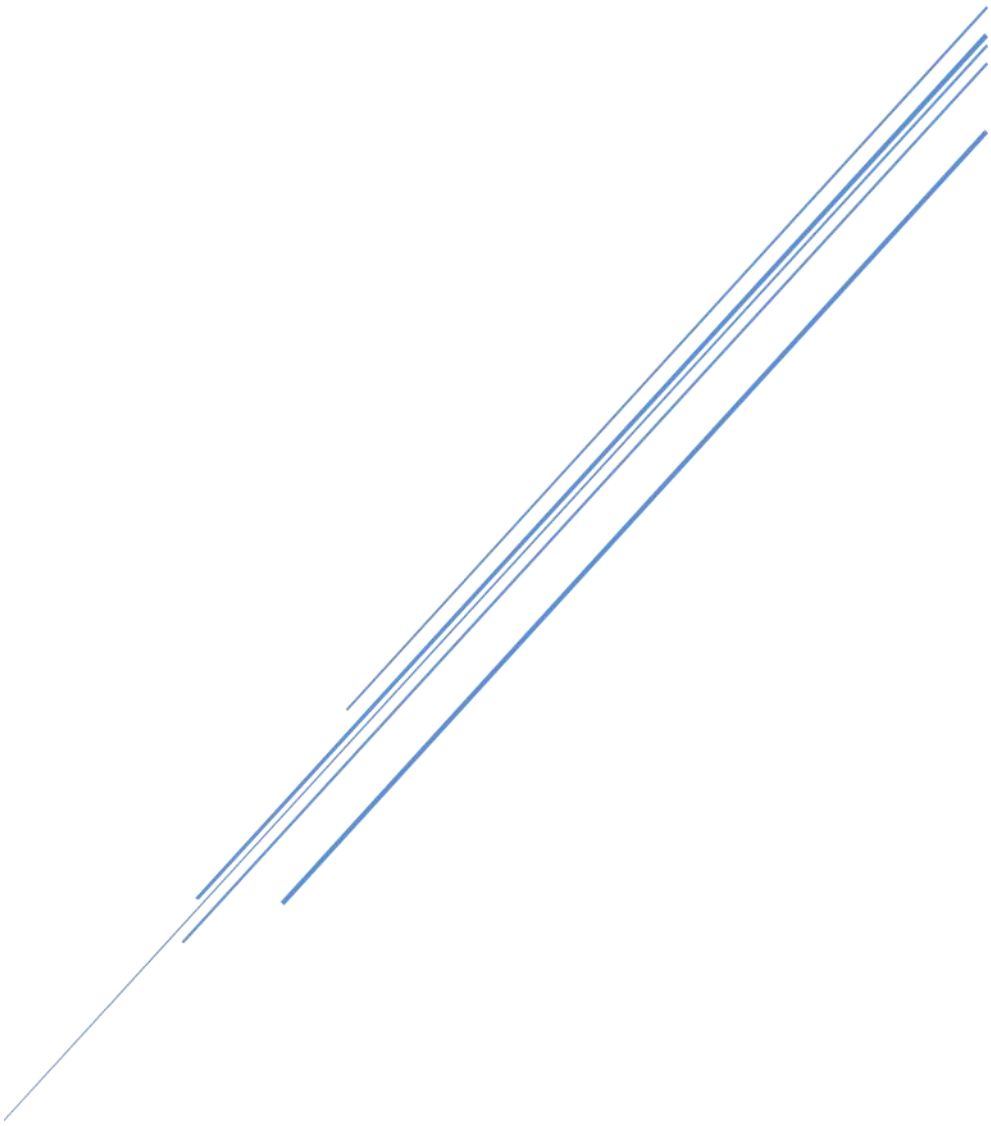

The present chapter is based on the following document:

- M. Herraiz-Carboné, S. Cotillas, E. Lacasa, C. Sainz de Baranda, E. Riquelme, P. Cañizares, M.A. Rodrigo, C. Sáez, *A review on disinfection technologies for controlling the antibiotic resistance spread*, Science of The Total Environment, 797 (2021) 149150.

2.1. Introduction

In recent years, the occurrence of antibiotic-resistant bacteria (ARB) has become a global concern because of the potential threats they can pose to human health [1, 2]. ARB are bacteria with the capacity of survive and multiply in the presence of the antibiotics specifically designed to kill them. The development of ARB is a complex process in which a microorganism can be intrinsically resistant to a drug or can acquire this resistance through different mechanisms [3]. Multiple pathways allow the exchange of genetic material within bacteria, specifically, the four major mechanisms for developed antibiotic resistance are drug inactivation, target modification, reduced antibiotic permeability and antibiotic efflux pumps [4]. Once the resistance has been acquired, this can be transferred to other bacteria, increasing the number of ARB. Consequently, diseases produced by these ARB cannot be effectively treated with antibiotics and being responsible for more than 700 000 human deaths per year [5, 6].

Furthermore, not only vertical transfer (i.e., cell division) but also horizontal gene transfer processes (conjugation, transduction and natural transformation) developing the Antibiotic Resistance Genes (ARGs) contributes to the spread of antibiotic resistance [7]. During conjugation, exchange of genetic elements occurs when the active donor cell and the recipient cell are able to initiate and maintain a physical contact. Conversely, after cell lysis, the transfer of foreign genetic elements only requires a metabolically active recipient capable of being infected (transduction) or of actively acquiring these genetic elements (natural transformation) into its own chromosome [8]. In addition, mobile genetic elements such as integrons and transposons have been widely studied in last years due to their contribution on the antibiotic resistance spread. Integrons are genetic structures able to capture gene cassettes that can encode antibiotic resistance. The mobility of integrons is directly related with transposons, jumping gene systems with resistance genes incorporated [9] and plasmids [10]. These moving elements carrying genetic information can be transfer to the bacterial genome, contributing to the spread of antibiotic resistance [11, 12].

The presence of ARB in water bodies has also become a major environmental challenge [13, 14]. This problem has been exacerbated by the increasing and uncontrolled consumption of antibiotics worldwide, and the absence of efficient technologies for killing these pathogens at large scale [15-18]. Hospitals present a friendly environment for the spread of ARB because of the high concentration of bacteria and drugs contained in their effluents. Most antibiotics are poorly metabolized in the human body, being excreted mainly by urine [19]. Furthermore, some pathogens from infected patients are removed from the body by the same way. This promotes the occurrence of larger concentrations of ARB in hospital urines, and therefore in hospital wastewater (HWW), in comparison with the population typically found in urban wastewater [20]. No restrictions are currently foreseen in the European Directive 91/271/EEC for hospital effluents and then, the management of HWW (including hospital urines) is carried out together with urban and industrial wastewater. Most of these effluents are merged and discharged into wastewater treatment plants (WWTPs) or even disposed poorly or untreated into the environment [21], being an important source of ARB [22].

WWTPs are the unique barrier for the reduction of pollution and toxicity in wastewater coming from different sources. Nevertheless, the technology implemented in conventional WWTPs is not capable to efficiently remove ARB [23, 24]. In addition, WWTPs environment may promote mutation mechanisms between bacteria and also enhance horizontal gene transfer processes, increasing the population of ARB and other mobile genetic elements in treated water [25-27]. The emergence of antibiotic resistance in different water matrices, such as rivers, seawater or HWW has been recently reported [28, 29] and defined by WHO as a potential risk for human health and environment [30]. For this reason, it is of crucial importance to develop efficient technologies that allow the removal of ARB and other mobile genetic elements from different water matrices to minimize the spread of antibiotic resistance. In this paper, a review of disinfection technologies in water, wastewater, and hospital wastewater (including urine matrices) is reported to discuss the most common treatment technologies for the removal of bacteria, ARB, ARGs and other genetic mobile elements in different matrices. To the

author's knowledge, a deep information is still needed related to the state of the art of disinfection technologies to properly manage hospital effluents and above all hospital urines.

2.2. Disinfection technologies for the removal of ARB

ARB from urinary tract infection (UTI) patients are excreted by urine which is merged with other wastewater produced in different areas of hospital facilities (kitchen, laundry…). Similarly, pathogens which do not present antibiotic-resistance, are also eliminated in the same way [31]. As discussed in the introduction, HWW also contain a multitude of antibiotics from patients' urine and faeces. Hence, these effluents present a favourable environment for both the generation of ARB and the spread of existing ones. In this context, the development and application of efficient technologies for killing pathogens, both multi-resistant and non-resistant, in sanitary effluents is critical from an engineering and environmental viewpoint.

The occurrence of ARB in different water bodies has become a major environmental issue. This problem has been aggravated by the misuse of antibiotics worldwide and the scarce legislation regulating the treatment of effluents containing ARB. However, concern in the scientific community related to the development of highly efficient technologies for killing microorganisms has increased considerably in recent years. Figure 2.1 summarizes the publications related to different water matrices disinfection reported from the early 80s. Specifically, Elservier's Scopus were the database used to develop the search using "drinking water disinfection", "wastewater disinfection", and "hospital wastewater disinfection" & "urine disinfection" as keywords.

Natural waters are directly related to consumption, so the presence of microorganisms in them poses a risk to human health [32, 33]. For this reason, a greater number of studies have been carried out on the disinfection of natural waters during the last 40 years. Also noteworthy is the number of publications related to wastewater

disinfection, which although lower than those related to natural water, represent up to the 35.57 % of the total publications on disinfection. This great concern by part of the scientific community may be related to the inefficiency of conventional WWTPs in the elimination of microorganisms, and the danger to the environment that their persistent presence may cause. On the other hand, as mentioned in the introduction, one of the major sources of pathogens are hospital effluents, and more specifically, hospital urines. Even so, only 3.83 % of the publications summarized in Figure 2.1 are referred to disinfection of urine and hospital effluents. However, due to the high environmental and human health threat posed by these outbreaks with such a high concentration of ARB [34, 35], in the coming years, it is expected a growing interest from the scientific community and the increase in the number of works related to urine and hospital effluents disinfection.

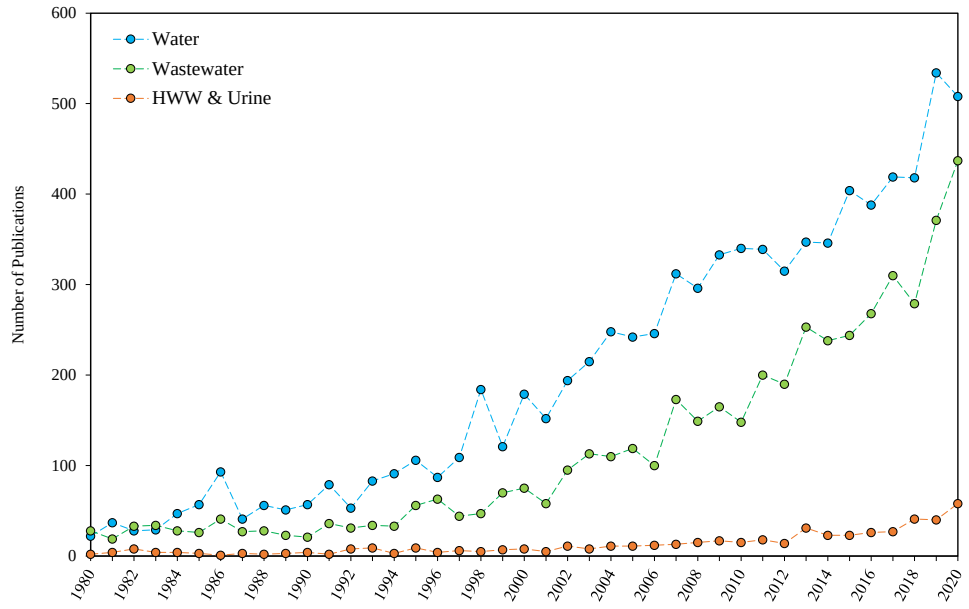

Figure 2.1. Publications related to water, wastewater and HHW and urine disinfection from 1980 to 2020.

2.2.1. Disinfection technologies for the treatment of natural water

Natural waters include rivers, lakes, rainwater or groundwater which naturally contain large amounts of inorganic ions and organic matter, although its composition can be altered by agricultural, domestic and industrial activities [36]. The presence of the different inorganic salts also depends on the water source since these compounds have a vast spectrum. According to literature, HCO_3^-, NO_3^-, NO_2^-, Cl^-, SO_4^- or NH_4^+ can be found in natural waters within the ranges 20 – 800 mg l^{-1}, 0.05 – 60 mg l^{-1}, 0.40 – 1 mg l^{-1}, 4 – 700 mg l^{-1}, 0 – 630 mg l^{-1} and 0.20 – 3 mg l^{-1}, respectively [37-39]. Regarding the organic content in natural water, both humic (hydrophobic) and non-humic (hydrophilic) fractions can be found, including microorganisms [40, 41]. These can promote the proliferation of ARB in these effluents and, hence, a potential risk for human health. Table 2.1 summarizes the most relevant disinfection technologies for different water matrices during the last two years (2019 and 2020).

Many technologies have been developed for pathogen disinfection in water matrices, including conventional, advanced oxidation and electrochemical advanced oxidation processes. Conventional technologies such as filtration, adsorption, coagulation, or precipitation are mainly applied at full scale for the removal of suspended solid, dissolved organic and inorganic contaminants, metals and ionic species, etc. [42]. However, novelty research has been attempted to improve the antibacterial capabilities of these conventional processes. Hence, conventional processes could be considered as a suitable alternative for water disinfection because of their low cost and easy application. These physical-chemical technologies are mainly based on the separation of microorganisms from polluted water [43]. Wang et al. [44] evaluated the removal of *S. aureus* in water by filtration using a modified filter-paper-based material. They developed a tannic acid crosslinked gelatine polymer network with an oxidized cellulose filter paper (OFP-GEL-TA) for bacteria removal. As a natural antibacterial agent, the cross-linker TA endowed the prepared OFP-GEL-TA with favourable antibacterial property. Disinfection efficiencies reached 99.00 % and decreased up to 98.00 % after five cycles. Additionally, the adsorption performance of a magnetic graphene oxide (MGO) was evaluated against microbial activity of *E. coli*,

Yersinia ruckeri (Y. ruckeri) and *Enterobacter agglomerans* (*E. agglomerans)* by Ain et al. [45]. Results showed that with the addition of 0.5, 0.5 and 0.45 mg ml^{-1} of MGO to water containing *E. coli*, *Y. ruckeri* and *E. agglomerans*, respectively, the maximum percentages of relative effectiveness were 98.79, 97.15 and 97.69 % in comparison with a control system (commercially available disinfectant).

Coagulation processes have been also tested for water disinfection. These technologies consist of adding a coagulant species to the water to be treated, which can be a chemical or natural compound. Iron and aluminium based inorganic salts are typically used as chemical coagulants. However, these metal species can promote the occurrence of coagulant traces as toxic by-products dissolved in treated effluents [46, 47]. This can be avoided by using natural coagulants, since these compounds are highly biodegradable [48]. Nonetheless, the main drawback of coagulation processes is the generation of a final sludge that should be treated later. Patchaiyappan et al. [49] tested an indigenous natural coagulant *Strychnos potatorum* (*S. potatorum*) for the disinfection of synthetic waters with high levels of turbidity. *S. potatorum* is a deciduous tree known as clearing-nut tree, commonly used in traditional medicine and water purification in some regions of South Asia. They concluded that an optimum coagulant dosage within the range 0.2 - 1 mg l^{-1} reduced 3.3 - 4.3 logs of *E. coli*. On the other hand, the bactericidal properties of a green and low-priced magnetic biochar/quaternary phosphonium salt (MBQ) were tested by Fu et al. [50]. Quaternary phosphonium salts are able to reach high disinfection efficiencies working in a wide range of pH (2 - 12), thus, they are presented as a new generation of cationic biocides [51]. Specifically, the use of 20 mg l^{-1} of MBQ-3 (with a mass ratio of magnetic biochar and quaternary phosphonium salt of 1:30) reduced the population of *E. coli* in 3.05 logs and achieved the complete removal of 10^6 CFU ml^{-1} of *S. aureus*. Microorganisms were captured by the electrostatic force of the cationic surfactant on the surface of MBQ and nanoparticles penetrating the cell wall and membrane into the cytoplasm may be responsible for the irreversible cell damage.

Other conventional processes based on the addition of chemical disinfectants or the irradiation of UV light have also been recently studied by Stange et al. for water

disinfection to attain the abatement of ARB and ARGs [52]. They compared ARB (*E. coli* and *E. faecalis*) and ARGs removal during three different processes: chlorination, ozonation and UV light irradiance. The chlorination process using 0.25 mg l^{-1} of free chlorine (30 min contact time) resulted in a reduction of 5.1 and 2.9 logs of *E. coli* and *E. faecalis*, respectively. Likewise, ARGs were decrease by only 0.4 (*amp*C), 0.5 (*tet(*A*)*), 0.9 (*erm*B) and 0.8 (*van*A) log. Higher free chlorine concentrations of 1.03 mg l^{-1} leads to remove ARGs up to their limit of detection for *ampC* and *tet(*A*)* and around 3 logs for *erm*B and *van*A. Otherwise, the ozonation process using about 1 mg l^{-1} of O_3 (5 min contact time) achieved a reduction of 5 logs for *E. coli* and *E. faecalis*, and higher than 4.3 logs for the 4 ARGs tested without reaching a totally removal of ARGs. Finally, the irradiation of a UV dosage of 100 J m^{-2} showed an inactivation of 2.5 log of *E. coli* and 4.2 log of *E. faecalis*, without noticeable changes for the removal of any ARGs.

Physical-chemical processes allow to reduce the population of microorganisms in natural water by using low-cost materials. However, the main drawback of these conventional technologies is that they do not kill pathogens but are retained in filters, adsorbents or coagulants and, hence, a complete disinfection can be limited. To overcome this issue, other technologies such as Advanced Oxidation Processes (AOPs) have been studied for water disinfection over the last years. AOPs can be defined as oxidation technologies based on the production of large amounts of highly reactive species which are directly involved in the destruction of target pollutants. Specifically, the generation of hydroxyl radical (·OH) is mainly promoted during AOPs because it is a powerful oxidant (E^0: 2.86 V) able to non-selectively attack the recalcitrant organic compounds and microorganisms present in different effluents.

Depending on the mechanism for hydroxyl radical generation, AOPs can be classified in two major groups (Figure 2.2): homogeneous and heterogeneous AOPs. These AOPs can be also divided in two different groups based on the energy requirements or the irradiation of UV light, respectively. The production of hydroxyl radicals takes place from chemicals completely dissolved in the effluents during homogeneous AOPs whereas a solid catalyst is commonly required for generating these radicals in heterogeneous AOPs.

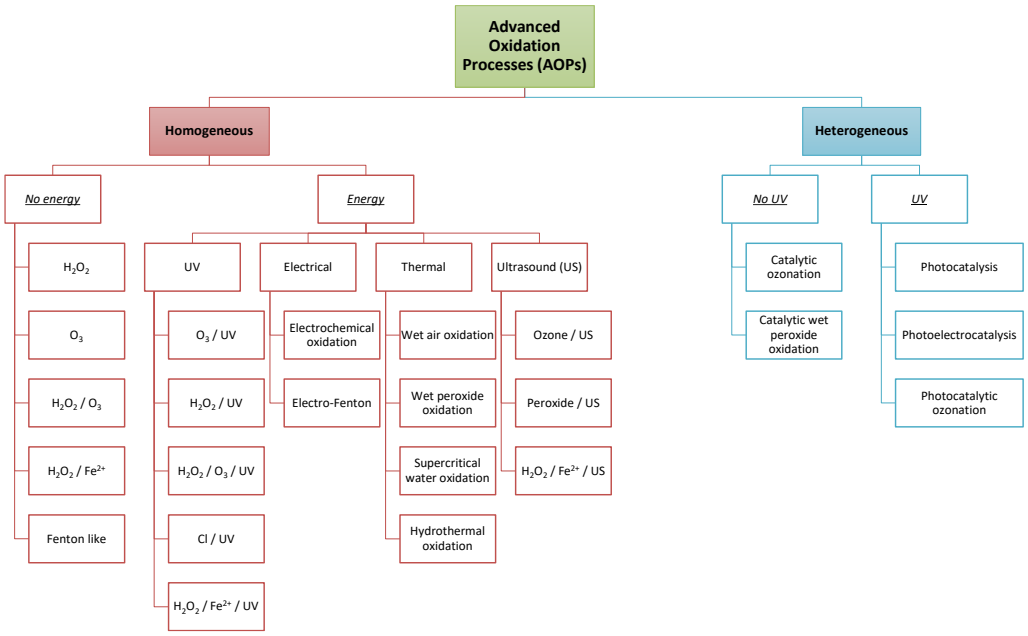

Figure 2.2. Classification of Advanced Oxidation Processes.

Hydrogen peroxide (H_2O_2) is a powerful oxidant (E^0: 1.78 V) which can be used for disinfection purposes. It is considered as a clean compound since H_2O_2 is usually decomposed in oxygen and water, avoiding the generation of by-products. The bactericidal effect of this species can be limited depending on the initial concentration [53]. For this reason, the activation of H_2O_2 with other oxidants or catalysts to improve the processes efficiencies has been reported in literature [54-56]. The combined effect of H_2O_2 and ozone (O_3) promotes the generation of large amounts of hydroxyl radicals (Equation 2.1) [57, 58]. This process (H_2O_2/O_3) has been investigated for the disinfection of water and wastewater [59].

$$O_3 + H_2O_2 \rightarrow \cdot OH + O_2 + HO_2\cdot \quad (2.1)$$

Nonetheless, Fenton oxidation (H_2O_2/Fe^{2+}) is the most widely investigated technology for water treatment [60-62]. It is based on the production of large amounts of hydroxyl radicals from the activation of hydrogen peroxide by using ferrous iron (Fe^{2+}) as catalyst (Equation 2.2) which, in turn, can be continuously regenerated during the process (Equations 2.3-2.4) [63].

$$Fe^{2+} + H_2O_2 \rightarrow Fe^{3+} + \cdot OH + OH^- \quad (2.2)$$

$$Fe^{3+} + H_2O_2 \rightarrow H^+ + Fe(HO_2)^{2+} \quad (2.3)$$

$$Fe(HO_2)^{2+} \rightarrow Fe^{2+} + HO_2\cdot \quad (2.4)$$

The ratio of reagents employed (H_2O_2:Fe^{2+}) in the Fenton's reaction significantly influences the process performance [62]. Likewise, another important operational parameter is pH since it is necessary to operate under acidic conditions to ensure the dissolution of catalyst. pH values around 3 usually leads to better performances during the Fenton process [64]. These operating conditions can limit the applicability of this technology because a subsequent neutralization step is required before discharging the treated effluents that increases the operational costs. For this reason, the use of solid catalysts can be considered as an excellent alternative for carrying out the Fenton process at a wide pH range (heterogeneous Fenton). This also allows to easily separate the catalyst from treated water after disinfection [65]. The development of novel catalysts for improving disinfection efficiencies has become a hot research topic in the last years. Gu et al. [66] tested the antibacterial capability of $CuFe_2O_4$ nanomaterial enhanced with hydroxylamine (NH_2OH) in a Fenton-like process (Figure 2.3). In a first step, NH_2OH acts as a reducing agent that promotes the generation of Cu(I) (Equation 2.5). Then, Cu(I) reacts with hydrogen peroxide, previously generated from the reaction between NH_2OH and O_2 (Equation 2.6), promoting the generation of hydroxyl radicals (Equation 2.7) [67]. Cu(I) also showed a higher binding affinity to proteins of cell membrane, favouring their reduction and, hence, the killing of microorganisms. Specifically, the process achieved a 2.71 log reduction of *E. coli*.

$$2\ NH_2OH + 4\ Cu(II) \rightarrow N_2O + H_2O + 4\ Cu(I) + 4H^+ \quad (2.5)$$

$$2\ NH_2OH + O_2 \rightarrow N_2 + H_2O_2 + 2\ H_2O \quad (2.6)$$

$$Cu(I) + H_2O_2 \rightarrow Cu(II) + \cdot OH + OH^- \quad (2.7)$$

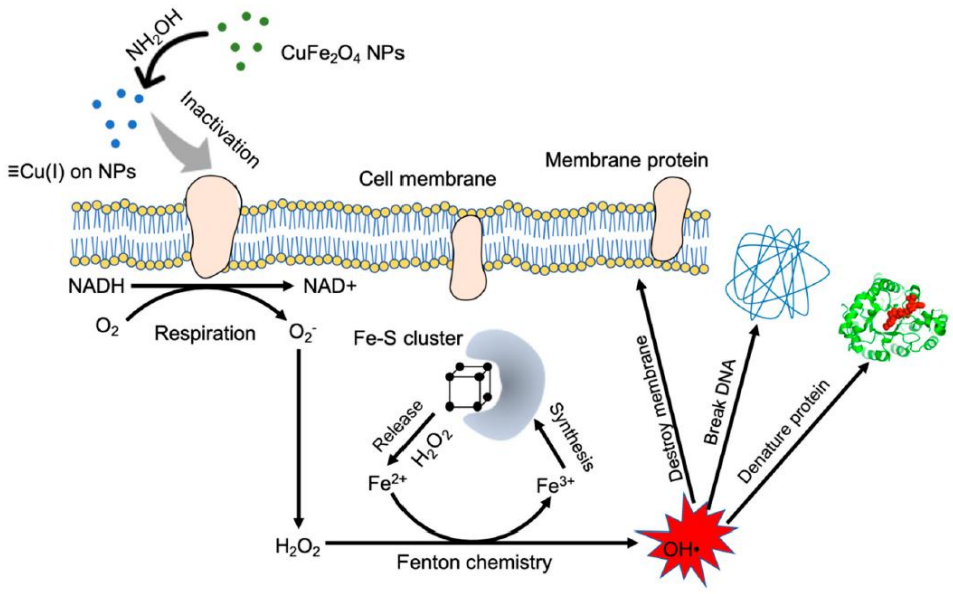

Figure 2.3. Proposed mechanism of $CuFe_2O_4/NH_2OH$ reaction inactivating *E. coli* cells. Reprinted from ref [66]. Open access 2020 MDPI.

Fenton oxidation process can also be enhanced by coupling ultraviolet (UV) irradiation (photo-Fenton). This promotes the massive production of hydroxyl radicals not only by the Fenton reaction (Equation 2.2) but also by the irradiation of UVA light ($315 < \lambda < 400$) over an iron complex ($Fe(HO)^{2+}$) previously formed during the process (Equation 2.8) [65]. Thus, it is possible to regenerate the iron catalyst used during photo-Fenton, minimizing the waste production. This fact can also be achieved during single Fenton process (Equations 2.3-2.4), although the regeneration rate is lower [68]. In addition, the irradiation of UVC light ($200 < \lambda < 280$) improves the production of hydroxyl radicals in the effluent because it photoactivates both iron (Equation 2.8) and hydrogen peroxide (Equation 2.9) [69]. Rubio et al. [70] reported the applicability of photo-Fenton process with UVC light for the removal of 10^6 CFU ml^{-1} of *E. coli* in different water matrices (milli-q water, lake water and seawater). They achieved a complete disinfection in all effluent at operating times of 5 min, although the process efficiency was higher in milli-q water.

$$Fe(HO)^{2+} + h\nu \rightarrow Fe^{2+} + \cdot OH \quad (2.8)$$

$H_2O_2 + h\nu \rightarrow 2\ \cdot OH$ (2.9)

The irradiation of UV light during Fenton process can significantly increase the treatment costs, which can be avoided by using solar light ($\lambda > 300$ nm) as renewable energy-saving alternative. The investigation of solar photo-Fenton process for the disinfection of water contaminated with *E. coli* was reported by Spuhler et al. [71]. They evaluated a solar simulator to irradiate an effluent containing 0.6 mg l^{-1} Fe^{2+} and 10 mg l^{-1} H_2O_2, achieving the complete disinfection (6-log reduction). The presence of ions in polluted water can affect the effectiveness of photo-Fenton. Rommozzi et al. tested the interaction of HCO_3^-, NO_3^-, NO_2^-, Cl^-, SO_4^{2-} and NH_4^+ during the *E. coli* inactivation by photo-Fenton [36]. They concluded that the disinfection can be enhanced by the presence of ions because of the generation of free radicals. For instance, the addition of 10 mg l^{-1} of HCO_3^- promoted the complete removal of *E. coli* in shorter times than those observed without the presence of HCO_3^- during photo-Fenton process. This was mainly attributed to the contribution of carbonate radicals generated from the reaction between carbonate ions and hydroxyl radicals (Equations 2.10-2.11) [36].

$HCO_3^- + \cdot OH \rightarrow CO_3^{\cdot -} + H_2O$ (2.10)

$CO_3^{2-} + \cdot OH \rightarrow CO_3^{\cdot -} + OH^-$ (2.11)

To overcome the pH limitations of the Fenton process, the use of iron and copper chelates for water and wastewater disinfection at near neutral pH values has been recently reported [72-74]. The most commonly studied chelating agents are aminopolicarboxylic acids such as EDTA (Ethylenediaminetetraacetic acid) or EDDS (Ethylenediamine-N,N‘-disuccinic acid), citric or oxalic acids [75]. These compounds can generate Fe^{2+} rather than other iron complexes and have molar absorption coefficients in the UV-vis region, allowing the solar photo-Fenton like process to operate under neutral pH conditions [76]. This technology has been investigated by Ahmed et al., which employed a modified photo-Fenton process using EDDS to chelate Fe(III) for the simultaneous removal of ARB, ARGs and micropollutants. Results showed that the concentration of ARB, extracellular ARGs and micropollutants

decreased to the limit of detection after 30, 15 and 10 min, respectively, when working in ultra-pure water [77].

Ferrous iron catalysts can also be used for the activation of other oxidants such as peroxymonosulphate and persulphate, favouring the formation of sulphate radicals (Equations 2.12-2.13). Furthermore, the irradiation of UV light also promotes the photoactivation of these oxidants, increasing the quantity of free radicals available for disinfection purposes (Equations 2.14-2.15). Rodriguez-Chueca et al. reported the activation of peroxymonosulphate and persulphate by different routes to form sulphate and hydroxyl radicals for enhancing the solar disinfection of drinking water [78]. Outcomes showed that it was possible to attain a complete removal of 10^6 CFU ml^{-1} of *E. coli* with both oxidants, although the use of HSO_5^- was more efficient to generate sulphate radicals than $S_2O_8^{2-}$, increasing the disinfection rates.

$$HSO_5^- + Fe^{2+} \rightarrow Fe^{3+} + SO_4^{\bullet -} + OH^- \quad (2.12)$$

$$S_2O_8^{2-} + Fe^{2+} \rightarrow Fe^{3+} + 2\ SO_4^{\bullet -} \quad (2.13)$$

$$HSO_5^- + h\nu \rightarrow SO_4^{\bullet -} + {}^{\bullet}OH \quad (2.14)$$

$$S_2O_8^{2-} + h\nu \rightarrow 2SO_4^{\bullet -} \quad (2.15)$$

Ferreira et al. [79] tested the photo activation of persulfate ($S_2O_8^{2-}$) under solar irradiation for the inactivation of water pathogens (*E. coli* and *E. faecalis*). The generation of sulphate radicals (Equation 2.15) led to the total bacteria removal during 20 min of solar exposure. The highest inactivation rates were obtained with 0.5 and 0.7 mM of $S_2O_8^{2-}$ for *E. coli* and *E. faecalis*, respectively. This process has also been used for the removal of carbapenem resistant *K. pneumoniae* and the elimination of bla_{KPC-3} genes in water [80]. In this work, the UV-C/$S_2O_8^{2-}$ process showed a faster removal rate of the genetic material compared with UV-C/H_2O_2 process, remarking the great potential of the sulphate radicals generation for water disinfection. However, the treatment time required to achieve the elimination of bla_{KPC-3} gene is higher than the 60 seconds needed to reach the complete removal of bacteria. More than 98 % of bla_{KPC-3} gene were removed after 300 seconds for both UV-C/$S_2O_8^{2-}$ and UV-C/H_2O_2 processes. In addition, no regrowth was observed after 24 h incubation in Brain Heart Infusion agar

for both processes, remarking the great potential of preventing the antibiotic resistance spread. Other homogeneous AOPs in which UV light is used to photoactivate chemical species without the presence of iron in the reaction are Cl/UV, CH_3CO_3H/UV, H_2O_2/UV, O_3/UV and H_2O_2/O_3/UV. These photochemical processes promote the generation of large amounts of hydroxyl radicals, improving the oxidation potential of Cl, CH_3CO_3H, O_3 and H_2O_2 [81-83].

On the other hand, in the last decades the heterogeneous photocatalytic processes have emerged as an interesting alternative for water disinfection. These AOPs are based on the production of reactive oxidizing species (ROS) by the irradiation of a UV light power source on a semiconductor material [84-87]. Energy from UV light greater than the band gap of the semiconductor excites an electron from the valence band to the conduction band, generating a positive hole in the valence band. These positive holes can oxidize OH^- or H_2O at the surface of the semiconductor material leading to the production of ROS. Specifically, hydrogen peroxide, ozone and hydroxyl radicals can be generated during the heterogeneous photocatalytic processes. These ROS significantly contribute to killing microorganisms and, hence, increase the disinfection efficiencies [88, 89]. The most common semiconductor used for the development of heterogeneous photochemical AOPs is TiO_2 which is photo-activated by UV irradiation at wavelengths lower than 387 nm [90, 91].

The efficiency of this photocatalyst in disinfection was firstly studied in the early 80s [92] and, recently, it has been reported by Nyangaresi et al., who obtained a maximum of 5 Log CFU reduction of *E. coli* by activating TiO_2 with UV light at 365 nm [93]. Likewise, other recent studies have described that the addition of dopants such us silver oxalate (under visible light, $\lambda > 400$ nm) [94] or carbon modified (activated with UV-A or artificial solar light (ASL)) [95] with TiO_2 allows to attain the complete removal of $2 \cdot 10^5$ and $1.5 \cdot 10^6$ CFU/ml of *E. coli*, respectively. The use of nanomaterials is becoming increasingly relevant as catalytic compounds for developing highly efficient AOPs. Song et al. [96] synthesized a nanofibrous membrane (g-C_3N_4@Co-TiO_2) with outstanding visible-light driven photocatalytic performance towards bacteria, reaching a removal of 10^6 CFU/ml of *E. coli* (Figure 2.4). The catalytic

disinfection activity caused surface collapse and shape destruction of bacteria cells after 90 min treatment, resulting in the complete inactivation of bacteria. This confirms the excellent photocatalytic disinfection properties of the synthesized membrane.

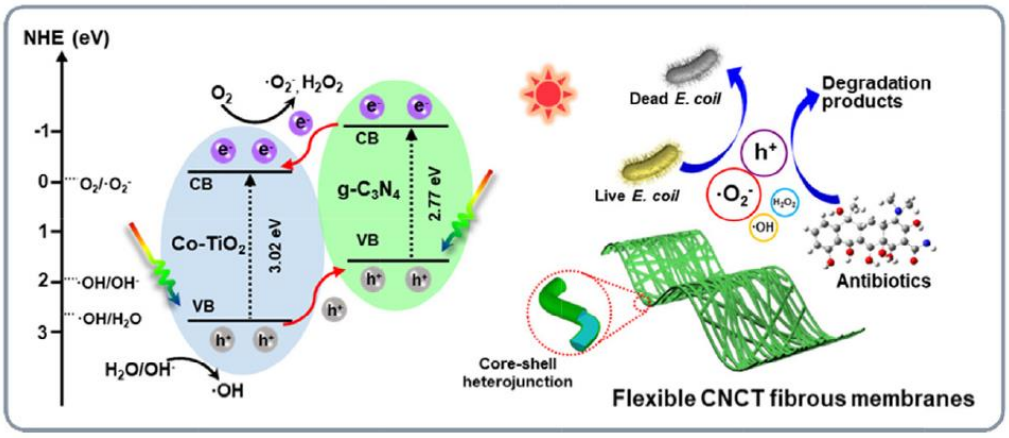

Figure 2.4. Proposed photocatalytic mechanism of the soft CNCT fibrous membrane. Reprinted with permission from ref [96]. Copyright 2020 Elsevier.

Wavelengths lower than 387 nm required for the photo-activation of TiO_2 can limit the efficiency of solar applications, in which light is emitted mostly in the spectrum range of λ = 400 - 700 nm [97, 98]. Manasa et al. [99] reported the photoactivation of TiO_2 by sunlight and no noticeable disinfection degree was reached. The use of cerium (Ce) and boron (B) as doping elements slightly increased the killing of microorganisms, but a complete disinfection was not attained. Doping plays a key role in modifying the properties of functional photocatalyst materials and, these modifications are determined by several factors such as the type and concentration of the dopant, the fabrication method, and the physicochemical properties of the catalyst [100].

To overcome the limitations related to TiO_2, and its low photoactivation by sunlight, the use of multi-component oxides is being studied to promote high-efficiency solar photocatalytic processes [101]. Bismuth-based multi-component oxides have been widely used for disinfection purposes because of their dielectric, ion-conductive, luminescent and catalytic properties [102, 103]. These compounds can be photoactivated by sunlight, favouring the production of large amounts of hydroxyl radicals and the subsequent water treatment [104-106]. Specifically, Cu-MoS_2-Bi_2S_3

[107] and Bi_2MoO_6/Ag-AgCl [108] have been proven efficient for water disinfection, promoting the complete removal of *E. coli* under visible light irradiation.

Other compounds such as silver (Ag) [109-111] or magnesium (Mg) [112] have also proven their excellent photocatalytic disinfection properties. The positive doping effect of Ag on the disinfection process have been tested by Yu et al. [111]. In this work, they used a AgBr-modified g-C_3N_4 composite for enhancing visible-light-driven photocatalytic disinfection. Removal rates of *E. coli* were improved from 0.6 to 3.68 log CFUs reduction for a molar ratio of 1 AgBr to g-C_3N_4. The photocatalytic disinfection efficiency of Ag increased to 4.8 log CFUs reduction for a molar ratio of 5, but it decreased to 3.04 log CFUs reduction by increasing the molar ratio to 20. This highlights the importance of balancing the doping materials to reach the best bacterial adsorption capacity. Additionally, other technologies can be coupled with multi-component oxides to improve the photocatalytic process. Kumar et al. have recently tested a piezoelectric material, poled $BaTiO_3$, in combination with UV irradiation and low frequency vibration (8 Hz) to design a piezo photo-catalytic process able to completely remove *E. coli* from a water matrix [113]. The oxidative stress caused by the electrostatic attraction between positive charged $BaTiO_3$ and negatively charged bacterial cell membranes is directly related to bacterial death. In addition, the concentration of intracellular ROS, which was notably enhanced during the piezo photo-catalytic process compared with UV and US processes, also played an important role in the disinfection process.

Non-metal doping has been also tested in photocatalytic processes because it promotes a great photocatalytic activity under UV-vis irradiation, being N-doped and C-doped TiO_2 the most studied systems [114, 115]. He et al. [116] proposed a novel metal-free 2D heterostructure made of black phosphorus (BP) and graphitic carbon nitride (CN) for the removal of ARB in water sources. Results indicated that the metal-free BP-CN made of low cost and hearth abundant materials with a 6 wt % BP-CN (6BP-CN) was able to reach the complete disinfection of 10^7 CFU/ml of *E. coli*. Other interesting study reported by Zeng et al. [117] compares the disinfection efficiencies of a metal-free photocatalytic process based on a versatile semiconductor (C_3N_4) for killing

E. coli and *E. faecalis* as models of gram-negative and gram-positive bacteria, respectively. They modified C_3N_4 nanosheets with polyethyleneimine (PEI) to improve its disinfection capabilities. Results showed the gradual destruction of cell membranes and leakage of interior components by the generated ROS. The damage to the cell structures of *E. coli* was worse than those of *E. faecalis* cells, and this was attributed to the thicker peptidoglycan layer in the cell wall of gram-positive bacteria.

The Glow Plasma Discharge (GPD) process can be considered as a kind of AOPs and it has also been studied for the removal of ARB and ARGs. The GPD process is able to generate plasma between an anode tip and a water surface by the strong electric field generated, promoting the formation of disinfectant species such as hydroxyl or chlorine radicals [118, 119]. Yang et al. studied the removal of *E. coli* by applying a DC voltage of 500 V and a current intensity of 100 mA into the anode platinum wire. The inactivation of *E. coli* was estimated by following the concentration of the 16S rRNA, which showed a decrease close to the detection limit of 4.7 logs after a discharge time of 15 min. Additionally, the reduction of *tet*A, *tet*R, *aph*A and *tnp*A genes was 5.8, 5.4, 5.3 and 5.5 logs with 30 min discharge treatment, respectively [120]. These results highlighted the potential capacity of the GDP process to reduce the risk of gene transfer.

Other AOPs applied to water disinfection are technologies based on electrochemistry which are commonly known as electrochemical advanced oxidation processes (EAOPs) [54, 121]. EAOPs are processes in which a direct current electric field is applied across the contaminated effluent, promoting the generation of large amounts of highly reactive species that destroy chemical and biological pollutants. There are different EAOPs that can be applied to water disinfection: electro-Fenton (EF), photoelectron-Fenton (PEF), sonoelectrochemistry (SE) or electrochemical oxidation (EO) [122]. These technologies can proceed without the need for chemicals storage as occur in methods such as chlorination, ozonation or Fenton process, reducing associated operating costs [123, 124]. During EO, ions naturally contained in the untreated effluents are oxidized or reduced on the anode or cathode surface, respectively. By these mechanisms, different disinfectants can be electrogenerated such as ozone, hypochlorite, chloramines or hydrogen peroxide. Likewise, other powerful

oxidizing species like hydroxyl, sulphate, carbonate or chlorine radicals can be also generated, favouring the killing of microorganisms during disinfection processes. EAOPs provide several advantages for the disinfection of contaminated sources because the electron is a clean reagent, and the process efficiencies are very high [122, 125-127]. For this reason, they are considered environmentally friendly processes.

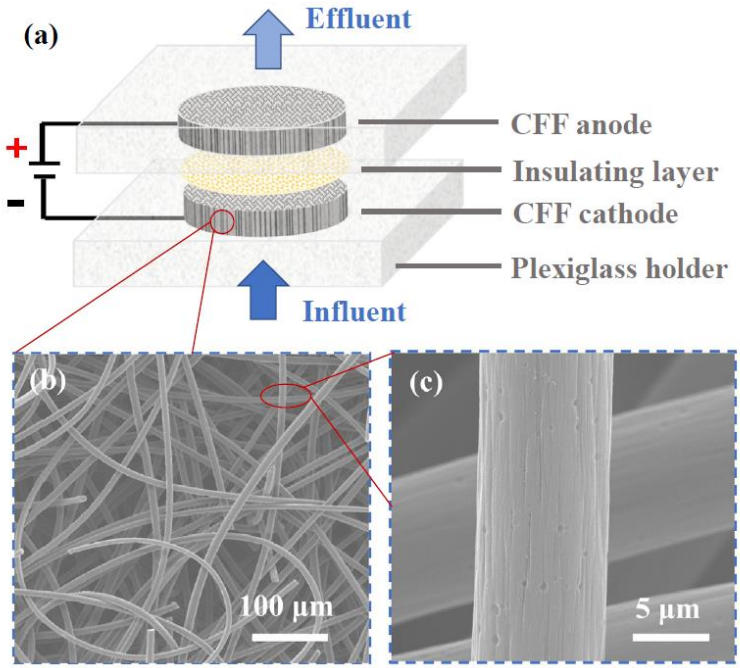

Figure 2.5. Construction and characterization of the flow-through electrode system (FES). (a) The schematic diagram of the FES including Plexiglass coaxial electrode holders, a filter paper as the insulating layer, and two CFF electrodes connected to the DC power. (b) Scanning electron microscopy (SEM) image of the micro-structure of CFF electrodes. (c) SEM image of the carbon fibers under high magnification. Reprinted with permission from ref [128]. Copyright 2020 Elsevier.

EO process is strongly influenced by the electrode material used and the applied current density. Electrode materials such as carbon fiber felt (CFF), boron doped diamond (BDD), or mixed metal oxides (MMO) are commonly used for water disinfection process [129-135]. Many authors have tested the viability of EO as disinfection process, obtaining total bacteria removal rates in water matrices with the application of low current densities and electric charges. Ni et al. [128] tested the

disinfection performance of a carbon fiber-based flow through electrode system towards gram-negative and gram-positive pathogens (Figure 2.5). Results showed that the complete removal of different bacteria was attained at low applied voltages (1-5V) and short HRTs (1-10s). Gram-positive bacteria (*E. faecalis* and *Bacillus subtilis*) were less vulnerable to the disinfection process than gram-negative bacteria (*E. coli* and faecal coliform), which may be associated to the different composition of cell walls (peptidoglycan and teichoic acids). Furthermore, authors stablished the direct oxidation as main disinfection mechanism since the indirect oxidation was negligible at low voltages.

Other authors have studied the applicability of nanowires electrodes for low-voltage electroporation disinfection process [136, 137]. These nanowire structures have a nanoscale tip structure that can amplify the strength of the electric field near the tips by several orders of magnitude [138], leading to the complete removal of pathogens. In the electroporation process, it is induced a damage in the cell membrane resulting in cell death when is exposed to an electric field of strength enough [139]. Conversely, different electrode materials and electrochemical reactors have been also proven efficient in the disinfection of water matrices. In the work reported by Isidro et al. [140], a special PEM-electrolyzer equipped with diamond anodes was studied for the removal of total coliforms and *P. aeruginosa*. The reactor employed was a commercial MIKROZON cell, especially designed to produce ozone as the main disinfectant specie in low-conductivity waters. Results showed that the reactor can be successfully used to disinfect water, being promising results for the future development of this type of cells.

EO can also be coupled with photolysis to enhance the photo-electro generation of disinfectant species and, hence, to obtain a more efficient process with a lower cost. The irradiation can be applied naturally (solar irradiation) or artificially (UV lamp). Thus, the photoactivation of the electrochemical generated reactive species such as hydrogen peroxide, ozone, persulfate or hypochlorite leads to the enhancement of the generation of hydroxyl, sulphate or chlorine radicals [141-143]. Specifically, photoelectrochemical technology has been recently proven to be efficient in the disinfection of water sources contaminated with *E. coli* [144, 145]. Another interesting

work has been published by Montenegro-Ayo et al. [146]. They designed a portable point-of-use photo-electrocatalytic device (e-DRINK) for rapid water disinfection. This device was composed of TiO_2 nanotubes acting as photo-anodes and a rechargeable battery to provide the power supply. This technology was able to reach 5-log inactivation of *E. coli* in just 10 seconds in sterile saline solution and in 4 min in a natural water matrix. The different disinfection behaviours were attributed to the hindrance of light transport in the presence of natural water components. The e-DRINK device provides an amazing opportunity to achieve access to safe drinking water in isolated areas and developing regions.

Other EAOPs have been also tested for water disinfection such as electro-Fenton. This technology is based on the production of hydroxyl radical by Fenton reaction (Equation 2.2) but, in this case, the hydrogen peroxide is electrochemically produced by oxygen reduction over the cathode surface (Equation 2.16) [147-149].

$$O_2 + 2H^+ + 2e^- \rightarrow H_2O_2 \quad (2.16)$$

Chen et al. [150], tested a granular activated carbon cathode (GAC) in an electro-Fenton process, to enhance the production of H_2O_2. This allowed to increase the generation of hydroxyl radicals, promoting an improvement in the *E. coli* removal rate. Results showed that the process could non-selectively inactivate the antibiotic-resistant *E. coli* with different ARGs in a 300 min treatment. ARGs present in the bacterial strain such as, ampicillin-, tetracycline-, or chloramphenicol-resistance genes, among others, were also completely removed after the treatment. The great cost-effectiveness ratio of GAC cathodes renders this electro-Fenton process as an affordable alternative for practical applications.

Table 2.1. Technologies for pathogen removal from water sources.

Technology	Operation parameters	Bacteria	$Bacteria_0$ (CFU/ml)	Bacteria removal [Log reduction]	Ref.
Filtration	FP / OFP-GEL / OFP-GEL-TA	*S. aureus*	$[10^5$-$10^6]$	0.08 / 0.18 / 2	[44]
Adsorption	0.5 mg ml^{-1} MGO 0.5 mg ml^{-1} MGO 0.45 mg ml^{-1} MGO Magnetic graphene oxide (MGO)	*E. coli* *Y. ruckeri* *E. agglomerans*	-	1.91 1.54 1.63	[45]
Coagulation	0.2 to 1 mg l^{-1} Indigenous natural coagulant (*S. potatorum*)	*E. coli*	$2.4 \cdot 10^4$ -	3.3 - 4.3	[49]
Precipitation / Ion exchange	20 mg l^{-1} Magnetic biochar/quaternary phosphonium salt (MBQ-3)	*E. coli* *S. aureus*	10^6	3.05 Total	[50]
Chlorination Ozonation UV	0.25 mg l^{-1} Cl-NaClO – 30 min 1 mg l^{-1} O_3 – 5 min 100 J m^{-2} - λ = 253.7 nm	*E. coli* *E. faecalis*	-	5.1 / 2.9 5 / 5 2.5 / 4.2	[52]
H_2O_2 / O_3	0.15 g O_3 $l^{-1}h^{-1}$ – 20 mg H_2O_2 l^{-1} - pH 6.25 – 6 min	*E. coli* *S. enteritidis*	10^6	Total Total	[59]
Fenton-like	0.2 g l^{-1} $CuFe_2O_4$ + 2mM NH_2OH – 3h	*E. coli*	10^8	2.71	[66]
Photo-Fenton	1 mg l^{-1} Fe^{2+} - 10 mg l^{-1} H_2O_2 – UV (λ=254) – 300s	*E. coli*	10^6	Total	[70]
Photo-Fenton	0.6 mg l^{-1} Fe^{2+} - 10 mg l^{-1} H_2O_2 Solar light simulation (λ > 290 nm) - 550 W m^{-2}	*E. coli*	10^6	Total	[71]

Table 2.1. (Cont.) Technologies for pathogen removal from water sources.

Technology	Operation parameters	Bacteria	Bacteria$_0$ (CFU/ml)	Bacteria removal [Log reduction]	Ref.
Photo-Fenton	PF + 10 mg l^{-1} HCO_3^- - Solar light (620 Wm^{-2}) - 45 min	*E. coli*	10^6	Total	[36]
Photo-Fenton	Fe(III):EDDS:H_2O_2 (0.1:0.2:0.3 mM) + SSL – 30 min SSL 130 mW cm^{-2}	*E. coli*	10^6	Total	[77]
Photochemical disinfection	UV + Fe^{2+} + HSO_5^- - 30 min / UV + Fe^{2+} + $S_2O_8^{2-}$ - 80min UV-B 900 Wm^{-2} - 40°C - $1.8 \cdot 10^5$ M (Fe^{2+} - HSO_5^- - $S_2O_8^{2-}$)	*E. coli*	10^6	Total Total	[78]
Photochemical disinfection	SODIS (26.38-44.44 Wm^{-2}) -55 min Solar + 0.5 mM $S_2O_8^{2-}$ - 20 min	*E. coli* / *E. faecalis*	10^6	Total / 1.5 Total / 4.2	[79]
Photochemical disinfection	UV-C (8W - 254 nm – 2.3 µW cm^{-2}) - 60 s UV-C + 1mM $S_2O_8^{2-}$ - 60 s UV-C + 1mM H_2O_2 - 60 s	*K. pneumoniae*	$5 \cdot 10^6$	Total Total Total	[80]
Photocatalysis	0.97 $mWcm^{-2}$ + 0.1 g l^{-1} TiO_2 / 1.98 $mWcm^{-2}$ + 0.1 g l^{-1} TiO_2 40 min - 365nm UV-LED	*E. coli*	-	4.3 / 5	[93]
Photocatalysis	$Ag_2C_2O_4$+TiO_2 Visible light (300W – $\lambda > 400$nm - 16mWcm^{-2}) - 40 min	*E. coli*	$2 \cdot 10^5$	Total	[94]
Photocatalysis	Carbon modified 0.1 g l^{-1} TiO_2-F-1 %-100 50 min (UV-A) / 70 min (ASL)	*E. coli*	$1.5 \cdot 10^6$	Total Total	[95]

Table 2.1. (Cont.) Technologies for pathogen removal from water sources.

Technology	Operation parameters	Bacteria	Bacteria$_0$ (CFU/ml)	Bacteria removal [Log reduction]	Ref.
Photocatalysis	0.5 g l^{-1} g-C_3N_4@Co-TiO_2 (CNCT-3) 90 min - Xe Lamp (300W - 420 nm)	*E. coli*	10^6	Total	[96]
Photocatalysis	0.5 g l^{-1} 1at. % (Ce-TiO_2 / B-TiO_2) - 180 min - Sunlight	*E. coli*	10^8	1.30 / 6.42	[99]
Photocatalysis	0.5 mg ml^{-1} Cu-MoS_2-Bi_2S_3 Light bulb (18W – $\lambda > 400$nm) – 60 min	*E. coli*	$8 \cdot 10^6$	Total	[107]
Photocatalysis	Bi_2MoO_6/Ag-AgCl Light (300W – $\lambda > 420$nm) - 30 min	*E. coli*	10^7	Total	[108]
Photocatalysis	G-C_3N_4 nanosheets (CNNS) / Ag-AgBr-CNNS-5 200 mg l^{-1} - 120min - Light (20 mWcm^{-2} - 420 nm)	*E. coli*	$8.9 \cdot 10^7$	0.64 / Total	[109]
Photocatalysis	18.7 µg ml^{-1} Ag-Fe_2O_3-ZnO - Visible light – 60 min	*E. coli*	$3 \cdot 10^7$	Total	[110]
Photocatalysis	AgBr/g-CeN_4-5 molar ratio) 150 min - 15 µg l^{-1} Ag^+ - light (300W - 13 Wcm^{-2} - 420 nm)	*E. coli*	$5 \cdot 10^7$	4.8	[111]
Photocatalysis	g-C_3N_4 (CN) / $MgTi_2O_5$ (MTO) / MTO-CN 4h - Xenon lamp (300W - 400 nm - 1000 Wm^{-2})	*E. coli*	$4 \cdot 10^7$	0 / 0 / Total	[112]
Piezo-Photocatalysis	Poled $BaTiO_3$ (BA) / BA + Vib + UV 30 min - 8Hz - UV (20 mW cm^{-2} - 375 nm)	*E. coli*	-	0.25 / Total	[113]
Metal-free Photocatalysis	6 wt% BP-CN - 60 min - UV (300W - $\lambda < 400$nm)	*E. coli*	10^7	Total	[116]

Table 2.1. (Cont.) Technologies for pathogen removal from water sources.

Technology	Operation parameters	Bacteria	Bacteria$_0$ (CFU/ml)	Bacteria removal [Log reduction]	Ref.
Metal-free Photocatalysis	Light + Polyethylenimine (PEI) + C_3N_4 (0.1 g l^{-1}) Simulated Solar Light 150 mW cm^{-2} - 45 min	*E. coli* *E. faecalis*	$2 \cdot 10^6$	Total / 3.6	[117]
Glow discharge plasma	Anode: platinum wire Cathode: stainless steal 500 V – 100 mA – 15 min	*E. coli*	10^6	4.7	[120]
Electrochemical Oxidation	Voltages (1-5 V) - HRT (1-10s) 1 cm diameter carbon fiber felt electrodes	*E. coli* Fecal coliform *E. faecalis* *B. subtilis*	[10^6-10^7]	Total Total Total Total	[128]
Electrochemical Oxidation	1.8 $m^3h^{-1}m^{-2}$ - 1V 1 cm diameter PDA-CuONW-Cu_24 (2h) Electroporation disinfection cell	*E. coli*	10^6	Total	[136]
Electrochemical Oxidation	1500 ml min^{-1} - 10V 200 nm diameter C/Cu_2O-AgNPs electrodes Electroporation disinfection cell	*E. coli* *S. aureus*	10^4	Total 2	[137]
Electrochemical Oxidation	0.3 A - 0.3 A h l^{-1} 113 mm^2 DDB electrodes MIKROZON cell	Total coliforms *P. aeruginosa*	$5.5 \cdot 10^5$ $2.7 \cdot 10^6$	Total 6	[140]
Solar Photo-EO	20 mA - 180 min 17.5 cm^2 Ti-RuO_2 anode - RVC cathode UV 25-835 W m^{-2}	*E. coli*	$3 \cdot 10^6$	Total	[144]
Photo-EO	30 cycles - 10 min - 1V – UV 2.5 $mWcm^{-2}$ 352 nm self-doped TiO_2 nanotubes (cathode)	*E. coli*	10^5	3	[145]

Table 2.1. (Cont.) Technologies for pathogen removal from water sources.

Technology	Operation parameters	Bacteria	Bacteria$_0$ (CFU/ml)	Bacteria removal [Log reduction]	Ref.
Photo-Electrocatalysis	5 mA - 10s TiO_2 nanotubes as photoanodes (λ=356 nm)	*E. coli*	10^5	Total	[146]
Electro-Fenton	3g GAC 100 mA + 0.2m M $FeSO_4$ (300 min)	*E. coli*	10^8	Total	[150]

2.2.2. Disinfection technologies for the treatment of wastewater

Wastewater is a very complex matrix of different organic and inorganic compounds which can be toxic and difficult to degrade. The wide range of wastewater sources consists of urban and industrial streams. Urban wastewater is generated from households, recreational areas, sanitary facilities, and all other sources that end up being mixed with these effluents. The composition of industrial wastewater depends on the type of industrial activity and, the number of different pollutants such as heavy metals, pharmaceutical products, dyes, toxic compounds derived from chlorine, nitrogen, phosphorus or sulphur… is practically endless [151]. The solid fraction of wastewater is generally made of a high percentage of volatile matter and medium to low content in fixed carbon, depending on the mineral content of the feedstock [152-156]. Inorganic compounds found in wastewater are mainly fluorides, chlorides, sulphates, nitrates phosphates or ammonium, among others.

Wastewater also contain microorganisms from human or animal urine and faeces, representing an environmental threat [157-160]. For this reason, disinfection technologies must assure the killing of pathogens in these effluents before discharge. A wide variety of processes have been tested in the last years for this purpose and the most significant disinfection technologies for different wastewater matrices during the years 2018-2020 are summarized in Table 2.2. Conventional technologies may represent a suitable alternative for practical applications, due to the large volumes of wastewater that need to be treated every day [161]. These conventional processes comprise bioreactors, wetland systems, UV light irradiation or solar disinfection among others.

The use of sequencing batch biofilter granular reactors (SBBGRs) has been tested for wastewater disinfection. This technology is based on a submerged biofilter in combination with a granular sequencing reactor that operates under batch conditions, showing a high filtering capacity [162]. The use of an innovative SBBGR was evaluated for the disinfection of sewage to be reuse for irrigation by De Sanctis et al. [163]. This process achieved average log reductions of 2.9 and 1.6 for *E. coli* and *Clostridium perfringens* (*C. perfringens*), respectively. Nonetheless, a subsequent sand filtration

stage was also required to improve the disinfection performance and to guarantee the quality of the treated effluent within the standards that reclaimed water must satisfy to be reused in agricultural activities in several countries.

On the other hand, wetlands are low operational and maintenance cost systems for wastewater disinfection. This technology combines different processes such as filtration, sedimentation, oxidation, oxygen release, production of bacteriological compounds, retention in biofilms, aggregation or competition for limiting nutrients which promote the removal of ARB [164]. Constructed wetlands (CWs) are semi-aquatic ecosystems with a large population of microorganisms and vegetation that proliferate in the environment, promoting physical-chemical reactions able to degrade contaminants [165]. Kaliakatsos et al. [166] tested the application of a CW system for wastewater disinfection, finding that the process was able to remove around 99 % of the bacteria present in wastewater (2-log reduction) in 14 days. Another interesting approach of wetlands for disinfection purposes was proposed by González et al. [167], who combined a wetland system with the irradiation of UV light. The coupling of both technologies improved the disinfection efficiencies of the constructed wetland up to 2.03-log reduction of faecal coliforms in 3-7 days. However, bacteria regrowth was observed around 27.8 % under visible UV light irradiation which represents an important drawback of the technology. This behaviour has been previously reported in literature where it has been checked that the damage caused on bacteria by UV light irradiation can be repaired after relative small times, promoting bacteria regrowth [168, 169].

The combination of biological processes with other treatment technologies has become a suitable choice for improving disinfection efficiencies. Bellucci et al. [170] tested the coupling of a microalgae-based reactor with the traditional UV disinfection process. The combined effect of microalgae (disinfectant and nutrient removal agent) together with the irradiation of UV light achieved around 5 log reduction of *E. coli* after a 48 h treatment.

However, the energy requirements for the implementation of light irradiation systems can also limit the applicability of these technologies due to the energy costs. To

overcome this limitation, the use of solar light irradiation has become an excellent alternative for wastewater disinfection. It is a well-known and broadly used technology which consists in the direct application of solar light to wastewater, although the inactivation process is complex because it depends on both exogenous and endogenous microbial inactivation pathways [171-173]. Solar disinfection has been recently studied for wastewater treatment by Voumard et al. [174]. They reported that the irradiation of solar light led to an *E. coli* removal percentage of 99.99 % (4-log reduction) in 1.7 h. This study also highlighted the possible risks for human health related to an incomplete killing of microorganisms.

One of the novel approaches for reducing ARB in wastewaters is the use of metal-exchanged natural zeolites. Zeolites are natural aluminosilicate minerals that show a high cation-exchange affinity, yielding materials with antibacterial properties. Ivankovic et al. [175] reported the disinfection of urban treated wastewater using a metal-exchanged zeolite clinoptilolite enriched with silver (AgNZ) in a bead filter system. This technology achieved the complete removal of an antibiotic-resistant *Acinetobacter baumannii* (*A. baumannii*), using a glass column filled with 5 g of AgNZ with a retention time of 4 min.

Recent advances in the development of nanomaterials have aroused the interest of the scientific community for their application in wastewater treatment [176, 177]. Magnetic nanoparticles have inherent disinfection capabilities which are directly related to the nanoparticle type and doses, contact times or effluent contamination levels [178]. Najafpoor et al. [179] tested the use of silver loaded magnetic nanoparticles (Ag-MNPs) for disinfection purposes. The nanomaterial performance was evaluated for the removal of total and faecal coliforms, and heterotrophic bacteria, reaching around 1-log reduction for all microorganisms. This study proved that the doping of Ag ions onto magnetic nanoparticles improved the magnetic properties and enhanced the disinfection removal rates of the nanocomposites. The synthesis and investigation of a novel magnetic nanostructure for the disinfection of wastewater was reported by Khazaei et al. [180]. They synthesized the nanomaterial by anchoring sodium dichloroisocyanurate (NaDCC) on the nano-Fe_3O_4@SiO_2@$Si(CH_2)_3Cl$ surface. NaDCC acted as a chlorine

reservoir with high disinfectant capacity. The process reached the complete removal of *E. coli* from wastewater which revealed that the Fe_3O_4@SiO_2@$Si(CH_2)_3$@DCC nanostructure was a clean and efficient disinfectant.

In recent years, ferrate (Fe(VI)) have emerged as a novel oxidizing agent with remarkable disinfectant capabilities for wastewater treatment [181-183]. Ni et al., studied the performance of Fe(VI) for the removal of intracellular ARGs from a secondary effluents of a WWTP [184]. They tested 15 ARGs which were frequently detected in wastewater and they also included the class 1 integron (*int*I1) because of its critical role in horizontal gene transfer. Results showed that the reduction in the 15 genes and *int*I1 studied ranged from 1.1-log to 4.37-log for 10 mg Fe(VI) l^{-1}. The combined effect of DNA damage induced by Fe(VI) and coagulation initiated by Fe(VI) reduction products was the main mechanism for ARGs removal (Figure 2.6).

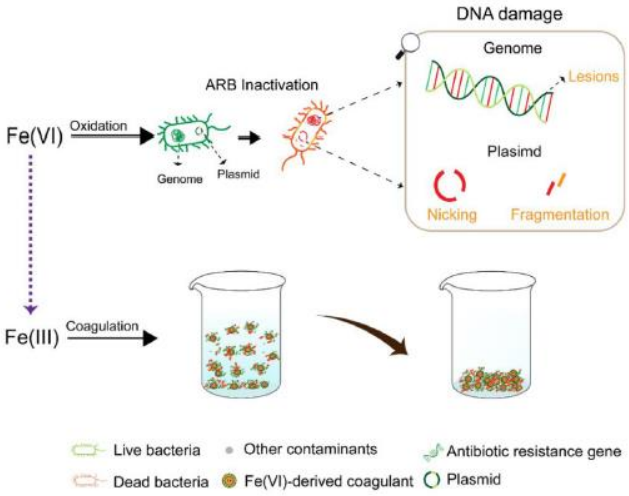

Figure 2.6. Schematic diagram representing the mechanisms of ARG/integrons removal in the wastewater through Fe(VI) treatment. Reprinted with permission from [184]. Copyright 2020 Elsevier.

The main drawbacks of most of conventional treatments for killing pathogens in wastewater are the low efficiencies and the limitations in achieving the complete disinfection of the effluents, which can lead to bacterial regrowth and the proliferation of ARB into the environment. To overcome these limitations, the application of AOPs for wastewater disinfection has been widely studied in the last decades since these

processes promote the generation of large amounts of free radicals that favour the removal of microorganisms [68, 185]. Homogeneous AOPs based on the generation of hydroxyl or sulfate radicals are promising technologies due to the strong oxidative power of these species. Xiao et al. [186] tested the use of a zerovalent iron/peroxydisulfate (ZVI/PS) process for wastewater disinfection. In an air-saturated PS solution, ZVI was oxidized to generate Fe^{2+} (Equation 2.17-2.19) and, consequently, Fe^{2+} activated PS to form sulfate radicals ($SO_4^{\bullet-}$) (Equation 2.20) in the solution.

$$2Fe^0 + O_2 + 2H_2O \rightarrow 2Fe^{2+} + 4OH^- \quad (2.17)$$

$$2Fe^0 + O_2 + 4H^+ \rightarrow 2Fe^{2+} + 2H_2O \quad (2.18)$$

$$2Fe^0 + S_2O_8^{2-} \rightarrow Fe^{2+} + 2SO_4^{2-} \quad (2.19)$$

$$Fe^{2+} + S_2O_8^{2-} \rightarrow SO_4^{\bullet-} + SO_4^{2-} + Fe^{3+} \quad (2.20)$$

Sulfate radicals were responsible for initiating a series of oxidative reactions on the cell membranes that affected its permeability (Figure 2.7). Results showed the loss of integrity in the wall/cell structures after 0, 40 and 80 min of ZVI/PS treatment, resulting in leakage of cytoplasm. The morphological changes observed in *E. faecalis* were similar to that of *E. coli*.

Likewise, the removal of ARGs in a secondary effluent was studied by Gao et al., using sodium persulfate activated by a nanoscale zero valent iron modified by *Ginkgo biloba L.* (G-NZVI) catalyst [187]. They selected bacterial 16S rRNA gene, eight ARGs and two mobile genetic elements as target pollutants. Four resistance mechanisms were present among the ARGs selected, including efflux (*tet*E and *mex*F), deactivate (bla_{TEM}, *cat*A1 and *aac*), protection (*tet*W and *van*G) and unknown (*qnr*S). Class 1 integron-integrase gene (*int*I1) and the conjugative transposon Tn916-Tn1545 family (*Tn916/1545*) were selected as mobile genetic elements. Results showed that 98.6 % (1.85 log) bacterial 16S rRNA gene was removed within 10 min and the removal efficiency of target ARGs and other mobile genetic elements decreased in the following order: *Tn916/1545=aac* (below the detection limit) > *int*I1 (99.99 %) > *tet*E (99.64 %) > *mex*F (99.10 %) > *tet*W (94.57 %) > *qnr*S (90.18 %) > *van*G (82.21 %) > bla_{TEM} (64.15 %) > *cat*A1 (23.13 %).

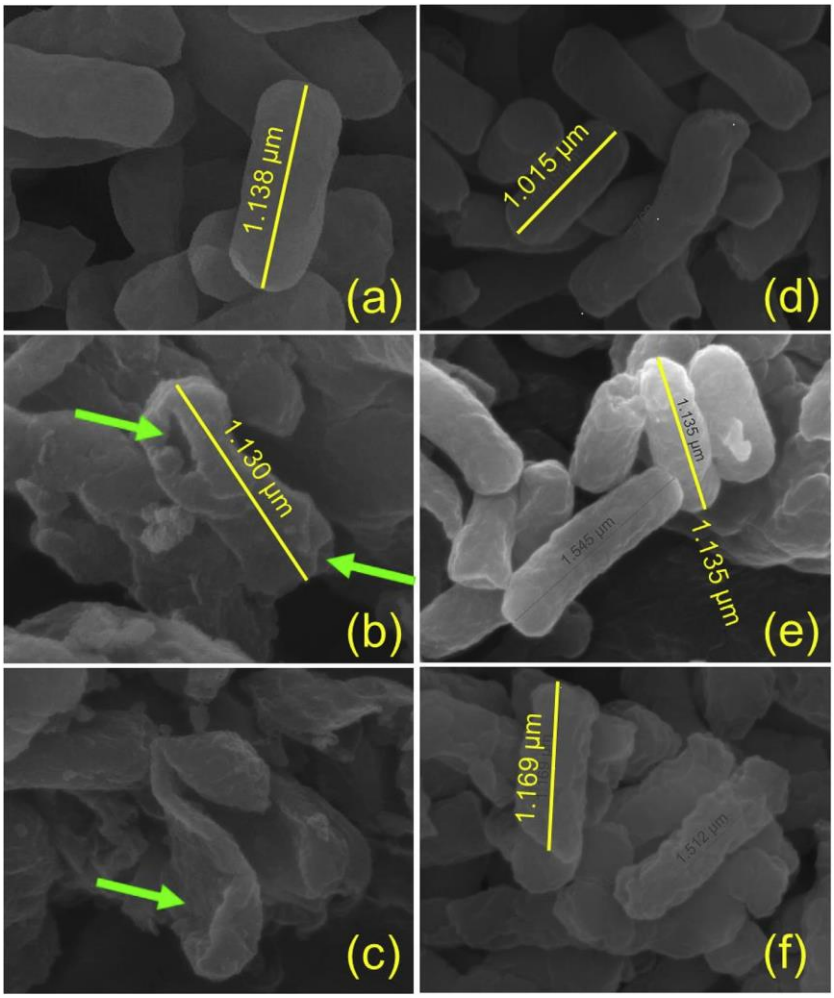

Figure 2.7. The morphological images of *E. coli* ($1.07x10^7$ CFU ml^{-1}) treated with ZVI/PS for (a) 0 min, (b) 40 min, (c) 80 min, and UV for (d) 0 s, (e) 20 s, (f) 40 s. The arrow indicates the deformation, pore–forming, and fracture of cells damaged by $SO_4^{\bullet-}$. Reprinted with permission from [186]. Copyright 2020 Elsevier.

Another homogeneous AOP that has been recently tested for the removal of *E. coli* and *Pseudomonas spp* in wastewater is catalytic ozonation [188]. This technology can also be considered as heterogeneous AOP if metals are added as dispersed solid oxides. Malvestiti et al. studied different metal ions (Fe^{2+}, Co^{2+} and Al^{3+}) to enhance the generation of powerful radicals with disinfectant capacity in a metal-catalyse ozonation process. The generation of hydroxyl radicals was promoted during the decomposition of O_3 in the presence of Fe^{2+} (Equations 2.21-2.22) [189]. In addition, the interaction of

ozone and water is well known to produce hydrogen peroxide (Equation 2.23) [190], which, subsequently can react with Fe^{2+} in the Fenton process (Equations 2.3-2.4) to generate hydroxyl radicals.

$$Fe^{2+} + O_3 \rightarrow FeO^{2+} + O_2 \quad (2.21)$$

$$FeO^{2+} + H_2O_2 \rightarrow FeO^{3+} + HO^{\bullet} + OH^{-} \quad (2.22)$$

$$O_3 + H_2O \rightarrow H_2O_2 + O_2 \quad (2.23)$$

Cobalt interacted directly in the presence of O_3 promoting the generation of hydroxyl radicals (Equations 2.24-2.26) [188].

$$Co^{2+} + O_3 + H_2O \rightarrow Co(OH)^{2+} + O_2 + HO^{\bullet} \quad (2.24)$$

$$HO^{\bullet} + O_3 \rightarrow HO_2^{\bullet} + O_2 \quad (2.25)$$

$$HO_2^{\bullet} + Co(OH)^{2+} \rightarrow Co^{2+} + H_2O + O_2 \quad (2.26)$$

Results showed that the inactivation process of both pathogens increased its efficiency up to 20 % with the use of 1 mg l^{-1} of Fe^{2+}, Co^{2+} and Al^{3+} and up to 40 % with 10 mg l^{-1} Fe^{2+} compared with single ozonation. Cellular adenosine triphosphate (ATP) was measured as an indirect indicator for disinfection. This molecule is used as a carrier of free energy and phosphate groups, which are directly involved in microbial activity [191]. The decrease of cellular ATP followed the same trend than that previously observed for pathogens inactivation. This study concluded that the presence of metal ions improved ozone disinfection performance, further increasing its efficiency in the presence of Fe^{2+}.

Within homogeneous photocatalytic AOPs, the PF process is one of the most developed technologies for disinfection and decontamination of wastewater matrices. Many studies have reported the application of PF with UV or solar irradiation for the inactivation of waterborne pathogens including *E. coli*, *S. enteritidis*, faecal coliforms or *P. aeruginosa* [192-195]. The efficiency of the PF process for the complete removal of ARB in wastewater matrices was successfully proven in these works. Nahim-Granados et al. [194] studied the inactivation of *E. coli* and *S. enteritidis* in synthetic fresh-cut wastewater by different solar based processes at pH values around 6. Results

showed that PF was able to reach the complete removal of both microorganisms in less than 30 min, using 2.5 mg l^{-1} Fe^{2+} and 5 mg l^{-1} H_2O_2. A similar disinfection behaviour was observed during the single solar photo-inactivation and, the best disinfection rates were obtained during the H_2O_2/Solar UV process. This was attributed to the limitations of the PF process when working at neutral pHs. Michael S.G. et al. [195] tested the solar PF process for the removal of ARB and ARGs from wastewater. The use of 5 mg l^{-1} Fe^{2+} and H_2O_2 doses of 18, 30, 40 and 18 mg l^{-1} under solar light irradiation promoted the inactivation of faecal coliforms, *Enterococcus spp.*, total heterotrophs and *P. aeruginosa*, respectively, avoiding undesirable bacteria regrowth. ARGs showed different performances and, their complete elimination was not achieved during the process. For instance, bla_{TEM} genes, whose resistance is associated to β-lactamases, were persistent after treatment. Di Cesare et al. studied the removal of antibiotic resistance determinants (16S rRNA, ARGs and *int*I1 gene) and pathogenic bacteria by a photo-Fenton like process (UV-C/H_2O_2/Cu-IDS) using an iminodisuccinic acid (IDS-Cu) complex as catalyst [196]. Results showed that the UV-C/H_2O_2/Cu-IDS process working under neutral pH conditions was more effective than the UV-C/H_2O_2 process in terms of bacterial removal. This was mainly attributed to the reaction of Cu^{+} and Cu^{2+} with H_2O_2 and the subsequent generation of hydroxyl radicals [197]. However, the UV-C/H_2O_2 process was more effective in decreasing the relative abundance of *int*I1 and *tet*A genes after a 24h storage in human pathogens favorable conditions (37ºC in rich medium, LB broth), which highlights the need of further investigation of the UV-C/H_2O_2/Cu-IDS process under more intensive operational conditions.

The irradiation of UV light to solutions containing powerful oxidants such as H_2O_2, HSO_5^-, $S_2O_8^{2-}$ or ClO^- promotes their photoactivation, favouring the generation of free radicals (Equations 2.9, 2.14, 2.15, 2.27) [198]. The role of these radicals in the disinfection of wastewater matrices has been reported in literature which significantly influence the inactivation of microorganisms, reaching a complete removal of ARB models such as *E. coli*, *E. faecalis* or *K. pneumoniae* [79, 80, 199-201].

$$ClO^- + h\nu \rightarrow O^{\bullet -} + Cl^{\bullet} \quad (2.27)$$

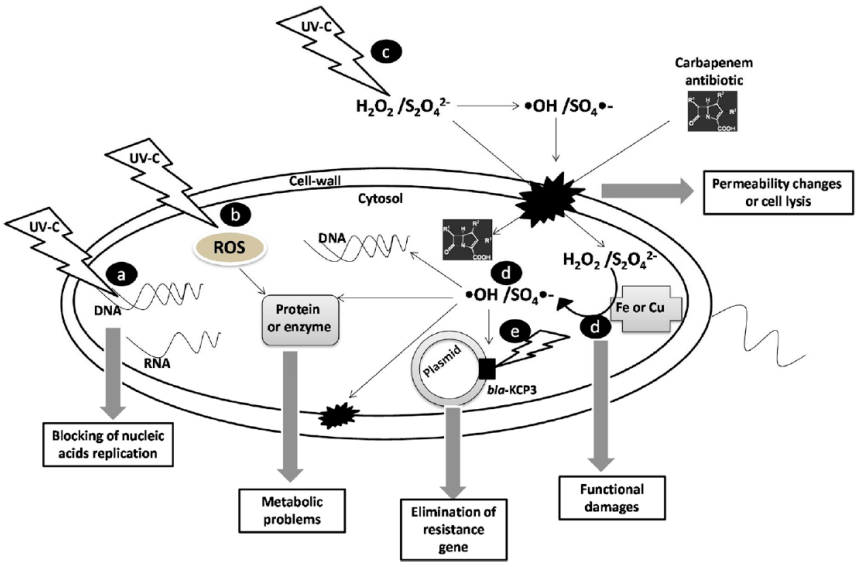

Figure 2.8. Proposed pathways for the inactivation of carbapenem resistant *Klebsiella pneumoniae* (CR-kp). Reprinted with permission from [80]. Copyright 2020 Elsevier.

The inactivation mechanisms of *K. pneumoniae* under photoactivated $S_2O_8^{2-}$ and H_2O_2 have been proposed by Serna-Galvis et al. (Figure 2.8): 1) DNA and RNA damage by UV-C, 2) degradation of proteins and enzymes by ROS, 3) modifications in membrane and cell-wall by photogenerated hydroxyl or sulfate radicals, 4) iron and cooper naturally contain in bacteria can react with H_2O_2 or $S_2O_8^{2-}$ to produce $^{\bullet}OH$ and $SO_4^{\bullet-}$, inducing bacterial death, 5) DNA plasmids can experiment dimerization reactions promoted by UV-C light [80]. The disinfection was achieved under an exposure time of 180 s using 1 mM of $S_2O_8^{2-}$ or H_2O_2.

Other studies have proposed the irradiation of UV-A light to favour the generation of radicals during disinfection processes, although the removal rates are lower than that obtained when using UV-C light. Rodriguez-Chueca et al. [200] reported the inactivation of *E. coli* under UV-A irradiation and its combination with $S_2O_8^{2-}$ and HSO_5^- to promote the generation of ROS. Results showed that a negligible disinfection was achieved by single photolysis with UV-A light. However, the photoactivation of 1 mM $S_2O_8^{2-}$ led to the total inactivation of *E. coli* in 30 min whereas a decrease around 2.2-log was achieved during a 90 min treatment with 1 mM HSO_5^-. These different behaviours were explained by the different production of radicals: hydroxyl and

sulphate radicals were generated during the photolysis of HSO_5^- (Equation 2.14) but large amounts of sulphate radicals were produced during the photoactivation of $S_2O_8^2$ (Equation 2.15). Michael et al. tested the UV-C/H_2O_2 and sunlight/H_2O_2 processes in a pilot scale to remove antibiotics, bacteria, ARB, 16S rRNA and ARGs [202]. Results showed that both processes were able to inactivate *E. coli* and *P. aeruginosa* with the use of 5 mg l^{-1} H_2O_2 and 0.06 kJ l^{-1} UV-C for the UV-C/H_2O_2 process and 30 mg l^{-1} H_2O_2 with 16-20 kJ l^{-1} for the sunlight/H_2O_2 process. However, bacterial regrowth occurred after a 48h storage for the treated samples with sunlight/H_2O_2 process. In addition, by increasing the treatment until 90 min and the UV-C irradiation until 0.8 kJ l^{-1}, the UV-C/H_2O_2 process attained 2.4 log reduction for 16S rRNA, 3.7 log reduction for bla_{OXA}, bla_{SHV}, bla_{TEM} and *qnr*S, 2.3 log reduction for *tet*M, 2.2 log reduction for *sul*1 and 2.1 log reduction for *sul*2. Likewise, logarithmic reductions of 0.8, 0.3, 1.7, 0.7, 1.6, 1.4, 0.8 and 1.0 for 16S rRNA, bla_{OXA}, bla_{SHV}, bla_{TEM}, *qnr*S, *tet*M, *sul*1 and *sul*2, respectively, were reached during the sunlight/H_2O_2 process after 300 min and 42 kJ l^{-1} of sunlight irradiance. Thus, the UV-C/H_2O_2 process was observed to attain higher log reduction values of ARGs than the sunlight/H_2O_2 process. However, these results still confirmed that both processes are not suitable to avoid the spread of ARGs into the environment.

Heterogeneous AOPs are based on the use of a solid catalyst to promote the generation of free radicals in wastewater. Solid semiconductor materials can be photoactivated by the irradiation of UV light, promoting the generation of ROS in wastewater that favour the killing of microorganisms [203, 204]. These heterogeneous photocatalytic processes have been widely studied for the disinfection of wastewater sources in literature [205-208]. Three different TiO_2 based materials were tested by Martín-Sómer et al. [209] for the removal of total aerobic bacteria in a real wastewater effluent. The higher disinfection rates were obtained with the use of commercial TiO_2 Evonik P25 as photocatalyst, reaching around 3.6-log reduction when 3.8 E/L of accumulated radiant energy were applied. The use of other TiO_2 based materials led to less than 2-log reduction units of total anaerobic bacteria. The development of other photocatalysts non-based on TiO_2 have been also carried out for wastewater

disinfection. A novel cerium-doped zinc oxide (Ce-ZnO) photocatalyst was compared with the commercial TiO_2-P25 for the disinfection of real wastewater by Zammit et al. [210]. The concentration of *E. coli* was completely inactivated and *P. aeruginosa* was reduced in more than 4-log units with Ce-ZnO photocatalyst in 180 min. Results obtained for both microorganisms with this novel material were more than 2-log units higher than those achieved when using commercial TiO_2-P25.

As discussed in section 2.1., EAOPs are a promising alternative for improving the disinfection efficiencies of AOPs. Specifically, EO is one of the most widespread technologies employed for wastewater treatment. During EO, oxidation and reduction reactions take place on the anode and cathode surface, respectively. The high concentration of inorganic ions contained in wastewater leads to the generation of disinfectant species such as hypochlorite (Equations 2.28-2.30) [211], hydroxyl radicals (Equation 2.31) [212], hydrogen peroxide (Equations 2.32-2.34) [213, 214], or ozone (Equations 2.35-2.36) [215, 216] that significantly contribute to bacteria removal [131, 217].

$$2Cl^- \rightarrow Cl_2 + 2e^- \quad (2.28)$$

$$Cl_2 + H_2O \rightarrow HClO + Cl^- + H^+ \quad (2.29)$$

$$HClO \leftrightarrow H^+ + ClO^- \quad (2.30)$$

$$H_2O \rightarrow OH^\bullet + H^+ + e^- \quad (2.31)$$

$$OH^\bullet \rightarrow O^\bullet + H^+ + e^- \quad (2.32)$$

$$2O^\bullet \rightarrow O_2 \quad (2.33)$$

$$2OH^\bullet \rightarrow H_2O_2 \quad (2.34)$$

$$H_2O_2 \rightarrow O_2 + 2H^+ + 2e^- \quad (2.35)$$

$$O_{2\,+}\, O^\bullet \rightarrow O_3 \quad (2.36)$$

The presence of organic compounds in wastewater may affect the efficiency of the electrochemical disinfection process since the disinfectant species generated can degrade these organic compounds, promoting competitive oxidative reactions between

bacteria and organics [218]. The EO process is significantly influenced by the anodic material employed and the current density [219]. Several materials may be suitable as anodes but BDD and MMO are more extensively used for wastewater disinfection processes [130, 220]. Li et al. [221] tested the electrochemical disinfection with BDD anodes for the removal of heterotrophic bacteria. The application of 20 mA cm^{-2} led to a 3.8-log reduction of bacteria, reaching almost the complete disinfection of the effluent. This process was also able to reduce the relative abundance of ARGs, which was mainly attributed to the different amounts of free chlorine and hydroxyl radicals generated. They studied the removal efficiency of 23 ARGs that confer resistance to 8 classes of antibiotics with different operational conditions. Results showed a total removal rate of ARGs of 56 % after 5 min at a current density of 80 mA cm^{-2}, meanwhile the total removal rate of ARGs decreases below 47 % after 20 min at a current density of 20 mA cm^{-2}, when 99 % inactivation was achieved by both treatments.

On the other hand, Rajasekhar et al. [222] evaluated the EO process with a Ti/Sb-SnO_2/PbO_2 anode for wastewater disinfection. This novel electrode consists of a Ti substrate, an interlayer made of Sb-SnO_2 and an outer layer of PbO_2. Results showed that the complete removal of $2 \cdot 10^5$ UFC ml^{-1} coliforms was achieved at applied current densities of 30 mA cm^{-2}. In addition, it was also confirmed the complete destruction and morphological changes of bacterial cells by SEM analysis.

One of the major challenges to be faced by electrochemical technologies is their scale-up, being many of the works described in this review at lab or bench scale. Cotillas et al. [223] studied the scale-up of an integrated electrodisinfection-electrocoagulation (ED-EC) process with BDD anodes and iron bipolar electrodes for the reclamation of urban treated wastewater. This process was operated in continuous mode and achieved the complete disinfection of urban treated wastewater at low applied electric charges (0.1 kAh m^{-3}). In-situ electrogenerated free and combined chlorine species were the main responsible for disinfection whereas iron coagulant species electrodissolved led to an efficient turbidity removal. This work supports the idea that the scale-up of electrochemical technology is possible and, an efficient and environmentally friendly disinfection process can be achieved.

Table 2.2. Technologies for pathogen removal from wastewater sources.

Technology	Operation parameters	Bacteria	acteria$_0$ (CFU/ml)	Bacteria removal [Log reduction]	Ref.
Sequencing batch biofilter granular reactor	240 l day^{-1} / 6h / 15-20 mg l^{-1} O_2	*E. coli* *C. perfringens*	$1.2 \cdot 10^4$ $4.9 \cdot 10^3$	2.9 1.6	[163]
Wetland system	HSSF - 1.4 m^{3}d^{-1} - HRT 14 days	Total coliforms *E. coli* Enterococci	$2.4 \cdot 10^4$ $4.7 \cdot 10^4$ $1.6 \cdot 10^4$	1.7 2.2 1.9	[166]
Wetland system + UV	30 mJ cm^{-2} / 0.4 m^3 h^{-1} / 3-7 d HRT / Winter	Total coliforms Fecal coliforms Somatic coliphages	$5.3 \cdot 10^4$ $7.1 \cdot 10^4$ $1.2 \cdot 10^5$	2.53 2.03 1.22	[167]
Photobioreactor	Algal suspension + Light (6x30W - 111 µmol m^{-2} s^{-1}) - 48 h	*E. coli*	-	5	[170]
Solar disinfection	1200 Wm^{-2} - 1.7 h	*E. coli*	10^6	4	[174]
Metal-exchanged natural zeolites	Natural / Copper / Silver Zeolite 5g of Zeolite – HRT 4 min - 30 ml h^{-1}	*A. baumannii*	10^3	0 / 0.38 / Total	[175]
Chemical disinfection	Ag-MNPs - 105 mg l^{-1} MNP - 70 min Magnetic nanoparticles (MNP)	Total coliforms Fecal coliforms Heterotrophic bacteria	-	0.68 0.51 0.61	[179]
Chemical disinfection	Nano structure Fe_3O_4@SiO_2@$Si(CH_2)_3$@DCC - 50 min	*E. coli*	-	Total	[180]
Chemical disinfection	FeO_4^{2-} (10 mg Fe l^{-1})	Total coliforms Fecal coliforms	-	3	[184]

Table 2.2. (Cont.) Technologies for pathogen removal from wastewater sources.

Technology	Operation parameters	Bacteria	Bacteria$_0$ (CFU/ml)	Bacteria removal [Log reduction]	Ref.
Persulfate activation	3mM $S_2O_8^{2-}$ + 0.6g l^{-1} ZVI - 80 min 1mM $S_2O_8^{2-}$ + 0.2g l^{-1} ZVI - 12min	*E. coli* *E. faecalis*	10^7	0.8 0.6	[186]
Persulfate activation	$S_2O_8^{-2}$ / NZVI – 10 min $S_2O_8^{-2}$ / G-NZVI – 10 min 2.5 g l^{-1} NZVI / G-NZVI – 20 g l^{-1} $S_2O_8^{-2}$	16S rRNA	-	1.85	[187]
Catalytic ozonation	O_3 / Fe^{2+} / Co^{2+} / Al^{3+} / 10 mg l^{-1} Fe^{2+} O_3 (0.2 l min^{-1} - 10 mg l^{-1}) - 20 mg l^{-1} O_3 transformation 1 mg l^{-1} (Fe^{2+} / Co^{2+} / Al^{3+})	*E. coli* *Pseudomonas spp.*	$2.1 \cdot 10^4$ $2.8 \cdot 10^3$	2.5 / 3.3 / 3.2 / 2.8 / 4.2 1.7 / 2.3 / 2.4 / 2.2 / 3.0	[188]
Photo-Fenton	0.36 mM $FeSO_4$ + 1.47 mM H_2O_2 – 40 min 0.1 mM Fe^{3+}- EDDS (1:1) + 0.88 mM H_2O_2 - 60min UVA 26 W m^{-2}	*E. coli*	$6 \cdot 10^2$	Total Total	[192]
Photo-Fenton	20 mg l^{-1} FeOx (Hematite) - 50 mg l^{-1} H_2O_2 Simulated solar light – 676 W m^{-2} - 120 min	*E. coli*	10^5	Total	[193]
Photo-Fenton	30 W m^{-2} UVA + 2.5/5 mg l^{-1} Fe^{2+}/H_2O_2 (25 min *E. coli* – 27.5 min *S. enteritidis*)	*E. coli* *S. enteritidis*	$5 \cdot 10^5$	Total Total	[194]
Photo-Fenton	18 mg l^{-1} H_2O_2 -90 min 30 mg l^{-1} H_2O_2 - 120 min 40 mg l^{-1} H_2O_2 – 180 min 18 mg l^{-1} H_2O_2 – 30 min Solar UV (30 W m^{-2}) - $[Fe^{2+}]_0$ 5 mg l^{-1} - $[H_2O_2]_0$ 100 mg l^{-1}	Fecal coliforms *Enterococcus spp.* Total heterotrophs *P. aeruginosa*	$9.33 \cdot 10^2$ $5.57 \cdot 10^1$ $8.27 \cdot 10^4$ $1.87 \cdot 10^3$	Total Total Total Total	[195]

Table 2.2. (Cont.) Technologies for pathogen removal from wastewater sources.

Technology	Operation parameters	Bacteria	Bacteria$_0$ (CFU/ml)	Bacteria removal [Log reduction]	Ref.
Photo-Fenton like	UV-C/H_2O_2 /Cu-IDS - 25 min 1.47 mM H_2O_2 - 0.02 mM Cu-IDS UV lamp 4.9 mW cm^{-2}	Total bacteria	$4.10 \cdot 10^7$-$8.75 \cdot 10^8$	0.05 - 0.5	[196]
Photochemical disinfection	Solar light + 1 mM $S_2O_8^{2-}$ - 50 min	*E. coli* *E. faecalis*	10^6	Total 3.7	[79]
Photochemical disinfection	UV-C + 1mM $S_2O_8^{2-}$ / UV-C + 1mM H_2O_2 UV-C (8W - λ=254 nm - 2.3 μW cm^{-2}) - 180 s	*K. pneumoniae*	$5 \cdot 10^6$	Total / Total	[80]
Photochemical disinfection	Cl_2 + UV - 5min Free chlorine 15 mg l^{-1} - UV (λ=275 nm)	*E. faecium*	-	Total	[199]
Photochemical disinfection	UV-A + 1 mM $S_2O_8^{2-}$ – 90 min UV-A + 1 mM HSO_5^- – 30 min UV-A (6W – λ=365 nm - 22.7 min)	*E. coli*	10^5	2.2 Total	[200]
Photochemical disinfection	UV-C + 2 mM (H_2O_2 / $S_2O_8^{2-}$ / HSO_5^-) UV-C (0.45 W m^{-2} - λ=254 nm) - 80 min	*E. coli*	-	6.52 / 6.7 / 6.58	[201]
Photochemical disinfection	UV-C/H_2O_2 (5 mg l^{-1} H_2O_2 - 0.06 kJ l^{-1} - 8 min) Sunlight/H_2O_2 (30 mg l^{-1} H_2O_2 – 16/20 kJ l^{-1} – 120/150 min) UV-C lamp (230W - 254 nm)	*E. coli* / *P. aeruginosa*	$5 \cdot 10^3$	Total / Total	[202]
Photocatalysis	TiO_2 based material – Evonik P25 Accumulated radiant energy (3.8 E/l) - 4h	Total aerobic bacteria	10^6	3.6	[209]

Table 2.2. (Cont.) Technologies for pathogen removal from wastewater sources.

Technology	Operation parameters	Bacteria	$Bacteria_0$ (CFU/ml)	Bacteria removal [Log reduction]	Ref.
Photocatalysis	380 cm^2 Ce-ZnO photocatalyst coated disc UVA 36W - 180 min	*E. coli* *P. aeruginosa*	$1 \cdot 10^4$ $5 \cdot 10^4$	Total 4.3	[210]
Electrochemical Oxidation	20 mA cm^{-2} – 20 min / 80 mA cm^{-2} - 5min 1 cm^2 BDD anode - SS cathode	Heterotrophic bacteria	$2.4 \cdot 10^4$	3.8 / 2.9	[221]
Electrochemical Oxidation	12 cm^2 Ti/Sb-SnO_2/PbO_2 anode - SS cathode 30 mA cm^{-2} - 30 min	Coliform bacteria	$2 \cdot 10^5$	Total	[222]
Electrodisinfection-electrocoagulation	5A m^{-2} (0.1kAhm^{-3}) – 1.6 mmol l^{-1} Fe dissolved 78.5 cm^{-2} BDD anode - SS cathode – 50 l h^{-1}	*E. coli*	$[1.1\text{-}2.2] \cdot 10^1$	Total	[223]

2.2.3. Disinfection technologies for the treatment of sanitary effluents

2.2.3.1. Disinfection of hospital wastewater (HWW)

In last years, concern about HWW treatment has sharply increased in the scientific community due to the complex composition of this type of effluents, including a great variety of drugs and high concentrations of pathogens, viruses, and fungi. HWW greatly affect the loads of contaminants arriving to WWTPs since contain high levels of chemical and biological residues [224-226]. ARB are easily spread among hospitalized patients via air, shower drains and/or the sewage systems as bacteria reservoirs, promoting the occurrence of nosocomial infections [227, 228]. This has led to the search for technological solutions to decrease the impact of HWW into the environment and human health. A review related to disinfection/denaturation treatments reported by Dodd et al. [8] stated that undamaged DNA residues from cellular debris could confer antibiotic resistance to bacterial populations present in the environment by natural transformation and/or transduction, despite ARB were inactivated during the disinfection process. Furthermore, dead bacteria can have intact plasmids which are capable of replicating autonomously within a suitable host [229]. The particular composition of HWW, in terms of pathogens, promotes a rapid vertical and/or horizontal gene transfer. For this reason, disinfection technologies should assure not only the complete removal of microorganisms but also the denaturation of genetic material. Table 2.3 summarizes the most significant disinfection technologies for HWW reported in literature until 2020.

Despite the major challenge posed by HWW, conventional biological and chemical processes have attempted to face its treatment. The use of pilot scale membrane bioreactors (MBRs) were tested by Nielsen et al. [230] for the removal of *E. coli*, total coliforms and total enterococci in HWW. Disinfection rates achieved a maximum of 3.69-log reduction in total coliforms with a 35-day sludge age. The main advantages of MBRs are the lower carbon footprint and the higher ARB removal efficiencies than those obtained with conventional biological processes located at WWTPs. On the other hand, chemical processes are based on the use of ozone or

chlorine for killing pathogens because of their excellent disinfectant properties. Gautam et al. [231] and Fijan et al. [232] evaluated the disinfection of HWW with chlorine and peracetic acid (PA), respectively. The use of 20 mg l^{-1} $Ca(ClO)_2$ achieved disinfection percentages up to 98.5 % in 30 min whereas the addition of 400 mg l^{-1} PA led to the complete removal of *E. faecium* in 15 min. These results point out the bactericidal effect of chlorine and PA for the removal of ARB in HWW. Furthermore, the monitorization of ARGs was studied in three different Hospital WasteWater Treatment Plants (HWWTPs), operating with several physical-chemical processes and a final disinfection stage based on chlorination. Results showed that ARGs removal rates ranged from 0.85 to 2.71 log with maximum decays approximately one order of magnitude observed for *qnr*S, bla_{SHV-1} and bla_{DHA-1} genes. However, HWWTPs were not efficient at removing all ARGs, and the concentration of five β-lactam ARGs (bla_{OXA-1}, bla_{OXA-10}, bla_{DHA-1}, bla_{SHV-1}, bla_{TEM-1}) and two quinolone ARGs (*qnr*A and *qnr*D) were even increased in the treated wastewater [233]. These results prove that an inadequate chlorine dosage can increase ARG concentrations, inducing the formation of more pili for conjugative transfer [234-236].

Disinfection systems based on ozone (E^0: 2.07 V) are highly effective because this species has an oxidation potential higher than other commonly disinfectants such as chlorine (E^0: 1.36 V) or hypochlorite (E^0: 1.49 V) [237]. Chiang et al. [238] studied the disinfection of hospital effluents by ozonation at neutral pH, finding that a complete removal of *P. aeruginosa* was attained with the addition of 3.5 mg O_3 l^{-1}. A similar ozone dosage was able to reduce the population of total coliforms in more than 4-log units.

The influence of pH on bacteria removal was evaluated in cholera treatment centers using hydrated lime (pH 11.4-12.2) and hydrochloric acid (pH 3.7-3.9) during 14 h since extreme values can significantly affect the survival of pathogens [239]. Results from a full-scale process showed that thermotolerant coliforms were removed up to 99.97 % in HWW, being higher the efficiency in acid conditions. Furthermore, treated effluents met the WHO bacteriological guideline values for agricultural reuse (fewer than 1000 CFU/100 ml) [240].

Chemical processes are cost-effective options for the reduction of the hazardousness associated with ARB in sanitary effluents. However, the use of chemicals can promote the occurrence of disinfection by-products due to the presence of organic compounds in HWW which are susceptible to react with chlorine-based disinfectants. These organochlorinated compounds are known to be mutagenic and cancerogenic for humans [241, 242] and, for this reason, the application of AOPs to the disinfection of HWW has been recently tested with the aim of improving disinfection efficiencies and avoiding the disinfection by-products [20, 243, 244].

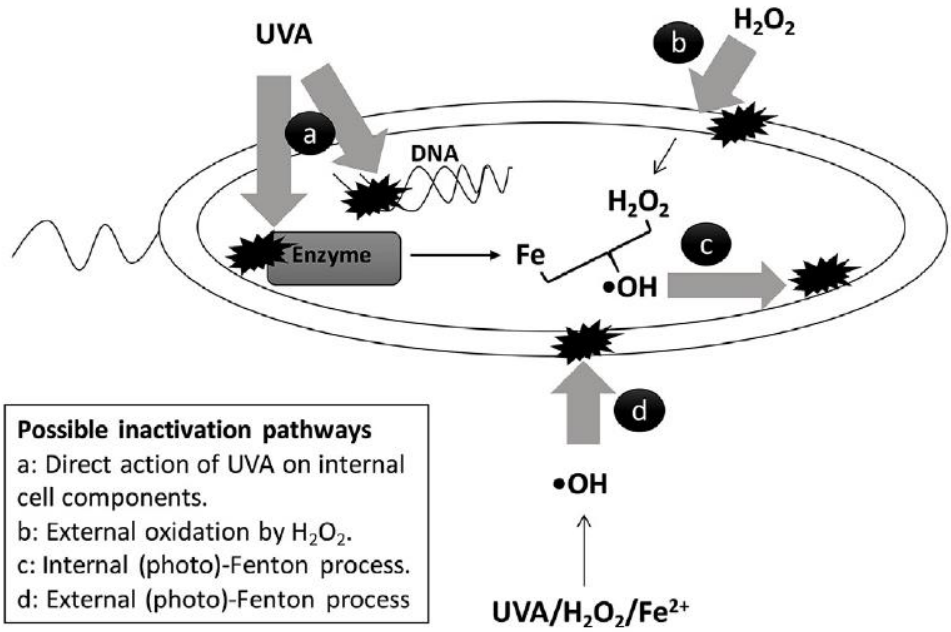

Figure 2.9. Schema of plausible inactivation routes of ARB *K. pneumoniae* during process application. Experimental conditions: V: 150 ml, $pH_{initial}$: 6.5, [Bacteria]: 10^6 CFU ml^{-1}, [Fe^{2+}]: 5 mg l^{-1}, [H_2O_2]: 50 mg l^{-1} and light intensity: 3.9 Wm^{-2}. Reprinted with permission from [245]. Copyright 2019 Elsevier.

Muñoz et al. [246] reported the efficiency of the Fenton process in the removal of total coliforms from real HWW. The process operated under temperatures within the range of 50-90 ºC, obtaining oxalic and formic acids as main by-products. Treated effluents exhibited 4 times less toxicity than the raw wastewater at temperatures higher than 70 ºC. The Fenton process with the irradiation of UVC light (PF) has been also

successfully tested for the complete removal of total coliforms and *E. coli* in HWW [76]. Likewise, Serna-Galvis et al. [245] evaluated the removal of carbapenem-resistant *K. pneumoniae* in HWW by PF, finding that the use of 5 mg l^{-1} Fe^{2+} and 50 mg l^{-1} H_2O_2 under UVA irradiation led to a reduction of 3.3-logs in the concentration of bacteria in 300 min. The addition of 9 µM of citric acid enhanced the PF process until the complete removal of *K. pneumoniae* in 300 min. Furthermore, the replacement of H_2O_2 by 1470 µM $Na_2S_2O_8$ improved the disinfection efficiencies, reaching the bacteria removal in 60 min. They also proposed different possible inactivation routes for *K. pneumoniae* (Figure 2.9): 1) direct action of UVA on internal cell components; 2) external oxidation by H_2O_2; 3) internal PF process, 4) external PF process.

The disinfection of HWW has been also carried out by AOPs based on the photoactivation of chemical oxidants to produce large amounts of free radicals that promote the killing of microorganisms. Luo et al. [247] compared the efficiencies of chemical and photochemical processes for the removal of faecal coliforms in HWW. Results showed that single photolysis was enhanced by the addition of 10 mg l^{-1} of Cl_2 in 0.72 log units, reaching a final decrease in bacteria concentration around 4-log units. Moussavi et al. [248] described two UV-based AOPs for the disinfection of sanitary effluents (10^{10} UFC ml^{-1} of *E. coli*): vacuum UV (VUV) with the addition of hydrogen peroxide (VUV/H_2O_2) and UVC/H_2O_2 process. They found that VUV/H_2O_2 was much more efficient than the UVC/H_2O_2 process since a complete removal of *E. coli* was attained with the first one whereas the irradiation of UVC light promoted a reduction of 6.1-log units. This was mainly attributed to the higher production of free radicals by the photoactivation of H_2O_2 using the VUV lamp ($100 > \lambda > 200$ nm) that emits radiation at wavelengths lower than UVC lamps ($200 > \lambda > 280$ nm). In fact, the molar ratio absorption of H_2O_2 is about 180 $l(mol \cdot cm)^{-1}$ at wavelengths around 200 nm and significantly decreases at 254 nm (19.6 $l(mol \cdot cm)^{-1}$) which is the typical operating value of UVC lamps [249].

Many studies have been focused on the disinfection of complex water matrices contaminated with bacteria and viruses by photodynamic inactivation (PDI) [250, 251]. This technology is based on the action of light on a photosensitizer that leads to the

production of ROS in presence of molecular oxygen, promoting the killing of microorganisms. Almeida et al. [252] tested the PDI technology for the treatment of sanitary effluents contaminated with *E. coli*, *P. aeruginosa*, *A. baumannii* and *S. aureus*. They employed 5 μM of Tetra-Py^{+}-Me as photosensitizer solution and irradiated the samples with white light (380-700nm) during 270 min. Results showed that reductions higher than 6-log units were obtained for each pathogen and for a mixture of the four bacteria.

Ozone is a powerful disinfectant that can be activated by ultrasound, favouring the production of free radicals which improve the disinfection efficiencies of single ozonation and ultrasound irradiation processes [253, 254]. Somensi et al. [255] studied the removal of total coliforms and DNA denaturation efficiency in sanitary effluents by O_3 and O_3/US at 70 and 100 W l^{-1}. No viable cells were observed in the inoculated Petri dishes after 40 min, although the O_3/US process at 100 W l^{-1} was the most efficient in killing pathogens. This was mainly due to the higher amount of free radicals in the effluent. Results from gel electrophoresis analysis showed that O_3/US processes achieved a higher degree of genetic denaturation than single ozonation. The denaturation rate reached was 64 and 81 % for the power densities applied of 70 and 100 W l^{-1}, respectively. These results point out the need for developing efficient treatment technologies focused on killing microorganisms and DNA denaturation to reduce the antibiotic resistance mechanisms in treated effluents.

Within heterogeneous photocatalytic AOPs, the predominant disinfection process for the treatment of HWW reported in literature is the catalytic photoozonation (UV/TiO_2/O_3). This process consists of providing an additional source of hydroxyl radicals from oxygen and ozone adsorbed ($O_{2(ads)}$ and $O_{3(ads)}$) on a solid catalyst (Equations 2.37-2.40) [256]. Furthermore, the irradiation of UV light not only contributes to the removal of microorganisms by its penetration into cells but also enhances the generation of hydroxyl radicals by the photoactivation of oxidants.

$$O_{2(ads)}, O_{3(ads)} + e^{-} \rightarrow O_2^{\bullet -} \quad (2.37)$$

$$O_2^{\bullet -} + H_2O \rightarrow 2HO_2^{\bullet} + HO^{-} \rightarrow O_2 + H_2O_2 \quad (2.38)$$

$H_2O_2 + O_2^{\bullet-} \rightarrow HO^- + HO^\bullet + O_2$ (2.39)

$O_3 + H_2O \rightarrow HO^- + HO^\bullet + O_2$ (2.40)

Machado et al. [257] studied the removal of thermotolerant coliforms in a secondary HWW by catalytic photoozonation using a ramp-type reactor equipped with a germicidal low-pressure mercury vapor lamp. They concluded that the use of 2.96 mg cm^{-2} TiO_2 (P25, Degussa) in the photoirradiation ramp together with the generation of 5.8 mg h^{-1} O_3 in the reactor´s inner air led to the complete disinfection of the effluent after a 60 min treatment. This UV/TiO_2/O_3 process was also tested for the disinfection of hospital laundry wastewater under the same operating conditions by Kist et al. [258]. Results showed that a complete removal of *E. coli* and thermotolerant coliforms was attained which reveals that catalitic photoozonation can be considered as an efficient alternative for the disinfection of HWW.

Finally, EAOPs have been also tested for the disinfection of HWW. Zhou et al. [259] reported the removal of faecal coliforms ($9 \cdot 10^1$ CFU ml^{-1}) by EO using a Ti/SnO_2-Sb_2O_3/PbO_2 anode and a carbon fibre cathode. A complete disinfection was attained in 12 min when applying a current density of 80 A m^{-2}. Initial concentrations of NaCl higher than 200 mg l^{-1} enhanced the disinfection rates because of the higher electrochemical production of free chlorine. Rieder et al. [260] studied a novel alternative for HWW treatment based on the pulsed electric field (PEF). The PEF technology is directly applied against membranes of biological cells. The phosphorus lipid double layer in membranes is broken during the PEF process and represents the main mechanism of this technique for cell lysis. Results showed that the complete disinfection of *P. aeruginosa* was achieved and molecular genomic DNA was released due to cell lysis. In addition, nuclease activities were determined degrading the genetic material in HWW, avoiding the promotion of genetic transfer events that could enhance the spreading of ARB.

2.2.3.2. Disinfection of urines

Wastewater generated in hospital facilities come from different sources (laundry, kitchen, toilets…) but hospital urine can be considered as the main hotspot of both drugs and microorganisms release, despite it only represents 2-3 % of the total volume of hospital wastewater [261]. Specifically, urines contribute to: 1) diffusion of PhCs and/or products metabolized by the human body because 55-80 % of ingested drugs are excreted in urine [262]; and 2) diffusion of pathogens (viruses, fungi and bacteria) due to the proliferation and/or accumulation of certain microorganisms in the urinary tract in immunocompromised patients whose immune system is unable to control the infection. The concentration of chemical and biological contaminants in urine is up to 3-fold higher than that found in hospital wastewater [263] and, hence, the direct treatment of urine at the point of generation could reduce the energy costs for downstream WWTPs and related ecotoxicity risks [264]. For these reasons, the treatment of urines becomes a key goal for reducing the environmental and health impact of hospital effluents. In last years, the number of scientific papers related to the disinfection of urines is increasing, but they are still limited. Table 2.3 summarizes recent studies related to this purpose.

Microbial fuel cells (MFCs) have been also tested as an environmentally friendly alternative for urine disinfection. Despite MFCs are bioelectrochemical reactors in which mainly organic contaminants are oxidized in the anodic chamber obtaining electricity in the process, the removal of *S. enterica* in urine by MFC technology has been reported by Leropoulos et al. [265] who concluded that the operation under closed-circuit conditions was the best MFC configuration since a reduction of 4.43 log units in bacteria concentration was attained. These same authors also studied the performance of the MFC under close circuit conditions for the disinfection of *S. enterica* and *P. aeruginosa* [266]. In this last work, MFC cascades were fed with a flow rate of 0.4 l d^{-1}, resulting in a hydraulic retention time (HRT) of 3.5 h. Results revealed that the new operating conditions improved the disinfection performance, achieving a reduction of 6.91 and 7.79 log units in *S. enterica* and *P. aeruginosa*, respectively. They proposed several disinfection mechanisms based on

high pH and the production of electric power in the anodic chamber, causing a stressful environment for the exogenous pathogenic organisms.

Urine is a complex matrix which not only contains inorganic salts but also natural organic compounds such as urea, creatinine and uric acid [267]. The application of AOPs to the disinfection of urines can promote the removal of both microorganisms and organics until their complete mineralization since hydroxyl radical is a non-selective oxidant [122]. Therefore, the occurrence of competitive oxidation reactions can promote a decrease in the disinfection efficiency. Giannakis et al. [268] compared the removal of *E. coli* from wastewater and urine by UV-C based AOPs, finding that total disinfection was achieved by single photolysis (UV-C) and a positive synergistic effect was obtained with the addition of 10 mg l^{-1} of hydrogen peroxide (UVC/H_2O_2). This last process promotes the generation of large amounts of hydroxyl radicals which not only contribute to the killing of microorganisms but also avoid the bacteria regrowth.

The electrochemical oxidation has been also tested for the disinfection of urines since this technology can promote the production of powerful oxidants from the ions naturally contained in urine, and the subsequent removal of microorganisms. Many authors have studied the feasibility of BDD anodes in the disinfection of urine matrices by EO. Raut et al. [269] studied the implementation of an electrochemical device equipped with BDD anodes to a modular outdoor toilet for the removal of *E. coli* from urine in developing countries. The influence of the applied voltage was evaluated on the disinfection process, finding that the higher the voltage applied, the higher the disinfection rate. Nonetheless, the removal of *E. coli* was attained for all the voltages tested (6-12 V). In a later work, Raut et al. [270] compared different operation modes for the same electrodisinfection system with the aim of minimizing the energy required for killing microorganisms: continuous voltage mode *vs.* pulse operation mode. Results showed energy saving of 68 % when applying a 10 % duty cycle at 6 V at pulse mode. However, the disinfection rates were lower under this novel operation mode.

Cotillas et al. [217] also tested the use of BDD anodes for the removal of *E. coli* and *P. aeruginosa* in polluted urines, obtaining the complete removal of both

microorganisms applying electric charges lower than 0.25 k Ah m^{-3} and current densities of 5 mA cm^{-2} (Figure 2.10).

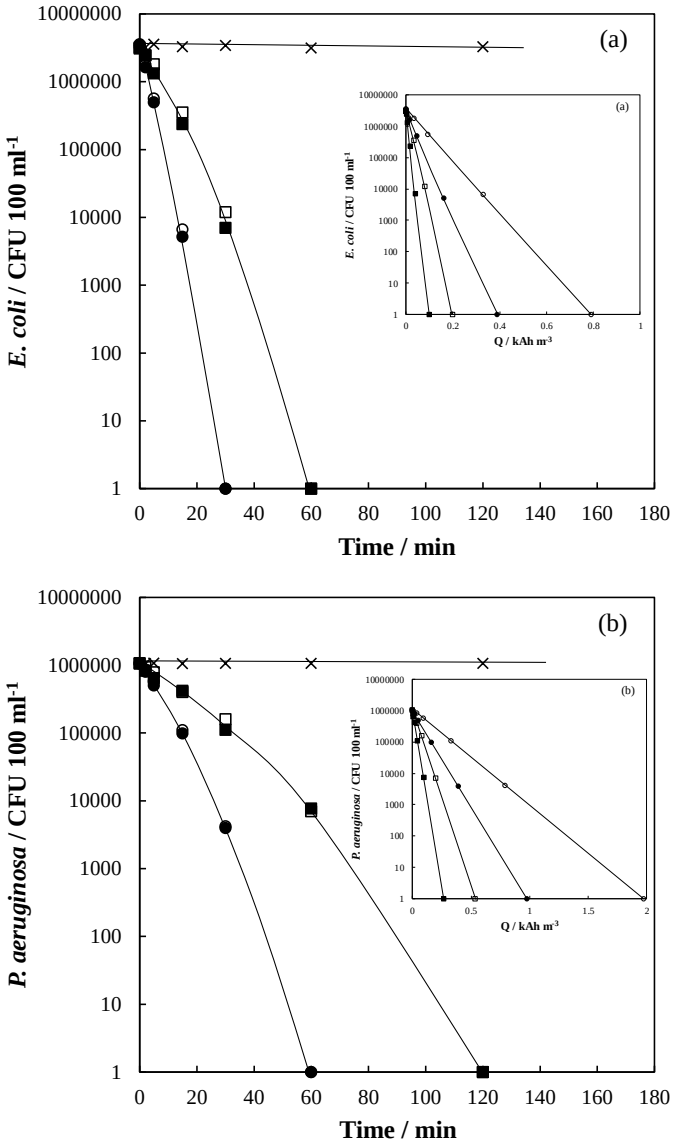

Figure 2.10. Variation of microorganisms as function of the operation time and the applied electric charge during the electrochemical disinfection of synthetic urine with diamond electrodes. (a) *E. coli*; (b) *P. aeruginosa*; (x) 0 Am^{-2}; (■) 5 Am^{-2}; (□) 10 Am^{-2}; (●) 50 Am^{-2}; (○) 100 Am^{-2}. Reprinted with permission from [217]. Copyright 2018 Elsevier.

Electrogenerated chlorine-based disinfectants were reported as the main responsible species for the disinfection. The presence of natural organics (urea, creatinine and uric acid) in urine seems to play a key role on the disinfection process by EO. The partial or total oxidation of organic compounds release a high nitrogen load to the effluent which can be transformed into other inorganic species [217, 271]. Specifically, nitrite is formed from the organic nitrogen released (Equation 2.41), which is rapidly oxidized to nitrate (Equations 2.42-2.43). This last one can be electrochemically reduced, favoring the generation of ammonium (Equations 2.44-2.45) [272].

$$N_2 + 2\ O_2 + 2\ e^- \rightarrow 2\ NO_2^- \quad (2.41)$$

$$3\ NO_2^- + 2\ H^+ \leftrightarrow 2\ NO + NO_3^- + H_2O \quad (2.42)$$

$$NO_2^- + ½\ O_2 \rightarrow NO_3^- \quad (2.43)$$

$$NO_3^- + 6\ H_2O + 8\ e^- \leftrightarrow NH_3 + 9\ OH^- \quad (2.44)$$

$$NH_3 + H_2O \leftrightarrow NH_4^+ + OH^- \quad (2.45)$$

Ammonium can react with electrogenerated free chlorine, promoting the production of combined chlorine species (chloramines) (Equations 2.46-2.48). These species have a disinfectant capacity that also contributes to the removal of microorganisms. Hence, the electrochemical oxidation with BDD anodes could be considered a suitable technology for the disinfection of urines since large amounts of disinfectants are generated without the addition of chemicals.

$$NH_3 + HClO \rightarrow NH_2Cl + H_2O \quad (2.46)$$

$$NH_2Cl + HClO \rightarrow NHCl_2 + H_2O \quad (2.47)$$

$$NHCl_2 + HClO \rightarrow NCl_3 + H_2O \quad (2.48)$$

However, the use of BDD anodes promotes the occurrence of chlorine compounds in high oxidation state during the electrochemical oxidation of solutions containing large amounts of chlorides, like urine. For this reason, the operating conditions should be controlled, working at low applied electric charges and current

densities for avoiding the generation of hazardous disinfection by-products. On the other hand, the use of other anode materials was also tested for the disinfection of urines with the aim of limiting the production of chlorates and/or perchlorates. Dbira et al. [273] reported the disinfection of urines by EO using BDD and different MMO (Ti-RuO_2, Ti-IrO_2 and Ti-Pt) anodes. The complete removal of *E. coli* was achieved with all anodes at 15 mA cm^{-2}, being BDD the most efficient material followed by Ti-RuO_2, Ti-IrO_2 and, finally, Ti-Pt anodes. The use of BDD anodes led to the highest production of ammonium and nitrates, which implies the degradation of organic compounds. Furthermore, high concentrations of perchlorates were obtained during the process with BDD anodes and large amounts of chlorates were detected using Ti-RuO_2 and Ti-IrO_2 anodes. These results reveal, once again, that very soft operating conditions should be applied for avoiding the formation of disinfection-by products during EO. Singla et al. [274] evaluated the EO and the photo-electrocatalytic process (PEC) for the disinfection of synthetic urines with MMO anodes. They concluded that the optimum conditions for the disinfection of urines by EO were 0.42 N/Cl ratios and current densities of 30.33 mA cm^{-2}. Likewise, EO could also be improved by the irradiation of UV light, being the removal of *E. coli* faster in the PEC process (40 min) than that observed in the EO process (60 min) under the optimum operating conditions. Toxicity analyses confirmed that treated urines were non-toxic.

Table 2.3. Technologies for pathogen removal from HWW and urine sources.

Effluent	Technology	Operation parameters	Bacteria	$Bacteria_0$ (CFU/ml)	Bacteria removal [Log reduction]	Ref.
HWW	Membrane bioreactor (MBR)	24.6 l $m^{-2}h^{-1}$ - Sludge age (35 days)	*E. coli* Total coliforms Total enterococci	$2.8 \cdot 10^3$ $1.2 \cdot 10^5$ $4.1 \cdot 10^4$	2.76 3.69 2.46	[230]
HWW	Chemical disinfection	20 mg l^{-1} $Ca(ClO)_2$ - pH=7.36 - 30 min	Heterotrophic bacteria	$2.5 \cdot 10^7$	1.82	[231]
HWW	Chemical disinfection	400 mg l^{-1} CH_3CO_3H - 15 min	*E. faecium*	$1.4 \cdot 10^9$	8.8	[232]
HWW	Chemical disinfection	3.5 mg O_3 l^{-1} - 6 l min^{-1} – pH (6.5 – 7.8)	Total coliforms *P. aeruginosa*	$2.8 \cdot 10^5$ $4 \cdot 10^4$	4.85 Total	[238]
HWW	Chemical disinfection	20 g l^{-1} $Ca(OH)_2$ - pH (11.4-12.2) – 14h HCl - pH (3.7-3.9) – 14h	Thermotolerant coliforms	$1.8 \cdot 10^3$ $1.8 \cdot 10^2$	2.31 3.52	[239]
HWW	Fenton	25 mg l^{-1} Fe^{3+} - 1000 mg l^{-1} H_2O_2 50 °C – 60 min	Total coliforms	$4.2 \cdot 10^4$	Total	[246]
HWW	Photo-Fenton	Solar irradiation 14.1 J cm^{-2} - 90 min UVC lamp 2x15W (λ=254 nm) - 90 min UVC + 10µM FeCit + 500µM H_2O_2 - 90 min	Total coliforms *E. coli*	$3.8 \cdot 10^5$ $2.5 \cdot 10^3$	3.7 / 2.4 Total / Total Total / Total	[76]
HWW	Photo-Fenton	PF– 300 min PF + 9µM $C_6H_8O_7$ (CitAc) – 300 min PF + 1470 µM $S_2O_8^{2-}$ - 60 min 5 mg l^{-1} Fe^{2+} - 50 mg l^{-1} H_2O_2 UV (λ=365 nm –3.9 Wm^{-2})	*K. pneumoniae*	10^6	3.3 Total Total	[245]

Table 2.3. (Cont.) Technologies for pathogen removal from HWW and urine sources.

Effluent	Technology	Operation parameters	Bacteria	Bacteria$_0$ (CFU/ml)	Bacteria removal [Log reduction]	Ref.
HWW	Photochemical disinfection	30 mg l^{-1} Cl_2 – 60 min 10 mg l^{-1} ClO_2 – 60 min 30 mg l^{-1} O_3 – 30 min UV (λ=254 nm – 7.84·10^{-8} El^{-1} s^{-1}) - 70 s UV 30 s + 10 mg l^{-1} Cl_2 - 60 min	Faecal coliforms	$4·10^3$	3.60 4.20 3 3 3.72	[247]
HWW	Photochemical disinfection	UVC (9W - λ=254nm) + 3 mM H_2O_2 VUV + 3 mM H_2O_2 VUV (6.83mWcm^{-2} – λ=185-254 nm) – 10HRT	*E. coli*	10^{10}	6.1 Total	[248]
HWW	Photochemical disinfection	5µM Tetra-Py^+-Me - 270 min 40 Wm^{-2} – (λ = 380-700 nm) Photodynamic inactivation (PDI)	*E. coli* *P. aeruginosa* *A. baumannii* *S. aureus*	10^8	6.5 Total 6 6.5	[252]
HWW	Ozonolysis Sonolysis	0.5 mg l^{-1} O_3 + 100 W l^{-1} US - 30 min	Total coliforms	$4.4·10^3$	Total	[255]
HWW	Catalytic photoozonation	5.8 mg h^{-1} O_3 - 2.96 mg TiO_2 cm^{-2} - 60 min UV (λ < 360 nm - 31.9 J cm^{-2}) 25°C – pH (9.5) - 180 lh^{-1}	Thermotolerant coliforms	$1.1·10^4$	Total	[257]
HWW	Catalytic photoozonation	5.8 mg h^{-1} O_3 - 2.96 mg TiO_2 cm^{-2} - 60 min UV (λ < 360 nm - 31.9 J cm^{-2}) 25°C - pH (8-9) - 180 lh^{-1}	Thermotolerant coliforms *E. coli*	$9·10^4$ $3·10^4$	Total Total	[258]
HWW	EO	Ti/SnO_2-Sb_2O_3/PbO_2 anode Carbon fibre cathode - 80 A m^{-2} - 12 min	Fecal coliform	$9·10^1$	Total	[259]
HWW	Pulse electric field (PEF)	Pulse (1 kJ – 10 Hz – 60 kV) – 1 µs Field strength 80 kV cm^{-1} Energy 162 J ml^{-1}	*P. aeruginosa*	$3·10^5$	Total	[260]

Table 2.3. (Cont.) Technologies for pathogen removal from HWW and urine sources.

Effluent	Technology	Operation parameters	Bacteria	Bacteria$_0$ (CFU/ml)	Bacteria removal [Log reduction]	Ref.
Urine	Microbial fuel cell (MFC)	9 MFCs closed circuit – 31.2 ± 9.2 µW 1000 Ω/MFC (1 1d) – 250 Ω/MFC (12-167d) / 0.9 l d^{-1}	*S. enterica*	-	4.43	[265]
Urine	Microbial fuel cell (MFC)	763 µW 763 µW 9 MFCs closed circuit – 100 Ω/MFC 0.4 l day^{-1} – HRT 3.5 h	*S. enterica* *P. aeruginosa*	10^{12} 10^{12}	6.91 7.79	[266]
Urine	Photochemical disinfection	UVC + 10 mg l^{-1} H_2O_2 - 10 min UVC (λ=254nm – $1.34 \cdot 10^{-5}$ E/l/s)	*E. coli*	10^6	Total	[268]
Urine	Electrochemical Oxidation	6 V - 30min 8V - 17min 10V - 9min 12 V - 6min 42 cm^2 BDD – W cathode	*E. coli*	10^8	Total Total Total Total	[269]
Urine	Electrochemical Oxidation	Single pulse mode (10 %) 6V - 3.7A 90 min - 42 cm^2 BDD	*E. coli*	10^8	Total	[270]
Urine	Electrochemical Oxidation	0.1 kAh m^{-3} 0.25 kAh m^{-3} 5 mA cm^{-2} - 78 cm^2 BDD – SS cathode	*E. coli* *P. aeruginosa*	$5 \cdot 10^4$ 10^4	Total Total	[217]
Urine	Electrochemical Oxidation	BDD / Ti-RuO_2 / Ti-IrO_2 / Ti-Pt 15 mA cm^{-2} - pH 8 – Q < 1.34 Ah l^{-1}	*E. coli*	[8.7-8.3] $\cdot 10^1$	Total	[273]
Urine	Electrochemical Oxidation Photo-Electrocatalysis	EO - 60 min / PEC - 40 min N/Cl=0.42 - 30.33 mA cm^{-2} - 42 cm^2 MMO-SS	*E. coli*	$8 \cdot 10^3$	Total Total	[274]

2.3. Bibliography

[1] D. Sano, A.L. Wester, H. Schmitt, M. Amarasiri, A. Kirby, K. Medlicott, A.M. de Roda Husman, Updated research agenda for water, sanitation and antimicrobial resistance, J. Water Health, 18 (2020) 858-866.

[2] P. Sivalingam, J. Poté, K. Prabakar, Extracellular DNA (eDNA): Neglected and potential sources of antibiotic resistant genes (ARGs) in the aquatic environments, Pathogens, 9 (2020) 1-18.

[3] J.M.A. Blair, M.A. Webber, A.J. Baylay, D.O. Ogbolu, L.J.V. Piddock, Molecular mechanisms of antibiotic resistance, Nat. Rev. Microbiol., 13 (2015) 42-51.

[4] S.M. Lim, S.A.R. Webb, Nosocomial bacterial infections in intensive care units. I: Organisms and mechanisms of antibiotic resistance, Anaesthesia, 60 (2005) 887-902.

[5] A. Cassini, L.D. Högberg, D. Plachouras, A. Quattrocchi, A. Hoxha, G.S. Simonsen, M. Colomb-Cotinat, M.E. Kretzschmar, B. Devleesschauwer, M. Cecchini, Attributable deaths and disability-adjusted life-years caused by infections with antibiotic-resistant bacteria in the EU and the European Economic Area in 2015: a population-level modelling analysis, The Lancet infectious diseases, 19 (2019) 56-66.

[6] T.P. Robinson, D.P. Bu, J. Carrique-Mas, E.M. Fèvre, M. Gilbert, D. Grace, S.I. Hay, J. Jiwakanon, M. Kakkar, S. Kariuki, R. Laxminarayan, J. Lubroth, U. Magnusson, P. Thi Ngoc, T.P. Van Boeckel, M.E.J. Woolhouse, Antibiotic resistance is the quintessential One Health issue, Transactions of The Royal Society of Tropical Medicine and Hygiene, 110 (2016) 377-380.

[7] M.G. Lorenz, W. Wackernagel, Bacterial gene transfer by natural genetic transformation in the environment, Microbiological reviews, 58 (1994) 563-602.

[8] M.C. Dodd, Potential impacts of disinfection processes on elimination and deactivation of antibiotic resistance genes during water and wastewater treatment, J. Environ. Monit., 14 (2012) 1754-1771.

[9] P. Bennett, Plasmid encoded antibiotic resistance: acquisition and transfer of antibiotic resistance genes in bacteria, British journal of pharmacology, 153 (2008) S347-S357.

[10] T.M. Ghaly, J.L. Geoghegan, S.G. Tetu, M.R. Gillings, The peril and promise of integrons: beyond antibiotic resistance, Trends in microbiology, 28 (2020) 455-464.

[11] S. Sütterlin, J.E. Bray, M.C. Maiden, E. Tano, Distribution of class 1 integrons in historic and contemporary collections of human pathogenic Escherichia coli, Plos one, 15 (2020) e0233315.

[12] P. Sabbagh, M. Rajabnia, A. Maali, E. Ferdosi-Shahandashti, Integron and its role in antimicrobial resistance: A literature review on some bacterial pathogens, Iranian Journal of Basic Medical Sciences, 24 (2021) 136.

[13] C.W. Yang, Y.T. Chang, W.L. Chao, I.I. Shiung, H.S. Lin, H. Chen, S.H. Ho, M.J. Lu, P.H. Lee, S.N. Fan, An investigation of total bacterial communities, culturable antibiotic-resistant bacterial communities and integrons in the river water environments of Taipei city, J. Hazard. Mater., 277 (2014) 159-168.

[14] E.T. Anthony, M.O. Ojemaye, O.O. Okoh, A.I. Okoh, A critical review on the occurrence of resistomes in the environment and their removal from wastewater using apposite treatment technologies: Limitations, successes and future improvement, Environ. Pollut., 263 (2020).

[15] B. Wang, X.L. Lv, D. Feng, L.H. Xie, J. Zhang, M. Li, Y. Xie, J.R. Li, H.C. Zhou, Highly Stable Zr(IV)-Based Metal-Organic Frameworks for the Detection and Removal of Antibiotics and Organic Explosives in Water, Journal of the American Chemical Society, 138 (2016) 6204-6216.

[16] O.A. Jones, J.N. Lester, N. Voulvoulis, Pharmaceuticals: A threat to drinking water?, Trends Biotechnol., 23 (2005) 163-167.

[17] J. Radjenović, M. Petrović, D. Barceló, Fate and distribution of pharmaceuticals in wastewater and sewage sludge of the conventional activated sludge (CAS) and advanced membrane bioreactor (MBR) treatment, Water Res., 43 (2009) 831-841.

[18] A.J. Watkinson, E.J. Murby, S.D. Costanzo, Removal of antibiotics in conventional and advanced wastewater treatment: Implications for environmental discharge and wastewater recycling, Water Res., 41 (2007) 4164-4176.

[19] A. Göbel, C.S. McArdell, M.J.F. Suter, W. Giger, Trace Determination of Macrolide and Sulfonamide Antimicrobials, a Human Sulfonamide Metabolite, and Trimethoprim in Wastewater Using Liquid Chromatography Coupled to Electrospray Tandem Mass Spectrometry, Analytical Chemistry, 76 (2004) 4756-4764.

[20] P. Verlicchi, A. Galletti, M. Petrovic, D. Barceló, Hospital effluents as a source of emerging pollutants: An overview of micropollutants and sustainable treatment options, Journal of Hydrology, 389 (2010) 416-428.

[21] J.I. Mubedi, N. Devarajan, S.L. Faucheur, J.K. Mputu, E.K. Atibu, P. Sivalingam, K. Prabakar, P.T. Mpiana, W. Wildi, J. Poté, Effects of untreated hospital effluents on the accumulation of toxic metals in sediments of receiving system under tropical conditions: Case of South India and Democratic Republic of Congo, Chemosphere, 93 (2013) 1070-1076.

[22] I. Michael, L. Rizzo, C.S. McArdell, C.M. Manaia, C. Merlin, T. Schwartz, C. Dagot, D. Fatta-Kassinos, Urban wastewater treatment plants as hotspots for the release of antibiotics in the environment: A review, Water Res., 47 (2013) 957-995.

[23] R.E. Beattie, T. Skwor, K.R. Hristova, Survivor microbial populations in post-chlorinated wastewater are strongly associated with untreated hospital sewage and include ceftazidime and meropenem resistant populations, Science of the Total Environment, 740 (2020).

[24] S.K. Behera, H.W. Kim, J.-E. Oh, H.-S. Park, Occurrence and removal of antibiotics, hormones and several other pharmaceuticals in wastewater treatment plants of the largest industrial city of Korea, Science of The Total Environment, 409 (2011) 4351-4360.

[25] F. Ju, K. Beck, X. Yin, A. Maccagnan, C.S. McArdell, H.P. Singer, D.R. Johnson, T. Zhang, H. Bürgmann, Wastewater treatment plant resistomes are shaped by bacterial

composition, genetic exchange, and upregulated expression in the effluent microbiomes, The ISME Journal, 13 (2019) 346-360.

[26] L. Rizzo, C. Manaia, C. Merlin, T. Schwartz, C. Dagot, M.C. Ploy, I. Michael, D. Fatta-Kassinos, Urban wastewater treatment plants as hotspots for antibiotic resistant bacteria and genes spread into the environment: A review, Science of The Total Environment, 447 (2013) 345-360.

[27] A. Di Cesare, G. Corno, C.M. Manaia, L. Rizzo, Impact of disinfection processes on bacterial community in urban wastewater: Should we rethink microbial assessment methods?, Journal of Environmental Chemical Engineering, 8 (2020) 104393.

[28] D.G. Sanchez, F.M. de Melo, E.A. Savazzi, E.G. Stehling, Detection of different β-lactamases encoding genes, including bla NDM, and plasmid-mediated quinolone resistance genes in different water sources from Brazil, Environmental monitoring and assessment, 190 (2018) 407.

[29] N. Makowska, A. Philips, M. Dabert, K. Nowis, A. Trzebny, R. Koczura, J. Mokracka, Metagenomic analysis of β-lactamase and carbapenemase genes in the wastewater resistome, Water Res., 170 (2020) 115277.

[30] W.H. Organization, Antimicrobial resistance: global report on surveillance, World Health Organization2014.

[31] M. Grabe, T. Bjerklund-Johansen, H. Botto, M. Çek, K. Naber, P. Tenke, F. Wagenlehner, Guidelines on urological infections, European association of urology, 182 (2015).

[32] F. Baquero, J.L. Martínez, R. Cantón, Antibiotics and antibiotic resistance in water environments, Curr. Opin. Biotechnol., 19 (2008) 260-265.

[33] K. Kümmerer, Drugs in the environment: Emission of drugs, diagnostic aids and disinfectants into wastewater by hospitals in relation to other sources - A review, Chemosphere, 45 (2001) 957-969.

[34] M. Mohammadali, J. Davies, Antimicrobial Resistance Genes and Wastewater Treatment, Antimicrobial Resistance in Wastewater Treatment Processes, wiley2017, pp. 1-13.

[35] K.D. Brown, J. Kulis, B. Thomson, T.H. Chapman, D.B. Mawhinney, Occurrence of antibiotics in hospital, residential, and dairy effluent, municipal wastewater, and the Rio Grande in New Mexico, Science of the Total Environment, 366 (2006) 772-783.

[36] E. Rommozzi, S. Giannakis, R. Giovannetti, D. Vione, C. Pulgarin, Detrimental vs. beneficial influence of ions during solar (SODIS) and photo-Fenton disinfection of E. coli in water: (Bi)carbonate, chloride, nitrate and nitrite effects, Appl. Catal. B Environ., 270 (2020).

[37] D. Vione, M. Minella, C. Minero, V. Maurino, P. Picco, A. Marchetto, G. Tartari, Photodegradation of nitrite in lake waters: role of dissolved organic matter, Environmental Chemistry, 6 (2009) 407-415.

[38] R. Bhateria, D. Jain, Water quality assessment of lake water: a review, Sustainable Water Resources Management, 2 (2016) 161-173.

[39] M. De Kwaadsteniet, P. Dobrowsky, A. Van Deventer, W. Khan, T. Cloete, Domestic rainwater harvesting: microbial and chemical water quality and point-of-use treatment systems, Water, Air, & Soil Pollution, 224 (2013) 1629.

[40] I. García, Removal of natural organic matter to reduce the presence of trihalomethanes in drinking water, KTH Royal Institute of Technology, 2011.

[41] E. Brillas, I. Sirés, M.A. Oturan, Electro-Fenton Process and Related Electrochemical Technologies Based on Fenton's Reaction Chemistry, Chemical Reviews, 109 (2009) 6570-6631.

[42] Y. Luo, W. Guo, H.H. Ngo, L.D. Nghiem, F.I. Hai, J. Zhang, S. Liang, X.C. Wang, A review on the occurrence of micropollutants in the aquatic environment and their fate and removal during wastewater treatment, Science of the Total Environment, 473-474 (2014) 619-641.

[43] A. Bhatnagar, M. Sillanpää, Removal of natural organic matter (NOM) and its constituents from water by adsorption – A review, Chemosphere, 166 (2017) 497-510.

[44] Y. Wang, S. Liu, J. Wang, F. Tang, Polymer network strengthened filter paper for durable water disinfection, Colloids Surf. A Physicochem. Eng. Asp., 591 (2020).

[45] Q.U. Ain, M.U. Farooq, M.I. Jalees, Application of Magnetic Graphene Oxide for Water Purification: Heavy Metals Removal and Disinfection, J. Water Process Eng., 33 (2020).

[46] A. Dalvand, E. Gholibegloo, M.R. Ganjali, N. Golchinpoor, M. Khazaei, H. Kamani, S.S. Hosseini, A.H. Mahvi, Comparison of Moringa stenopetala seed extract as a clean coagulant with Alum and Moringa stenopetala-Alum hybrid coagulant to remove direct dye from Textile Wastewater, Environ. Sci. Pollut. Res., 23 (2016) 16396-16405.

[47] U. Gassenschmidt, K.D. Jany, T. Bernhard, H. Niebergall, Isolation and characterization of a flocculating protein from Moringa oleifera Lam, Biochimica et Biophysica Acta (BBA) - General Subjects, 1243 (1995) 477-481.

[48] T.K.F.S. Freitas, V.M. Oliveira, M.T.F. de Souza, H.C.L. Geraldino, V.C. Almeida, S.L. Fávaro, J.C. Garcia, Optimization of coagulation-flocculation process for treatment of industrial textile wastewater using okra (A. esculentus) mucilage as natural coagulant, Ind. Crops Prod., 76 (2015) 538-544.

[49] A. Patchaiyappan, S. Sarangapany, Y.A. Saksakom, S.P. Devipriya, Feasibility study of a point of use technique for water treatment using plant-based coagulant and isolation of a bioactive compound with bactericidal properties, Sep. Sci. Technol., 55 (2020) 112-122.

[50] Y. Fu, F. Wang, H. Sheng, M. Xu, Y. Liang, Y. Bian, S.A. Hashsham, X. Jiang, J.M. Tiedje, Enhanced antibacterial activity of magnetic biochar conjugated quaternary phosphonium salt, Carbon, 163 (2020) 360-369.

[51] X. Cai, S. Tan, M. Lin, A. Xie, W. Mai, X. Zhang, Z. Lin, T. Wu, Y. Liu, Synergistic Antibacterial Brilliant Blue/Reduced Graphene Oxide/Quaternary

Phosphonium Salt Composite with Excellent Water Solubility and Specific Targeting Capability, Langmuir, 27 (2011) 7828-7835.

[52] C. Stange, J.P.S. Sidhu, S. Toze, A. Tiehm, Comparative removal of antibiotic resistance genes during chlorination, ozonation, and UV treatment, Int. J. Hyg. Environ. Health, 222 (2019) 541-548.

[53] H. Ölmez, U. Kretzschmar, Potential alternative disinfection methods for organic fresh-cut industry for minimizing water consumption and environmental impact, LWT - Food Sci. Technol., 42 (2009) 686-693.

[54] H.F. Diao, X.Y. Li, J.D. Gu, H.C. Shi, Z.M. Xie, Electron microscopic investigation of the bactericidal action of electrochemical disinfection in comparison with chlorination, ozonation and Fenton reaction, Process Biochemistry, 39 (2004) 1421-1426.

[55] X. Yang, J. Peng, B. Chen, W. Guo, Y. Liang, W. Liu, L. Liu, Effects of ozone and ozone/peroxide pretreatments on disinfection byproduct formation during subsequent chlorination and chloramination, J. Hazard. Mater., 239-240 (2012) 348-354.

[56] J. Liu, C. Dong, Y. Deng, J. Ji, S. Bao, C. Chen, B. Shen, J. Zhang, M. Xing, Molybdenum sulfide Co-catalytic Fenton reaction for rapid and efficient inactivation of Escherichia coli, Water Res., 145 (2018) 312-320.

[57] U. Von Gunten, Ozonation of drinking water: Part I. Oxidation kinetics and product formation, Water Res., 37 (2003) 1443-1467.

[58] J.P. Duguet, E. Brodard, B. Dussert, J. Mallevialle, Improvement in the Effectiveness of Ozonation of Drinking Water Through the Use of Hydrogen Peroxide, Ozone: Science & Engineering, 7 (1985) 241-258.

[59] S. Nahim-Granados, G. Rivas-Ibáñez, J. Antonio Sánchez Pérez, I. Oller, S. Malato, M.I. Polo-López, Synthetic fresh-cut wastewater disinfection and decontamination by ozonation at pilot scale, Water Res., 170 (2020) 115304.

[60] P.L. Huston, J.J. Pignatello, Degradation of selected pesticide active ingredients and commercial formulations in water by the photo-assisted Fenton reaction, Water Res., 33 (1999) 1238-1246.

[61] J. Kiwi, C. Pulgarin, P. Peringer, Effect of Fenton and photo-Fenton reactions on the degradation and biodegradability of 2 and 4-nitrophenols in water treatment, Applied Catalysis B, Environmental, 3 (1994) 335-350.

[62] E. Neyens, J. Baeyens, A review of classic Fenton's peroxidation as an advanced oxidation technique, J. Hazard. Mater., 98 (2003) 33-50.

[63] N. Thomas, D.D. Dionysiou, S.C. Pillai, Heterogeneous Fenton catalysts: A review of recent advances, J. Hazard. Mater., 404 (2021).

[64] S.M. Arnold, W.J. Hickey, R.F. Harris, Degradation of atrazine by Fenton's reagent: condition optimization and product quantification, Environmental science & technology, 29 (1995) 2083-2089.

[65] J.J. Pignatello, E. Oliveros, A. MacKay, Advanced oxidation processes for organic contaminant destruction based on the Fenton reaction and related chemistry, Crit. Rev. Environ. Sci. Technol., 36 (2006) 1-84.

[66] Y. Gu, F. Xiao, L. Luo, X. Zhou, X. Zhou, J. Li, Z. Li, Bacterial disinfection by CuFe2O4 nanoparticles enhanced by NH2OH: A mechanistic study, Nanomaterials, 10 (2020).

[67] H.-E. Kim, T.T.M. Nguyen, H. Lee, C. Lee, Enhanced Inactivation of Escherichia coli and MS2 Coliphage by Cupric Ion in the Presence of Hydroxylamine: Dual Microbicidal Effects, Environmental Science & Technology, 49 (2015) 14416-14423.

[68] S. Malato, P. Fernández-Ibáñez, M.I. Maldonado, J. Blanco, W. Gernjak, Decontamination and disinfection of water by solar photocatalysis: Recent overview and trends, Catal Today, 147 (2009) 1-59.

[69] F. Zaviska, P. Drogui, G. Mercier, J.-F. Blais, Procédés d'oxydation avancée dans le traitement des eaux et des effluents industriels: Application à la dégradation des

polluants réfractaires, Revue des sciences de l'eau/Journal of Water Science, 22 (2009) 535-564.

[70] D. Rubio, E. Nebot, J.F. Casanueva, C. Pulgarin, Comparative effect of simulated solar light, UV, UV/H2O2 and photo-Fenton treatment (UV-Vis/H2O2/Fe2+,3+) in the Escherichia coli inactivation in artificial seawater, Water Res., 47 (2013) 6367-6379.

[71] D. Spuhler, J. Andrés Rengifo-Herrera, C. Pulgarin, The effect of Fe2+, Fe3+, H2O2 and the photo-Fenton reagent at near neutral pH on the solar disinfection (SODIS) at low temperatures of water containing Escherichia coli K12, Appl. Catal. B Environ., 96 (2010) 126-141.

[72] L. Clarizia, D. Russo, I. Di Somma, R. Marotta, R. Andreozzi, Homogeneous photo-Fenton processes at near neutral pH: A review, Appl. Catal. B Environ., 209 (2017) 358-371.

[73] S. Nahim-Granados, I. Oller, S. Malato, J.A. Sánchez Pérez, M.I. Polo-Lopez, Commercial fertilizer as effective iron chelate (Fe3+-EDDHA) for wastewater disinfection under natural sunlight for reusing in irrigation, Appl. Catal. B Environ., 253 (2019) 286-292.

[74] U.J. Ahile, R.A. Wuana, A.U. Itodo, R. Sha'Ato, J.A. Malvestiti, R.F. Dantas, Are iron chelates suitable to perform photo-Fenton at neutral pH for secondary effluent treatment?, J. Environ. Manage., 278 (2021).

[75] S. Giannakis, M.I.P. López, D. Spuhler, J.A.S. Pérez, P.F. Ibáñez, C. Pulgarin, Solar disinfection is an augmentable, in situ-generated photo-Fenton reaction—Part 2: A review of the applications for drinking water and wastewater disinfection, Appl. Catal. B Environ., 198 (2016) 431-446.

[76] J.A.L. Perini, A.L. Tonetti, C. Vidal, C.C. Montagner, R.F.P. Nogueira, Simultaneous degradation of ciprofloxacin, amoxicillin, sulfathiazole and sulfamethazine, and disinfection of hospital effluent after biological treatment via photo-Fenton process under ultraviolet germicidal irradiation, Appl. Catal. B Environ., 224 (2018) 761-771.

[77] Y. Ahmed, J. Zhong, Z. Yuan, J. Guo, Simultaneous removal of antibiotic resistant bacteria, antibiotic resistance genes, and micropollutants by a modified photo-Fenton process, Water Res., 197 (2021).

[78] J. Rodríguez-Chueca, S. Giannakis, M. Marjanovic, M. Kohantorabi, M.R. Gholami, D. Grandjean, L.F. de Alencastro, C. Pulgarín, Solar-assisted bacterial disinfection and removal of contaminants of emerging concern by Fe2+-activated HSO5- vs. S2O82- in drinking water, Appl. Catal. B Environ., 248 (2019) 62-72.

[79] L.C. Ferreira, M. Castro-Alférez, S. Nahim-Granados, M.I. Polo-López, M.S. Lucas, G. Li Puma, P. Fernández-Ibáñez, Inactivation of water pathogens with solar photo-activated persulfate oxidation, Chemical Engineering Journal, 381 (2020).

[80] E.A. Serna-Galvis, L. Salazar-Ospina, J.N. Jiménez, N.J. Pino, R.A. Torres-Palma, Elimination of carbapenem resistant Klebsiella pneumoniae in water by UV-C, UV-C/persulfate and UV-C/H2O2. Evaluation of response to antibiotic, residual effect of the processes and removal of resistance gene, J. Environ. Chem. Eng., 8 (2020).

[81] R. Munter, Advanced oxidation processes–current status and prospects, Proc. Estonian Acad. Sci. Chem, 50 (2001) 59-80.

[82] T. Zhang, Y. Hu, L. Jiang, S. Yao, K. Lin, Y. Zhou, C. Cui, Removal of antibiotic resistance genes and control of horizontal transfer risk by UV, chlorination and UV/chlorination treatments of drinking water, Chemical Engineering Journal, 358 (2019) 589-597.

[83] B.K. Biswal, R. Khairallah, K. Bibi, A. Mazza, R. Gehr, L. Masson, D. Frigon, Impact of UV and peracetic acid disinfection on the prevalence of virulence and antimicrobial resistance genes in uropathogenic escherichia coli in wastewater effluents, Appl. Environ. Microbiol., 80 (2014) 3656-3666.

[84] J. Feng, X. Hu, P.L. Yue, Effect of initial solution pH on the degradation of Orange II using clay-based Fe nanocomposites as heterogeneous photo-Fenton catalyst, Water Res., 40 (2006) 641-646.

[85] S. Bossmann, E. Oliveros, S. Göb, M. Kantor, A. Göppert, L. Lei, P.L. Yue, A. Braun, Degradation of polyvinyl alcohol (PVA) by homogeneous and heterogeneous photocatalysis applied to the photochemically enhanced Fenton reaction, Water science and technology, 44 (2001) 257-262.

[86] G. Puma, P. Yue, Heterogeneous photo-assisted Fenton oxidation of Indigo carmine dye on iron-Nafion pellet, Proceedings of the Sixth International Conference on Advanced Oxidation Technologies for Water and Air Remediation, London, Ont., Canada, 2000, pp. 105.

[87] J. Fernandez, J. Bandara, J. Kiwi, A. Lopez, P. Albers, Efficient photo-assisted Fenton catalysis mediated by Fe ions on Nafion membranes active in the abatement of non-biodegradable azo-dye, Chemical Communications, (1998) 1493-1494.

[88] A.J. Hoffman, E.R. Carraway, M.R. Hoffmann, Photocatalytic Production of H2O2 and Organic Peroxides on Quantum-Sized Semiconductor Colloids, Environmental Science and Technology, 28 (1994) 776-785.

[89] M. Pelaez, N.T. Nolan, S.C. Pillai, M.K. Seery, P. Falaras, A.G. Kontos, P.S.M. Dunlop, J.W.J. Hamilton, J.A. Byrne, K. O'Shea, M.H. Entezari, D.D. Dionysiou, A review on the visible light active titanium dioxide photocatalysts for environmental applications, Appl. Catal. B Environ., 125 (2012) 331-349.

[90] H. Irie, Y. Watanabe, K. Hashimoto, Carbon-doped anatase TiO2 powders as a visible-light sensitive photocatalyst, Chemistry Letters, 32 (2003) 772-773.

[91] T. Morikawa, R. Asahi, T. Ohwaki, K. Aoki, Y. Taga, Band-gap narrowing of titanium dioxide by nitrogen doping, Japanese Journal of Applied Physics, 40 (2001) L561.

[92] J.H. Carey, B.G. Oliver, The photochemical treatment of wastewater by ultraviolet irradiation of semiconductors, WATER POLLUT. RES. J. CAN., 15 (1980) 157-185.

[93] P.O. Nyangaresi, Y. Qin, G. Chen, B. Zhang, Y. Lu, L. Shen, Comparison of UV-LED photolytic and UV-LED/TiO2 photocatalytic disinfection for Escherichia coli in water, Catal Today, 335 (2019) 200-207.

[94] X. Wu, L. Cao, J. Song, Y. Si, J. Yu, B. Ding, Thorn-like flexible Ag2C2O4/TiO2 nanofibers as hierarchical heterojunction photocatalysts for efficient visible-light-driven bacteria-killing, J. Colloid Interface Sci., 560 (2020) 681-689.

[95] P. Rokicka-Konieczna, A. Markowska-Szczupak, E. Kusiak-Nejman, A.W. Morawski, Photocatalytic water disinfection under the artificial solar light by fructose-modified TiO2, Chemical Engineering Journal, 372 (2019) 203-215.

[96] J. Song, X. Wu, M. Zhang, C. Liu, J. Yu, G. Sun, Y. Si, B. Ding, Highly flexible, core-shell heterostructured, and visible-light-driven titania-based nanofibrous membranes for antibiotic removal and E. coil inactivation, Chemical Engineering Journal, 379 (2020).

[97] K. Qi, B. Cheng, J. Yu, W. Ho, A review on TiO2-based Z-scheme photocatalysts, Chinese Journal of Catalysis, 38 (2017) 1936-1955.

[98] X. Li, J. Xie, C. Jiang, J. Yu, P. Zhang, Review on design and evaluation of environmental photocatalysts, Frontiers of Environmental Science & Engineering, 12 (2018) 14.

[99] M. Manasa, P.R. Chandewar, H. Mahalingam, Photocatalytic degradation of ciprofloxacin & norfloxacin and disinfection studies under solar light using boron & cerium doped TiO2 catalysts synthesized by green EDTA-citrate method, Catal Today, (2020).

[100] S. Dong, J. Feng, M. Fan, Y. Pi, L. Hu, X. Han, M. Liu, J. Sun, J. Sun, Recent developments in heterogeneous photocatalytic water treatment using visible light-responsive photocatalysts: A review, RSC Adv., 5 (2015) 14610-14630.

[101] L. Zhang, T. Xu, X. Zhao, Y. Zhu, Controllable synthesis of Bi2MoO6 and effect of morphology and variation in local structure on photocatalytic activities, Appl. Catal. B Environ., 98 (2010) 138-146.

[102] M. Saiful Islam, S. Lazure, R.-n. Vannier, G. Nowogrocki, G. Mairesse, Structural and computational studies of Bi2WO6 based oxygen ion conductors, Journal of Materials Chemistry, 8 (1998) 655-660.

[103] O.M. Bordun, Luminescence Centers in Bi2WO6 and Bi2W2O9 Thin Films, Inorg. Mater., 34 (1998) 1270-1272.

[104] F. Duan, Q. Zhang, Q. Wei, D. Shi, M. Chen, Control of photocatalytic property of bismuth-based semiconductor photocatalysts, Progress in Chemistry, 26 (2014) 30.

[105] S. Dong, C. Yu, Y. Li, Y. Li, J. Sun, X. Geng, Controlled synthesis of T-shaped BiVO4 and enhanced visible light responsive photocatalytic activity, Journal of Solid State Chemistry, 211 (2014) 176-183.

[106] K. Rusevova, R. Köferstein, M. Rosell, H.H. Richnow, F.-D. Kopinke, A. Georgi, LaFeO3 and BiFeO3 perovskites as nanocatalysts for contaminant degradation in heterogeneous Fenton-like reactions, Chemical Engineering Journal, 239 (2014) 322-331.

[107] W.P.C. Lee, T.L. Perix, K.A.R. Packiam, M.M. Gui, C.W. Ooi, S.P. Chai, Highly-efficient photocatalytic disinfection of Escherichia coli by copper-doped molybdenum disulfide/bismuth sulfide under low-powered visible light irradiation, Catal. Commun., 140 (2020).

[108] M. Li, D. Li, Z. Zhou, P. Wang, X. Mi, Y. Xia, H. Wang, S. Zhan, Y. Li, L. Li, Plasmonic Ag as electron-transfer mediators in Bi2MoO6/Ag-AgCl for efficient photocatalytic inactivation of bacteria, Chemical Engineering Journal, 382 (2020).

[109] Y. Yan, X. Zhou, P. Yu, Z. Li, T. Zheng, Characteristics, mechanisms and bacteria behavior of photocatalysis with a solid Z-scheme Ag/AgBr/g-C3N4 nanosheet in water disinfection, Appl Catal A Gen, 590 (2020).

[110] A. Kaur, W.A. Anderson, S. Tanvir, S.K. Kansal, Solar light active silver/iron oxide/zinc oxide heterostructure for photodegradation of ciprofloxacin, transformation products and antibacterial activity, J. Colloid Interface Sci., 557 (2019) 236-253.

[111] P. Yu, X. Zhou, Y. Yan, Z. Li, T. Zheng, Enhanced visible-light-driven photocatalytic disinfection using AgBr-modified g-C 3 N 4 composite and its mechanism, Colloids Surf. B Biointerfaces, 179 (2019) 170-179.

[112] Z. Jiang, B. Wang, Y. Li, H.S. Chan, H. Sun, T. Wang, H. Li, S. Yuan, M.K.H. Leung, A. Lu, P.K. Wong, Solar-light-driven rapid water disinfection by ultrathin magnesium titanate/carbon nitride hybrid photocatalyst: Band structure analysis and role of reactive oxygen species, Appl. Catal. B Environ., 257 (2019).

[113] S. Kumar, M. Sharma, A. Kumar, S. Powar, R. Vaish, Rapid bacterial disinfection using low frequency piezocatalysis effect, J. Ind. Eng. Chem., 77 (2019) 355-364.

[114] A. Fujishima, X. Zhang, D.A. Tryk, TiO2 photocatalysis and related surface phenomena, Surface Science Reports, 63 (2008) 515-582.

[115] A.V. Emeline, V.N. Kuznetsov, V.K. Rybchuk, N. Serpone, Visible-light-active titania photocatalysts: the case of N-doped s—properties and some fundamental issues, International Journal of Photoenergy, 2008 (2008).

[116] D. He, Z. Zhang, Y. Xing, Y. Zhou, H. Yang, H. Liu, J. Qu, X. Yuan, J. Guan, Y.-n. Zhang, Black phosphorus/graphitic carbon nitride: A metal-free photocatalyst for "green" photocatalytic bacterial inactivation under visible light, Chemical Engineering Journal, 384 (2020) 123258.

[117] X. Zeng, Y. Liu, Y. Xia, M.H. Uddin, D. Xia, D.T. McCarthy, A. Deletic, J. Yu, X. Zhang, Cooperatively modulating reactive oxygen species generation and bacteria-photocatalyst contact over graphitic carbon nitride by polyethylenimine for rapid water disinfection, Appl. Catal. B Environ., 274 (2020).

[118] O. Polyakov, A. Badalyan, L. Bakhturova, Relative contributions of plasma pyrolysis and liquid-phase reactions in the anode microspark treatment of aqueous phenol solutions, High Energy Chemistry, 38 (2004) 131-133.

[119] A. Motyka, A. Dzimitrowicz, P. Jamroz, E. Lojkowska, P. Pohl, W. Sledz, Direct current atmospheric pressure glow discharge generated in contact with a flowing liquid cathode as a method for rapid eradication of phytopathogenic bacteria, New Biotechnology, 44 (2018) S162.

[120] Y. Yang, K. Wan, Z. Yang, D. Li, G. Li, S. Zhang, L. Wang, X. Yu, Inactivation of antibiotic resistant Escherichia coli and degradation of its resistance genes by glow discharge plasma in an aqueous solution, Chemosphere, 252 (2020).

[121] M. Griessler, S. Knetsch, E. Schimpf, A. Schmidhuber, B. Schrammel, W. Wesner, R. Sommer, A.K.T. Kirschner, Inactivation of Pseudomonas aeruginosa in electrochemical advanced oxidation process with diamond electrodes, Water Science and Technology, 63 (2011) 2010-2016.

[122] I. Sirés, E. Brillas, M.A. Oturan, M.A. Rodrigo, M. Panizza, Electrochemical advanced oxidation processes: today and tomorrow. A review, Environ. Sci. Pollut. Res., 21 (2014) 8336-8367.

[123] D. Ghernaout, B. Ghernaout, From chemical disinfection to electrodisinfection: The obligatory itinerary?, Desalin. Water Treat., 16 (2010) 156-175.

[124] I. Sirés, E. Brillas, Remediation of water pollution caused by pharmaceutical residues based on electrochemical separation and degradation technologies: A review, Environment International, 40 (2012) 212-229.

[125] I. Sirés, E. Brillas, Remediation of water pollution caused by pharmaceutical residues based on electrochemical separation and degradation technologies: a review, Environment international, 40 (2012) 212-229.

[126] M. Panizza, G. Cerisola, Direct and mediated anodic oxidation of organic pollutants, Chemical reviews, 109 (2009) 6541-6569.

[127] M. Rodrigo, N. Oturan, M.A. Oturan, Electrochemically assisted remediation of pesticides in soils and water: a review, Chemical reviews, 114 (2014) 8720-8745.

[128] X.Y. Ni, H. Liu, L. Xin, Z.B. Xu, Y.H. Wang, L. Peng, Z. Chen, Y.H. Wu, H.Y. Hu, Disinfection performance and mechanism of the carbon fiber-based flow-through electrode system (FES) towards Gram-negative and Gram-positive bacteria, Electrochim Acta, 341 (2020).

[129] J. Jeong, C. Kim, J. Yoon, The effect of electrode material on the generation of oxidants and microbial inactivation in the electrochemical disinfection processes, Water Res., 43 (2009) 895-901.

[130] J. Jeong, J.Y. Kim, J. Yoon, The role of reactive oxygen species in the electrochemical inactivation of microorganisms, Environmental Science and Technology, 40 (2006) 6117-6122.

[131] S. Cotillas, J. Llanos, P. Cañizares, S. Mateo, M.A. Rodrigo, Optimization of an integrated electrodisinfection/electrocoagulation process with Al bipolar electrodes for urban wastewater reclamation, Water Research, 47 (2013) 1741-1750.

[132] M. Mascia, A. Vacca, S. Palmas, Fixed bed reactors with three dimensional electrodes for electrochemical treatment of waters for disinfection, Chemical Engineering Journal, 211-212 (2012) 479-487.

[133] S. Cotillas, J. Llanos, K. Castro-Ríos, G. Taborda-Ocampo, M.A. Rodrigo, P. Cañizares, Synergistic integration of sonochemical and electrochemical disinfection with DSA anodes, Chemosphere, 163 (2016) 562-568.

[134] H. Liu, X.Y. Ni, Z.Y. Huo, L. Peng, G.Q. Li, C. Wang, Y.H. Wu, H.Y. Hu, Carbon Fiber-Based Flow-Through Electrode System (FES) for Water Disinfection via Direct Oxidation Mechanism with a Sequential Reduction-Oxidation Process, Environmental Science and Technology, 53 (2019) 3238-3249.

[135] X.Y. Ni, H. Liu, C. Wang, W.L. Wang, Z.B. Xu, Z. Chen, Y.H. Wu, H.Y. Hu, Comparison of carbonized and graphitized carbon fiber electrodes under flow-through electrode system (FES) for high-efficiency bacterial inactivation, Water Res., 168 (2020).

[136] Z.Y. Huo, H. Liu, C. Yu, Y.H. Wu, H.Y. Hu, X. Xie, Elevating the stability of nanowire electrodes by thin polydopamine coating for low-voltage electroporation-disinfection of pathogens in water, Chemical Engineering Journal, 369 (2019) 1005-1013.

[137] S. Wang, W. Wang, L. Yue, S. Cui, H. Wang, C. Wang, S. Chen, Hierarchical Cu2O nanowires covered by silver nanoparticles-doped carbon layer supported on Cu foam for rapid and efficient water disinfection with lower voltage, Chemical Engineering Journal, 382 (2020).

[138] J.A. Rojas-Chapana, M.A. Correa-Duarte, Z. Ren, K. Kempa, M. Giersig, Enhanced introduction of gold nanoparticles into vital acidothiobacillus ferrooxidans by carbon nanotube-based microwave electroporation, Nano Letters, 4 (2004) 985-988.

[139] M. Shahini, J.T.W. Yeow, Cell electroporation by CNT-featured microfluidic chip, Lab on a Chip, 13 (2013) 2585-2590.

[140] J. Isidro, D. Brackemeyer, C. Sáez, J. Llanos, J. Lobato, P. Cañizares, T. Matthée, M.A. Rodrigo, Electro-disinfection with BDD-electrodes featuring PEM technology, Sep. Purif. Technol., 248 (2020).

[141] R. Pelegrini, J. Reyes, N. Duran, P. Zamora, A. De Andrade, Photoelectrochemical degradation of lignin, Journal of Applied Electrochemistry, 30 (2000) 953-958.

[142] Y.-J. Shih, W.N. Putra, Y.-H. Huang, J.-C. Tsai, Mineralization and deflourization of 2, 2, 3, 3-tetrafluoro-1-propanol (TFP) by UV/persulfate oxidation and sequential adsorption, Chemosphere, 89 (2012) 1262-1266.

[143] P.Y. Chan, M.G. El-Din, J.R. Bolton, A solar-driven UV/Chlorine advanced oxidation process, Water Res., 46 (2012) 5672-5682.

[144] Y. Jin, Y. Shi, Z. Chen, R. Chen, X. Chen, X. Zheng, Y. Liu, R. Ding, Enhancement of solar water disinfection using H2O2 generated in situ by electrochemical reduction, Appl. Catal. B Environ., 267 (2020).

[145] K. Cho, S. Lee, H. Kim, H.E. Kim, A. Son, E.J. Kim, M. Li, Z. Qiang, S.W. Hong, Effects of reactive oxidants generation and capacitance on photoelectrochemical water disinfection with self-doped titanium dioxide nanotube arrays, Appl. Catal. B Environ., 257 (2019).

[146] R. Montenegro-Ayo, A.C. Barrios, I. Mondal, K. Bhagat, J.C. Morales-Gomero, M. Abbaszadegan, P. Westerhoff, F. Perreault, S. Garcia-Segura, Portable point-of-use photoelectrocatalytic device provides rapid water disinfection, Science of the Total Environment, 737 (2020).

[147] H. Zhao, Q. Wang, Y. Chen, Q. Tian, G. Zhao, Efficient removal of dimethyl phthalate with activated iron-doped carbon aerogel through an integrated adsorption and electro-Fenton oxidation process, Carbon, 124 (2017) 111-122.

[148] K. Chatterjee, M. Ashokkumar, H. Gullapalli, Y. Gong, R. Vajtai, P. Thanikaivelan, P.M. Ajayan, Nitrogen-rich carbon nano-onions for oxygen reduction reaction, Carbon, 130 (2018) 645-651.

[149] J. Lu, Z. Chen, B.A. Ayele, X. Liu, Q. Chen, Electrocatalytic activities of engineered carbonaceous cathodes for generation of hydrogen peroxide and oxidation of recalcitrant reactive dye, J Electroanal Chem, 878 (2020).

[150] L. Chen, A. Pinto, A.N. Alshawabkeh, Activated carbon as a cathode for water disinfection through the electro-fenton process, Catalysts, 9 (2019).

[151] G. Yuksek, D. Okutman Tas, E. Ubay Cokgor, G. Insel, B. Kirci, O. Erturan, Effect of eco-friendly production technologies on wastewater characterization and treatment plant performance, Desalin. Water Treat., 57 (2016) 27924-27933.

[152] M. Lucian, M. Volpe, L. Gao, G. Piro, J.L. Goldfarb, L. Fiori, Impact of hydrothermal carbonization conditions on the formation of hydrochars and secondary chars from the organic fraction of municipal solid waste, Fuel, 233 (2018) 257-268.

[153] Y. Lin, X. Ma, X. Peng, Z. Yu, A Mechanism Study on Hydrothermal Carbonization of Waste Textile, Energy & Fuels, 30 (2016) 7746-7754.

[154] C. Gai, Y. Guo, T. Liu, N. Peng, Z. Liu, Hydrogen-rich gas production by steam gasification of hydrochar derived from sewage sludge, International Journal of Hydrogen Energy, 41 (2016) 3363-3372.

[155] M.T. Reza, C. Coronella, K.M. Holtman, D. Franqui-Villanueva, S.R. Poulson, Hydrothermal Carbonization of Autoclaved Municipal Solid Waste Pulp and

Anaerobically Treated Pulp Digestate, ACS Sustainable Chemistry & Engineering, 4 (2016) 3649-3658.

[156] A.A. Azzaz, B. Khiari, S. Jellali, C.M. Ghimbeu, M. Jeguirim, Hydrochars production, characterization and application for wastewater treatment: A review, Renewable Sustainable Energy Rev, 127 (2020).

[157] J. Gomes, A. Matos, M. Gmurek, R.M. Quinta-Ferreira, R.C. Martins, Ozone and photocatalytic processes for pathogens removal from water: A review, Catalysts, 9 (2019).

[158] C. Casado, J. Moreno-SanSegundo, I. De la Obra, B. Esteban García, J.A. Sánchez Pérez, J. Marugán, Mechanistic modelling of wastewater disinfection by the photo-Fenton process at circumneutral pH, Chemical Engineering Journal, 403 (2021).

[159] T. Zhang, H. Yu, J. Li, H. Song, S. Wang, Z. Zhang, S. Chen, Green light–triggered antimicrobial cotton fabric for wastewater disinfection, Mat. Today Phy., 15 (2020).

[160] P. Ragazzo, N. Chiucchini, V. Piccolo, M. Spadolini, S. Carrer, F. Zanon, R. Gehr, Wastewater disinfection: long-term laboratory and full-scale studies on performic acid in comparison with peracetic acid and chlorine, Water Res., 184 (2020).

[161] P. Cornel, S. Krause, Membrane bioreactors in industrial wastewater treatment - European experiences, examples and trends, Water Science and Technology, 2006, pp. 37-44.

[162] C. Di Iaconi, M. De Sanctis, S. Rossetti, R. Ramadori, Technological transfer to demonstrative scale of sequencing batch biofilter granular reactor (SBBGR) technology for municipal and industrial wastewater treatment, Water Science and Technology, 58 (2008) 367-372.

[163] M. De Sanctis, V.G. Altieri, V. Piergrossi, C. Di Iaconi, Aerobic granular-based technology for water and energy recovery from municipal wastewater, New Biotechnol., 56 (2020) 71-78.

[164] V.K. Sharma, N. Johnson, L. Cizmas, T.J. McDonald, H. Kim, A review of the influence of treatment strategies on antibiotic resistant bacteria and antibiotic resistance genes, Chemosphere, 150 (2016) 702-714.

[165] L. Liu, Y.-h. Liu, Z. Wang, C.-x. Liu, X. Huang, G.-f. Zhu, Behavior of tetracycline and sulfamethazine with corresponding resistance genes from swine wastewater in pilot-scale constructed wetlands, J. Hazard. Mater., 278 (2014) 304-310.

[166] A. Kaliakatsos, N. Kalogerakis, T. Manios, D. Venieri, Efficiency of two constructed wetland systems for wastewater treatment: removal of bacterial indicators and enteric viruses, J. Chem. Technol. Biotechnol., 94 (2019) 2123-2130.

[167] Y. González, P. Salgado, G. Vidal, Disinfection behavior of a UV-treated wastewater system using constructed wetlands and the rate of reactivation of pathogenic microorganisms, Water Sci. Technol., 80 (2020) 1870-1879.

[168] G. Wen, Q. Wan, X. Deng, R. Cao, X. Xu, Z. Chen, J. Wang, T. Huang, Reactivation of fungal spores in water following UV disinfection: Effect of temperature, dark delay, and real water matrices, Chemosphere, 237 (2019).

[169] W.A.M. Hijnen, E.F. Beerendonk, G.J. Medema, Inactivation credit of UV radiation for viruses, bacteria and protozoan (oo)cysts in water: A review, Water Research, 40 (2006) 3-22.

[170] M. Bellucci, F. Marazzi, L.S. Naddeo, F. Piergiacomo, L. Beneduce, E. Ficara, V. Mezzanotte, Disinfection and nutrient removal in laboratory-scale photobioreactors for wastewater tertiary treatment, J. Chem. Technol. Biotechnol., 95 (2020) 959-966.

[171] M. Berney, H.U. Weilenmann, A. Simonetti, T. Egli, Efficacy of solar disinfection of Escherichia coli, Shigella flexneri, Salmonella Typhimurium and Vibrio cholerae, Journal of applied microbiology, 101 (2006) 828-836.

[172] T. Kohn, K.L. Nelson, Sunlight-mediated inactivation of MS2 coliphage via exogenous singlet oxygen produced by sensitizers in natural waters, Environmental science & technology, 41 (2007) 192-197.

[173] M.J. Mattle, D. Vione, T. Kohn, Conceptual model and experimental framework to determine the contributions of direct and indirect photoreactions to the solar disinfection of MS2, phiX174, and adenovirus, Environmental science & technology, 49 (2015) 334-342.

[174] M. Voumard, S. Giannakis, A. Carratalà, C. Pulgarin, E. coli – MS2 bacteriophage interactions during solar disinfection of wastewater and the subsequent post-irradiation period, Chemical Engineering Journal, 359 (2019) 1224-1233.

[175] T. Ivankovic, J. Dikic, S.R. Du Roscoat, S. Dekic, J. Hrenovic, M. Ganjto, Removal of emerging pathogenic bacteria using metal-exchanged natural zeolite bead filter, Water Sci. Technol., 80 (2019) 1085-1098.

[176] X. Qu, P.J.J. Alvarez, Q. Li, Applications of nanotechnology in water and wastewater treatment, Water Res., 47 (2013) 3931-3946.

[177] F. Hossain, O.J. Perales-Perez, S. Hwang, F. Román, Antimicrobial nanomaterials as water disinfectant: Applications, limitations and future perspectives, Science of the Total Environment, 466-467 (2014) 1047-1059.

[178] X. Zhang, W. Wang, Y. Zhang, T. Zeng, C. Jia, L. Chang, Loading Cu-doped magnesium oxide onto surface of magnetic nanoparticles to prepare magnetic disinfectant with enhanced antibacterial activity, Colloids and Surfaces B: Biointerfaces, 161 (2018) 433-441.

[179] A. Najafpoor, R. Norouzian-Ostad, H. Alidadi, T. Rohani-Bastami, M. Davoudi, F. Barjasteh-Askari, J. Zanganeh, Effect of magnetic nanoparticles and silver-loaded magnetic nanoparticles on advanced wastewater treatment and disinfection, J Mol Liq, 303 (2020).

[180] A. Khazaei, N. Sarmasti, J. Yousefi Seyf, Z. Merati, Anchoring N-Halo (sodium dichloroisocyanurate) on the nano-Fe3O4 surface as “chlorine reservoir”: Antibacterial properties and wastewater treatment, Arab. J. Chem., 13 (2020) 2219-2232.

[181] S. Licht, A high capacity Li-ion cathode: the Fe (III/VI) super-iron cathode, Energies, 3 (2010) 960-972.

[182] V.K. Sharma, Oxidation of inorganic contaminants by ferrates (VI, V, and IV)–kinetics and mechanisms: a review, J. Environ. Manage., 92 (2011) 1051-1073.

[183] V.K. Sharma, R. Zboril, R.S. Varma, Ferrates: Greener Oxidants with Multimodal Action in Water Treatment Technologies, Accounts of Chemical Research, 48 (2015) 182-191.

[184] B.J. Ni, X. Yan, X. Dai, Z. Liu, W. Wei, S.L. Wu, Q. Xu, J. Sun, Ferrate effectively removes antibiotic resistance genes from wastewater through combined effect of microbial DNA damage and coagulation, Water Res., 185 (2020).

[185] L.S. Zhang, K.H. Wong, H.Y. Yip, C. Hu, J.C. Yu, C.Y. Chan, P.K. Wong, Effective photocatalytic disinfection of E. coli K-12 using AgBr-Ag-Bi 2WO6 nanojunction system irradiated by visible light: The role of diffusing hydroxyl radicals, Environmental Science and Technology, 44 (2010) 1392-1398.

[186] R. Xiao, L. Bai, K. Liu, Y. Shi, D. Minakata, C.H. Huang, R. Spinney, R. Seth, D.D. Dionysiou, Z. Wei, P. Sun, Elucidating sulfate radical-mediated disinfection profiles and mechanisms of Escherichia coli and Enterococcus faecalis in municipal wastewater, Water Res., 173 (2020).

[187] J.F. Gao, W.J. Duan, W.Z. Zhang, Z.L. Wu, Effects of persulfate treatment on antibiotic resistance genes abundance and the bacterial community in secondary effluent, Chemical Engineering Journal, 382 (2020).

[188] J.A. Malvestiti, A. Cruz-Alcalde, N. López-Vinent, R.F. Dantas, C. Sans, Catalytic ozonation by metal ions for municipal wastewater disinfection and simulataneous micropollutants removal, Appl. Catal. B Environ., 259 (2019).

[189] I. Arslan, I. Akmehmet Balcioglu, T. Tuhkanen, Advanced treatment of dyehouse effluents by Fe(II) and Mn(II)-catalyzed ozonation and the H2O2/O3 process, Water Science and Technology, 42 (2000) 13-18.

[190] A. Rodríguez, R. Rosal, J. Perdigón-Melón, M. Mezcua, A. Agüera, M. Hernando, P. Letón, A. Fernández-Alba, E. García-Calvo, Ozone-based technologies in water and

wastewater treatment, Emerging Contaminants from Industrial and Municipal Waste, Springer2008, pp. 127-175.

[191] G. Liu, F. Ling, E. Van Der Mark, X. Zhang, A. Knezev, J. Verberk, W. Van Der Meer, G. Medema, W.-T. Liu, J. Van Dijk, Comparison of particle-associated bacteria from a drinking water treatment plant and distribution reservoirs with different water sources, Scientific reports, 6 (2016) 20367.

[192] P. Soriano-Molina, S. Miralles-Cuevas, B. Esteban García, P. Plaza-Bolaños, J.A. Sánchez Pérez, Two strategies of solar photo-Fenton at neutral pH for the simultaneous disinfection and removal of contaminants of emerging concern. Comparative assessment in raceway pond reactors, Catal Today, (2019).

[193] I. de la Obra Jiménez, S. Giannakis, D. Grandjean, F. Breider, G. Grunauer, J.L. Casas López, J.A. Sánchez Pérez, C. Pulgarin, Unfolding the action mode of light and homogeneous vs. heterogeneous photo-Fenton in bacteria disinfection and concurrent elimination of micropollutants in urban wastewater, mediated by iron oxides in Raceway Pond Reactors, Appl. Catal. B Environ., 263 (2020).

[194] S. Nahim-Granados, J.A. Sánchez Pérez, M.I. Polo-Lopez, Effective solar processes in fresh-cut wastewater disinfection: Inactivation of pathogenic E. coli O157:H7 and Salmonella enteritidis, Catal Today, 313 (2018) 79-85.

[195] S.G. Michael, I. Michael-Kordatou, V.G. Beretsou, T. Jäger, C. Michael, T. Schwartz, D. Fatta-Kassinos, Solar photo-Fenton oxidation followed by adsorption on activated carbon for the minimisation of antibiotic resistance determinants and toxicity present in urban wastewater, Appl. Catal. B Environ., 244 (2019) 871-880.

[196] A. Di Cesare, M. De Carluccio, E.M. Eckert, D. Fontaneto, A. Fiorentino, G. Corno, P. Prete, R. Cucciniello, A. Proto, L. Rizzo, Combination of flow cytometry and molecular analysis to monitor the effect of UVC/H2O2 vs UVC/H2O2/Cu-IDS processes on pathogens and antibiotic resistant genes in secondary wastewater effluents, Water Res., 184 (2020).

[197] S. Giannakis, M.I. Polo López, D. Spuhler, J.A. Sánchez Pérez, P. Fernández Ibáñez, C. Pulgarin, Solar disinfection is an augmentable, in situ-generated photo-Fenton reaction—Part 1: A review of the mechanisms and the fundamental aspects of the process, Appl. Catal. B Environ., 199 (2016) 199-223.

[198] J. Fang, Y. Fu, C. Shang, The roles of reactive species in micropollutant degradation in the UV/free chlorine system, Environmental science & technology, 48 (2014) 1859-1868.

[199] T.K. Kim, T. Kim, H. Park, I. Lee, A. Jo, K. Choi, K.D. Zoh, Degradation of ciprofloxacin and inactivation of ciprofloxacin resistant E. faecium during UV-LED (275 nm)/chlorine process, Chemical Engineering Journal, 394 (2020).

[200] J. Rodríguez-Chueca, S. Guerra-Rodríguez, J.M. Raez, M.J. López-Muñoz, E. Rodríguez, Assessment of different iron species as activators of S2O82- and HSO5- for inactivation of wild bacteria strains, Appl. Catal. B Environ., 248 (2019) 54-61.

[201] I. Arslan-Alaton, A. Karatas, Ö. Pehlivan, O. Koba Ucun, T. Ölmez-Hancı, Effect of UV-A-assisted iron-based and UV-C-driven oxidation processes on organic matter and antibiotic resistance removal in tertiary treated urban wastewater, Catal Today, (2020).

[202] S.G. Michael, I. Michael-Kordatou, S. Nahim-Granados, M.I. Polo-López, J. Rocha, A.B. Martínez-Piernas, P. Fernández-Ibáñez, A. Agüera, C.M. Manaia, D. Fatta-Kassinos, Investigating the impact of UV-C/H2O2 and sunlight/H2O2 on the removal of antibiotics, antibiotic resistance determinants and toxicity present in urban wastewater, Chemical Engineering Journal, 388 (2020).

[203] M. Cho, H. Chung, W. Choi, J. Yoon, Linear correlation between inactivation of E. coli and OH radical concentration in TiO2 photocatalytic disinfection, Water Res., 38 (2004) 1069-1077.

[204] H.A. Foster, I.B. Ditta, S. Varghese, A. Steele, Photocatalytic disinfection using titanium dioxide: Spectrum and mechanism of antimicrobial activity, Appl. Microbiol. Biotechnol., 90 (2011) 1847-1868.

[205] A.G. Rincón, C. Pulgarin, Photocatalytical inactivation of E. coli: Effect of (continuous-intermittent) light intensity and of (suspended-fixed) TiO_2 concentration, Appl. Catal. B Environ., 44 (2003) 263-284.

[206] R.J. Watts, S. Kong, M.P. Orr, G.C. Miller, B.E. Henry, Photocatalytic inactivation of coliform bacteria and viruses in secondary wastewater effluent, Water Res., 29 (1995) 95-100.

[207] A.G. Rincón, C. Pulgarin, Bactericidal action of illuminated TiO2 on pure Escherichia coli and natural bacterial consortia: Post-irradiation events in the dark and assessment of the effective disinfection time, Appl. Catal. B Environ., 49 (2004) 99-112.

[208] H. Choi, M.G. Antoniou, A.A. de la Cruz, E. Stathatos, D.D. Dionysiou, Photocatalytic TiO2 films and membranes for the development of efficient wastewater treatment and reuse systems, Desalination, 202 (2007) 199-206.

[209] M. Martín-Sómer, C. Pablos, A. de Diego, R. van Grieken, Á. Encinas, V.M. Monsalvo, J. Marugán, Novel macroporous 3D photocatalytic foams for simultaneous wastewater disinfection and removal of contaminants of emerging concern, Chemical Engineering Journal, 366 (2019) 449-459.

[210] I. Zammit, V. Vaiano, A.R. Ribeiro, A.M.T. Silva, C.M. Manaia, L. Rizzo, Immobilised cerium-doped zinc oxide as a photocatalyst for the degradation of antibiotics and the inactivation of antibiotic-resistant bacteria, Catalysts, 9 (2019).

[211] P. Cañizares, C. Sáez, A. Sánchez-Carretero, M. Rodrigo, Synthesis of novel oxidants by electrochemical technology, Journal of Applied Electrochemistry, 39 (2009) 2143.

[212] B. Marselli, J. Garcia-Gomez, P.-A. Michaud, M. Rodrigo, C. Comninellis, Electrogeneration of hydroxyl radicals on boron-doped diamond electrodes, Journal of the Electrochemical Society, 150 (2003) D79.

[213] A.M. Polcaro, A. Vacca, M. Mascia, S. Palmas, R. Pompei, S. Laconi, Characterization of a stirred tank electrochemical cell for water disinfection processes, Electrochimica Acta, 52 (2007) 2595-2602.

[214] H. Särkkä, A. Bhatnagar, M. Sillanpää, Recent developments of electro-oxidation in water treatment - A review, J Electroanal Chem, 754 (2015) 46-56.

[215] Y. Chu, Y. Qian, W. Wang, X. Deng, A dual-cathode electro-Fenton oxidation coupled with anodic oxidation system used for 4-nitrophenol degradation, J. Hazard. Mater., 199 (2012) 179-185.

[216] A. Dhaouadi, L. Monser, N. Adhoum, Anodic oxidation and electro-Fenton treatment of rotenone, Electrochimica Acta, 54 (2009) 4473-4480.

[217] S. Cotillas, E. Lacasa, C. Sáez, P. Cañizares, M.A. Rodrigo, Disinfection of urine by conductive-diamond electrochemical oxidation, Appl. Catal. B Environ., 229 (2018) 63-70.

[218] M. Herraiz-Carboné, S. Cotillas, E. Lacasa, P. Cañizares, M.A. Rodrigo, C. Sáez, Removal of antibiotic resistant bacteria by electrolysis with diamond anodes: A pretreatment or a tertiary treatment?, J. Water Process Eng., 38 (2020).

[219] G. Chen, Electrochemical technologies in wastewater treatment, Sep. Purif. Technol., 38 (2004) 11-41.

[220] M.R. Cruz-Díaz, E.P. Rivero, F.A. Rodríguez, R. Domínguez-Bautista, Experimental study and mathematical modeling of the electrochemical degradation of dyeing wastewaters in presence of chloride ion with dimensional stable anodes (DSA) of expanded meshes in a FM01-LC reactor, Electrochimica Acta, 260 (2018) 726-737.

[221] H. Li, Z. Zhang, J. Duan, N. Li, B. Li, T. Song, M.F. Sardar, X. Lv, C. Zhu, Electrochemical disinfection of secondary effluent from a wastewater treatment plant: Removal efficiency of ARGs and variation of antibiotic resistance in surviving bacteria, Chemical Engineering Journal, 392 (2020).

[222] B. Rajasekhar, U. Venkateshwaran, N. Durairaj, G. Divyapriya, I.M. Nambi, A. Joseph, Comprehensive treatment of urban wastewaters using electrochemical advanced oxidation process, J. Environ. Manage., 266 (2020).

[223] S. Cotillas, J. Llanos, I. Moraleda, P. Cañizares, M.A. Rodrigo, Scaling-up an integrated electrodisinfection-electrocoagulation process for wastewater reclamation, Chemical Engineering Journal, 380 (2020).

[224] P. Verlicchi, A. Galletti, M. Petrovic, D. Barceló, Hospital effluents as a source of emerging pollutants: an overview of micropollutants and sustainable treatment options, Journal of Hydrology, 389 (2010) 416-428.

[225] L.H. Santos, M. Gros, S. Rodriguez-Mozaz, C. Delerue-Matos, A. Pena, D. Barceló, M.C.B. Montenegro, Contribution of hospital effluents to the load of pharmaceuticals in urban wastewaters: identification of ecologically relevant pharmaceuticals, Science of the Total Environment, 461 (2013) 302-316.

[226] P. Verlicchi, A. Galletti, M. Al Aukidy, Hospital wastewaters: quali-quantitative characterization and for strategies for their treatment and disposal, Wastewater reuse and management, Springer2013, pp. 225-251.

[227] B. Aslam, W. Wang, M.I. Arshad, M. Khurshid, S. Muzammil, M.H. Rasool, M.A. Nisar, R.F. Alvi, M.A. Aslam, M.U. Qamar, M.K.F. Salamat, Z. Baloch, Antibiotic resistance: a rundown of a global crisis, Infect Drug Resist, 11 (2018) 1645-1658.

[228] J. Hopman, C. Meijer, N. Kenters, J.P. Coolen, M.R. Ghamati, S. Mehtar, R. van Crevel, W.J. Morshuis, A.F. Verhagen, M.M. van den Heuvel, Risk assessment after a severe hospital-acquired infection associated with Carbapenemase-producing Pseudomonas aeruginosa, JAMA network open, 2 (2019) e187665-e187665.

[229] J.H. So, J. Kim, I.K. Bae, S.H. Jeong, S.H. Kim, S.-k. Lim, Y.H. Park, K. Lee, Dissemination of multidrug-resistant Escherichia coli in Korean veterinary hospitals, Diagnostic Microbiology and Infectious Disease, 73 (2012) 195-199.

[230] U. Nielsen, C. Hastrup, M.M. Klausen, B.M. Pedersen, G.H. Kristensen, J.L.C. Jansen, S.N. Bak, J. Tuerk, Removal of APIs and bacteria from hospital wastewater by MBR plus O 3, O3 + H2O2, PAC or ClO2, Water Science and Technology, 67 (2013) 854-862.

[231] A.K. Gautam, S. Kumar, P.C. Sabumon, Preliminary study of physico-chemical treatment options for hospital wastewater, J. Environ. Manage., 83 (2007) 298-306.

[232] S. Fijan, S.S. Turk, Inactivation of enterococcus faecium in water and hospital laundry wastewater by disinfection processes utilizing peroxyacetic acid or ultraviolet radiation, J. Pure Appl. Microbiol., 8 (2014) 531-538.

[233] S. Yao, J. Ye, Q. Yang, Y. Hu, T. Zhang, L. Jiang, S. Munezero, K. Lin, C. Cui, Occurrence and removal of antibiotics, antibiotic resistance genes, and bacterial communities in hospital wastewater, Environ. Sci. Pollut. Res., (2021).

[234] H. Wang, J. Wang, S. Li, G. Ding, K. Wang, T. Zhuang, X. Huang, X. Wang, Synergistic effect of UV/chlorine in bacterial inactivation, resistance gene removal, and gene conjugative transfer blocking, Water Res., 185 (2020) 116290.

[235] Y. Hu, T. Zhang, L. Jiang, Y. Luo, S. Yao, D. Zhang, K. Lin, C. Cui, Occurrence and reduction of antibiotic resistance genes in conventional and advanced drinking water treatment processes, Science of the Total Environment, 669 (2019) 777-784.

[236] M.-T. Guo, Q.-B. Yuan, J. Yang, Distinguishing effects of ultraviolet exposure and chlorination on the horizontal transfer of antibiotic resistance genes in municipal wastewater, Environmental science & technology, 49 (2015) 5771-5778.

[237] C. Huang, C. Dong, Z. Tang, Advanced chemical oxidation: its present role and potential future in hazardous waste treatment, Waste management, 13 (1993) 361-377.

[238] C.F. Chiang, C.T. Tsai, S.T. Lin, C.P. Huo, K.V. Lo, Disinfection of Hospital Wastewater by Continuous Ozonization, J. Environ. Sci. Health Part A Toxic Hazard. Subst. Environ. Eng., 38 (2003) 2895-2908.

[239] E. Sozzi, K. Fabre, J.F. Fesselet, J.E. Ebdon, H. Taylor, Minimizing the risk of disease transmission in emergency settings: Novel in situ physico-chemical disinfection of pathogen-laden hospital Wastewaters, PLoS. Negl. Trop. Dis., 9 (2015).

[240] D.D. Mara, S. Cairncross, W.H. Organization, Guidelines for the safe use of wastewater and excreta in agriculture and aquaculture: measures for public health protection, World Health Organization1989.

[241] H. Yang, H. Cheng, Controlling nitrite level in drinking water by chlorination and chloramination, Sep. Purif. Technol., 56 (2007) 392-396.

[242] J. Lu, T. Zhang, J. Ma, Z. Chen, Evaluation of disinfection by-products formation during chlorination and chloramination of dissolved natural organic matter fractions isolated from a filtered river water, J. Hazard. Mater., 162 (2009) 140-145.

[243] B. Pauwels, W. Verstraete, The treatment of hospital wastewater: An appraisal, J. Water Health, 4 (2006) 405-416.

[244] C.A. Somensi, E.L. Simionatto, J.B. Dalmarco, P. Gaspareto, C.M. Radetski, A comparison between ozonolysis and sonolysis/ozonolysis treatments for the degradation of the cytostatic drugs methotrexate and doxorubicin: Kinetic and efficiency approaches, Journal of Environmental Science and Health, Part A, 47 (2012) 1543-1550.

[245] E.A. Serna-Galvis, E. Vélez-Peña, P. Osorio-Vargas, J.N. Jiménez, L. Salazar-Ospina, Y.M. Guaca-González, R.A. Torres-Palma, Inactivation of carbapenem-resistant Klebsiella pneumoniae by photo-Fenton: Residual effect, gene evolution and modifications with citric acid and persulfate, Water Res., 161 (2019) 354-363.

[246] M. Munoz, P. Garcia-Muñoz, G. Pliego, Z.M. De Pedro, J.A. Zazo, J.A. Casas, J.J. Rodriguez, Application of intensified Fenton oxidation to the treatment of hospital wastewater: Kinetics, ecotoxicity and disinfection, J. Environ. Chem. Eng., 4 (2016) 4107-4112.

[247] Y. Luo, L. Feng, Y. Liu, L. Zhang, Disinfection by-products formation and acute toxicity variation of hospital wastewater under different disinfection processes, Sep. Purif. Technol., 238 (2020).

[248] G. Moussavi, E. Fathi, M. Moradi, Advanced disinfecting and post-treating the biologically treated hospital wastewater in the UVC/H2O2 and VUV/H2O2 processes: Performance comparison and detoxification efficiency, Process Saf. Environ. Prot., 126 (2019) 259-268.

[249] J.C. Mierzwa, R. Rodrigues, A.C.S.C. Teixeira, Chapter 2 - UV-Hydrogen Peroxide Processes, in: S.C. Ameta, R. Ameta (Eds.) Advanced Oxidation Processes for Waste Water Treatment, Academic Press2018, pp. 13-48.

[250] A. Almeida, Â. Cunha, N. Gomes, E. Alves, L. Costa, M.A. Faustino, Phage therapy and photodynamic therapy: low environmental impact approaches to inactivate microorganisms in fish farming plants, Marine drugs, 7 (2009) 268-313.

[251] A. Almeida, Â. Cunha, M. Faustino, A. Tomé, M. Neves, Photodynamic Inactivation of Microbial Pathogens, Medical and Environmental Applications in Porphyrins as Antimicrobial Photosensitizing Agents, ed. MR Hamblin and G. Jori, RSC Publishing, Cambridge, 2011.

[252] J. Almeida, J.P.C. Tomé, M.G.P.M.S. Neves, A.C. Tomé, J.A.S. Cavaleiro, A. Cunha, L. Costa, M.A.F. Faustino, A. Almeida, Photodynamic inactivation of multidrug-resistant bacteria in hospital wastewaters: Influence of residual antibiotics, Photochem. Photobiol. Sci., 13 (2014) 626-633.

[253] V. Naddeo, V. Belgiorno, D. Kassinos, D. Mantzavinos, S. Meric, Ultrasonic degradation, mineralization and detoxification of diclofenac in water: Optimization of operating parameters, Ultrasonics Sonochemistry, 17 (2010) 179-185.

[254] V. Naddeo, D. Ricco, D. Scannapieco, V. Belgiorno, Degradation of Antibiotics in Wastewater during Sonolysis, Ozonation, and Their Simultaneous Application: Operating Conditions Effects and Processes Evaluation, International Journal of Photoenergy, 2012 (2012) 624270.

[255] C.A. Somensi, A.L.F. Souza, E.L. Simionatto, P. Gaspareto, M. Millet, C.M. Radetski, Genetic material present in hospital wastewaters: Evaluation of the efficiency of DNA denaturation by ozonolysis and ozonolysis/sonolysis treatments, J. Environ. Manage., 162 (2015) 74-80.

[256] M.I. Litter, Heterogeneous photocatalysis: transition metal ions in photocatalytic systems, Appl. Catal. B Environ., 23 (1999) 89-114.

[257] Ê.L. Machado, L.T. Kist, R. Schmidt, J.M. Hoeltz, D. Dalberto, E.L.A. Alcayaga, Secondary hospital wastewater detoxification and disinfection by advanced oxidation processes, Environ. Technol., 28 (2007) 1135-1143.

[258] L.T. Kis, C. Albrech, Ê.L. Machado, Hospital laundry wastewater disinfection with catalytic photoozonation, Clean Soil Air Water, 36 (2008) 775-780.

[259] J. Zhou, S. Wang, Z. Xue, X. Song, Disinfection of hospital wastewater by Ti/SnO2-Sb2O3/β-PbO2 anode, Chin. J. Environ. Eng., 8 (2014) 4110-4114.

[260] A. Rieder, T. Schwartz, K. Schön-Hölz, S.M. Marten, J. Süß, C. Gusbeth, W. Kohnen, W. Swoboda, U. Obst, W. Frey, Molecular monitoring of inactivation efficiencies of bacteria during pulsed electric field treatment of clinical wastewater, J. Appl. Microbiol., 105 (2008) 2035-2045.

[261] J. Lienert, M. Koller, J. Konrad, C.S. McArdell, N. Schuwirth, Multiple-Criteria Decision Analysis Reveals High Stakeholder Preference to Remove Pharmaceuticals from Hospital Wastewater, Environmental Science & Technology, 45 (2011) 3848-3857.

[262] M. Al Aukidy, P. Verlicchi, N. Voulvoulis, A framework for the assessment of the environmental risk posed by pharmaceuticals originating from hospital effluents, Science of the Total Environment, 493 (2014) 54-64.

[263] R. Zhang, P. Sun, T.H. Boyer, L. Zhao, C.-H. Huang, Degradation of pharmaceuticals and metabolite in synthetic human urine by UV, UV/H2O2, and UV/PDS, Environmental science & technology, 49 (2015) 3056-3066.

[264] J. Lienert, M. Koller, J. Konrad, C.S. McArdell, N. Schuwirth, Multiple-criteria decision analysis reveals high stakeholder preference to remove pharmaceuticals from hospital wastewater, ACS Publications, 2011.

[265] I. Ieropoulos, G. Pasternak, J. Greenman, Urine disinfection and in situ pathogen killing using a Microbial Fuel Cell cascade system, PLoS ONE, 12 (2017).

[266] I. Ieropoulos, O. Obata, G. Pasternak, J. Greenman, Fate of three bioluminescent pathogenic bacteria fed through a cascade of urine microbial fuel cells, J. Ind. Microbiol. Biotechnol., 46 (2019) 587-599.

[267] S. Dbira, N. Bensalah, A. Bedoui, P. Cañizares, M.A. Rodrigo, Treatment of synthetic urine by electrochemical oxidation using conductive-diamond anodes, Environmental Science and Pollution Research, 22 (2015) 6176-6184.

[268] S. Giannakis, B. Androulaki, C. Comninellis, C. Pulgarin, Wastewater and urine treatment by UVC-based advanced oxidation processes: Implications from the interactions of bacteria, viruses, and chemical contaminants, Chemical Engineering Journal, 343 (2018) 270-282.

[269] A.S. Raut, G.B. Cunningham, C.B. Parker, E.J.D. Klem, B.R. Stoner, M.A. Deshusses, J.T. Glass, Disinfection of E. coli contaminated urine using boron-doped diamond electrodes, J Electrochem Soc, 161 (2014) G81-G85.

[270] A.S. Raut, C.B. Parker, E.J.D. Klem, B.R. Stoner, M.A. Deshusses, J.T. Glass, Reduction in energy for electrochemical disinfection of E. coli in urine simulant, J Appl Electrochem, 49 (2019) 443-453.

[271] M.J. Martin De Vidales, M. Millán, C. Sáez, P. Cañizares, M.A. Rodrigo, What happens to inorganic nitrogen species during conductive diamond electrochemical oxidation of real wastewater?, Electrochemistry Communications, 67 (2016) 65-68.

[272] E. Lacasa, P. Cañizares, J. Llanos, M.A. Rodrigo, Effect of the cathode material on the removal of nitrates by electrolysis in non-chloride media, Journal of Hazardous Materials, 213-214 (2012) 478-484.

[273] S. Dbira, N. Bensalah, M.I. Ahmad, A. Bedoui, Electrochemical oxidation/disinfection of urine wastewaters with different anode materials, Mater., 12 (2019).

[274] J. Singla, V.K. Sangal, A. Singh, A. Verma, Application of mixed metal oxide anode for the electro-oxidation/disinfection of synthetic urine: Potential of harnessing molecular hydrogen generation, J. Environ. Manage., 255 (2020).

CHAPTER 3:

BACKGROUND RESEARCH, OBJECTIVES AND EXPERIMENTAL PLANNING

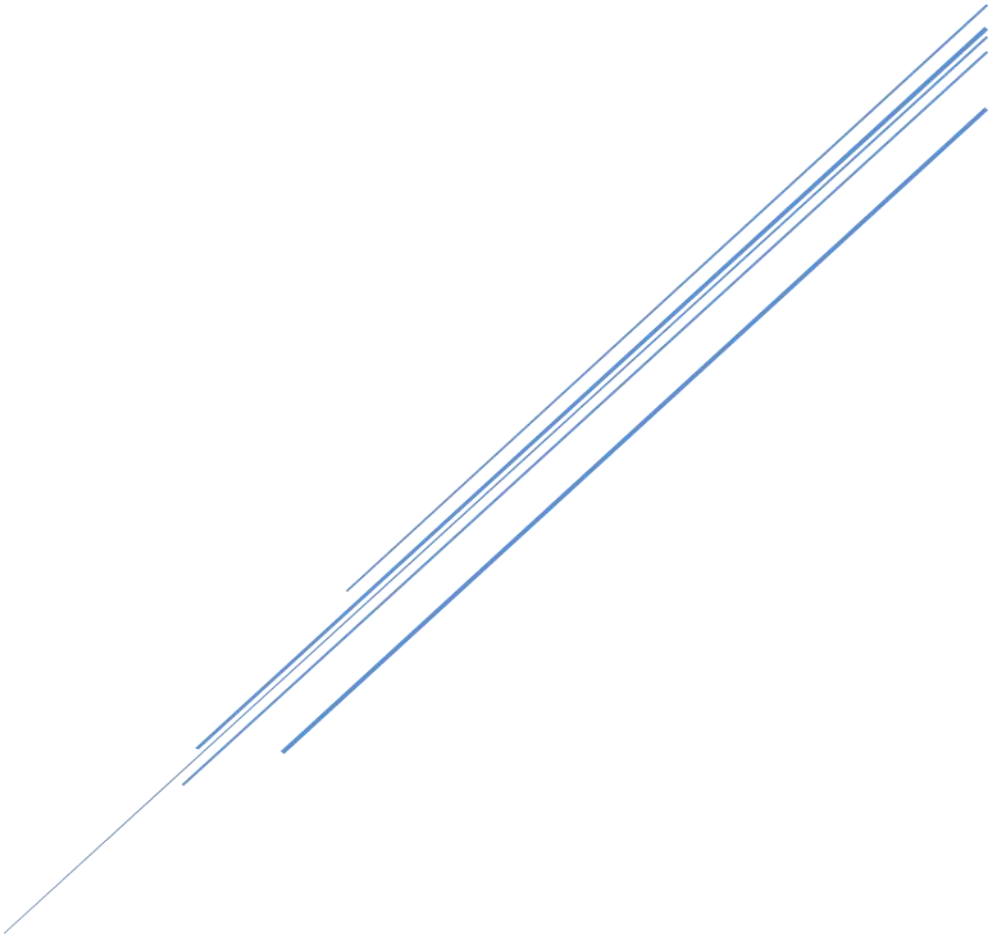

The presence of antibiotic-resistant bacteria (ARB) and other pathogens in water bodies has become a major environmental challenge because of the potential threats they can pose to human health. This problem has been exacerbated by the increasing and uncontrolled consumption of antibiotics worldwide, and the absence of efficient technologies for killing these pathogens at large scale.

Hospitals present a friendly environment for the spread of ARB because of the high concentration of pathogens, viruses, fungi and drugs contained in their effluents. Thus, the proper management of the hospital effluents is fundamental to minimize its adverse effects on health and the environment. Currently no restrictions are foreseen in the European Directive 91/271/EEC for hospital effluents. Hospital wastewater greatly affect the loads of contaminants arriving to WWTPs, prompting the scientific community to question the acceptability of the general practice of discharging it into public sewers to be treated in municipal WWTPs together with urban wastewater. The inefficiency of biological treatments from WWTPs to treat sanitary effluents leads the spread of chemicals, pathogens and ARB in the environmental water sources, negatively affecting aquatic organisms and human health. This has led to the proliferation of numerous studies searching for technological solutions in order to decrease the impact of sanitary effluents into the environment.

Within effluents generated in a hospital complex, urine can be considered one of the most dangerous ones because they contribute to: 1) diffusion of products metabolized by the human body, between 55-80% of ingested drug is excreted in the urine; and 2) diffusion of pathogens (viruses, fungi and bacteria) due to the proliferation and/or accumulation of certain microorganisms in the urinary tract in mainly immunocompromised patients in whom their immune system is unable to control the infection. Generally, hospital urine (with a generation rate of around 2.5 L person-1 day^{-1}) is mixed with the rest of the liquid waste generated in the hospital (grey water, water from cafeterias / restaurants ...), and mixed hospital effluent (generation rate around 100-1400 l bed^{-1} day^{-1}) reaches conventional urban wastewater treatment plants without prior treatment. The contribution of hospital urine to the total effluent does not amount to more than 2-3% by volume, but the concentration of contaminants can be up to 3-

fold higher than the average concentration of hospital wastewater. Then, the inappropriate management of urine can lead to discharges and mixtures with other less dangerous effluents, which facilitates the diffusion of these agents and makes urine a potential vector for the transmission of dangerous diseases. All this makes urine treatment a key objective for reducing the environmental and health impact of hospital effluents.

In this context, this PhD Thesis has been intended to develop a process based on electrochemical technologies to reduce the environmental and sanitary impact of hospital effluents by direct treatment of hospital urine, due to their chemical and biological risk. The thesis has been carried out in the Laboratory of Chemical Engineering (Higher Technical School of Industrial Engineering in Albacete) belonging the Laboratory of Electrochemical and Environmental Engineering (E3L, inside the TEQUIMA research group) (Faculty of Chemical Sciences and Technologies in Ciudad Real) of the Chemical Engineering Department of the University of Castilla la Mancha, and it is included in the Doctorate Program "Ingeniería Química y Ambiental", which is regulated through the Spanish Law RD 99/2011. The E3L has been working in the development of electrochemical processes for wastewater treatment since 1999. In this general topic, eighteen doctoral theses have been carried out to evaluate the applicability of electrochemical processes for the treatment of wastewater, the disinfection of water as well as the production of powerful oxidants.

The research background in electrochemical disinfection in aqueous effluents began with the development of the doctoral thesis of Dr. S. Cotillas (2015), in which the integration of different electrochemical technologies (electrodisinfection, electrocoagulation, electrodialysis, electrochlorination, electroFenton) was evaluated in a single stage to reduce the investment and operating costs in regeneration processes of real urban treated wastewater according to the *Real Decreto 1620/2007*. This research study continued with the development of the doctoral thesis of Dra. J. Isidro (2020), financed by the European project SafeWaterAfrica (grant agreement No 689925), in which one of the main objectives was to evaluate if the electrochemical technology developed by CONDIAS GmbH was efficient in the disinfection of low-quality surface

water to provide high-quality water to rural population in African countries. In this study, it was observed that the cell design and the disinfection strategy had a significant influence on the performance of the electrodisinfection processes and on the formation of undesirable by-products. In this point, more scientific effort is needed mainly in the aspect of reducing the formation of un-desirable by-products and the ecotoxicity risk, as well as improving energy efficiency by optimizing cell design to reduce operational cost. In fact, one of the challenges of research community is the design of appropriate electrochemical reactor to make this technology competitive with conventional technologies. This implies not only the implementation of a suitable anode but also the synergistic use of the cathode reaction and the promotion of mediated oxidation processes in the bulk during the treatment. In addition, the increase in the mass transfer rate inside the cell is also important. Thus, an efficient mechanical design of the cell and a careful choice of the operation conditions are critical to achieve good performance. In this field, during the doctoral thesis of J.F. Pérez (2018) a novel flow-through electrochemical reactor with microfluidic geometry, which allows to reduce ohmic resistance and maximize the mass transfer (two of the main restrictions of electrochemical reactors), was developed to generate hydrogen peroxide.

In this context, the present doctoral thesis is framed within the regional project entitled “Electrochemical technologies for the treatment of hospital urines: reduction of environmental and health impact (SBPLY/17/180501/000396)”, funded by *Junta de Comunidades de Castilla-La Mancha* and European Union (European Regional Development Fund), and the national project entitled “Electrochemical technologies facing the challenge of hospital urine treatment (PID2019-110904RB-I00)”, funded by the Ministry of Science and Innovation. The main objective of the present PhD Thesis is to assess the technical feasibility of different electrochemical processes including electrolysis and photoelectrolysis, to reduce the environmental and health impact of ARB from hospital urines, avoiding the formation of undesired disinfection by-products. To attain this goal, it is planned to work in parallel on two levels: 1) Knowledge generation: field study to define the problem of hospital urines, taking as a case of study the University Hospital of Albacete (*Complejo Hospitalario Universitario*

de Albacete, CHUA), 2) Scientific-technical development: to evaluate the most appropriate electrochemical reactor to reduce the biological risk of hospital urines. Based on this, the partial objectives of this thesis are:

1. *To analyse in a prospective way the urine generated in a hospital, taking into account its biological risk, to clarify the real impact of the urine to hospital wastewater.* A statistical and prevalence study is carried out to identify the main pathogens (fungi and bacteria) causing urinary tract infections (UTIs) in hospitalized patients from the University Hospital Complex of Albacete (Spain) as a case of study. This study is faced in section 5.1.
2. *To evaluate the feasibility of electrodisinfection to treat hospital urines with biological risk*. This allows to shed light on the role of water matrix on the disinfection performance and, hence, to stablish the best treatment point (as tertiary treatment of urban wastewater or as pretreatment of the main pollution source) for decreasing the sanitary and environmental hazardousness associated to ARB. The reduction of the potential chemical risk of urine during the disinfection process is also tested. This study is faced in section 5.2.
3. *To evaluate different electrochemical reactors to be used for the removal of pathogens in synthetic urine*, with the aim of optimizing operating conditions and evaluating disinfection mechanisms involved in the electrochemical disinfection process. To do this, the role of the main disinfectant species (hypochlorite, chloramines, hydrogen peroxide and ozone) that can be electrogenerated during the electrochemical disinfection of hospital urines is evaluated in depth in section 5.3.
4. *To evaluate the combination of electrolysis with another commonly used disinfection technology, UV light irradiation.* The evaluation of synergies or antagonisms of electrogenerated oxidants when coupling UV irradiation on the electrochemical disinfection process is carried out in section 5.4.
5. *To verify and adjust the operating conditions of the selected electrochemical technology for the treatment of complex synthetic urine matrices (polymicrobial urines),* that are selected based on the results in the statistical and prevalence study.

The denaturation of antibiotic resistance genes and the disinfection mechanisms of the oxidants electrogenerated are also described in section 5.5.

CHAPTER 4:

MATERIALS, METHODOLOGY AND EXPERIMENTAL PROCEDURES

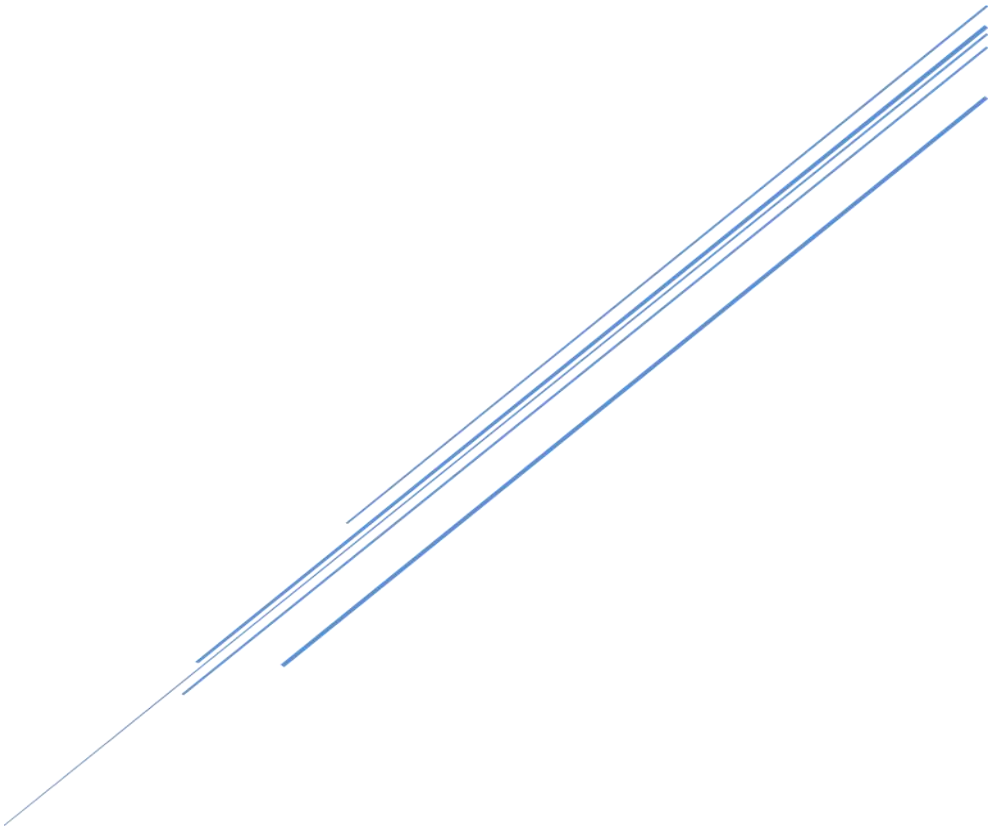

4.1. Reagents, biological strains and water matrices.

In this section, the main chemical reagents used are listed in Table 4.1.

Table 4.1. Reagents employed.

Reagent	Purity	Supplier
Formic acid (CH_2O_2)	90 %	VWR
Methanol (CH_3OH)	100 %	VWR
Acetone (C_3H_6O)	100 %	VWR
Sodium carbonate (Na_2CO_3)	99.95 -100.05 %	Sigma Aldrich
Dipicolinic acid (2,6-$(HOOC)_2C_5H_3N$)	0.02 M	Sigma Aldrich
Nitric acid (HNO_3)	65 %	VWR
Sodium thiosulphate ($Na_2S_2O_3 \cdot 5H_2O$)	1 N	Sigma Aldrich
Potassium iodide (KI)	99 %	Panreac
Starch ($(C_6H_{10}O_5)n$)	1	Panreac
Arsenic trioxide (As_2O_3)	99.999 %	Sigma Aldrich
Potassium phosphate monobasic (KH_2PO_4)	≥ 99 %	Sigma Aldrich
Sodium phosphate dibasic (Na_2HPO_4)	≥ 99 %	Sigma Aldrich
Ethylenediaminetetraacetic acid (EDTA)	≥ 98 %	Sigma Aldrich
N,N-Diethyl-p-phenylenediamine sulfate	≥ 98 %	Sigma Aldrich
Sulfuric acid (H_2SO_4)	98 %	VWR
Sodium hydroxide (NaOH)	98,0 - 100,5 %	Panreac
Hydrogen peroxide (H_2O_2)	33 %	Panreac
Urea (CH_4N_2O)	≥ 98 %	Sigma Aldrich
Uric acid ($C_5H_4N_4O_3$)	≥ 99 %	Sigma Aldrich
Creatinine ($C_4H_7N_3O$)	≥ 98 %	Sigma Aldrich
Potassium chloride (KCl)	≥ 99 %	Sigma Aldrich
Magnesium sulfate ($MgSO_4$)	≥ 97 %	Sigma Aldrich
Calcium phosphate ($(Ca)_3(PO_4)_2$)	≥ 96 %	Sigma Aldrich
Sodium carbonate (Na_2CO_3)	≥ 99.95 %	Sigma Aldrich
Ammonium phosphate ($(NH_4)_2HPO_4$)	≥ 98 %	Sigma Aldrich
Sodium chloride (NaCl)	≥ 99.95 %	Sigma Aldrich
Ammonium sulfate ($(NH_4)_2SO_4$)	99 %	Panreac
Magnesium chloride ($MgCl_2$)	99,0 – 102,0 %	Panreac
Calcium sulfate ($CaSO_4$)	98-101 %	Sigma Aldrich
Sodium nitrate ($NaNO_3$)	99 %	Panreac
Sodium phosphate (Na_3PO_4)	≥ 99 %	Sigma Aldrich
Humic acid	100 %	Sigma Aldrich
Chloramphenicol ($C_{11}H_{12}Cl_2N_2O_5$)	≥ 98 %	Sigma Aldrich

The bacterial strains used during the disinfection tests carried out in this work are summarized in Table 4.2.

Table 4.2. Bacterial strains used.

Bacteria	Strains	Supplier
E. faecalis	ATCC 19433	CECT, Spain
	ATCC 51299	CECT, Spain
E. coli	ATCC 25922	CECT, Spain
	ATCC 35218	CECT, Spain
K. pneumoniae	ATCC 4352	CECT, Spain
	ATCC BAA-1705	ThermoFisher Scientific, Spain

Additionally, two main water sources were selected to simulate different samples composition: urban treated wastewater and hospital urine. The urban treated wastewater was prepared according to the typical chemical composition found at the outlet of the municipal Wastewater Treatment Plant of Albacete (Spain). The hospital urine was prepared based on the chemical composition given by Dbira et al. [1]. The compositions of both water matrices are shown in Table 4.3.

Table 4.3. Target effluents composition.

Species	Urban treated wastewater (mg dm^{-3})	Hospital urine (mg dm^{-3})
Cl^-	148.22	475.52
NO_3^-	10.94	-
PO_4^{3-}	5.79	59.94
SO_4^{2-}	299.37	135.58
CO_3^{2-}	90.58	94.35
Na^+	97.39	72.34
K^+	31.47	524.45
NH_4^+	40.87	22.72
Ca^{2+}	79.48	10.99
Mg^{2+}	30.63	34.33
Humic acids	20.00	-
CH_4N_2O (Urea)	-	3,333.33
$C_4H_7N_3O$ (Creatinine)	-	166.67
$C_5H_4N_4O_3$ (Uric acid)	-	50.00

To simulate water matrices polluted with pathogenic microorganisms, urban treated wastewater and hospital urine were intensified with pure cultures of bacteria. The target bacteria were *K. pneumoniae*, *E. coli* and/or *E. faecalis* detailed in Table 4.2. Prior to each experiment, bacteria were incubated at 37 ºC for 18-24 h using the culture medium Tryptone Soy Agar ISO. Then, bacteria were added to water matrices to reach initial concentrations around 10^7 CFU ml^{-1}.

4.2. Electrodes

4.2.1. Mixed metal oxide

The mixed metal oxides (MMO) electrodes were supplied by Ti-Anode (India). In this work, both plate and mesh electrodes were used depending on the hydrodynamic design of the electrochemical cell tested. Plate electrodes were circular shape with a diameter of 10 cm (active area of 78.54 cm^2) and consisted of RuO_2/IrO_2 coatings supported on titanium plates. Mesh electrodes were square shape with dimensions of 9.5 × 8 cm^2 (active are of 53 cm^2) and consisted of IrO_2/Ta_2O_5 (70:30) coatings supported on titanium meshes. As a previous stage to electrochemical tests, MMO electrodes were typically electrolyzed for 10 minutes with 5000 mg dm^{-3} sodium sulfate (pH 2.0) at 300 A m^{-2} to remove any impurity contained on their surface.

4.2.2. Boron-doped diamond

Different geometrical shapes and dimensions of boron-doped diamond (BDD) electrodes were tested depending on the hydrodynamic design of the electrochemical cell tested:

- BDD plate electrode was supplied by Adamant Technologies (currently NeoCoat/WaterDiam, France). This electrode was circular shape with a diameter of 10 cm (active area of 78.54 cm^2) and consisted of a boron layer of 2.93 µm thickness and a concentration in the coatings of 500 ppm with a ratio sp^3/sp^2 of 256.

- BDD mesh electrodes were supplied by Condias GmbH (Germany). These electrodes were thin-film BDD electrodes supported on a niobium mesh (Diachem®) with a square shape of 9.5 × 8 cm^2 (active area of 50 cm^2). Additionally, BDD electrodes DIACHEM® (15 x 7.5 x 0.725 mm^3) synthetized on a structured silicon substrate were also employed.

As a previous stage to electrochemical tests, BDD electrodes were typically electrolyzed for 10 minutes with 5000 mg dm^{-3} sodium sulfate (pH 2.0) at 300 A m^{-2} to remove any impurity contained on their surface.

4.2.3. Stainless steel

The electrodes used as cathodes were a stainless-steel plate type AISI 304 with a diameter of 10 cm (total surface of 78.54 cm^2) and a stainless-steel mesh electrode with a square shape of 9.5 x 8 cm^2. The steel is subjected to several pre-treatment steps including degreasing with acetone, sanding with silicon carbide and rinsing with deionised water in an ultrasonic bath. In addition, before each electrochemical process, a pre-treatment was carried out for 10 minutes with 5000 mg dm^{-3} sodium sulfate (pH 2.0) at 300 A m^{-2} to remove any possible oxide produced in the surface.

4.3. Experimental setups

4.3.1. Electrolysis facilities and reactors

Two experimental facilities and three different reactors have been used during the development of this work. Firstly, the bench experimental setup integrated an electrochemical cell with a power supply, a peristaltic pump, a reservoir tank and a heat exchanger (Figure 4.1). The cell was connected to the reservoir tank by a peristatic pump (JP Selecta Percom N-M) and powered by a power supply (Delta Electronika ES030-10, 0-30 V, 0-10 A). Synthetic water matrices were stored in a glass tank (1.0 dm^3). The flow rate was kept constant, and the temperature was maintained at the desired set point (25 °C) by means of a thermostatic bath (Digiterm S-150 JP Selecta).

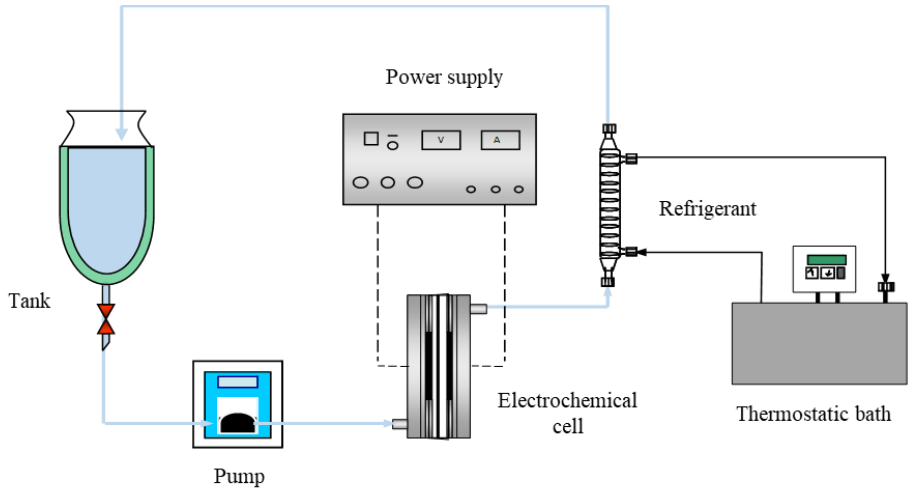

Figure 4.1. Experimental setup of electrolysis tests in discontinuous mode. Bench scale.

The experimental setup shown in Figure 4.1 has been used with two different electrochemical reactors; a parallel-flow cell and a MIKROZON® cell.

- A single-compartment electrochemical parallel-flow cell was selected because its technology is easy to be scaled-up and it fits well to the treatment of polluted effluents since it has a large surface/volume ratio, which helps to attain an optimum performance of the electrochemical processes (Figure 4.2a). The cell can be equipped with circular electrodes (10 cm diameter), and it had an interelectrode gap of 9 mm. The electrochemical tests were carried out in a galvanostatic mode selecting a constant current intensity and the flow rate was kept constant at 40 $dm^3\ h^{-1}$. The applied current density was in the range of 5 to 50 A m^{-2} for disinfection experiments and in the range of 12.5 to 50 A m^{-2} for the removal of antibiotics.
- A PEM-electrolyzer especially designed to produce ozone in low-conductivity water, the MIKROZON® cell (Figure 4.2b), manufactured by CONDIAS GmbH (Germany). It is equipped with two DIACHEM® electrodes (diamond coating on a structured silicon substrate), which are arranged in a membrane electrode assembly with a fumasep® cation exchange membrane. Table 4.4 shows the specification data sheet of

this commercial cell. The electrochemical disinfection tests were carried out in a galvanostatic mode selecting a constant current intensity in the MIKROZON® cell and the flow rate was kept constant at 30 dm^3 h^{-1} due to pump limitations. The applied intensity was in the range of 0.1 to 1.0 A.

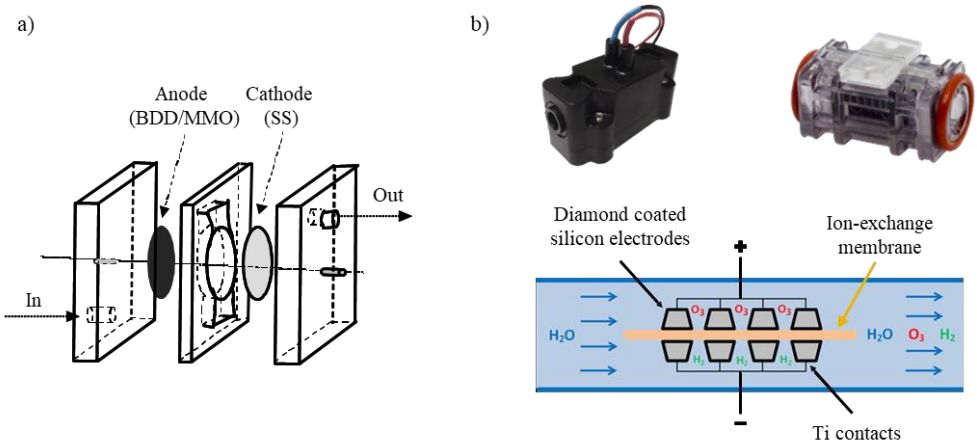

Figure 4.2. a) Single-compartment electrochemical parallel-flow cell. b) MIKROZON® cell.

Table 4.4. Specification data sheet of the MIKROZON® cell.

Technical information	
Temperature limits of medium	40 ºC
Pressure (max.)	10 bar
Flow rate	0.5 up to 1.5 l min^{-1}
Current (Continuous operation)	1.2 A
Voltage (max.)	24 V
Wetted materials	PVDF, PSU, Titanium, EPDM, Silicone
Stack properties	
Anodes	DIACHEM® electrode
Cathodes	DIACHEM® electrode
Electrode dimensions	15 mm x 7.5 mm x 0.725 mm
Membrane	Fumasep®
Active anodic area	112.5 mm^2
Cell dimension	61 mm x 31 mm x 36 mm
Weigh	70 g

Secondly, another experimental setup was modified to meet with the requirements of the last reactor employed. This experimental setup is based on the one previously shown (Figure 4.1) but integrating another design of electrochemical cell with a power supply, a peristaltic pump, a reservoir tank and a heat exchanger (Figure 4.3). The electrochemical cell used was a microfluidic flow-through reactor in which the electrodes of mesh-type geometry faced parallel to each other, allowing the effluent to pass through them. The cell consists in two symmetric pieces held together by compression where each piece holds one electrode which were separated by means of a solid PTFE plastic film (thickness 100 μm). Thin aluminium foils (≈25 μm) were attached at both sides of the PTFE film and were in contact with the electrodes (but not with the electrolyte) acting as current feeders, creating an inter-electrode gap of about 150 μm. This cell minimises the ohmic drop while maximising the mass transport [2, 3].

The cell was connected to the reservoir tank self-priming liquid ring pump by a peristatic pump (JP Selecta Percom N-M) or a self-priming liquid ring pump (Rover Pompe BE-M 10) and powered by a power supply (Delta Electronika ES030-10, 0-30 V, 0-10 A). Synthetic water matrices were stored in a plastic tank (2.0 dm^3) fabricated with polyvinyl chloride (PVC) and polyamide (Tecalan®). The flow rate was kept constant at 40 $dm^3\ h^{-1}$ or 160 $dm^3\ h^{-1}$, and the temperature was maintained at 25 °C by means of a thermostatic bath (Digiterm S-150 JP Selecta).

The electrochemical disinfection tests were carried out in a galvanostatic mode selecting a constant current intensity in the microfluidic electrochemical flow-through reactor. The applied current density was in the range of 5 to 50 A m^{-2}.

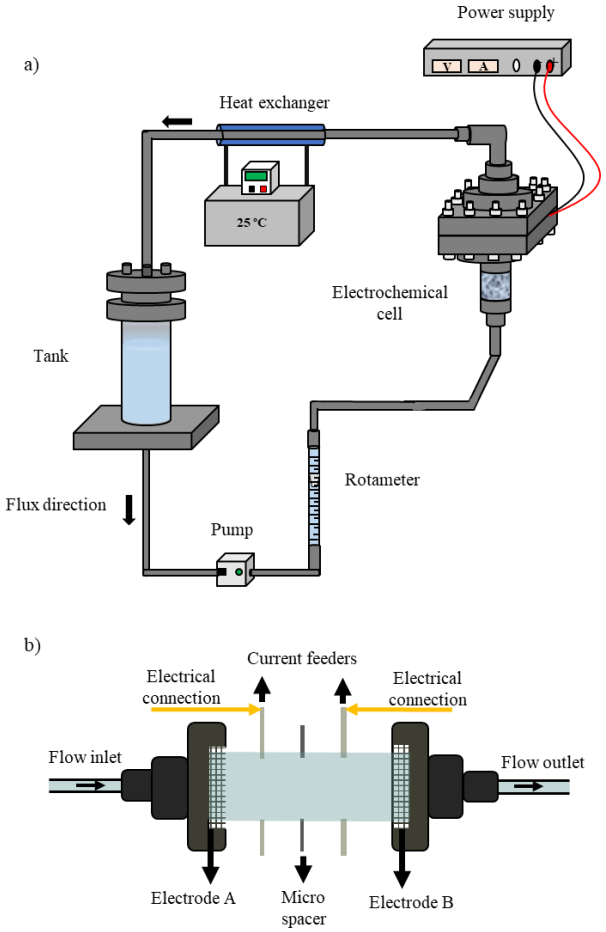

Figure 4.3. a) Experimental setup of electrochemical disinfection with a microfluidic flow-through reactor in discontinuous mode. Bench scale. b) Microfluidic flow-through reactor.

4.3.2. Photo-electrolysis facilities and reactors

Photo-electrolysis disinfection experiments were carried out employing the experimental setups and reactors used for the electrolysis tests. To integrate the UV light irradiation into the system, a UV germicidal lamp of 5 W (λ = 254 nm) was located in the middle of reservoir tanks as shown in Figure 4.4.

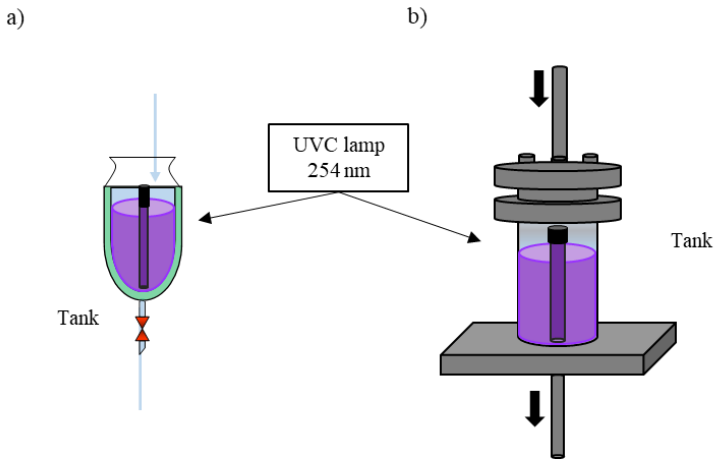

Figure 4.4. UVC light irradiation setup for different reactors: a) parallel flow cell and MIKROZON® cell, b) microfluidic flow-through reactor.

4.3.3. Chemical disinfection tests

Chemical disinfection experiments were conducted using a multi-stirrer device shown in Figure 4.5.

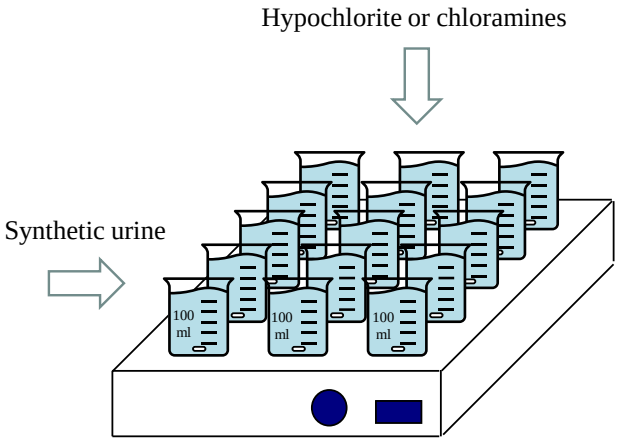

Figure 4.5. Multi-stirrer laboratory scale unit for chemical disinfection tests with hypochlorite and chloramines.

Beakers containing each one 100 ml of synthetic hospital urines inoculated with bacteria were added different concentrations of hypochlorite and/or chloramines. Hypochlorite stock solution was freshly prepared from commercial calcium hypochlorite. Chloramines were pre-formed by mixing aqueous ammonium sulfate and calcium hypochlorite solutions at a Cl/N weight ratio of 5:1 and testing that more than 97.2 % of available chlorine was combined chlorine. The same chlorine doses from hypochlorite or chloramine aqueous solutions were added to the raw water to achieve the target initial disinfectant concentrations of 0.07, 0.14, 0.28, and 0.56 mmol Cl dm^{-3}.

4.4. Analytical techniques

4.4.1. pH and conductivity

The pH and conductivity were simultaneously measured using a Sension+ MM150 Portable Multi-Parameter Meter (HACH®). The multi-parameter meter was previously calibrated with standard solutions before each set of measures.

4.4.2. Total Organic Carbon (TOC)

Total Carbon (TC) was measured on a Shimadzu TOC-VWP analyser with ASI-V autosampler. The measurement is based on the complete combustion of the sample with a pure oxygen stream at a temperature of 680°C in a furnace containing a platinum catalyst supported on alumina. The carbon dioxide produced is measured by infrared spectrophotometry and is directly related to the TC of the sample.

For the measurement of inorganic carbon (IC), the sample is acidified by the addition of 10 % phosphoric acid, which shifts the equilibrium of carbonates and bicarbonates towards carbonic acid. Again, the release of carbon dioxide is measured by infrared spectrophotometry and related to the IC value associated with the analysed sample.

Once the TC and CI measurements are known, the Total Organic Carbon (TOC) value is obtained by difference of the previous ones. The equipment performs a minimum of three measurements per sample, giving a valid result if the variation between them is less than 2 %.

4.4.3. Organic compounds

4.4.3.1. Spectrophotometry

The urea concentration was determined by a spectrophotometric method using the Cary Series UV–Vis Spectrophotometer (Agilent Technologies). For this purpose, p-dimethylaminobenzaldehyde (PDMAB), an organic compound which has a yellowish colour in the presence of urea in an acidic medium, was used as indicator [4]. The indicator was prepared by adding 20 g of PDMAB to 1.1 dm^3 of ethanol, containing 100 ml of hydrochloric acid. To determine the urea concentration, 15 ml of sample was mixed with 10 ml of the indicator and allowed to react for 10 min. Subsequently, the absorbance of the mixture was measured at 420 nm. Figure 4.6 shows the calibration curve with standard urea solutions, ranging from 0 to 500 mg dm^{-3}.

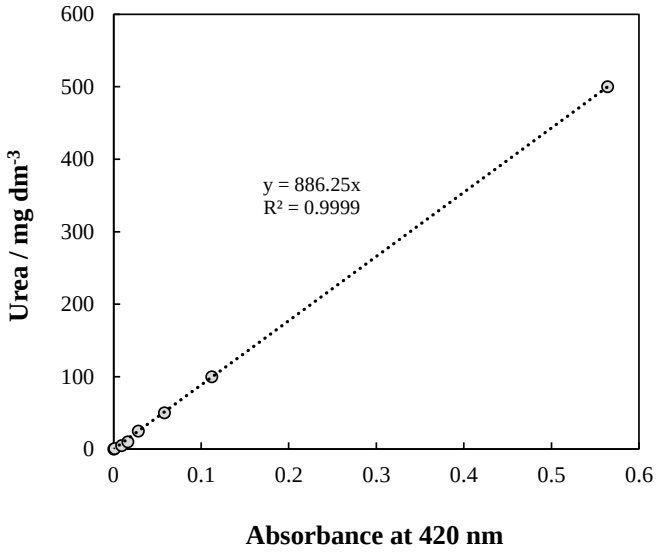

Figure 4.6. Calibration curve for the quantification of urea at 420 nm.

4.4.3.2. High-Performance Liquid Chromatography (HPLC)

High-Performance Liquid Chromatography (HPLC) was used to determine the concentration of uric acid using an Agilent 1200 series coupled with a DAD detector. A ZORBAX Eclipse Plus C18 analytical column was used and its temperature was maintained at 25 °C. The mobile phase consisted of 2 % acetonitrile / 98 % aqueous solution with 0.1 % of formic acid, applying a flow rate of 1.0 cm^3 min^{-1}. The injection volume was 10 μl and the DAD detection wavelength was 292 nm. Under these conditions, the retention time of uric acid was 2.1 min. Additionally, for the determination of chloramphenicol, the mobile phase used consisted of 50 % methanol / 50 % milli-q water applying a flow rate of 0.6 cm^3 min^{-1}, an injection volume of 20 μL and a DAD detection wavelength of 270 nm.

4.4.3.3. Gas chromatography

The concentration of trihalomethanes (THMs) was determined by gas chromatography (Young Lin YL6100GC) equipped with an ECD detector (SDM6100) and a DuraBond DB-624UI (30 m x 0.25 mm) column from Agilent Technologies, Inc. The flow was 3 ml min^{-1}, the detector temperature was maintained at 350 ºC and nitrogen was used as carrier gas (30 ml min^{-1}).

4.4.4. Inorganic compounds (including creatinine)

4.4.4.1. Ion chromatography

An ion chromatograph Metrohm 930 Compact IC Flex coupled to a conductivity detector, was used to analyze the ionic species. The columns Metrosep A Supp 7 and Metrosep C6 250 were used to measure anions and cations, respectively. A mobile phase of 85:15 v/v 3.6 mM Na_2CO_3/acetone with a flow rate of 0.8 cm^3 min^{-1} was used to measure anions and a mobile phase of 1.7 mM HNO_3 + 1.7 mM 2,6-pyridinedicarboxylic acid with a flow rate of 0.9 cm^3 min^{-1} was employed for cations. The volume injection of each sample was 20 μl. Table 4.5 shows the retention times for the different ionic species.

Table 4.5. Retention time of ionic species and creatinine.

Compound	Column	Retention time (min)
F^-	Metrosep A Supp 7 (Anions)	6.18
Cl^-		9.29
ClO^-		9.29
NO_2^-		10.77
Br^-		13.56
ClO_3^-		14.24
NO_3^-		15.08
PO_4^{3-}		26.32
SO_4^{2-}		29.06
ClO_4^-		60.77
Na^+	Metrosep C6 250 (Cations)	11.23
NH_4^+		12.96
K^+		19.39
Ca^{2+}		25.55
$C_4H_7N_3O$		29.27
Mg^{2+}		33.6

4.4.4.2. Automatic titration

i) I^-/I_2 method

The determination of total oxidants which is a colorimetric titration was conducted by the I^-/I_2 method, according to Kolthoff & Carr [5]. This technique was used to quantify all the oxidising species present in the solution which oxidise the iodide ion to molecular iodine.

The analysis consists of adding to 10 ml of sample, solid potassium iodide in excess and 5 ml of 20 % sulphuric acid solution, since the reaction must take place in a strongly acidic medium. The oxidants present in the medium react with the iodide. Subsequently, the iodine generated is titrated with a 0.01 M sodium thiosulphate solution (Equation 4.1), using a starch solution of 10 g dm^{-3} as an indicator to determine more accurately the end point of the titration. Thus, this titration method may be applied for the quantification of peroxomono-phosphate (Equation 4.2), peroxodisulfate

(Equation 4.3) and total chlorine oxoanions (Equation 4.4). The titrations were developed using an automatic titrator model Methrom 702 SM Titrino.

$$I_2 + 2\ S_2O_3^{2-} \rightarrow 2\ I^- + S_4O_6^{2-} \quad (4.1)$$

$$2\ I^- + PO_5^{3-} \rightarrow I_2 + 2\ PO_4^{3-} \quad (4.2)$$

$$2\ I^- + S_2O_8^{2-} \rightarrow I_2 + 2\ SO_4^{2-} \quad (4.3)$$

$$2n\ I^- + XO_n^- \rightarrow x\ I_2 + X^- \quad (4.4)$$

ii) Arsenic method

The peak of the chromatogram for hypochlorite interferes with the chloride peak in the IC technique (Table 4.5). Therefore, the concentration of hypochlorite ions was separately measured using an automatic titrator model Methrom 702 SM Titrino. The analytical method used is based on the redox reaction between arsenite and hypochlorite (Equation 4.5).

$$As_2O_3 + 2\ ClO^- + 6\ OH^- \rightarrow 2\ AsO_4^{3-} + 2\ Cl^- + 3\ H_2O \quad (4.5)$$

Hypochlorite is reduced to chloride by the continuous addition of arsenite, which in turn is oxidised to arsenate. The excess arsenite added results in a marked decrease in the electrolyte potential (relative to a platinum electrode), which is detected by means of the automatic titrator.

A 0,001 M solution of arsenic trioxide and 2 M sodium hydroxide was used as titrant, which was placed in the titrator vessel. The pre-treatment of the sample consisted of its basification by adding 2 ml of a 2 M sodium hydroxide solution to 10 ml of the sample whose hypochlorite concentration would be determined. Finally, the concentration of hypochlorite generated was calculated by equivalents (Equations 4.6-4.7) [6, 7].

$$Eq\ (As^{3+}) = Eq\ (ClO^-) \quad (4.6)$$

$$M\ (As^{3+}) \cdot V\ (As^{3+}) \cdot n^o e^-_{lost} = M\ (ClO^-) \cdot V\ (ClO^-) \cdot n^o e^-_{gained} \quad (4.7)$$

4.4.4.3. Colorimetric methods

i) Colorimetric method to measure inorganic chloramines

The determination of inorganic chloramines was developed following the DPD (N,N-diethyl-phenylenediamine) standard colorimetric method [8], using a spectrophotometer Libra S70 (Biochrom). This is a selective method that allows to determine the presence of monochloramine (NH_2Cl), dichloramine ($NHCl_2$) and trichloramine (NCl_3) without the interferences of other oxidizing species formed during the process. The reagent used is DPD, which generates a pink colour in the aqueous solution on reaction with chlorine species. The minimum and maximum detectable concentrations of chlorine are 10 μg dm^{-3} and 4 mg dm^{-3}, respectively.

This colorimetric method requires a previous calibration of the spectrophotometer. Calibration is performed starting from a stock solution containing 891 mg dm^{-3} of $KMnO_4$ (sol.1), from which 10 ml are taken and brought to 100 ml with distilled water (sol.2). Thus, 1 ml of sol.2 will correspond to a solution of 1 mg dm^{-3} of chlorine.

The procedure for determining the concentration of inorganic chloramines is based on dividing the sample into two portions (10 ml each):

- To the first portion, 0,5 ml of DPD indicator (8,1 mM DPD, 37,8 mM H_2SO_4 and 0,5 mM EDTA) and 0,5 ml of KH_2PO_4/Na_2HPO_4 buffer (338,1 mM KH_2PO_4, 169 mM Na_2HPO_4 and 21,5 mM EDTA) are added, mixed and immediately measured (reading A). The resulting colour will correspond to the amount of free chlorine. Subsequently, a small amount of KI (0,1 mg) is added, mixed and immediately measured (reading B). The KI allows the activation of monochloramine, so that the colour now results from the appearance of monochloramine and free chlorine. Approximately 0,1 g of KI is then added and the reading is taken after 2 minutes (reading C). The addition of iodide ion in excess results in a dichloramine colorimetric response.

- In the presence of iodide ion, part of the nitrogen trichloride (or trichloramine) is included with the dichloramine and part with the free chlorine. Therefore, it is necessary to carry out an additional procedure based on the prior addition of iodide ion, in order to estimate the proportion of nitrogen trichloride, which appears with the free chlorine. Thus, a small crystal of KI (approximately 0,1 mg) is placed in a beaker to which 10 ml of the sample is subsequently added and mixed. To a second beaker, 0,5 ml of KH_2PO_4/Na_2HPO_4 buffer (338,1 mM KH_2PO_4, 169 mM Na_2HPO_4 and 21,5 mM EDTA) and 0,5 ml of DFD reagent (8,1 mM DPD, 37,8 mM H_2SO_4 and 0,5 mM EDTA) are added and mixed. The content of the first beaker is then added to the second beaker and mixed to read the colour immediately (reading N).

The combination of the four spectrophotometric readings at 515 nm allows to calculate the amounts of inorganic chloramines according to Table 4.6.

Table 4.6. Determination of chlorine species based on spectrophotometry.

Reading	**NCl_3 absent**	**NCl_3 present**
A	Free Cl	Free Cl
B-A	NH_2Cl	NH_2Cl
C-B	$NHCl_2$	$NHCl_2 + {}^1/_2\, NCl_3$
N	-	Free Cl $+ {}^1/_2\, NCl_3$
2(N-A)	-	NCl_3
C-N	-	$NHCl_2$

ii) Colorimetric method to measure ozone

Ozone quantification was determined by an Ozone Test Spectroquant® (Merk KGaA, Germany). This test is based on the reaction between ozone and dipropyl-p-phenylenediamine (DPD) in weakly acidic solution (4<pH<8), giving a reddish violet dye. The procedure to quantify ozone in solution consisted of mixing 10 ml of sample with two drops of reagent O_3-1 and one level microspoonful of reagent O_3-2. Then, the mixture was allowed to stand for one minute (reaction time) before its measured at 550

nm, using a spectrophotometer Spectroquant® Prove 100 (Merck). Figure 4.7 shows the calibration curve directly obtained from the spectrophotometer Spectroquant® Prove 100, ranging from 0.05 to 0.2 mg dm^{-3}.

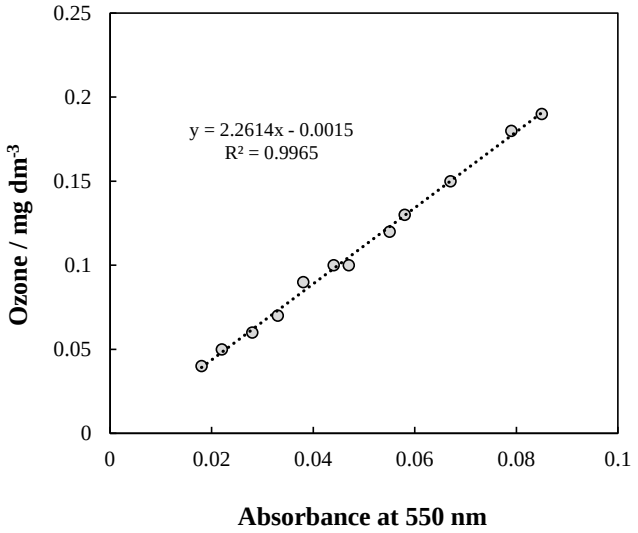

Figure 4.7. Calibration curve for the quantification of ozone at 550 nm.

4.4.5. Biodegradation and toxicity assays

4.4.5.1. Rapid biodegradability assay

Rapid biodegradability assays were carried out in glass reactors (250 ml) with 95 ml of endogenous activated sludge and 5 ml of target sample. Before the assay, the activated sludge was maintained in starvation and continuous aeration overnight to eliminate any residual organic matter and to avoid oxygen limitation. The dissolved oxygen concentration was monitored by using an oximeter (HI9146, Hanna Instruments) as function of the experimental time. The rapid biodegradability of samples was calculated as a relation between rapid biochemical oxygen demand (BOD) and chemical oxygen demand (COD) by using Equation (4.8).

$$\text{Rapid biodegradability (\%)} = \frac{BOD_{rapid} \cdot V_{biological\ reactor}}{COD_{sample} \cdot V_{sample}} \cdot 100 \quad (4.8)$$

The rapid BOD is calculated as the difference, in terms of dissolved oxygen decay (mg O_2 dm^{-3}), between the slope of endogenous activated sludge and the slope when sample is added into endogenous activated sludge.

4.4.5.2. Standard biodegradability assay

Standard biodegradability assays were carried out in Erlenmeyer glass reactors (250 ml) with 240 ml of sample following the Zahn-Wellens test (OECD 302 B 1992). Sludge in the ratio 1:3 for inoculum/TOC and mineral medium (10 ml A + 1 ml B + 1 ml C + 1 ml D + H_2O to 1 l) were added. The stocks solutions for the preparation of mineral medium were:

- A (0.85 g KH_2PO_4 + 2.175 g K_2HPO_4 + 3.34 g $Na_2HPO_4 \cdot 2H_2O$ + 0.05 g NH_4Cl + H_2O to 100 ml)
- B (2.75 g $CaCl_2$ + H_2O to 100 ml)
- C (2.25 g $MgSO_4 \cdot 7H_2O$ + H_2O to 100 ml)
- D (0.025g $FeCl_3 \cdot 6H_2O$ + H_2O to 100 ml)

The mixture was stirred softly at room temperature for 28 days. Samples were taken periodically to quantify the evolution of TOC and target contaminant concentrations. Glucose was used as reference compound to ensure the activity of microorganisms.

4.4.5.3. Acute toxicity assays

Acute toxicity towards *Vibrio fischeri* (marine luminescent bacterium) was measured using a Microtox® M500 Analyzer (Azur Environmental), according to standard Microtox test procedure (ISO 11348, 2007). Lyophilized bacteria are reconstituted by suspension in 1 ml of ultrapure water. Samples were tested for 15 min of exposure at 15 ºC. Toxic effects were monitored as a percent decrease of the light emission of *Vibrio fischeri* and compared to that obtained for the blank sample, which contains 2% NaCl in deionized water.

4.4.6. Biological analyses

4.4.6.1. Determination of Minimum Inhibitory Concentration (MIC)

The resistance of the selected bacterial strains to other antibiotic classes was evaluated by means of Minimum Inhibition Concentration (MIC) assay.

Bacteria were incubated in agar plates for 18–24 h at 37 ºC after which, colonies were transferred from the agar plates to 5 ml of sterile demineralized water (Cat no. T3339, ThermoFisher Scientific). Then, suspensions were mixed by vortexing until cells were completely dispersed and adjusted accordingly by adding more colonies until 0.5 McFarland is reached using a Nephelometer (Sensititre™ Nephelometer, ThermoFisher Scientific). This suspension (10 µl) was then added into a vial containing 11 ml of Mueller-Hinton broth (Cat no. T3462, ThermoFisher Scientific) and mixed by vortexing. 50 µl of the vial contents was transferred into each well of a Sensititre plate using an Sensititre AutoInoculator/AIM (Sensititre AIM™ Automated Inoculation Delivery System, ThermoFisher Scientific). After inoculation, the plates were sealed with plate film and incubated at 37 ºC for 24 h. The plates were read manually using a Sensititre Vizion (Thermo Scientific™ Sensititre™ Vizion™ Digital MIC Viewing System, ThermoFisher Scientific). Sensititre plate results were interpreted according to European Committee on Antimicrobial Susceptibility Testing (EUCAST) established breakpoints 2021 available on the European Society of Clinical Microbiology and Infectious Diseases website. Test results are summarized in Table 4.7.

Table 4.7. Antibiotic sensitivity study using minimum inhibitory concentration (MIC) assays with various antibiotic classes. R: Resistant, S: Sensible.

Antibiotic	Class	*Klebsiella pneumoniae* ATCC 4352			*Escherichia coli* ATCC 25922			*Enterococcus faecalis* ATCC 19433		
		MIC	MIC EUCAST 2021	Result	MIC	MIC EUCAST 2021	Result	MIC	MIC EUCAST 2021	Result
Ampicillin	Penicillins	64	R>8	R	8	R>8	S	2	R>4	S
Azithromycin	Macrolides	≤2	-	-	8	R>16	S	≤2	-	-
Cefotaxime	Cephalosporins	>4	R>2	R	≤0,25	R>0,25	S	>4	- (R>2)	R
Ceftazidime	Cephalosporins	>8	R>4	R	≤0,5	R>0,5	S	>8	- (R>8)	R
Chloramphenicol	Amphenicols	≤8	R>8	S	≤8	R>16	S	≤8	R>32	S
Ciprofloxacin	Fluoroquinolones	1	R>0,5	R	≤0,015	R>0,064	S	1	R>4	S
Colistin	Polypeptides	>16	R>2	R	≤1	R>2	S	>16	-	-
Gentamicin	Aminoglycosides	16	R>2	R	≤0,5	R>2	S	16	R>32	S
Meropenem	Carbapenems	8	R>8	S	≤0,03	R>0,125	S	8	R>16	S
Nalidixic acid	Fluoroquinolones	>128	-	-	≤4	R>16	S	>128	-	-
Sulfamethoxazole	Sulfonamides	>1024	-	-	16	R>64	S	>1024	-	-
Tetracycline	Tetracyclines	≤2	R>8	S	≤2	R>8	S	≤2	R>4	S
Tigecycline	Glycylcycline	≤0,25	R>2	S	≤0,25	R>1	S	≤0,25	R>0,25	S
Trimethoprim	-	≤0,25	R>4	S	0,5	R>2	S	0,5	R>1	S

Table 4.7 (Cont.). Antibiotic sensitivity study using minimum inhibitory concentration (MIC) assays with various antibiotic classes. R: Resistant, S: Sensible.

Antibiotic	Class	*Klebsiella pneumoniae* ATCC BAA-1705			*Escherichia coli* ATCC 35218			*Enterococcus faecalis* ATCC 51299		
		MIC	MIC EUCAST 2021	Result	MIC	MIC EUCAST 2021	Result	MIC	MIC EUCAST 2021	Result
Ampicillin	Penicillins	>64	R>8	R	>64	R>8	R	≤1	R>4	S
Azithromycin	Macrolides	>64	-	-	4	R>16	S	64	-	-
Cefotaxime	Cephalosporins	>4	R>2	R	≤0,25	R>0,25	S	>4	- (R>2)	R
Ceftazidime	Cephalosporins	>8	R>4	R	≤0,5	R>0,5	S	>8	- (R>8)	R
Chloramphenicol	Amphenicols	>128	R>8	R	64	R>16	R	64	R>32	R
Ciprofloxacin	Fluoroquinolones	>8	R>0,5	R	≤0,015	R>0,064	S	1	R>4	S
Colistin	Polypeptides	≤1	R>2	S	≤1	R>2	S	>16	-	-
Gentamicin	Aminoglycosides	1	R>2	S	1	R>2	S	>32	R>32	R
Meropenem	Carbapenems	8	R>8	S	≤0,03	R>0,125	S	4	R>16	S
Nalidixic acid	Fluoroquinolones	>128	-	-	≤4	R>16	S	128	-	-
Sulfamethoxazole	Sulfonamides	>1024	-	-	>1024	R>64	R	>1024	-	-
Tetracycline	Tetracyclines	8	R>8	S	≤2	R>8	S	≤2	R>4	S
Tigecycline	Glycylcycline	0,5	R>2	S	≤0,25	R>1	S	≤0,25	R>0,25	S
Trimethoprim	-	>32	R>4	R	0,5	R>2	S	≤0,25	R>1	S

Minimum inhibition concentrations (MICs) of *K. pneumoniae*, *E. coli* and *E. faecalis* isolates were measured by their susceptibility to a panel of 14 antimicrobics by broth microdilution using the Sensititre EU Surveillance *Salmonella* / *E. coli* EUVSEC Plate (Figure 4.8).

Figure 4.8. Panel of 14 antimicrobics tested in the Minimum Inhibition Concentration (MIC) assay.

4.4.6.2. Measurement of Colony-Forming Units (CFU) per ml

i) Measurement of CFU ml^{-1} using a μ-Trac® 4200 system

Bacterial counts were performed by an indirect impedance method using a μ-Trac® 4200 system (SY-LAB). It uses a standard impedance signal (Media Impedance = M-value) that is registered as the result of microbial metabolism, which causes the change of the impedance in an AC field. During the growth of microorganisms low or non-charged nutrient molecules are metabolized. This break down of nutrients generates small and highly charged metabolites that result in a change of the impedance of the nutrient media that is recorded by the instrument [9, 10]. In this work, the nutrient media used are shown in Table 4.8.

Table 4.8. Nutrient media used to quantify bacteria at μ-Trac® 4200 system.

Bacterial strains	Nutrient media	Supplier
E. faecalis ATCC 19433	BiMedia 001B (Total viable count medium)	SY-LAB
E. faecalis ATCC 51299	BiMedia 330A (Selective medium for the determination of Enterococci)	SY-LAB
E. coli ATCC 25922 *E. coli* ATCC 35218	BiMedia 155A (Selective medium for the determination of *E. coli*)	SY-LAB
K. pneumoniae ATCC 4352 *K. pneumoniae* ATCC BAA-1705	BiMedia 001B (Total viable count medium)	SY-LAB

An initial calibration using the membrane filtration technique was developed for each bacterium tested to correlate the impedance values of samples with the bacteria concentration. The correlation of bacteria concentration (CFU ml^{-1}) and time (h) to reach the exponential growth stage for each bacterium is shown in Figure 4.9. An impedance threshold value of 5 % has been stablished to reach the exponential growth stage for every strain tested. The equations obtained to correlate bacterial concentration and time (Figure 4.9) are subsequently introduced in the μ-Trac® 4200 software to enable it to measure samples on the basis of these calibrations.

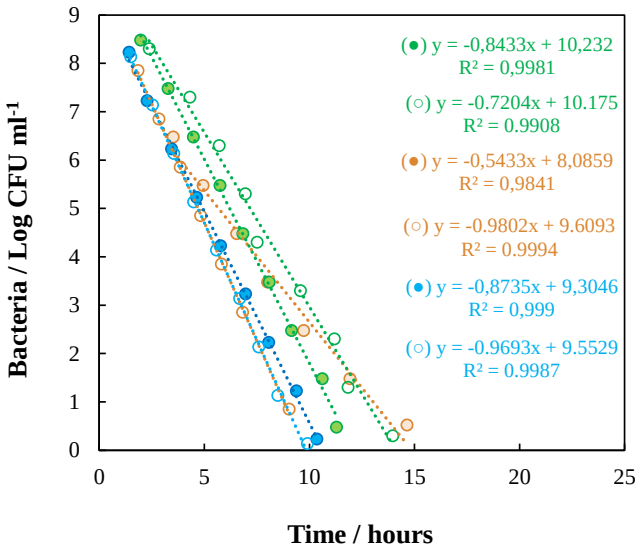

Figure 4.9. Calibration curves for the µ-Trac® 4200 system for each bacterial strain tested: (●) *E. faecalis* ATCC 19433, (○) *E. faecalis* ATCC 51299, (●) *E. coli* ATCC 25922, (○) *E. coli* ATCC 35218, (●) *K. pneumoniae* ATCC 4352, (○) *K. pneumoniae* ATCC BAA-1705.

ii) Measurement of CFU ml^{-1} using the membrane filtration technique

Occasionally, bacterial concentration was also measured following the ISO 8199 regulation by the membrane filtration technique. The test portion was passed through a membrane filter of 45 mm of diameter and a pore size diameter of 45 µm (certified according to the standard ISO 7704:1985) which retained the microorganisms sought. The membrane was placed facing up in a specific culture medium (usually Tryptone Soy Agar ISO) for each microorganism. Here, it is important to highlight that for the measure of *K. pneumoniae* under the simultaneous presence of other bacteria, it was necessary to use a selective culture medium nutrient media (Klebsiella ChromoSelect Selective Agar base with the addition of Klebsiella Selective Supplement). Formation of bubbles and winkles must be avoided. Then, the culture plates were incubated during 18-24 h and, the bacterial growth was determined by plate counting. Result was expressed as a number of Colony-Forming Units (CFU) in a 100 ml of sample.

4.4.6.3. Measurement of cell wall permeability

Changes in cell wall permeability were monitored by the crystal violet assay [11]. The main steps of this assay are schematized in Figure 4.10 and summarized below:

- A previous stage to obtain a biological pellet (aggregation of bacteria obtained by centrifugation) from 100 ml sample were carried out. This process allows to discard undesirable substances that could interfere with the biological measurements.
    - Sample volumes of 50 ml were centrifuged in Falcon® 50 ml conical centrifuge tubes at 5320 x g for 15 minutes.
    - After the first centrifugation, 37.5 ml of supernatant were discarded and the other 12.5 ml of suspension at the bottom of each tube were mixed in a same new 50 ml tube to reach a final volume of 25 ml. This tube was centrifuged again (5320 x g for 15 min).
    - After the second centrifugation, as much supernatant as possible was removed and the pellet was resuspended into a 25 ml of sterile saline solution (0.9 % NaCl). Once resuspended, the solution was centrifuged again (5320 x g for 15 min) and the supernatant was discarded to obtain a clean pellet.
- The clean pellet was dissolved in 1.5 ml of phosphate-buffered saline (PBS) solution containing 10 $\mu g\ ml^{-1}$ crystal violet. Then, the tubes were incubated at 37 °C for 10 minutes.
- After incubation, the solution was transferred to Eppendorf® safe-lock tubes and centrifuged at 13400 x g for 15 minutes.
- The supernatant was transferred to a cuvette (taking care not to move the pellet) to be measured in the spectrophotometer (Biochrom Libra S70) at 590 nm.

The Abs_{590} value of the crystal violet solution standard (10 µg ml^{-1}) was considered as an uptake percentage of 100 %. The percentage uptake of crystal violet for each sample was calculated using the Equation 4.9 [12].

$$\% \text{ uptake} = \frac{Abs_{sample}}{Abs_{\text{crystal violet standard (10 µg ml}^{-1})}} \cdot 100 \quad (4.9)$$

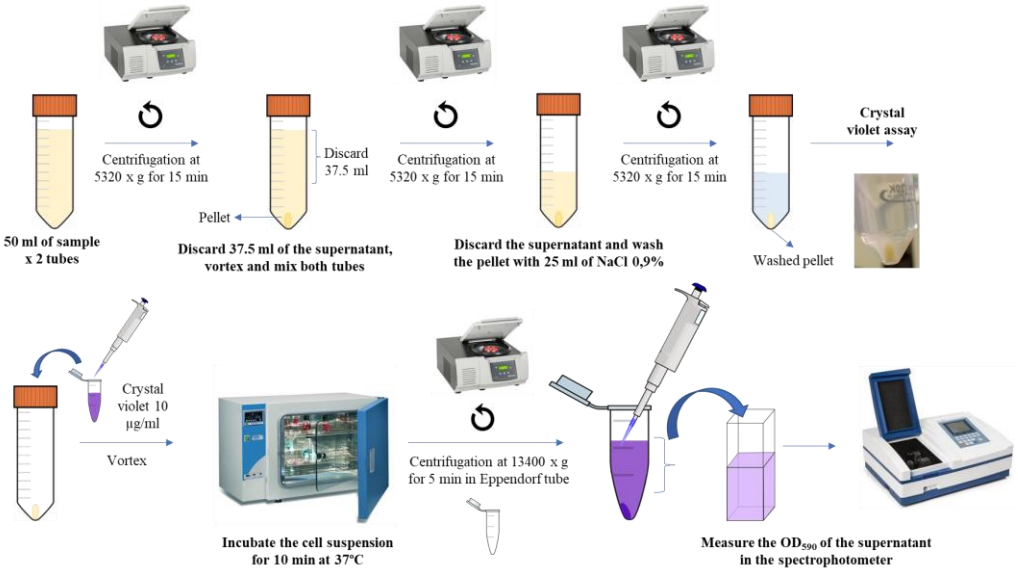

Figure 4.10. Steps to measure the cell wall permeability by the crystal violet assay.

4.4.6.4. Measurement of total proteins concentration

The concentration of total proteins was analysed following the procedure described by Long et al. [13]. Figure 4.11 shows the main steps follow to carried out this procedure. Firstly, the cell lysis of the sample was conducted using the Bacterial Protein Extraction Reagent (B-PER®, Thermo Fisher Scientific) as follows:

- Obtain a biological pellet (aggregation of bacteria obtained by centrifugation) from 100 ml sample were carried out. This process allows to discard undesirable substances that could interfere with the biological measurements.

- Sample volumes of 50 ml were centrifuged in Falcon® 50 ml conical centrifuge tubes at 5320 x g for 15 minutes.
- After the first centrifugation, 37.5 ml of supernatant were discarded and the other 12.5 ml of suspension at the bottom of each tube were mixed in a same new 50 ml tube to reach a final volume of 25 ml. This tube was centrifuged again (5320 x g for 15 min).
- After the second centrifugation, as much supernatant as possible was removed and the pellet was resuspended into a 25 ml of sterile saline solution (0.9 % NaCl). Once resuspended, the solution was centrifuged again (5320 x g for 15 min) and the supernatant was discarded to obtain a clean pellet.

- The pellet was put inside a Falcon® 50 ml conical centrifuge tube and 4 ml of B-PER® per gram of cell pellet was added. It was incubated 15 minutes at room temperature and transferred the suspension to an Eppendorf® tube.
- Eppendorf® tubes (containing lysate) were centrifuged at 15000 x g for 5 minutes to separate soluble and insoluble proteins. The insoluble proteins remain in the precipitate and the supernatant was used for the determination of total proteins.

Once the cell lysis was carried out, the total proteins in the lysate was photochemically determined using the Pierce™ BCA Protein Assay Kit (Thermo Fisher Scientific) following the next steps:

- 0.1 ml of the supernatant were introduced into a 10 ml tube and added 2 ml of a reagent (BCA Reagent A and BCA Reagent B were mixed in a ratio 50:1). The solution was strongly agitated to achieve homogenization.
- The tubes were incubated at 37 °C for 30 minutes. Subsequently, they were cooled to room temperature.
- After that, samples were measured in the spectrophotometer (Biochrom Libra S70) at 562 nm.

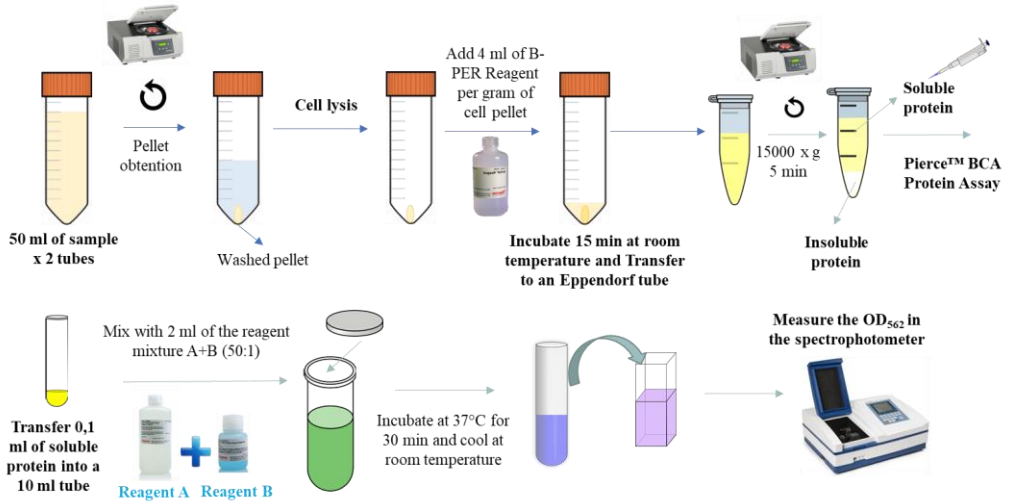

Figure 4.11. Steps to measure the concentration of total proteins.

The Abs_{562} values were related to the concentration of total proteins by means of a previous calibration with bicinchoninic acid (BCA) as shown in Figure 4.12. The concentration of BCA is directly related with the concentration of total proteins in a ratio 1:1.

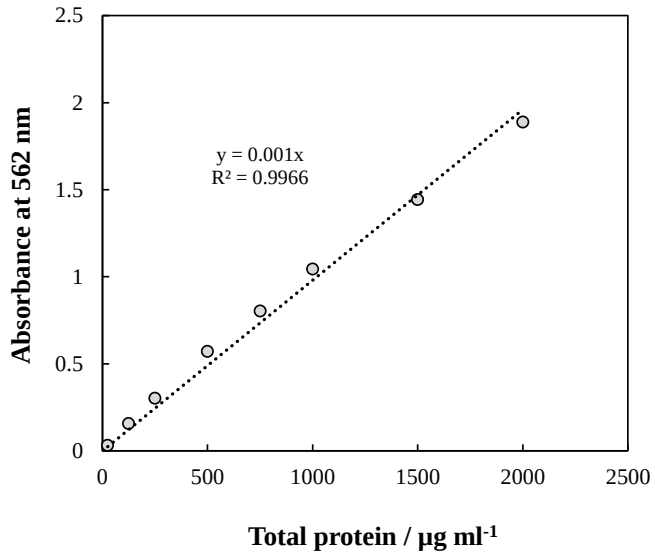

Figure 4.12. Calibration curve for the quantification of total proteins at 562 nm.

4.4.6.5. Measurement of DeoxyriboNucleic Acid (DNA)

DeoxyriboNucleic Acid (DNA) concentration was determined according to the methodology reported in literature [14, 15]. A commercial Urine DNA Isolation Kit for Exfoliated Cells or Bacteria (Norgen Biotek) was employed for the DNA extraction. Figure 4.13 shows the main steps to measure DNA of bacteria in urine matrices and may be described as follows:

- Pellet obtention from 100 ml sample were carried out:
  - Sample volumes of 50 ml were centrifuged in Falcon® 50 ml conical centrifuge tubes at 5320 x g for 15 minutes.
  - After the first centrifugation, 37.5 ml of supernatant were discarded and the other 12.5 ml of suspension at the bottom of each tube were mixed in a same new 50 ml tube to reach a final volume of 25 ml. This tube was centrifuged again (5320 x g for 15 min).
  - After the second centrifugation, as much supernatant as possible was removed and the pellet was resuspended into a 25 ml of sterile saline solution (0.9 % NaCl). Once resuspended, the solution was centrifuged again (5320 x g for 15 min) and the supernatant was discarded to obtain a clean pellet.
- 200 µl of the resuspension solution A were added to the pellet and resuspended by gentle vortexing to obtain a cell suspension.
- Subsequently, 600 µl of Lysis Buffer B, 20 µl of lysozyme stock solution (400 mg ml^{-1}) and 20 µl of proteinase K were added to the cell suspension. The mixture was gentle vortexed and incubated in the thermoblock (already preheated) at 55°C for 30 minutes to obtain the lysate.
- 160 µl of pure isopropanol were added to the lysate and mixed by gentle vortexing to obtain a lysate mixture.
- 500 µl of the lysate mixture were added to a spin column which is inside a collection tube. The spin column with the collection tube was capped and centrifugated at 8,000 rpm for 2 min. After centrifugation, the collected liquid at the bottom of the collection tube was discarded.

- 500 µl of wash solution A were added to the spin column and centrifuged at 14,000 rpm for 1 min. Then, the collected liquid at the bottom of the collection tube was discarded. 500 µl of wash solution A were again added to the spin column and centrifuged at 8,000 rpm for 1 min. After that, the collected liquid at the bottom of the collection tube was discarded again. The spin column was centrifuged at 14,000 rpm for 2 min, discarding the collected liquid at the bottom of the collection tube and the collection tube itself. The spin column was introduced into an Eppendorf® tube.
- 20 - 100 µl of elution buffer B was added to the Eppendorf® tube. This tube was centrifuged at 8,000 rpm for 2 min and, subsequently, it was centrifuged at 14,000 rpm for 1 min again to obtain the extracted DNA in liquid phase.

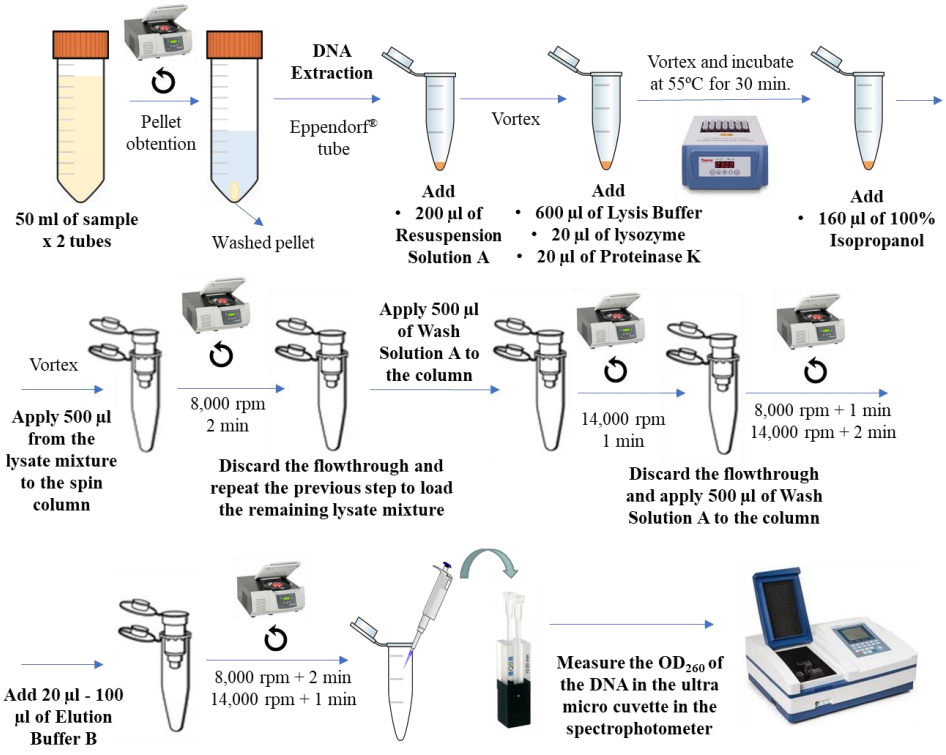

Figure 4.13. Steps to measure the DNA of bacteria in urine matrices.

The amount of DNA was quantified by spectrophotometry, using an ultra-Micro absorption cuvette (Hellma®). The measurement was carried out by adding 5 µl of extracted DNA to the cuvette and measuring the absorbance at 260 nm in the spectrophotometer (Biochrom Libra S70). The concentration of DNA has been quantified at 260 nm because it is well stablished that solutions of DNA in 10 mm pathlength cells with an absorbance of 1.0 have concentrations of 50 µg/ml [16].

4.4.6.6. Measurement of Antibiotic Resistance Genes (ARGs)

The nucleotide sequence was obtained from the data base of the National Center for Biotechnology Information (NCBI). These sequencies demonstrated an above 99 % of homology between *E. faecalis* (ATCC 51299) and *erm*B gene, *K. pneumoniae* (ATCC BAA-1705) and bla_{KPC} gene, and *E. coli* (ATCC 35218) and bla_{TEM} gene.

i) Measurement of ermB and bla_{KPC} genes

Commercial primers and probes (TaqMan® Gene Expression Assays (FAM)) were supplied by Thermo Fischer Scientific. The quantification of genes was conducted through amplification in a QuantStudio™ 5 Real-Time PCR System (Thermo Fischer Scientific). The qPCR amplification was performed in a 20 µl reaction mixture containing 10 µl of TaqMan™ Fast Advanced Master Mix, 1 µl of TaqMan® Gene Expression Assays (FAM), 50 ng of extracted DNA and ultrapure water. The conditions of the qPCR for the amplification of genes were 50 ºC for 2 min and 95 ºC for 2 min followed by 40 cycles (cycle: 95 ºC for 1 second and 60 ºC for 20 seconds). The measure of genes is obtained in threshold cycles.

ii) Measurement of bla_{TEM} gene

The primers were designed based on a previous study by Bibbal et al. [17], and ordered for its preparation in Thermo Fischer Scientific. The forward and reverse primers chosen were 5'-TTCCTGTTTTTGCTCACCCAG-3' and 5'-CTCAAGGATCTTACCGCTGTTG-3', respectively. The quantification of genes was conducted through amplification in a QuantStudio™ 5 Real-Time PCR System (Thermo Fischer Scientific). The gene amplification was performed in a 20 µl reaction mixture

containing 10 µl of PowerUp™ SYBR™ Green Master Mix, 1 µl of each primer, 50 ng of extracted DNA and ultrapure water. The operation conditions of the qPCR were 50 ºC for 2 min and 95 ºC for 2 min followed by 40 cycles (cycle: 95 ºC for 15 second and 60 ºC for 1 minute). The measure of genes is obtained in threshold cycles.

4.4.6.7. Measurement of bacterial morphology

The ARB morphology was observed by a Scanning Electron Microscope (SEM). Prior to the analysis, samples were prepared to obtain a pellet as follows:

- Sample volumes of 50 ml were centrifuged in Falcon® 50 ml conical centrifuge tubes at 5320 x g for 15 minutes.
- After the first centrifugation, 37.5 ml of supernatant were discarded and the other 12.5 ml of suspension at the bottom of each tube were mixed in a same new 50 ml tube to reach a final volume of 25 ml. This tube was centrifuged again (5320 x g for 15 min).
- After the second centrifugation, as much supernatant as possible was removed and the pellet was resuspended into a 25 ml of sterile saline solution (0.9 % NaCl). Once resuspended, the solution was centrifuged again (5320 x g for 15 min) and the supernatant was discarded to obtain a clean pellet.

Then, the clean pellet was mixed with 2.5 % glutaraldehyde and 4 % paraformaldehyde. Subsequently, the mixture was fixed in osmium tetroxide ReagentPlus®. Analyses were carried out in the Central Service for Experimental Research (SCSIE) at the University of Valencia using a SEM-FEG Hitachi S-4800.

4.5. Electrochemical parameters

4.5.1. Current density

Current density is defined as the amount of electric current flowing through a unit of electrodic area. It is calculated following the Equation 4.10, where j is the current density (A m^{-2}), I is the intensity applied (A) and A is the electrodic area (m^2).

$$j=\frac{I}{A} \quad (4.10)$$

4.5.2. Applied electric charge

The applied electric charge is a parameter used in electrochemical processes instead of the time, to express the progress of reactions. This electrochemical parameter is related to the operating conditions and can be calculated by Equation 4.11 when operating at constant current (galvanostatic mode) in discontinuous mode.

$$Q=\frac{j\cdot S\cdot t}{V} \quad (4.11)$$

Where Q is the applied electric charge (Ah l^{-1}), j is the current density (A m^{-2}), S is the anodic surface (m^2), t is the time (h), and V is the wastewater volume treated (l).

4.5.3. Hydraulic retention time

The Hydraulic Retention Time (HRT) is the average amount of time that a given volume of liquid stays in a reactor or tank. Thus, it is defined as the volume of a reactor per the influent flowrate.

$$HRT=\frac{V}{q} \quad (4.12)$$

Where HRT is the Hydraulic Retention Time (h), V is the volume of the electrochemical cell (m^3), and q is the flowrate ($m^3\,h^{-1}$).

4.6. Bibliography

[1] S. Dbira, N. Bensalah, A. Bedoui, P. Cañizares, M.A. Rodrigo, Treatment of synthetic urine by electrochemical oxidation using conductive-diamond anodes, Environmental Science and Pollution Research, 22 (2015) 6176-6184.

[2] J.F. Pérez, J. Llanos, C. Sáez, C. López, P. Cañizares, M.A. Rodrigo, Towards the scale up of a pressurized-jet microfluidic flow-through reactor for cost-effective electro-generation of H2O2, Journal of Cleaner Production, 211 (2019) 1259-1267.

[3] J. Pérez, J. Llanos, C. Sáez, C. López, P. Cañizares, M. Rodrigo, Development of an innovative approach for low-impact wastewater treatment: A microfluidic flow-through electrochemical reactor, Chemical Engineering Journal, 351 (2018) 766-772.

[4] G.W. Watt, J.D. Chrisp, Spectrophotometric Method for Determination of Urea, Analytical Chemistry, 26 (1954) 452-453.

[5] I.M. Kolthoff, E.M. Carr, Volumetric determination of persulfate in the presence of organic substances, Analytical Chemistry, 25 (1953) 298-301.

[6] A.v. Wilpert, Über die Analyse von Hypochlorit und Chlorit in einer Lösung, Z. Anal. Chem., 155 (1957) 378-378.

[7] H. Freytag, Zur Bestimmung von Hypochlorit, Chlorid und Chlorat in Chlorkalk, Z. Anal. Chem., 171 (1959) 458-458.

[8] A. WPCF, APHA, Standard Methods for the Examination of Water and Wastewater, 20th Ed, American Public Health Association (APHA), Washington DC, (1998).

[9] J. Dupont, F. Dumont, C. Menanteau, M. Pommepuy, Calibration of the impedance method for rapid quantitative estimation of Escherichia coli in live marine bivalve molluscs, Journal of Applied Microbiology, 96 (2004) 894-902.

[10] S. Zhu, S. Schnell, M. Fischer, Rapid detection of Cronobacter spp. with a method combining impedance technology and rRNA based lateral flow assay, Int. J. Food Microbiol., 159 (2012) 54-58.

[11] M. Vaara, T. Vaara, Outer membrane permeability barrier disruption by polymyxin in polymyxin-susceptible and-resistant Salmonella typhimurium, Antimicrobial agents and chemotherapy, 19 (1981) 578-583.

[12] S.J. Ahmad, H.H. Lian, D.F. Basri, N.M. Zin, Mode of action of endophytic Streptomyces sp., SUK 25 extracts against MRSA; microscopic, biochemical and time-kill analysis, Int. J. Pharm. Sci. Rev. Res, 30 (2015) 11-17.

[13] Y. Long, J. Ni, Z. Wang, Subcellular mechanism of Escherichia coli inactivation during electrochemical disinfection with boron-doped diamond anode: a comparative study of three electrolytes, Water Res., 84 (2015) 198-206.

[14] K.A. Alexander, C.E. Sanderson, M.H. Larsen, S. Robbe-Austerman, M.C. Williams, M.V. Palmer, Emerging tuberculosis pathogen hijacks social communication behavior in the group-living banded mongoose (Mungos mungo), MBio, 7 (2016).

[15] K.L. Nielsen, P. Dynesen, P. Larsen, L. Jakobsen, P.S. Andersen, N. Frimodt-Møller, Role of urinary cathelicidin LL-37 and human β-defensin 1 in uncomplicated Escherichia coli urinary tract infections, Infection and Immunity, 82 (2014) 1572-1578.

[16] J. Sambrook, E.F. Fritsch, T. Maniatis, Molecular cloning: a laboratory manual, Cold spring harbor laboratory press1989.

[17] D. Bibbal, V. Dupouy, J.-P. Ferré, P.-L. Toutain, O. Fayet, M.-F. Prère, A. Bousquet-Mélou, Impact of three ampicillin dosage regimens on selection of ampicillin resistance in Enterobacteriaceae and excretion of bla TEM genes in swine feces, Appl. Environ. Microbiol., 73 (2007) 4785-4790.

CHAPTER 5:

RESULTS AND DISCUSSION

The present chapter is based on the following documents:

- M. Herraiz-Carboné, S. Cotillas, E. Lacasa, C. Sainz de Baranda, E. Riquelme, P. Cañizares, M.A. Rodrigo, C. Sáez, *Are we correctly targeting the research on disinfection of antibiotic-resistant bacteria (ARB)?* Journal of Cleaner Production, 320 (2021) 128865.
- M. Herraiz-Carboné, S. Cotillas, E. Lacasa, P. Cañizares, M.A. Rodrigo, C. Sáez. *Removal of antibiotic resistant bacteria by electrolysis with diamond anodes: A pretreatment or a tertiary treatment?* Journal of Water Process Engineering, 38 (2020) 101557.
- M. Herraiz-Carboné, S. Cotillas, E. Lacasa, A. Moratalla, P. Cañizares, M.A. Rodrigo, C. Sáez. *Improving the biodegradability of hospital urines polluted with chloramphenicol by the application of electrochemical oxidation,* Science of the Total Environment, 725 (2020) 138430.
- M. Herraiz-Carboné, E. Lacasa, S. Cotillas, M. Vasileva, P. Cañizares, M.A. Rodrigo, C. Sáez, *The role of chloramines on the electrodisinfection of Klebsiella pneumoniae in hospital urines*, Chemical Engineering Journal, 409 (2021) 128253.
- M. Herraiz-Carboné, S. Cotillas, E. Lacasa, P. Cañizares, M.A. Rodrigo, C. Sáez, *Disinfection of urines using an electro-ozonizer*, Electrochimica Acta, 383 (2021) 138343.
- M. Herraiz-Carboné, S. Cotillas, E. Lacasa, P. Cañizares, M.A. Rodrigo, C. Sáez, *Enhancement of UV disinfection of urine matrixes by electrochemical oxidation*, Journal of Hazardous Materials, (2020) 124548.
- M. Herraiz-Carboné, S. Cotillas, E. Lacasa, M. Vasileva, C. Sainz de Baranda, E. Riquelme, C. Sáez, *Disinfection of polymicrobial urines by electrochemical oxidation: removal of antibiotic-resistant bacteria and genes*, Journal of Hazardous Materials, submitted.

5.1. Case of study: prevalence study of pathogens in urines from a university hospital

Since the beginning of 2020, the outbreak of COVID-19 has caused more than 3.12 million deaths worldwide in just over a year. Early advances in vaccines development help to control the pandemic, however, the proliferation of new variants may threaten the effectiveness of vaccines to deal with the virus [1, 2]. This important epidemic has also helped to highlight another important health problems which need for urgent actions: the rapid global spread of antibiotic-resistance bacteria (ARB) since the treatment of serious diseases with antibiotics is becoming more difficult or nearly impossible. Novel broad-spectrum antibiotics are continuously being developed to kill ARB, but the occurrence of new strains hampers their effectiveness [3]. Antibiotics belonging to the beta-lactam family are broadly used for the treatment of severe bacterial infections such as urinary tract infections (UTIs), pneumonia, or intra-abdominal infections [4]. This family comprises all type of penicillins, cephalosporins, cephamycins, monobactams, carbapenems, most of which, kill bacteria by inhibiting bacterial wall synthesis [5, 6]. An alarming rise in the resistance to beta-lactams in recent years is causing great concern in the scientific community [7]. Beta-lactam resistance is common, but not exclusive, to Enterobacteriaceae, due to the expression of beta lactamase enzymes [8]. Specifically, significant nosocomial outbreaks are mainly identified among *Escherichia coli* (*E. coli*) and *Klebsiella pneumoniae* (*K. pneumoniae*) in sanitary facilities [9].

E. coli is one of the main intestinal bacterium causing gastroenteritis, UTIs or neonatal meningitis [10]. This gram-negative, coliform bacillus has been extensively studied in the scientific literature for its virulent and antibiotic resistance strains [11-13]. Bala et al. have recently reported the prevalence of beta-lactam producing *E. coli* from hospitalized patients of a sanitary complex in India. 470 samples were analyzed and 244 (51.9 %) were resistant to cefoxitin, confirming the high prevalence of antibiotic-resistant strains in *E. coli* [14]. Antimicrobial use, prolonged hospitalization, and interventions were associated risk factors for antibiotic-resistant *E. coli*

dissemination. Similarly, *K. pneumoniae* is a gram negative, rod-shaped bacterium, commonly found in mouth, skin and intestines [15]. Pneumonia, UTIs, wound infections or respiratory tract infections are included in the range of clinical diseases derived from *K. pneumoniae* [16, 17]. An antibiotic-resistant strain, *K. pneumoniae* carbapenemases (KPCs) is of particular relevance, since it efficiently hydrolyses most beta-lactam antibiotics, exhibiting high mortality rates [18, 19].

The real danger posed by ARB and their attributable mortality in the European Union (EU) and the European Economic Area (EEA) have been evaluated by Cassini et al. [20]. From European Antimicrobial Resistance Surveillance Network (EARS-Net) data collected during 2015, they estimated 671,689 infections with ARB which accounted for around 33,110 (4.93 %) attributable deaths. They also highlighted four ARB with the largest effect on health in the study: *E. coli*, *K. pneumoniae*, *Staphylococcus aureus* (*S. aureus*) and *Pseudomonas aeruginosa* (*P. aeruginosa*).

The high presence of antibiotic-resistant strains combined with the large number of reported cases of ARB derived infections and deaths raises the necessity to gain insight into their clinical epidemiology. In order to develop treatment technologies capable to destroy these ARB, it is extremely important to know more about them and, particularly, on the extension of the problem associated with each particular ARB. In this section, a prospective study of pathogens causing UTIs was used to discuss the proper management of ARB removal. This study was carried out in collaboration with the University Hospital Complex of Albacete, Spain (CHUA) as model of sanitary facility. The CHUA depends on the health service of Castilla-La Mancha (SESCAM) and is integrated by the General University Hospital of Albacete, the University Hospital of Perpetuo Socorro and the Mental Health Care Centre of Albacete. It is equipped with 752 beds, representing a total of 2.54 beds per 1000 inhabitants. Data on positive urine pathogens were provided by the Microbiology and Parasitology Service of CHUA. The patients under study have a clinical diagnosis of UTI and belong to different hospital units. This allows to evaluate the occurrence and fate of ARB in a real environment as well as the problematic associated with ARB in a hospital complex.

To reach this global aim, the following partial objectives were developed:

- A statistical study to identify the isolated pathogens causing UTIs in hospitalized patients.
- A prevalence study to quantify ARB causing UTIs in hospitalized patients.

To meet these objectives, 4,453 positive urine samples were accounted for the prevalence study from CHUA in the period 2014-2018 as shown in Table 5.1.

Table 5.1. Urine samples analysed.

TOTAL URINE SAMPLES (4,453)	*K. pneumoniae* (426 samples) (9.57 %)	ARB (143 samples) (33.56 %)	*ESBL (138 samples) (96.51 %)
			**CPB (5 samples) (3.49 %)
		No ARB (283 samples) (66.44 %)	
	E. coli (1,866 samples) (41.90 %)	ARB (269 samples) (14.41 %)	*ESBL (268 samples) (99.63 %)
			**CPB (1 samples) (0.37 %)
		No ARB (1,597 samples) (85.58 %)	
	S. aureus (65 samples) (1.46 %)	ARB (32 samples) (49.23 %)	***MRSA (32 samples) (100 %)
		No ARB (33 samples) (50.77 %)	
	Others (2,096 samples) (47.07 %)		

**extended spectrum beta-lactamases (ESBLs)*

***carbapenemase-producing bacteria (CPB)*

**** methicillin resistant (MRSA)*

5.1.1. Statistical study of pathogens in urine

UTIs are some of the most common infections in hospitals and represent a significant cause of morbidity of males and females of all ages [21]. Severe health problems associated with UTIs include pyelonephritis with sepsis, renal damage, pre-term birth and complications caused by frequent antimicrobial use [22]. Several risk factors are associated with UTIs, including female gender, sexual activity, vaginal infection, diabetes, obesity or genetic susceptibility among others [23, 24]. For this reason, the prevalence of gender in the presence of pathogens in urine has been considered in this study.

There are many areas in a sanitary complex where patients can present UTIs and, consequently, urines analysed come from different units of CHUA: geriatrics, haematology, oncology, reanimation, and intensive care unit (ICU). A total of 14,368 urine samples were analysed and 4,453 (30.99 %) were positive for the presence of pathogens from 2014 to 2018. Within these positive urines (PUs), 2,874, 286, 371, 421 and 528 correspond to geriatrics, haematology, oncology, reanimation and ICU, respectively. The distribution of these PUs over the 5-year period studied and the differences in infected patients between males and females are shown in Table 5.2.

As previously commented, UTIs have a gender factor, making women be more likely to develop them. This is supported by Table 5.2, where during the 5-year period, 62.36 % of PUs correspond to females. The number of PUs increases over the years, peaking in 2018, which could be attributed to the ageing of the population. As expected, geriatrics is more affected by this phenomenon with 473 PUs registered in 2014 and were almost doubled (836) 5 years later. PUs from geriatrics represent 64.54 % of all PUs which could be related to the particularities that characterize patients from this unit such as being elderly people (over 65) or presenting several pathologies with greater incidence of illness in the same individual [25-27]. PUs from haematology, oncology, reanimation and ICU are within the range 50-121 samples for all the years analysed, being higher in the last years. Differences in the age of patients of each unit are also noticeable. Specifically, elderly patients $\geq$ 65 years represent 99.23, 63.64, 54.18, 57.72

and 53.79 % of the total PUs of geriatrics, haematology, oncology, reanimation and ICU, respectively. These data reveal that the potential for developing an UTI could be directly related to the age and gender of the patient.

Table 5.2. Distribution of PUs in each hospital unit from 2014 to 2018 in CHUA. T: Total, F: Female (%), M: Male (%).

		Geriatrics	Haematology	Oncology	Reanimation	ICU
PUs 2014	**T**	473	50	51	74	91
	F (%)	71.04	78.00	50.98	43.24	51.65
	M (%)	28.96	22.00	49.02	56.76	48.35
PUs 2015	**T**	482	70	70	76	120
	F (%)	70.54	40.00	57.14	46.05	57.50
	M (%)	29.46	60.00	42.86	53.95	42.50
PUs 2016	**T**	457	52	83	72	91
	F (%)	64.77	61.54	53.01	56.94	54.95
	M (%)	35.23	38.46	46.99	43.06	45.05
PUs 2017	**T**	599	57	85	78	108
	F (%)	69.62	63.16	57.65	43.59	44.44
	M (%)	30.38	36.84	42.35	56.41	55.56
PUs 2018	**T**	836	57	82	121	118
	F (%)	65.07	64.91	37.80	46.28	59.32
	M (%)	34.93	35.09	62.20	53.72	40.68

Many studies focused on the epidemiology of UTIs have demonstrated that UTIs are caused by a wide range of pathogens, including gram-negative and gram-positive bacteria, and yeasts [28-30]. Despite the above-mentioned microorganisms are found in greater proportion in PUs, the number of pathogens that can be found in a smaller percentage is quite extensive. In this case of study, only pathogens that represent more than 1.00 % of the total pathogens have been included. Likewise, it is important to mention that two or more pathogens can result positive for a single urine sample analysed, being 5,036 the number of pathogens for the 4,453 PUs reported in the study. The distribution of pathogens in the different hospital units during the 5-year period is represented in Figure 5.1.

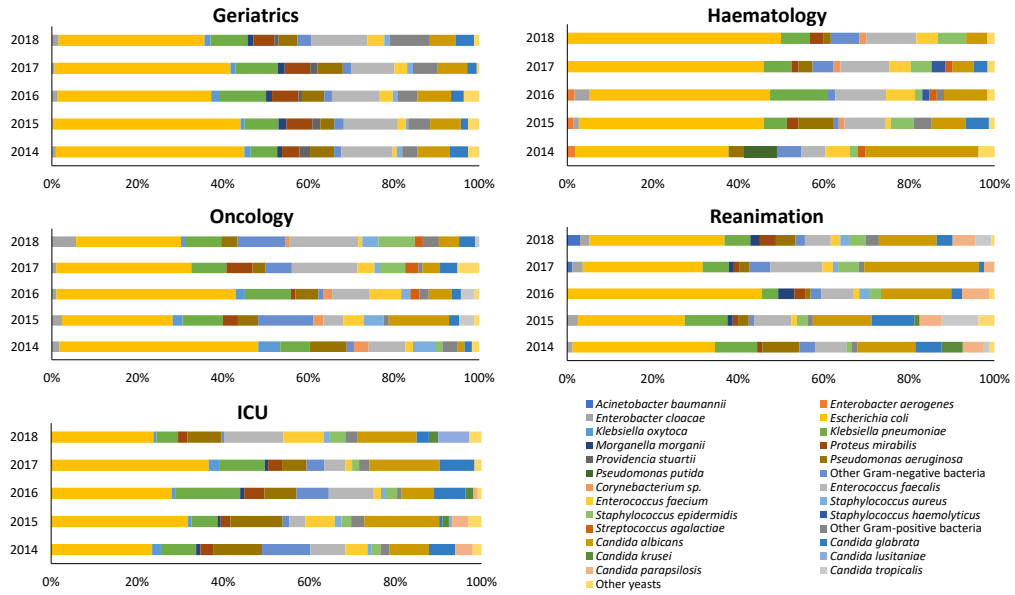

Figure 5.1. Percentage of positive microorganisms, representing more than 1.00 % of total PUs, in the different hospital units during the period 2014-2018.

E coli was the most significant pathogen in the PUs of all hospital units, being present in 1866 patients, 1365 women and 501 men. Specifically, it ranges from 20.00 to 50.00 %, with a mean value of 37.05 % of the total pathogens in the different hospital units over the years. This value is slightly lower than that previously reported in literature (65.00 - 75.00 %) [22]. Nonetheless, other studies have demonstrated that the microbiology of UTIs depends on its pathology. For instance, in a review of multicenter data on Catheter-associated Urinary Tract Infections (CAUTI), *E. coli* was only present in 23.90 % of PUs between 2011 and 2014 [31].

Regarding other gram-negative bacteria, *K. pneumoniae* (3.80 – 15.00 %), *P. aeruginosa* (0.00 - 12.10 %) and *Proteus mirabilis* (*P. mirabilis*) (0.00 - 6.20 %) are the most representative ones, considering all hospital units. Gram-positive bacteria are mainly represented by *E. faecalis*, the most significant pathogen of the family of *Enterococcus spp.*, ranging from 3.80 to 16.00 % in all PUs. The genus of *Staphylococcus* is poorly represented by *Staphylococcus aureus* (*S. aureus*) and *Staphylococcus epidermidis* (*S. epidermidis*), both with low prevalence percentages. The presence of *Staphylococcus saprophyticus* (*S. saprophyticus*), which was

previously introduced as the main specie of *Staphylococcus spp*. in UTIs, was below 1.00 % in PUs, so it was neglected. Group *B Streptococcus* is weakly constituted by *Streptococcus agalactiae* (*S. agalactiae*) with only presence in haematology and oncology. Finally, *Candida spp*, represents the most predominant yeasts family in all hospital services. *Candida albicans* (*C. albicans*) is the species found in the highest percentage, followed by *Candida glabrata* (*C. glabrata*) and *Candida parapsilosis* (*C. parapsilosis*).

Paying special attention to each hospital unit individually, geriatrics seems to be the unit with the least variability in the ranges of pathogens over the years. In this hospital unit, *E. coli* was the most common pathogen ranging from 34.10 to 44.10 % followed by *E. faecalis* (10.10-13.10 %), *K. pneumoniae* (6.20-11.00 %), *C. albicans* (6.10-7.80 %) and *P. mirabilis* (4.10-6.20 %). Similar results have been recently reported in Denmark, in a study with elderly patients ≥ 60 years where 15,242 cases of nosocomial UTIs were registered. The most common pathogens found were *E. coli*, *E. faecalis*, *K. pneumoniae* and *Enterococcus faecium* (*E. faecium*), present in 58.00, 28.00, 9.00 and 5.00 % of the total cases [32]. On the other hand, it is worth noting the elevated presence of *E. coli* in the unit of haematology, where in most of the years the percentage of prevalence were higher than 40.00 %. Conversely, in the unit of oncology, the presence of this pathogen has decreased over the years, from 46.60 % in 2014 to 24.50 % in 2018. Reanimation and ICU units have an important prevalence of *C. albicans* (13.50 - 26.80 % and 7.50 - 17.40 %, respectively), being the most significant pathogen in PUs after *E. coli*. These results are supported by the National Nosocomial Infection Surveillance system reports where *C. albicans* is reported as the second cause of nosocomial UTIs in ICUs [33].

To evaluate the prevalence of the total gram-negative and gram-positive bacteria, and yeasts in PUs from different hospital units, Figure 5.2 shows the percentage distribution of each type of microorganism over the 5-year period in the different hospital units.

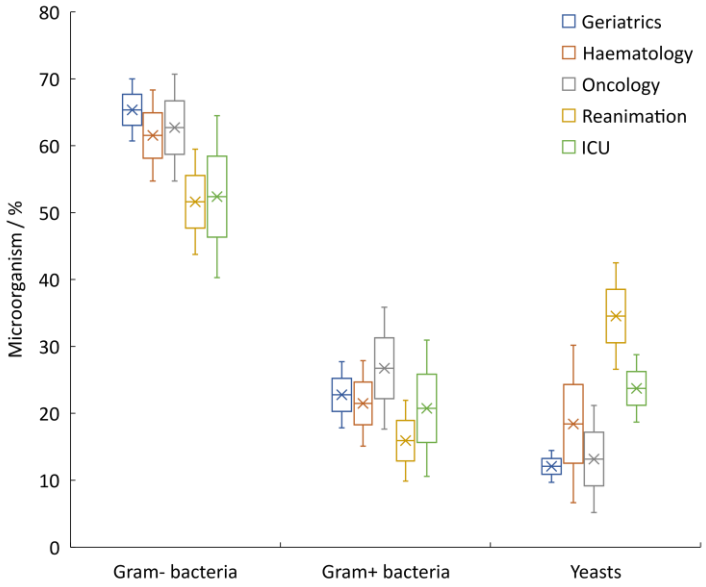

Figure 5.2. Distribution of total microorganisms corresponding to gram-negative, gram-positive bacteria and yeasts for each hospital unit during the years 2014-2018. Maximum, minimum, and mean value (*).

Results clearly depict the dominance of gram-negative pathogens in PUs with a presence between 40.30 and 70.70 % of the total pathogens for all the units studied. This agrees the *E. coli* prevalence in UTIs reported in the literature [22] and, it is also supported by several studies related to the pathology of gram-negative organisms in nosocomial UTIs [34, 35]. Regarding the distribution of gram-positive bacteria, their presence is within the range of 9.87-35.84 % in all PUs from the different hospital units, being clearly lower than the percentages registered for gram-negative bacteria. However, it is worth noting the highest percentages of gram-positive bacteria exhibited in the PUs from the oncology unit (35.84 – 17.64 %), which can be related with the higher risk of oncology patients of being colonized or infected by microorganisms of *Enterococcus* genus [36]. On the other hand, the prevalence of yeasts is higher in reanimation and ICU units which agrees with other studies reported in literature [37-39]. For instance, a study at a University Hospital in Turkey showed that the presence of *Candida spp.* was predominant for the Anaesthesiology and Reanimation Unit [40]. Besides, patients hospitalized in ICUs are at great risk for developing nosocomial fungal

infections presenting common risk factors. Some of them act primarily by inducing immunosuppression (e.g., corticosteroids, chemotherapy, malnutrition, malignancy, and neutropenia) while others primarily provide a route of infection (e.g., extensive burns, indwelling catheter), and some act in combination [41]. This could also explain the lower percentages of gram-negative bacteria registered in these units in comparison with geriatrics, haematology and oncology.

As stated above, women are more likely to suffer UTIs and, for this reason, the influence of gender in the presence of gram-negative and gram-positive bacteria, and yeasts in PUs is represented in Figure 5.3.

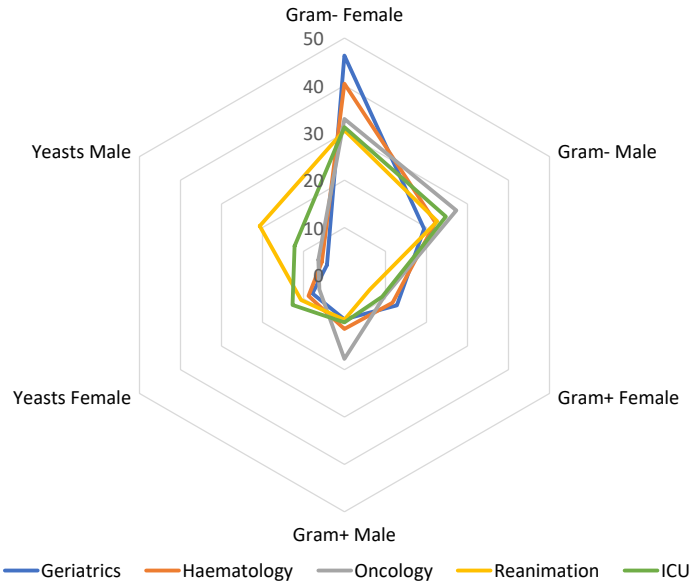

Figure 5.3. Gender prevalence in the distribution of total microorganisms corresponding to gram-negative, gram-positive bacteria and yeasts for each hospital unit during the years 2014-2018.

Furthermore, a chi-square (X^2) study of the gender prevalence in the different hospital units has been carried out from the data of Figure 5.3. The X^2 study is one of the tests belonging to the descriptive statistics applied to the study of two variables. It is a hypothesis test that compares the observed distribution of the data with an expected distribution of the data. The test uses an approximation of the X^2 distribution to evaluate the probability of a discrepancy equal to or greater than that between the data and the

expected frequencies according to the null hypothesis. The independence of two variables means that they are unrelated, and therefore one does not depend on the other, nor vice versa [42]. Results obtained from the X^2 study conclude that there is a statistically relevant relationship between the gender and PUs in geriatrics, oncology and reanimation units. On the contrary, there is no such relationship, independent variables, in haematology and ICU. The X^2 study stablishes for geriatrics, oncology and reanimation units that; 1) if a patient suffers a UTI associated with a gram-negative bacteria, the probability of being female would be 70.40, 54.70 and 57.40 %, respectively, 2) if a patient suffers a UTI associated with a gram-positive bacteria, the probability of being female would be 57.80, 35.00 and 39.40 %, respectively, and 3) if a patient suffers a UTI associated with a yeast, the probability of being female would be 64.70, 49.10 and 33.80 % for the same units, respectively.

UTIs can be caused by a wide variety of pathogens, however, those with antibiotic resistance involve a big challenge for their elimination. Infections caused by ARB cannot be treated with commonly used clinical antimicrobials, leading to serious health problems and high associated costs [43]. Extended spectrum beta-lactamases (ESBLs) are enzymes able to hydrolyse third and fourth generation cephalosporins and monobactams [44]. The epidemiology of ESBLs changes rapidly worldwide and, hence, there is no general overview of these enzymes in UTIs. Specifically, the antibiotic resistance of *E. coli* and *K. pneumoniae* associated to ESBLs is particularly high in some countries of the European Union, where UTIs can no more be treated with the common antibacterial classes, according to the European Antimicrobial Resistance Surveillance Network (EARS-Net). Therefore, ESBLs represent a public health concern due to the high prevalence in these common pathogens [45, 46]. In the case of study, the percentage of *K. pneumoniae* and *E. coli* producing ESBLs (ARB_{ESBL}) in PUs from the different hospital units of CHUA over the 5-year period is represented in Figure 5.4.

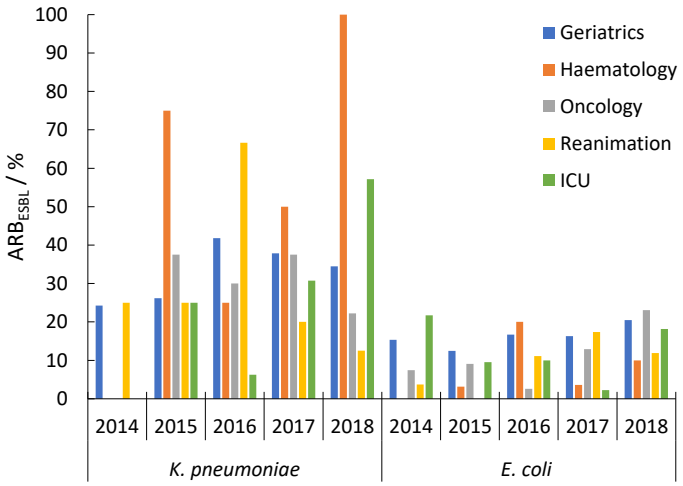

Figure 5.4. Evolution of the percentage of ARB_{ESBL} in the different hospital units during the period 2014-2018.

Overall, 32.39 % of total *K. pneumoniae* in PUs from all hospital units are ARB_{ESBL}. The percentage of this bacterium increased gradually throughout the years, from 9.80 % in 2014 to 45.30 % in 2018, being noticeable the higher percentages of ARB_{ESBL} in the reanimation unit in 2016 (66.70 %), and in the haematology unit in 2015 (75.00 %) and 2018 (100.00 %). On the other hand, the presence of *E. coli* producing ESBLs was much lower than that shown by *K. pneumoniae*, representing just the 14.36 % of total *E. coli* in PUs from all hospital units. The presence of this bacterium also showed an increasing tendency through the 5-year period of the study, from 9.60 % in 2014 to 16.70 % in 2018. These results highlight the greater threat to human health posed by *K. pneumoniae* (ARB_{ESBL}) and support the world's growing concern for this bacterium.

Other mechanisms of antibiotic resistance are possible for *E. coli* and *K. pneumoniae*. Specifically, in the late 90s, the carbapenem-resistant *K. pneumoniae* began to emerge and, currently, is the most common carbapenemase detected globally [47, 48]. Carbapenemase-Producing Bacteria (CPB) have a large and shallow active site, allowing these enzymes to accommodate a wide range of β-lactam molecules, including cephalosporins, monobactams, and carbapenems [49]. Acquired serine carbapenemase enzymes are resistant to most β-lactams and they encode a multitude of

other resistance genes, offering multidrug resistance [50]. In the present study, the percentage of *K. pneumoniae* and *E. coli* producing CPB (ARB_{CPB}) in PUs from the different hospital units over the 5-year period is represented in Figure 5.5.

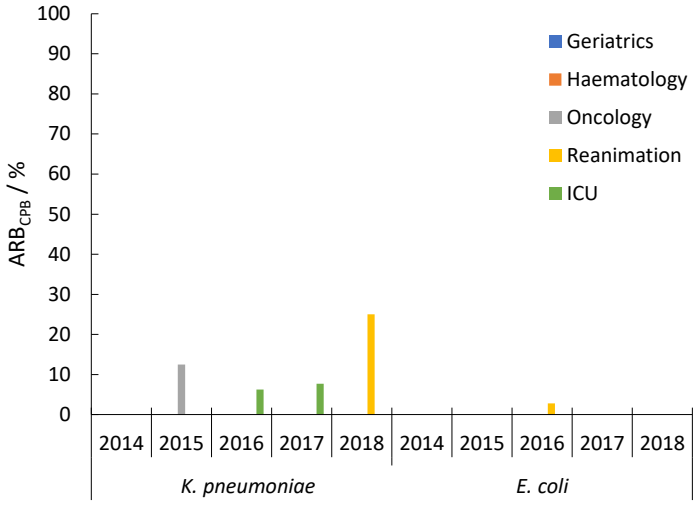

Figure 5.5. Evolution of the percentage of ARB_{CPB} in the different hospital units during the period 2014-2018.

In this case, 1.17 % of total *K. pneumoniae* in PUs from all hospital units were ARB_{CPB}. Nonetheless, these data were only obtained from oncology, ICU and reanimation because the presence of ARB_{CPB} in geriatrics and haematology was null. Despite the low percentage of ARB_{CPB} in all years analysed, this increased up to 25.00 % in reanimation unit in 2018. Once again, *K. pneumoniae* presented a higher percentage of resistance than *E. coli*, in which only 1 case out of 1,866 positives (0.05 %) were ARB_{CPB}. These results reveal that ARB_{ESBL} are more widespread than ARB_{CPB} and the higher resistance percentages of *K. pneumoniae* point out again the need to control this bacterium.

On the other hand, methicillin-resistant *S. aureus* (MRSA) strains are common causes of nosocomial infections in hospital facilities, including ITUs [31, 51]. The prevalence of MRSA strains has significantly increased over the years. In fact, the spread of MRSA infections from healthcare facilities to various community settings has raised considerable concern in recent decades [52]. The *mec*A gene is responsible for

carrying resistance to methicillin. This gene has a large heterologous mobile genetic element called Staphylococcal Cassette Chromosome mec (SCCmec) that promotes *S. aureus* resistance to Methicillin. The increasing emergence of resistance to currently available antimicrobial agents among MRSA strains has limited the choice of therapeutic options and is becoming a serious threat to public health [53]. Figure 5.6 shows the percentage of *S. aureus* producing MRSA (ARB_{MRSA}) in PUs from the different hospital units over the 5-year period.

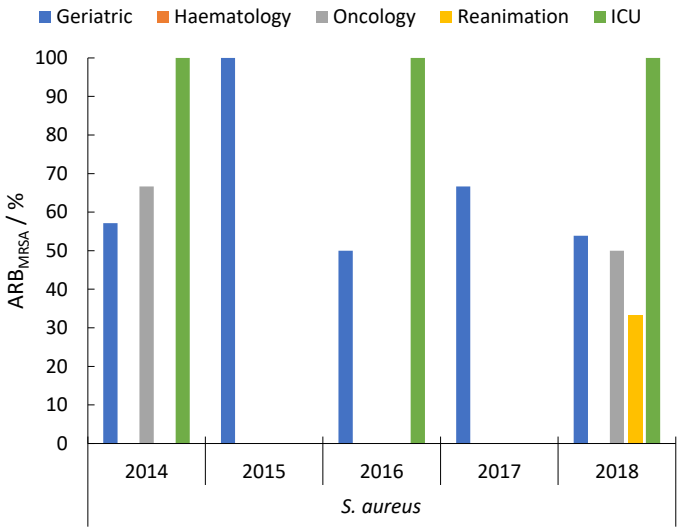

Figure 5.6. Evolution of the percentage of ARB_{MRSA} in the different hospital units during the period 2014-2018.

A total of 65 samples were positive for *S. aureus*, of which, 32 presented methicillin resistance. Although MRSA strains are less common, their occurrence is much higher than those of ESBL (Figure 5.4) and CPB (Figure 5.5) in the CHUA since almost 50.00 % of analysed cases exhibited antibiotic resistance. Specifically, the presence of ARB_{MRSA} is most remarkable in geriatrics, reaching percentages of 100.00 % in 2015, and in ICU, where values of 100.00 % in the years 2014, 2016 and 2018 were achieved. However, no ARB_{MRSA} were registered in haematology unit within the years analysed.

In summary, 426 samples were positive for *K. pneumoniae* where a percentage of 33.56 % were ARB, being 96.51 % ARB_{ESBL} and 3.49 % ARB_{CPB}. Conversely, 1,866 samples were positive for *E. coli*, finding 14.41 % as ARB of which 99.63 % were ARB_{ESBL} and 0.37 % ARB_{CPB}. Eventually, ARB_{MRSA} represent 49.23 % of the total *S. aureus* in PUs (65 samples). Thus, ARB represent 9.97 % of the total PUs (4,453) reported in the study, 8.81 % of the total microorganisms (5,036) reported, and 18.83 % of the three bacteria presenting ARB, *K. pneumoniae*, *E. coli*, and *S. aureus* (2,357).

Based on previously data (figures 5.4-5.6), *K. pneumoniae, E. coli* and *S. aureus* can be considered as bacteria that pose a higher risk for human health. Furthermore, these ARB and their ARGs have been commonly detected in wastewater, surface water, drinking water biofilms and urban treated wastewater [54, 55]. For this reason, it is necessary to develop novel and efficient technologies that allow to kill these pathogens for avoiding their spread not only in sanitary facilities but also in the environment. In this context, a literature search focused on these specific bacteria and the disinfection technologies proposed for their elimination in three different scenarios (water disinfection, wastewater disinfection and hospital wastewater disinfection) was carried out. This allows us to compare the importance given to the main ARB found in the case study from a sanitary and environmental-technological viewpoint. The search has been carried out using SCOPUS as database and the following keywords (April 30th, 2021): "disinfection", the type of effluent ("water", "wastewater" or "hospital wastewater") and the specific bacteria ("*Escherichia coli*", "*Klebsiella pneumoniae*" or "*Staphylococcus aureus*"), finding 3,977 documents for water, 987 documents for wastewater and only 33 documents for hospital wastewater. Figure 5.7 summarizes the percentage of scientific papers related to the disinfection of each ARB in the different scenarios.

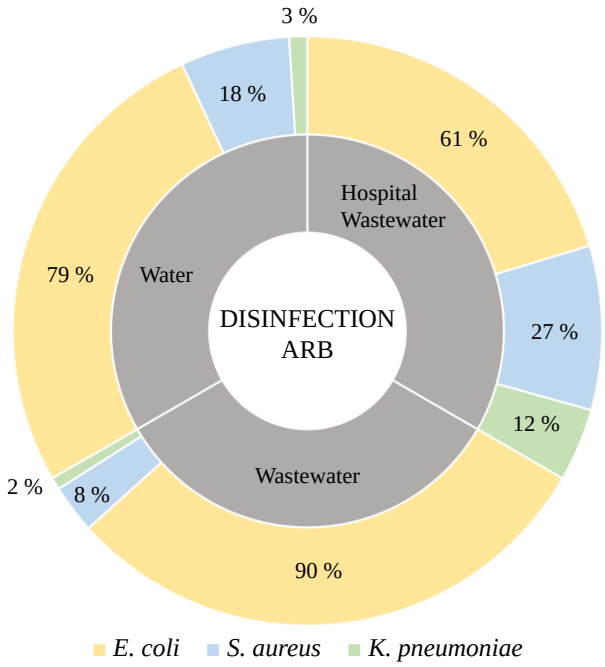

Figure 5.7. Literature reported on disinfection of ARB.

As can be observed, most studies reported in literature are focused on the removal of *E. coli* followed by *S. aureus* and, finally, *K. pneumoniae*. This is more remarkable in the disinfection of wastewater where scientific papers related to *E. coli* achieve 90 % (888 documents). This is an expected outcome because this pathogen is the most common indicator of faecal pollution, and their removal is critical for very important applications such as wastewater reclamation. On the other hand, the research reported on the disinfection of hospital wastewater shows the lowest percentage of documents related to *E. coli* (61 %; 20 documents) in comparison with the disinfection of water (79 %; 3,142 documents) and wastewater (90 %; 888 documents). In this scenario, the manuscripts related to the removal of *S. aureus* and *K. pneumoniae* are higher, reaching values of 27 (9 documents) and 12 % (4 documents), respectively. The studies reported in water and wastewater based on the removal of these bacteria are lower than 20 % for *S. aureus* (water: 716 documents; wastewater: 79 documents) and, only 2-3 % of all documents for *K. pneumoniae* (water: 119 documents; wastewater: 20 documents). This points out the importance given for these ARB in hospital wastewater

by scientists because of the sanitary risks associated to both bacteria. Nonetheless, the research carried out in the disinfection of hospital wastewater is mainly focused on the removal of *E. coli* since is the pathogen found in the highest incidence in urines from the different hospital areas (Figure 5.1).

These results reveal that the importance given to the disinfection of the main ARB found in hospital urine by scientific community is not directly related to their hazardousness from a sanitary viewpoint since *K. pneumoniae* can be considered as the main ARB in hospital urine but the research about its disinfection is scarce.

5.1.2. Conclusions

E. coli was the most significant bacteria found in PUs regardless the hospital unit studied. The UTIs were significantly affected by the age and gender of patients. Gram-negative bacteria (*E. coli*, *K. pneumoniae*, *P. aeruginosa* and *P. mirabilis*) predominate over gram-positive bacteria (*E. faecalis*) and yeasts (*C. albicans*). However, *K. pneumoniae* showed the highest percentages of ARB_{ESBL} and ARB_{CPB}, confirming its greater hazardousness to human health from a sanitary viewpoint. On the contrary, the research carried out on the disinfection of ARB is mainly related to the removal of *E. coli* since is the pathogen found in the highest proportion in water bodies. The importance given to *K. pneumoniae* as ARB from a sanitary viewpoint does not correspond to the research carried out on the disinfection of ARB by the scientific community because the literature reported is scarce and the likelihood of finding antibiotic resistant is higher in *K. pneumoniae* than in *E. coli*, despite the last one is found in greater extension. Hence, it is necessary to search and to develop novel technologies that allow to remove *K. pneumoniae* ARB for decreasing the sanitary and environmental impact of the effluents infected with this bacterium.

5.2. Treatment of hospital urines with electrolysis

Regarding the environmental problem related to the presence of ARB in natural water, it should be pointed out that the critical source of these ARB is found in hospital facilities because many of these bacteria are excreted by urine of immunocompromised patients in whom their immune system is unable to control the infection. Hospital urines are merged with wastewater from other services (laundry, kitchen…) and, finally, it is discharged to the sewerage system [56] allowing the spread of these hazardous bacteria into the environment [57, 58]. Additionally, urine is also considered as one of the most dangerous pollution sources since high concentration of pharmaceuticals and their metabolites are excreted by this media [59]. This has promoted the searching for technological solutions to decrease the impact of sanitary effluents into the environment, grouped in two main strategies: 1) boosting efficient treatments at WWTPs by the implementation of additional treatments, 2) pre-treatment before their discharge into WWTPs, that is in the pollution source. The second option is emerging as the key alternative, as it addresses the problem in more concentrated effluents and the volume of wastewater treated is further much lower than in the other case. Additionally, the treatment of urine at the point of generation could reduce the ecotoxicity risks of hospital effluents.

Electrolysis with diamond anodes could be considered as an appropriate technology for the removal of ARB due to its efficiency in the disinfection of urban treated and surface water [60-62]. This process is based on the in-situ production of disinfectants from the oxidation of the ions naturally contained in the effluent. The main advantages of electrolysis include that the addition of chemicals is not required and the operating conditions for disinfection are usually soft [63]. These good prospects have encouraged some researchers to propose the use of diamond electrolysis as tertiary treatment after conventional wastewater treatment plants (WWTPs) [64]. Nonetheless, electrochemical processes are generally limited by mass transfer [65, 66] and by the formation of hazardous by-products [67]. These drawbacks have limited the use of this

technology and have encouraged the search of different strategies to solve these problems [68, 69].

The search for suitable treatment strategies is needed to help reduce both the environmental and sanitary impact of hospital effluents. In this regard, to reach this global aim, the following partial objectives were developed in this section:

- A preliminary study of the electrochemical technology as an alternative for the removal of bacteria in two different treatment scenarios: 1) synthetic urban wastewater rich in ammonium (similar to that obtained in stabilization ponds, where additional disinfection is taking place by sunlight), 2) synthetic hospital urines. This study is faced in section 5.2.1 and is intended to shed light on the role of water matrix on the disinfection performance and, hence, to stablish the best treatment point (as tertiary treatment of urban wastewater or as pretreatment of the main pollution source) for decreasing the sanitary and environmental hazardousness associated to ARB.
- An evaluation of electrolysis for the reduction of the potential chemical risk of hospital urine during the disinfection process. This study is discussed in section 5.2.2 and it was designed to test whether under the operation conditions used in the electrodisinfection process the removal of other organic contaminants present in urine, such as antibiotics, can be also attained.

To attain these partial objectives, the following experimental planification was outlined:

- Electrodisinfection with BDD electrodes of synthetic water matrixes (see Table 4.3) intensified with three different target bacteria: two bacteria commonly found in hospital urines (*K. pneumoniae* as gram-negative bacteria and *Enterococcus faecalis* (*E. faecalis*) as gram-positive bacteria), and a third bacterium commonly found in urban treated wastewater (*E. coli*). Table 5.3 shows the experimental conditions used in each test.

Table 5.3. Experimental planification of different treatment strategies for the removal of bacteria.

Exp. Nº	Tech.	Reactor	Anode / Cathode	*Current density (A m^{-2})	Treated effluent	Bacterial strains
1	Electrolysis	Single compartment electrochemical cell	BDD / SS	10	Synthetic urban wastewater	*E. coli* ATCC 25922
2						*K. pneumoniae* ATCC 4352
3						*E. faecalis* ATCC 19433
4	Electrolysis	Single compartment electrochemical cell	BDD / SS	10	Synthetic hospital urines	*E. coli* ATCC 25922
5						*K. pneumoniae* ATCC 4352
6						*E. faecalis* ATCC 19433

*This current density value was selected considering other results reported in the literature related to the applicability of electrodisinfection process [70].

- Electrolysis of synthetic urine polluted with chloramphenicol (selected as a model of antibiotic). The role of anodic material (BDD and MMO) and current density (50, 25, 12.5 A m^{-2}) was evaluated. Table 5.4 shows the experimental conditions used in each test.

Table 5.4. Experimental planification of electrolysis tests for the removal of chloramphenicol in synthetic urines.

Exp. Nº	Tech.	Reactor	Anode / Cathode	*Current density (A m^{-2})	Treated effluent	Antibiotic
1	Electrolysis	Single compartment electrochemical cell	BDD / SS	12.5	Synthetic hospital urines	Chloramphenicol 100 mg dm^{-3}
2				25		
3				50		
4	Electrolysis	Single compartment electrochemical cell	MMO / SS	12.5	Synthetic hospital urines	Chloramphenicol 100 mg dm^{-3}
5				25		
6				50		

*This current density value was selected considering the selected value for disinfection purposes and other typical higher values found in literature for the degradation of antibiotics.

5.2.1. Removal of antibiotic resistant bacteria by electrolysis with diamond anodes: a pretreatment or a tertiary treatment?

Figure 5.8 shows the decay in the population of three different bacteria with the applied electric charge during the electrochemical disinfection with diamond anodes of synthetic urban treated wastewater and hospital urine. All electrolysis tests were carried out at 10 A m^{-2}. The initial bacteria population used was similar in both effluents to evaluate the process efficiency in similar conditions, although a lower population may be expected in a real urban treated wastewater [71].

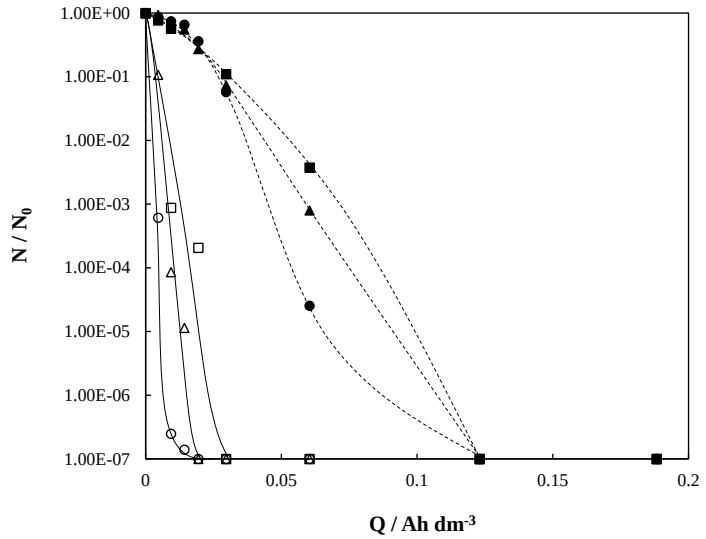

Figure 5.8. Influence of water matrix of the removal of antibiotic resistant bacteria by electrolysis with diamond anodes. (■) *E. coli*; (▲) *K. pneumoniae*; (●) *E. faecalis*; white symbols: urban wastewater; black symbols: hospital urine; j: 10 A m^{-2}.

As can be observed, the disinfection efficiency depends on the nature of the bacteria and on the complexity of the aqueous matrix. The population of all microorganisms decreases with the applied electric charge and the complete disinfection is reached at values below 0.15 Ah dm^{-3}. This is due to the action of disinfectant species generated during electrolysis. The occurrence of these species is detailed later. Comparing results of the three bacteria tested, *E. faecalis* shows a higher depletion efficiency followed by *K. pneumoniae* and, finally, *E. coli*. This difference can be related to the cell morphology of each bacterium since *E. faecalis* is a gram-positive

bacterium whereas *K. pneumoniae* and *E. coli* are gram-negative bacteria. Specifically, gram-positive bacteria present a cytoplasmic membrane and a cell wall in its structure, while gram-negative bacteria are constituted by a cytoplasmic membrane, the cell wall and an additional external membrane [72]. This supplementary membrane in gram-negative bacteria could be the responsible for the higher resistance against the disinfection process.

The differences observed also depend on the water matrix. Thus, the disinfection efficiency is higher when working with urban treated wastewater since the complete removal of microorganisms is attained at electric charges below 0.05 Ah dm^{-3}, regardless the bacteria tested. This marked influence of water matrix on the electrochemical disinfection can be related to a competitive oxidation of other compounds during the treatment. In this context, hospital urine also contains organic compounds in high concentration that consume electrons and oxidants for being oxidized: urea, creatinine, and uric acid [70]. On the contrary, urban treated wastewater may contain humic acids as organic load but in low concentration in comparison with the other organics from urine. Therefore, the oxidation of this species is negligible during the electrochemical disinfection, but this is relevant in the case of hospital urine [67]. Hence, the lower disinfection efficiency during the treatment of hospital urine may be related to the simultaneous oxidation of microorganisms and organics.

Experimental data were fitted to a first order kinetics model and the resulting constants are shown in Figure 5.9. For comparison purposes, kinetic constants from the degradation of organics contained in hospital urine have been also plotted.

As can be observed, the disinfection rate of urban treated wastewater is higher than that of hospital urine, being the kinetic constants within the range 0.81-1.02 and 0.13-0.18 min^{-1} for both media, respectively. The ratio $k_{wastewater}/k_{urine}$ (which compares disinfection in wastewater and urine media) confirms that the disinfection rate of *E. faecalis*, *K. pneumoniae* and *E. coli* in urban treated wastewater is 7.02, 6.27 and 5.43 times faster than in urine, respectively. Additionally, the resulting kinetic values for urea, creatinine and uric acid are some orders of magnitude lower ($k < 0.003$ min^{-1}), but, despite this, it confirms the existence of competitive oxidation between bacteria and

organics contained in hospital urine and reveals the importance of the water matrix on the disinfection process.

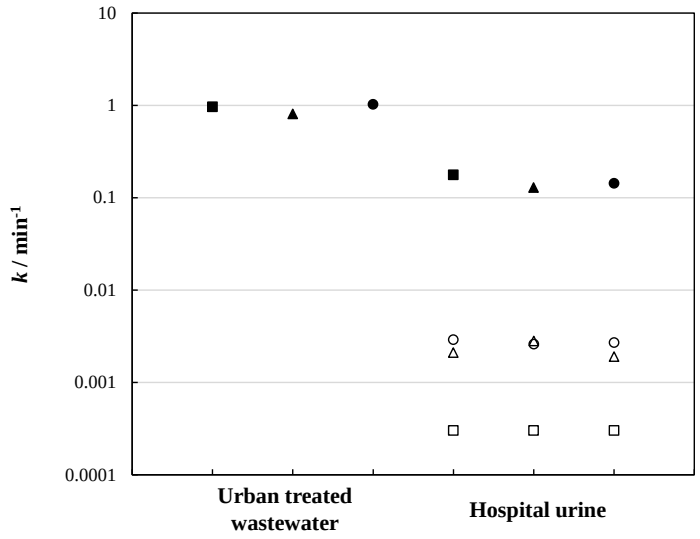

Figure 5.9. Kinetic constants calculated for the removal of ARB by electrolysis with diamond anodes. j: 10 A m^{-2}; (■) *E. coli*; (▲) *K. pneumoniae*; (●) *E. faecalis*; (□) urea; (Δ) creatinine; (○) uric acid.

In this point, it is important to remark that the electrochemical disinfection mainly takes place by the action of disinfectant species electrochemically generated during the process [63]. Therefore, the type and concentration of inorganic species present in aqueous matrix that are susceptible to form strong disinfectants will mark the efficiency of the process. From the disinfection viewpoint, chloride is the ion with the most interest because its oxidation leads to hypochlorite, which shows a high disinfection capacity. Additionally, it can react with ammonium, typically contained in both effluents, to form chloramines which are also disinfectants. On the other hand, hypochlorite can also react with organics present in the reaction media (chlorination reaction) or it can be further oxidized to other undesirable chlorine compounds in high oxidation state (chlorate and perchlorate) [73], whose presence in treated water is not desirable. For this reason, the evolution of chlorine species was monitored during the process and results are plotted in Figure 5.10.

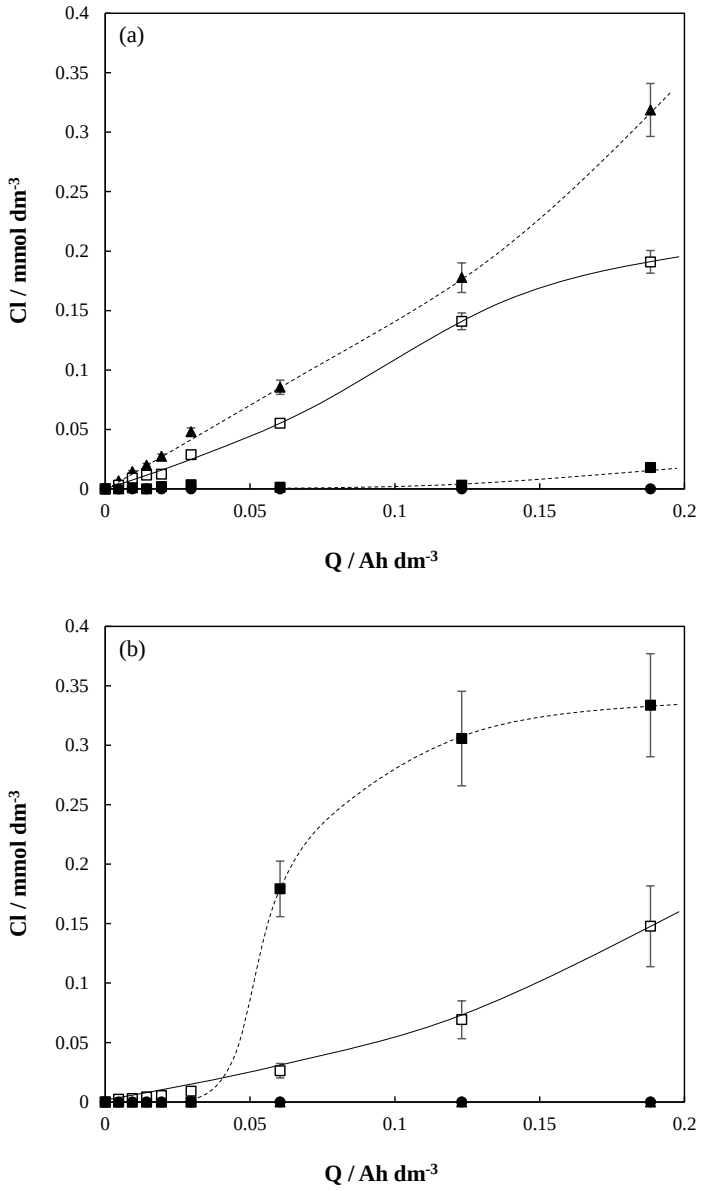

Figure 5.10. Influence of water matrix on chlorine speciation during the removal of antibiotic resistant bacteria by electrolysis with diamond anodes in (a) urban treated wastewater and (b) hospital urine. (■) Hypochlorite; (▲) chlorate; (●) perchlorate; (□) chloramines. j: 10 A m^{-2}.

As can be observed, the concentration of chlorine species increases with the applied electric charge, although the trend and the maximum concentration depend on the water matrix composition. In the case of urban treated wastewater (Figure 5.10a), the concentration of hypochlorite is not relevant (lower than 0.02 mmol dm^{-3}) in

comparison with chloramine and chlorate ones. This indicates that once hypochlorite is generated by the oxidation of chlorides, it rapidly reacts. According to disinfection results shown in Figure 5.8 and to chemical disinfection tests carried out (data not shown), hypochlorite reacts rapidly with bacteria (kinetic constants ranging from 0.81 to 1.02 min^{-1}). Then, once bacteria have decreased the hypochlorite electrogenerated continuous to react with ammonium contained in the treated wastewater, and chloramines are accumulated in the reaction media. The trend observed reveals that the generation rate of these species decreases at higher electric charges which may be related to a limited concentration of ammonium in wastewater or to the promotion of hypochlorite to chlorate (competitive reaction) whose generation rate increases at the end of the treatment. Chlorate is a hazardous species that should be avoided.

On the other hand, in urine media the trend of chlorine species is different, and this could be related to its higher complexity (see Table 4.3). As observed in Figure 5.10b, in the first stages of the process (electric charges below 0.05 Ah dm^{-3}), the accumulation of chloro-species is not favored, and only chloramines start to be detected in the solution (but in very low concentration). The formation of chloramines only can come from the breakpoint reaction which requires the presence of hypochlorite. Then, it confirms that hypochlorite is formed, but its rate of disappearance is greater than its rate of generation. Chloramines profile suggests that its concentration could be increased by the continuous nitrogen release from the oxidation of organics. Unlike urban treated wastewater, the concentration of organics naturally contained in urine is not negligible and they can consume part of the hypochlorite generated. This, together with the hypochlorite used in the disinfection, may justify the delay in hypochlorite accumulation observed in urine. Additionally, the higher initial concentration of chlorides in urine (475.52 *vs.* 148.22 mg dm^{-3}) may explain the higher concentration of hypochlorite accumulated at the end of the process. Furthermore, it is important to highlight the null concentration of chlorate registered in hospital urine. This may indicate that while there are other species in the reaction media that may be attacked (such as uric acid, urea or creatinine), the hypochlorite is not available to be oxidized to chlorate. These results are quite relevant and point out that the formation of hazardous

chlorine by-products can be avoided if the removal of bacteria by electrodisinfection with diamond anodes is directly carried out in hospital urine since the formation of hypochlorite and chloramines is mainly promoted as chlorine species. In addition, from a technical and economic point of view, another advantage of disinfecting hospital urine is its low generation volume compared to that of treated urban wastewater, since hospital urine represents around 2-3 % of the total volume of hospital effluents [74] and these, in turn, represent around 20 % of the volume of urban wastewater [75]. Therefore, although the electric charge necessary for the complete elimination of bacteria is around 6 times higher in urine, the volume to be treated is 5 log units lower, so that both the investment and operation costs would be much lower. This makes direct electrodisinfection of hospital urine an excellent option from a techno-economic point of view to decrease the presence of ARB in the aquatic environment.

5.2.2. Testing the electrochemical oxidation in soft operation conditions to reduce the chemical and environmental risk of hospital urines

Figure 5.11 shows the removal of chloramphenicol (CAP) in urine matrix with the applied electric charge at different current densities (ranging from 12.5 to 50 A m^{-2}) using BDD and MMO anodes. These values of current density were selected to verify the degradation of organic in conditions closer to those typical of electrodisinfection (12.5 A m^{-2}) and closer to those typically used in the electrooxidation of wastewater (25 and 50 A m^{-2}). Under these conditions, it is expected a selective oxidation process and a competitive cost-effective technology. Likewise, BDD and MMO were tested as anodic materials due to their different electrocatalytic behaviour as non-active and active anodes, respectively [76, 77].

As it can be seen, electrolysis with BDD and MMO exhibits different behaviour in terms of CAP degradation efficiency. Specifically, a complete CAP degradation is attained with BDD anode after passing 6 Ah dm^{-3} of applied electric charge for the lowest current density (12.5 A m^{-2}), being the most efficient condition. Likewise, the trend observed with this anodic material follows an exponential decay which is directly

related to a mass-transfer control of the degradation route [76, 78]. The process efficiency is higher when working at very low current densities which suggests that other parasitic reactions take place at high current densities. Hence, electrons are used not only in the antibiotic removal but also are wasted in other side reactions such as oxygen evolution [79, 80]. Regarding CAP removal with MMO anodes, only degradation percentages of 15-35 % are attained at the operating conditions studied. These values are considerably lower than those obtained with BDD anodes. Specifically, BDD anode seems to be up to 5-fold more efficient on CAP degradation in urine media than MMO anode that requires higher applied electric charges to reach a similar CAP removal.

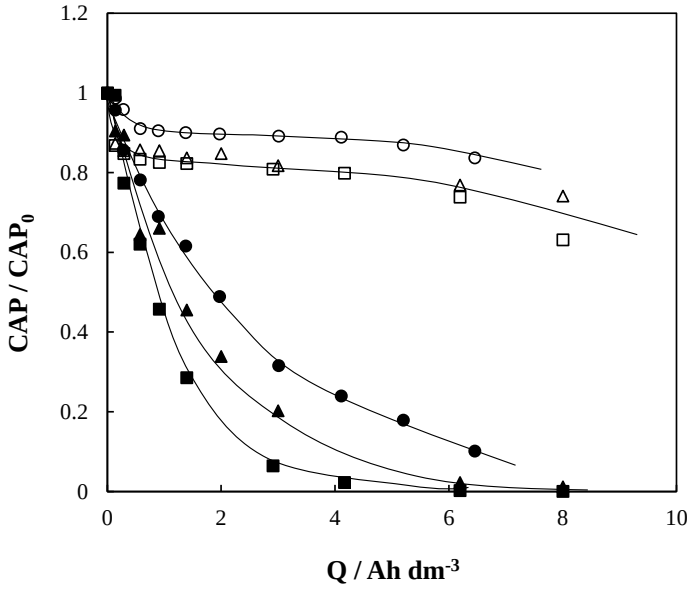

Figure 5.11. Evolution of chloramphenicol as function of the applied electric charge during the electrochemical oxidation of 100 mg dm^{-3} CAP in urine media. Current density: (■, □) 12.5 A m^{-2}; (▲, Δ) 25 A m^{-2}; (●, ○) 50 A m^{-2}. Anodic material: (black symbols) BDD; (white symbols) MMO.

Urine is a complex water media containing different inorganic anions including sulphate, chloride, phosphate or carbonate [81, 82]. These compounds can be also oxidized during electrolysis, favouring the production of powerful oxidants such as hypochlorite, persulfate, peroxodiphosphate and percarbonates [83, 84]. In addition, hypochlorite is known to chemically react with ammonium ions during electrolysis,

resulting in the in-situ production of inorganic chloramines [85]. These generated inorganic oxidants may contribute to CAP degradation by mediated oxidation processes and, for this reason, their concentration was monitored during the process. Figure 5.12 shows the maximum concentration of total oxidants, hypochlorite and chloramines as function of the current density during the treatment of urines polluted with 100 mg dm^{-3} CAP.

As can be observed, the higher the current density, the higher is the maximum concentration of total oxidants remained in solution. BDD anode leads to a lower concentration of total oxidants than MMO anode which is an unexpected behaviour according to literature [84, 86, 87]. This fact is more noticeable at the highest current density (50 A m^{-2}) where the maximum concentration of oxidants is 7.0 mmol dm^{-3} for BDD anode *vs.* 12.8 mmol dm^{-3} for MMO anode. This is mainly related to the stability of the different oxidants generated in each case. In this context, the formation of free and combined chlorine species (hypochlorite and chloramines) and peroxocompounds (persulfate, peroxodiphosphate, percarbonates) are expected to be generated using BDD anodes from the oxidation of the ions contained in urine [84] whereas only chlorine species are expected to be generated with MMO anodes due to their different electrocatalytic properties [88]. Nonetheless, it is important to highlight that measured oxidants inform about the residual concentration of oxidants (after reaction with organics) but not about the total amount of oxidants formed. This means that electrolysis with diamond anodes can be producing more unstable oxidants (peroxocompounds), helping to explain the higher oxidation of organics observed.

Regarding chlorine speciation, hypochlorite concentration attains a maximum value of 0.7 and 0.5 mmol dm^{-3} at a current density of 25 A m^{-2} with BDD and MMO anodes, respectively. Likewise, the maximum concentration of chloramines formed is around two orders of magnitude lower in the case of using BDD and it seems to depend on the current density. The stronger oxidation conditions during BDD-electrolysis seems to favour chloramines decomposition [89, 90], whereas the current density seems to favour the accumulation of dichloramine and trichloramine during MMO-electrolysis [91].

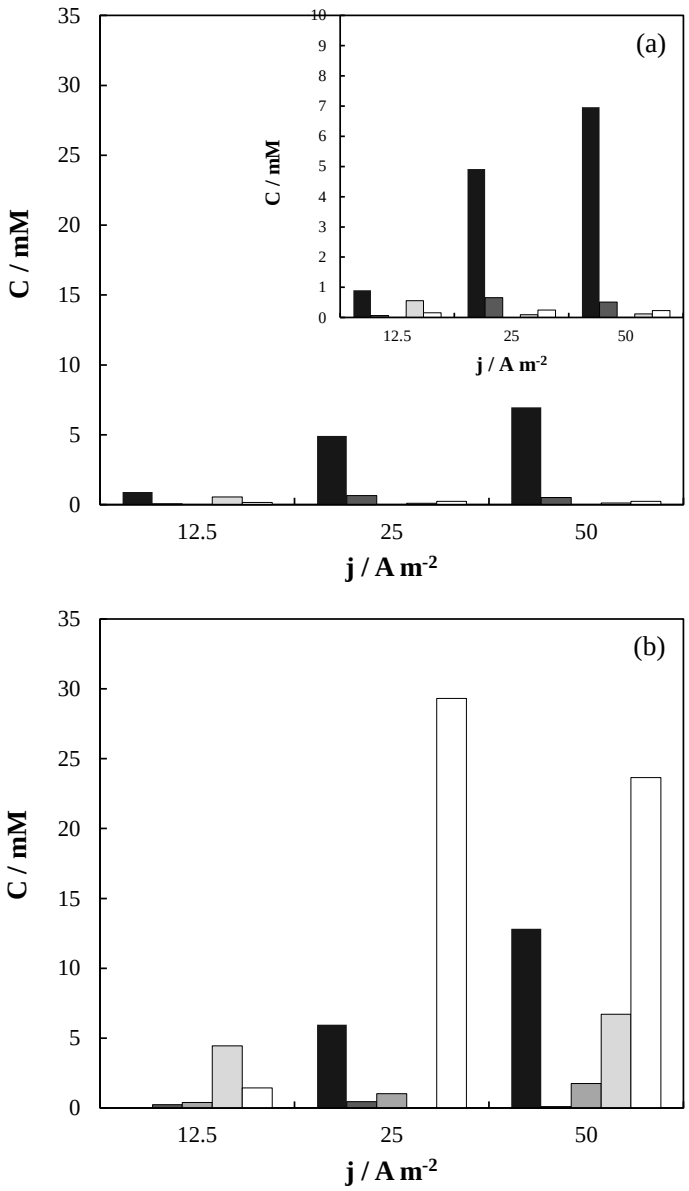

Figure 5.12. Maximum molar concentration of total oxidants, hypochlorite and chloramines as function of the current density applied during the electrochemical oxidation of 100 mg dm^{-3} CAP in urine media. Anodic material: (a) BDD; (b) MMO. (■) total oxidants, (■) Cl-ClO^-, (■) Cl-NH_2Cl, (■) Cl-$NHCl_2$, (□) Cl-NCl_3.

Finally, it is noteworthy to mention that the generation of volatile active chlorine species such as Cl_2, Cl_2O or ClO_2 can be generated during the electrolysis with both anodes, enhancing the oxidation of organics in urine [92]. However, the operating

conditions tested (current density and pH) in this work promote the formation of hypochlorite as the main free chlorine species. On the other hand, chlorine compounds in high oxidation state such as chlorates or perchlorates are not detected anytime in solution at the operating conditions used. This is an excellent output that allow to consider electrochemical oxidation as an appropriate advanced oxidation process for the removal of pharmaceuticals in hospital urines. Combination of hypochlorite with ammonium to form chloramines prevent the further oxidation of hypochlorite to chlorates and perchlorates.

The oxidation of CAP by electrolysis can lead to the formation of other intermediate organic compounds or to progress up to the complete mineralization. The first case can be very worrying since other organics formed can be more hazardous than the initial pollutant, increasing the toxicity of the resulting effluent. On the other hand, the main drawback associated to the complete mineralization is the increase in the energy requirements and, thus, in the treatment costs. At this point, it is important to highlight that the organic load of urine is not only related to the presence of CAP but also to other organics such as urea (3333.33 mg dm^{-3}), creatinine (166.67 mg dm^{-3}) and uric acid (50 mg dm^{-3}) present in its composition at much higher concentrations. For this reason, the evolution of urea, creatinine and uric acid, as well as the mineralization were monitored during the treatment and results are presented in Figure 5.13.

The evolution of TOC is not significantly influenced by the current density applied, regardless the anodic material tested. A negligible mineralization is observed during electrolysis with MMO anode whereas 60 % of mineralization is reached for 8 Ah dm^{-3} using the BDD anode. In this last case, the residual organic matter is expected to be aliphatic compounds, mainly carboxylic acids such as formic, oxalic or oxamic acid [89, 93, 94]. These results suggest that the operating conditions used (low current densities and electric charges) do not favour a complete removal of the organic matter present in the effluent, being more noticeable in the case of MMO anodes. Nonetheless, similar mineralization percentages can be attained with lower energy consumption and higher efficiency when working at very low current densities.

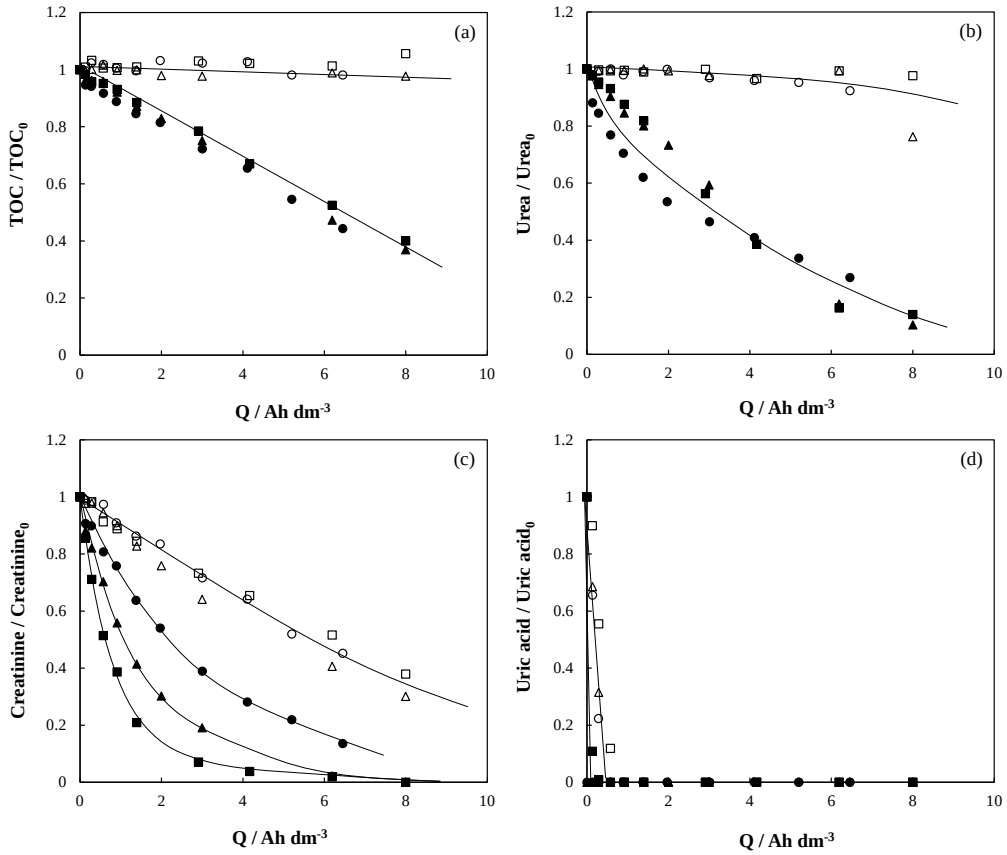

Figure 5.13. Evolution of TOC (a) and urine organic compounds (urea (b), creatinine (c), uric acid (d)) as function of the applied electric charge during the electrochemical oxidation of 100 mg CAP dm^{-3} in urine media. Current density: (■, □) 12.5 A m^{-2}; (▲, Δ) 25 A m^{-2}; (●, ○) 50 A m^{-2}. Anodic material: (black symbols) BDD; (white symbols) MMO. TOC intermediates: (dark grey symbols) BDD; (light grey symbols) MMO.

Regarding the evolution of organic compounds from urine composition, different behaviours can be seen in urea, creatinine and uric acid trends which are related to the different initial concentration of each compound and their different molecular structure [67]. The removal of urea is observed to follow a similar profile than mineralization shown in Figure 5.13a because initial concentration of urea corresponds to most of the initial TOC (83.7 %). Hence, there is a remarkable degradation of urea with BDD anodes whereas a negligible oxidation is observed using MMO anodes. This could be one of the main advantages of these electrodes (MMO) since it allows a selective oxidation of antibiotic, avoiding the potential degradation of urea. On the other

hand, creatinine removal percentages range between 60-93 % in the case of using BDD anodes whereas only around 30 % of creatinine degradation is achieved using MMO anode despite the current density applied. Finally, uric acid is the most efficiently degraded independently of the current densities tested and applied electric charges below 0.3 and 0.6 Ah dm^{-3} are required with BDD and MMO anodes, respectively.

In order to evaluate the competitive oxidation of organics contained in urine, a simple kinetic studied was carried out. Hence, experimental data of CAP, uric acid, creatinine and urea were fitted to a first order kinetics model according to Equation 5.1 (where C is the concentration of target compound at time t in mg dm^{-3}, C_0 is the initial concentration of the target compound in mg dm^{-3}, k is the kinetic constant in min^{-1} and t is the time in min). Resulting kinetic constants are shown in Table 5.5.

$$\text{Ln}\,(C/C_0) = -k \cdot t \qquad (5.1)$$

As can be observed, the kinetic constant of CAP (k_{CAP}) increases with the current density and the degradation rate is higher when working with BDD anodes, which is in line with lower removal percentage attained with MMO electrodes for a given electric charge passed. In the case of urine organic compounds, similar behaviours can be seen: the higher current density, the higher degradation rate for both electrodes, being the values higher with BDD anodes again. The kinetic constants values are higher for uric acid followed by CAP, creatinine and, finally, urea ($k_{UA} > k_{CAP} > k_C > k_U$). Hence, to evaluate the competitive oxidation of antibiotic with other organics naturally present in urine during electrolysis, the ratio k_{CAP}/k_i has been calculated where i is the target organic compound of urine (urea, creatinine or uric acid). Furthermore, electrochemical oxidation of 100 mg dm^{-3} CAP in 3000 mg dm^{-3} perchloric acid (inert media) as electrolyte was carried out and the ratio k_{CAP}/k_i has been also calculated. This study helps to explain the interferences of urine organic compounds on CAP removal. Figure 5.14 shows the ratio k_{CAP}/k_i as function of the applied current density during the electrolysis of 100 mg dm^{-3} CAP with BDD (Figure 5.14a) and MMO (Figure 5.14b) anodes. Values higher than 1 indicates that the degradation rate of CAP is favoured *vs.* the degradation of other organics whereas ratios lower than 1 reveals that the elimination rate of organics naturally contained in urine is favoured instead of antibiotic removal.

Table 5.5. k values for all the applied current densities and anode materials with the corresponding interval of adjustment, residual variance (S^2_R) and coefficient of determination (R^2).

Anode / current density (A m^{-2})	Q (Ah dm^{-3})	Time interval for complete removal (min)	k_{CAP} (10^{-3} min^{-1})	S^2_R (mg^2/L^2)	R^2
		CAP			
BDD / 12.5	8.00	0 -3600	2.08 ± 0.03	0.0176	0.9975
BDD / 25	8.00	0 -1800	2.54 ± 0.07	0.0149	0.9940
BDD / 50	6.46	0 -720	3.04 ± 0.07	0.0035	0.9941
MMO / 12.5	8.00	0 - 3600 (36.86 % removal)	0.08 ± 0.02	0.0033	0.7566
MMO / 25	8.00	0 - 1800 (25.88 % removal)	0.11 ± 0.02	0.0020	0.6842
MMO / 50	6.46	0 - 720 (16.26 % removal)	0.18 ± 0.04	0.0008	0.7232
		URIC ACID			
BDD / 12.5	0.57	0 - 160	29.46 ± 0.06	0.0000	0.9999
BDD / 25	0.14	0 - 39	25.02 ± 0.00	0.0000	1.0000
BDD / 50	0.14	0 - 20	49.96 ± 0.07	0.0000	1.0000
MMO / 12.5	0.91	0 - 310	7.11 ± 1.42	0.1066	0.8897
MMO / 25	0.57	0 - 80	14.46 ± 2.67	0.0228	0.9341
MMO / 50	0.58	0 - 40	37.44 ± 9.43	0.0712	0.8807
		CREATININE			
BDD / 12.5	8.00	0 - 2880	1.42 ± 0.10	0.0760	0.9638
BDD / 25	8.00	0 - 1440	2.60 ± 0.07	0.0073	0.9949
BDD / 50	6.46	0 - 720	2.65 ± 0.06	0.0023	0.9948
MMO / 12.5	8.00	0 - 3600	0.25 ± 0.01	0.0019	0.9812
MMO / 25	8.00	0 - 1800	0.67 ± 0.01	0.0005	0.9969
MMO / 50	6.46	0 - 720	1.10 ± 0.05	0.0015	0.9808
		UREA			
BDD / 12.5	8.00	0 - 3600	0.58 ± 0.03	0.0165	0.9710
BDD / 25	8.00	0 - 1800	1.26 ± 0.08	0.0203	0.9679
BDD / 50	6.46	0 - 720	1.68 ± 0.07	0.0035	0.9806
MMO / 12.5	8.00	0 - 3600 (2.31 % removal)	$3.68 \cdot 10^{-3}$	0.0002	0.0533
MMO / 25	8.00	0 - 1800 (23.72 % removal)	0.10 ± 0.03	0.0037	0.4645
MMO / 50	6.46	0 - 720 (7.63 % removal)	0.09 ± 0.02	0.0001	0.7718

Overall, the ratio follows a similar trend regardless the anode material in urine: the higher current density, the lower ratio. Likewise, a similar behaviour is observed during the treatment of CAP in perchloric acid at different current densities. On the

other hand, urea ratios (k_{CAP}/k_U) obtained are higher than 1 with both electrodes which reveals that degradation of urea is not favoured in comparison with CAP, despite its higher initial concentration (3333.34 mg dm^{-3} *vs.* 100 mg dm^{-3} of CAP). A similar behaviour can be seen in creatinine ratio (k_{CAP}/k_C) with BDD anodes (Figure 5.14a) where values are slightly higher. However, the ratios obtained for creatinine are very similar to CAP removal because the initial concentration of both organics are similar (166.67 mg dm^{-3} creatinine *vs.* 100 mg dm^{-3} CAP). In the case of MMO (Figure 5.14b), k_{CAP}/k_C decreases down to 1 when applying current densities higher than 25 A m^{-2}. This may indicate the important role of mediated oxidation in each case and of the molecule structure in the competitive oxidation of organics in urine media.

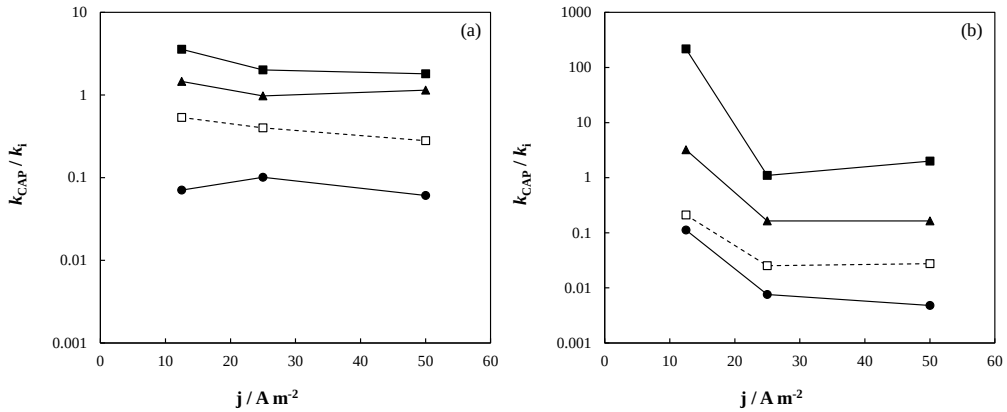

Figure 5.14. Ratio k_{CAP}/k_i as function of the current density for the different organic compounds from urine and the antibiotic in perchloric acid media. (a) BDD; (b) MMO; (■) urea; (▲) creatinine; (●) uric acid; (□) CAP in perchloric acid.

Regarding uric acid, the ratios for uric acid are lower than 1 for all the current densities and anode materials studied. This reveals that uric acid is more easily degraded than CAP during the electrolysis of urine. In this point, it is important to point out that uric acid is a more complex cyclic molecule and, it seems to be easier to break due to more available functional groups in its structure. Therefore, the rapid degradation of this compound suggests that it may be easily transformed to another intermediate organic compound. In this context, the removal of uric acid by electrolysis with MMO anodes has been reported in literature, being 2,3,6,7,8,9-hexahydro-1H-purine-2,6-diol and (5-amino-2,3-dihydro-1H-imidazol-2-yl)((hydroxymethyl)amino)methanol the first

intermediates generated [95]. The first one comes from the reduction of uric acid whereas the second is formed from the C-N bond cleavage of the first intermediate. Hence, 2,3,6,7,8,9-hexahydro-1H-purine-2,6-diol could be the main intermediate formed at the beginning of urine electrolysis at the operating conditions tested due to its easy formation.

Finally, the comparison of the degradation rate of CAP in urine and perchloric media may help to confirm the relevance of competitive oxidation in a complex media (hospital urine). Thus, ratios below 1 indicate the faster degradation of CAP in perchloric acid ($k_{CAP\text{-}ClO4} > k_{CAP\text{-}urine}$) where other organics are not present. This confirms that there is a clear competitive oxidation between CAP and the other organics present in hospital urine. Additionally, in perchloric acid media, the degradation process can only take place by direct oxidation of the pollutant on the anode surface or mediated oxidation by hydroxyl radicals since perchloric acid is a non-reactive media at the operating conditions tested. Therefore, these results suggest that an increase in the current density leads to a potential production of oxidant species in the effluent and, consequently, an enhancement in organics removal.

The soft oxidative conditions studied allows to remove CAP from urine (up to 100 and 35 % CAP with BDD and MMO anodes, respectively, after passing 8 Ah dm^{-3}) but additional information is required to estimate the potential hazardousness of treated effluents, due to intermediates formed. Figure 5.15 depicts the profiles of organic intermediates formed during the electrochemical oxidation of 100 mg dm^{-3} CAP in urine media. The chromatographic area is plotted as function of the applied electric charge to evaluate the influence of the current density and the anodic material on the formation of organic intermediates.

There are significant differences in the intermediate organic compounds formed when working with BDD or MMO anodes, regardless the current density tested. Specifically, large amounts of organics are monitored during MMO-electrolysis despite the low degradation of CAP observed in Figure 5.11. Nonetheless, the amount of these intermediates could decrease if higher electric charges will be applied, favouring the formation of aliphatic compounds [89, 94]. Conversely, BDD anode led to the formation

of few organic intermediates and their maximum concentration in solution occurs at applied electric charges around 2 Ah dm^{-3}, and they disappear almost completely at the end of each test (8 Ah dm^{-3}).

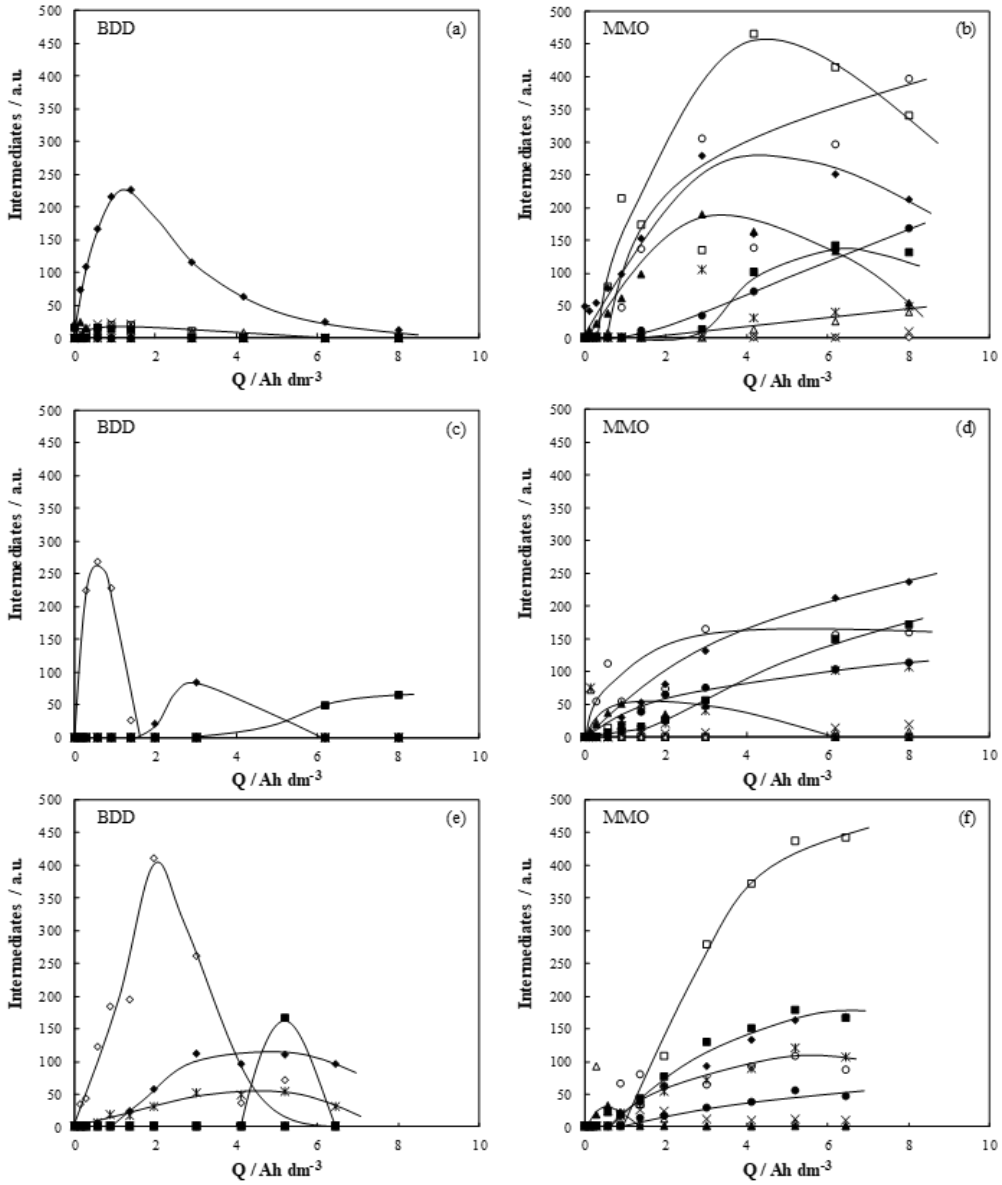

Figure 5.15. Profiles of intermediates chromatographic area as function of the applied electric charge during the electrochemical oxidation of 100 mg dm^{-3} CAP in urine media. (□) i1, (◊) i2, (Δ) i3, (x) i4, (∗) i5, (○) i6, (■) i7, (♦) i8, (▲) i9, (●) i10. Anodic material / Current density: (a) BDD / 12.5 A m^{-2}; (b) MMO / 12.5 A m^{-2}; (c) BDD / 25 A m^{-2}; (d) MMO / 25 A m^{-2}; (e) BDD / 50 A m^{-2}; (f) MMO / 50 A m^{-2}.

To shed light on the nature of the intermediates formed during the treatment of hospital urines polluted with CAP, electrochemical oxidation of 100 mg dm^{-3} antibiotic in 3000 mg dm^{-3} perchloric acid (inert media) as electrolyte was carried out (data not shown). This study allows to evaluate the intermediate compounds that come directly from the oxidation of CAP and not from other organics present in hospital urines. Results showed similar profiles in perchloric acid than that previously described during CAP degradation in urine media. Hence, most of organic intermediates monitored in this complex matrix can be attributed to CAP degradation instead of urea, creatinine or uric acid. Table 5.6 summarizes the ratio between the maximum area (MA) of intermediates in urine and perchloric acid during the electrolysis of CAP with BDD and MMO anodes at different current densities. Values higher than 1 indicates that the maximum area is higher during the electrolysis in urine matrix whereas ratios lower than 1 reveals that the maximum area of intermediates is higher when working in perchloric acid.

Table 5.6. Ratio $MA_{urine}/MA_{perchloric\ acid}$ of intermediates during the electrolysis of 100 mg dm^{-3} CAP with BDD and MMO anodes at different current densities.

Intermediate	j_{BDD} / A m^{-2}			j_{MMO} / A m^{-2}		
	12.5	**25**	**50**	**12.5**	**25**	**50**
i1	0.57	-	-	4.46	0.31	4.99
i2	-	8.90	33.40	-	-	-
i3	0.35	-	-	0.39	1.61	0.94
i4	0.49	-	-	0.69	0.57	0.53
i5	-	-	0.54	1.48	4.54	0.89
i6	-	-	-	11.72	4.69	3.03
i7	0.47	13.47	7.01	5.09	4.51	8.21
i8	0.38	0.13	0.49	2.64	8.12	2.54
i9	0.34	-	-	9.33	1.17	1.30
i10	-	-	-	3.84	1.58	0.52

Overall, the areas of intermediates formed are higher in urine matrix during the electrolysis with MMO anodes since the ratio is higher than 1. However, an opposite behaviour can be seen when working with BDD anodes where the ratios are mainly lower than 1. This can be due to mediated oxidation mechanisms. In this context, the

removal of CAP in perchloric acid can only take place by the direct oxidation of the pollutant on the anode surface or by hydroxyl radical mediated oxidation. On the other hand, the electrolysis in urine matrix leads to the formation of a cocktail of oxidants (hypochlorite, peroxodisulfate, peroxodiphosphate…). Nonetheless, the nature of the anodic material (electrocatalytic properties) favours the formation of different oxidants [84]. Specifically, MMO leads to the production of large amounts of hypochlorite as main oxidant whereas BDD anodes promote the formation not only of hypochlorite but also of other peroxocompounds. These last species present a higher oxidant capacity and, hence, they can significantly contribute to a rapid degradation of the intermediates formed during the electrolysis of CAP in urine. For this reason, the number and area of intermediates are lower during the electrolysis in urine matrix with BDD anodes. In literature, it has been reported the intermediates formed during the mineralization of synthetic solutions polluted with CAP [93]. Table 5.7 shows the main intermediate organic compounds reported in these works. However, the soft operating conditions used in this work can lead to the formation of other intermediate compounds.

Table 5.7. Main intermediates formed during electrochemical treatment of CAP polluted effluents.

Chemical name	Molecular formula	Method	Reference
2,2-Dichloro-N-[1,3-dihydroxy-1-(4-hydroxyphenyl)-propan-2-yl]acetamide	$C_{11}H_{13}O_4NCl_2$	GC-MS / LC-MS	[93, 94, 96]
4-(2-Nitro-1,3-dihydroxy-propanyl)-nitrobenzene	$C_9H_{10}O_6N_2$	GC-MS / LC-MS	[93, 94]
4-(2-Amino-1,3-dihydroxy-propanyl)-nitrobenzene	$C_8H_8O_4N_2$	GC-MS / LC-MS	[93, 94]
4-Nitrobenzoic acid	$C_7H_5O_4N$	GC-MS / LC-MS	[93, 94, 96]
Allatoic acid	$C_4H_8N_4O_4$	GC-MS	[89]
Ethyl hydrazine	$C_2H_8N_2$	GC-MS	[89]
Dichloroacetamide	$C_2H_3Cl_2NO$	GC-MS / LC-MS	[96, 97]
Acetic acid	$C_2H_4O_2$	GC-MS / LC-MS	[89, 94]

In this point, it is essential to take in mind that these results only confirm the removal of CAP, its reaction intermediates and organics contained in urine but do not give information about the remaining riskiness of the treated urine. Thus, to assess the hazardousness of treated urine before their direct discharge to sewage network and the subsequent treatment in municipal WWTPs, toxicity analyses were carried out to the treated hospital urines. Specifically, acute toxicity towards *Vibrio fischeri* luminescence inhibition was evaluated by Microtox® standard method. Figure 5.16a shows the EC_{50} percentages during the electrochemical oxidation of 100 mg dm^{-3} CAP in urine media with BDD anodes at different current densities. For comparison purposes, three different values of applied electric charge were selected in order to evaluate the hazardousness of the treated urine in three different stages: initially ([CAP]: 100 mg dm^{-3}), when CAP has been partial degraded, and intermediates remain in the reaction media (2 Ah dm^{-3}) and when CAP and total organic load has been almost degraded (6 Ah dm^{-3}). Likewise, Figure 5.16b shows the EC_{50} values obtained with MMO anodes but, in this case, CAP removal was only about 20 % at the maximum electric charge selected.

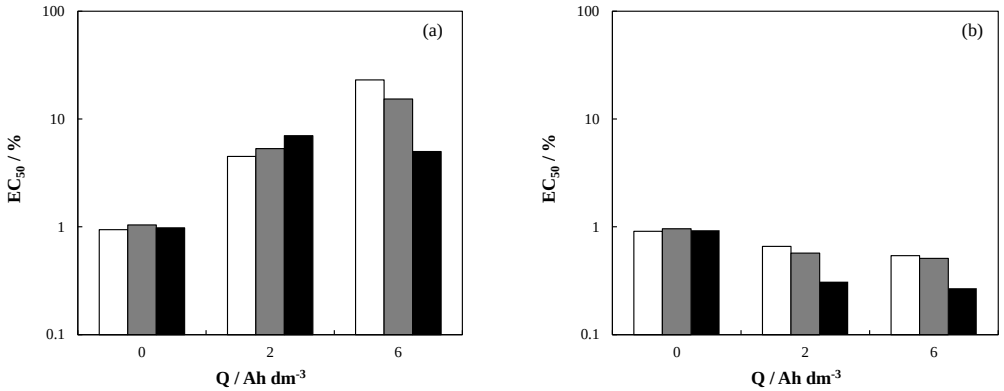

Figure 5.16. EC_{50} values at different applied electric charges (0, 2 and 6 Ah dm^{-3}) during the electrochemical oxidation of 100 mg dm^{-3} CAP in urine media. (□) 12.5 A m^{-2}; (■) 25 A m^{-2}; (■) 50 A m^{-2}. (a) BDD; (b) MMO.

As can be observed, EC_{50} values are lower than 1 % at the beginning of the treatment with BDD anodes (Figure 5.16a) which can be directly associated to the presence of 100 mg dm^{-3} CAP in urine and, hence, it reveals the high toxicity of untreated hospital urine. This is an expected behaviour taking into account the pharmacological properties of CAP: a wide spectrum antibiotic [98]. At this point, it is

important to highlight that urine matrix without CAP was analysed, resulting in EC_{50} values around 90 %. This result confirms that urine matrix is not the responsible of hospital urine initial toxicity. Then, the EC_{50} increases at 2 Ah dm^{-3} due to the CAP removal for all the current densities studied. However, there is not a significant increase in this parameter, which can be related to the presence of the primary intermediates from the oxidation of CAP (mainly aromatics). At this point, it is important to highlight that the oxidants were neutralized in samples with thiosulphate (1:1) when passing 2 Ah dm^{-3} and toxicity was measured again. After neutralization process, EC_{50} values were quite similar (4-7 %) and, hence, this clearly indicates that the initial toxicity is due to the primary organic intermediates formed from CAP oxidation. Furthermore, a complete antibiotic removal was not attained at these conditions and, therefore, it also influences on the *V. fischeri* luminescence inhibition. Likewise, it can be seen that the current density has not a remarkable influence on toxicity at this charge value with BDD anodes. Finally, EC_{50} values are higher at applied electric charges of 6 Ah dm^{-3} when working at current densities of 12.5 and 25 A m^{-2}. However, this parameter decreases at the end of the electrochemical treatment at 50 A m^{-2}. This different behaviour can be attributed to the residual CAP that has still not been removed at 50 A m^{-2} (Figure 5.11). In addition, the different EC_{50} values obtained at higher electric charges can be also influenced by the amount of oxidants accumulated in urine during the treatment. In this context, oxidants concentrations are lower at 12.5 A m^{-2} than the results obtained at 50 A m^{-2} (Figure 5.12). This is the expected outcome since the production of oxidants during electrolysis is strongly influenced by the current density [86]. Hence, it suggests that the oxidants electrogenerated at low current densities are mainly wasted in the removal of organics whereas higher concentrations of these species remain in the bulk at 50 A m^{-2} which can contribute to increase the toxicity towards *V. fischeri*. To check this hypothesis, toxicity analyses were carried out using a urine matrix without antibiotic and polluted with different concentrations of hypochlorite as model of oxidant that can be easily generated during electrolysis. Results showed that a low concentration of 1 mg dm^{-3} ClO^- leads to EC_{50} values lower than 1 %. This reveals that the higher

concentration of oxidants at 50 A m^{-2} significantly influences the EC_{50} values and, therefore, the toxicity of treated urines.

On the other hand, the EC_{50} values obtained during the treatment of hospital urines with MMO anodes (Figure 5.16b) are lower than 1 % for all the applied electric charges studied. In this case, it can be attributed to the presence of antibiotic in urine (Figure 5.11) which has still not been removed (around 80 %). Furthermore, the toxicity can be also explained in terms of the generation of hypochlorite during the process, since MMO anodes mainly promotes the formation of large amounts of hypochlorite from the oxidation of chlorides due to their electrocatalytic properties [99].

Once the toxicity of hospital urines was evaluated, rapid biodegradability assays were performed during the treatment of urines polluted with 100 mg dm^{-3} CAP at different current densities using BDD and MMO anodes. This study is an approach that allows to evaluate if it will be possible to carry out an efficient conventional biological treatment after electrolysis [100]. Therefore, rapid biodegradability together with toxicity analyses will initially allow to evaluate the final environmental and sanitary risk of treated hospital urine. Figure 5.17 shows the influence of the current density on the evolution of the rapid biodegradability during the treatment of hospital urines polluted with 100 mg dm^{-3} CAP using BDD and MMO anodes. This rapid test also informs about the biodegradability of treated effluents based on the oxygen consumed by microorganisms present in an activated sludge, relating the biological oxygen demand and the chemical oxygen demand.

The initial rapid biodegradability determined was around 25 % which can be attributed to an easy degradation of natural organic compounds present in hospital urine (urea, creatinine and uric acid). This initial value decreases during electrochemical oxidation at 2 Ah dm^{-3} despite the current density values and anodic materials. Lower percentages of rapid biodegradability are obtained with MMO anodes (4 – 15 %) in comparison with BDD anodes (11 – 15 %). This decrease may be a consequence of the maximum presence of poorer biodegradable organic intermediates than the parental ones. However, different performances are observed for the rapid biodegradability percentages during electrochemical oxidation at 6 Ah dm^{-3} depending on the current

density and anodic materials. Specifically, the rapid biodegradability remains constant from 2 to 6 Ah dm^{-3} during electrolysis with MMO anodes, regardless the current density applied. This steady state in the rapid biodegradability may occurs due to different behaviours, simultaneously: the lower CAP removal efficiency, the amount of accumulated intermediates and/or the presence of oxidants (mainly hypochlorite). Therefore, higher electric charges should be applied to attain a complete CAP removal with MMO anode and a subsequent biodegradability improvement. Conversely, rapid biodegradability increases during electrochemical oxidation with BDD anodes despite the current density. Here, similar trends are observed during electrolysis at 25 and 50 A m^{-2} where rapid biodegradability increases up to 22 % (similar than initial rapid biodegradability value). Meanwhile, rapid biodegradability increases up to 36 % for the lowest value of current density. Overall, these performances lead to explain that rapid biodegradability is directly affected not only by the presence of organic intermediates (less biodegradable with MMO anodes, more biodegradable with BDD anodes) but mainly by the presence of antibiotic and oxidants electrogenerated in hospital urines.

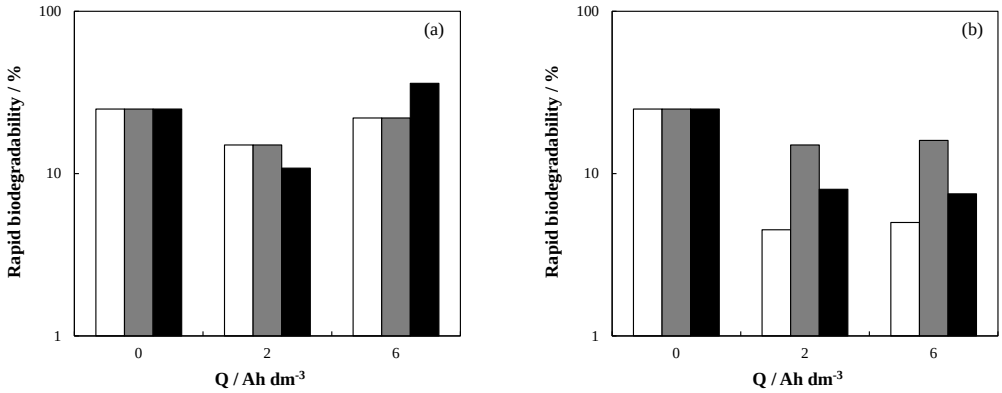

Figure 5.17. Evolution of rapid biodegradability percentage as function of different applied electric charges during the electrochemical oxidation of 100 mg dm^{-3} CAP in urine media. Current density: (■) 12.5 A m^{-2}; (▲) 25 A m^{-2}; (●) 50 A m^{-2}. (a) BDD; (b) MMO.

Electrochemical oxidation of 100 mg dm^{-3} CAP in urine media with BDD anodes applying a current density value of 12.5 A m^{-2} could be considered as the most appropriate technology to reduce the hazard of hospital urines under the experimental conditions studied since this technology completely removes the antibiotic, increases

the EC_{50} and the rapid biodegradability up to 23 and 36 %, respectively. For this reason, the Zahn-Wellens standard biodegradability test was performed to the resulting hospital urine after the electrolysis with BDD anodes at 12.5 A m^{-2} and, the results obtained are plotted in Figure 5.18. The procedure control effluent of 1593 mg dm^{-3} glucose were also tested for comparison purposes.

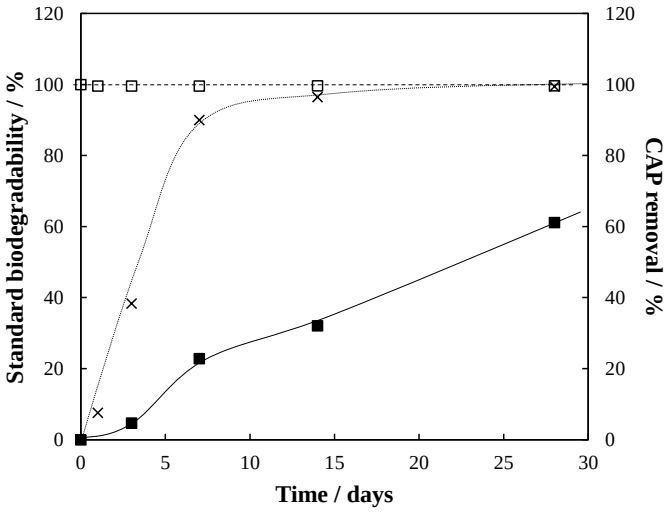

Figure 5.18. Time-course of standard biodegradability percentage for the final effluent (8 Ah dm^{-3}) obtained during the electrochemical oxidation of 100 mg dm^{-3} CAP in urine media with BDD anodes at 12.5 A m^{-2}. Effluents: (x) procedure control, (■) final effluent. Symbols: (black symbols) standard biodegradability, (white symbols) CAP removal.

The blank reference test (1593 mg dm^{-3} glucose) is observed to attain the 100 % of standard biodegradability after 28 days. This performance ensures the proper conditions of microorganisms from the activated sludge used to develop Zahn-Wellens procedure. After electrochemical oxidation where CAP is not presented in solution, the standard biodegradability rises almost linearly up to 60 % after 28 days. These results reveal that electrochemical oxidation can be considered as a promising technology to reduce toxicity and enhance biodegradability of hospital urines at the operating conditions tested (j: 12.5 A m^{-2}; Q: 8 Ah dm^{-3}) since, as reported in literature, effluents may be considered as easily biodegradable when its biodegradability percentage is above 40 % [101, 102].

5.2.3. Conclusions

From this study, the following conclusions can be drawn:

- Bacterial removal efficiency is lower in hospital urine because of the existence of other competitive oxidation reactions during electrolysis. Gram-positive bacteria are easier to deplete than gram-negative bacteria. The occurrence of hazardous disinfection by-product is avoided when the removal of bacteria is carried out in hospital urine since the production of hypochlorite and the subsequent formation of inorganic chloramines are favoured.
- Electrolysis with BDD anodes allows to decrease the hazardousness of hospital urines, achieving a complete removal of the antibiotic CAP at very low current densities and electric charges. Opposite to that, the use of MMO anodes only attains a 20 % of CAP removal applying the same conditions. Free and combined chlorine species and peroxocompounds are generated from the oxidation of the ions contained in the effluent which are the main responsible of antibiotic removal and also contribute to the degradation of natural organics present in hospital urine (urea, creatinine and uric acid).
- A competitive oxidation takes place during the electrolysis of urine polluted with CAP between the target antibiotic and the other organic compounds (urea, creatinine and uric acid) for all the current densities and anode materials tested in this work. Specifically, uric acid degradation rate is higher than CAP removal rate whereas creatinine and urea show a lower rate.
- The acute toxicity evolution towards *Vibrio fischeri* luminescence inhibition during the electrochemical oxidation at 6 Ah dm^{-3} showed EC_{50} percentages up to 23 % with BDD-electrolysis at 12.5 A m^{-2}. However, EC_{50} values lower than 1 % were obtained during electrolysis with MMO anodes despite the current density applied. Likewise, the rapid biodegradability percentage increased in a range from 22 to 36 % during

the electrochemical oxidation with BDD anode at 6 Ah dm^{-3} whereas remained constant around 15 % with MMO anodes. Overall, the evolution of both parameters seems to be directly related to the residual antibiotic concentration, the amount of intermediates and the electrogenerated oxidants.

- Electrochemical oxidation with BDD anodes applying 12.5 A m^{-2} and electric charges of 8 Ah dm^{-3} can be considered as an appropriate technology for the pre-treatment of hospital urines before their disposal into municipal sewers since the final standard biodegradability (Zahn-Wellens method) was higher than 40 %.

5.3. Contribution of disinfectant species on the electrodisinfection process

The most common and widely used conventional disinfection process is chlorination due to the high biocidal efficacy of chlorine species. Chlorine disinfection leads to alter cell permeability, degrades the intracellular DNA, reacts with the lipids of the cell wall to its destruction, etc. [103]. Among others, hypochlorite, chlorine dioxide, and chloramines are used as chlorine disinfectants for urban wastewater treatment [104, 105]. Consequently, Guatam et al. [106] reported that the addition of a calcium hypochlorite dosage of 20 mg l^{-1} reached an almost 98.5 % of microbial reduction in hospital wastewater.

Similarly, ozone-based systems for disinfection purposes have recently aroused a great interest due to the pandemic caused by coronavirus [107, 108]. Ozone is a powerful oxidant (E^0: 2.07 V) that has been used as disinfectant since is more effective than chlorine systems for killing microorganisms (bacteria, viruses or fungi) because its oxidation potential is higher than hypochlorous acid (E^0: 1.49 V) or chlorine (E^0: 1.36 V) [109]. Oh et al. [110] compared the efficiency of electron beam, chlorination and ozonation processes on the removal of ARB and ARGs, finding that it was needed

chlorine doses of 30 mg dm^{-3} to remove over 90 % ARB and ARGs whereas only 3 mg dm^{-3} ozone led to the removal of more than 90 % ARB and ARGs.

However, the use of chemicals can promote their reaction with organic compounds naturally contained in hospital effluents to develop organochlorinated compounds, that are known to be mutagenic and cancerogenic for humans. Alternatively, Advanced Oxidation Processes (AOPs) such as Fenton [111], photo-Fenton [112], photoactivation of hydrogen peroxide [113] or ozonation [114] have been tested successfully for the removal of bacteria in hospital effluent matrices. Furthermore, Electrochemical Advanced Oxidation Processes (EAOPs) have been also tested for disinfection since this technology can promote the production of powerful oxidants from the ions naturally contained in hospital effluents, depending on the electrocatalytic properties of the electrode material used [70, 115, 116]. Free and combined chlorine compounds are the main disinfectant species formed during the electrolysis of wastewater containing chlorides. In addition, other disinfectant species such as hydrogen peroxide, ozone or hydroxyl radicals can be generated by the electrochemical oxidation process. Indeed, the selection of a cell design is a critical endeavour to provide a well-defined reaction environment. The performance of the electrochemical reactor is determined by a complex interaction among different factors including 1) electrode material (metal oxide, doped diamond, etc.), 2) electrode configuration (plates, meshes, etc.), 3) flow conditions (parallel flow, flow-through, microfluidic flow-through, parallel flow with an ion exchange membrane, etc.) and 4) operating conditions (current density, searching synergies of combined electrochemical processes, etc.). In last years, the development of efficient electrochemical reactors has aroused great interest to make the electrochemical technology competitive with the conventional technologies to face the challenge of hospital urine disinfection.

A critical input for the industrial scale of electrochemical technologies is the design of electrochemical reactors since they are mostly limited by mass transport. To overcome it, flow-through cells have been applied to improve the efficiency of the electro-Fenton degradation of organics [117, 118]. Comparison with a commercial flow-by showed that the microfluidic flow-through reactors required up to 10 times less

electric charge and up to 15 times less energy consumption and, therefore, they can be an interesting approach for the development of low environmental impact electrochemical wastewater technologies. In addition, the nature of the anode materials conditions to generation of large amounts of powerful oxidants from the oxidation of the ions naturally contained in wastewater. Thus, the use of anodes based on Mixed Metal Oxides (MMO) such as RuO_2, IrO_2, or Ta_2O_5 promotes the evolution of chlorine during electrolysis [119-121]. On the other hand, Boron Doped Diamond (BDD) anodes favour the formation of a cocktail of oxidants (e.g., hypochlorite, persulfate, peroxodiphosphate, percarbonate, ozone) which seems to be the main responsible for the good performance of this electrode in the treatment of industrial wastewater [122, 123] and wastewater disinfection [62, 124]. Furthermore, novel solid-electrolyte electrolyzers have been developed [125] to overcome the main drawback of using ozone in wastewater treatment that is the mass transfer limitation from gas to the liquid phase [126]. In this electro-ozonizer, the ozone is directly produced in the liquid phase, avoiding limitations in the transport from the gaseous to the liquid phase and, hence, increasing the efficiency of the degradation processes [62, 127].

The development of efficient disinfection technologies as a pre-treatment to remove microorganisms from hospital urines is a suitable treatment strategy to avoid both the progress of antimicrobial resistance and the production of hazardous disinfection by products. In this section, the main objective is to gain insight into the role of the electro-generated oxidants on the disinfection process to remove *K. pneumoniae* as bacterium model from hospital urines. To reach this global aim, the following partial objectives were stablished:

- To evaluate the contribution of chloramines on the electrochemical disinfection testing two concepts of electrochemical cell design with MMO anodes: a conventional parallel flow reactor and a microfluidic flow-through reactor.
- To evaluate the contribution of ozone on the electrochemical disinfection testing a solid-electrolyte electro-ozonizer (MIKROZON®).

Table 5.8 shows the experimental conditions used in each test to attain this first partial objective. The influence of current density (5-50 A m^{-2}) is also studied, and results are compared with those obtained with other simpler "urine" matrixes. Additionally, for comparison purposes, chemical disinfection tests are also carried out.

Table 5.8. Experimental planification for evaluating the contribution of chloramines in the electrochemical disinfection of *K. pneumoniae* ATCC 4352.

Exp. Nº	Technology	Reactor	Anode / Cathode	Current density (A m^{-2})	Treated effluent
1	Electrolysis	Single compartment electrochemical cell	MMO / SS	5	Hospital urine
2				50	
3	Electrolysis	Single compartment electrochemical cell	MMO / SS	5	1000 mg dm^{-3} Na_2SO_4
4				50	
5	Electrolysis	Microfluidic flow-through reactor	MMO / SS	5	Hospital urine
6				50	
7	Electrolysis	Microfluidic flow-through reactor	MMO / SS	5	1000 mg dm^{-3} KCl
8				50	
9	Electrolysis	Microfluidic flow-through reactor	MMO / SS	5	1000 mg dm^{-3} KCl + 83.34 mg dm^{-3} $(NH_4)_2HPO_4$.
10				50	
11	Electrolysis	Microfluidic flow-through reactor	MMO / SS	5	1000 mg dm^{-3} Na_2SO_4
12				50	
13	Chemical disinfection	-	Disinfectant concentration: 0.07 / 0.14 / 0.28 and 0.56 mmol dm^{-3} Cl		Ultrapure water with NH_xCl_y
14					Ultrapure water with ClO^-

Table 5.9 shows the experimental conditions used to evaluate of the role of ozone electrogenerated from an electro-ozonizer with solid-electrolyte technology using BDD anodes (MIKROZON®) on the electrochemical disinfection processes. Experiments are carried out applying current intensities within the range 0.1-1.0 A. The influence of the hospital urine composition is also tested within conventional hospital urines, hospital urines without chlorides and diluted (1:10) hospital urines.

Table 5.9. Experimental planification for evaluating the contribution of ozone in the electrochemical disinfection of *K. pneumoniae* ATCC 4352.

Exp. Nº	Technology	Reactor	Anode / Cathode	Current density (A m^{-2})	Treated effluent
1	Electrolysis	MIKROZON® cell	BDD / BDD	0.1 A	Hospital urine
2				0.5 A	
3				1 A	
4	Electrolysis	MIKROZON® cell	BDD / BDD	0.1 A	Hospital urine without KCl
5				0.5 A	
6				1 A	
7	Electrolysis	MIKROZON® cell	BDD / BDD	1 A	Diluted hospital urine (1:10)

5.3.1. The role of chloramines on the electrodisinfection process

Figure 5.19 shows the electrochemical disinfection of hospital urines intensified with *K. pneumoniae* as function of the experimental time, using two different reactor configurations: a flow-through reactor with a three-dimensional mesh MMO anode and a conventional parallel flow reactor with a two-dimensional plate MMO anode. The tests were performed at a flow rate of 40 l h^{-1} and the influence of the current density was studied: 5 mA cm^{-2} at which direct oxidation is promoted and 50 mA cm^{-2} at which mediated oxidation mechanisms are expected [78, 128].

As can be observed, the inactivation of *K. pneumoniae* is significantly influenced by the current density and the reactor layout. An almost negligible removal of *K. pneumoniae* is observed at the lowest current density (5 A m^{-2}) since less than 1 log reduction is achieved, regardless the electrochemical reactor tested. Under these experimental conditions, the bacteria decay is slightly faster using the parallel flow reactor. On the other hand, rapid disinfection is observed during electrolysis at 50 A m^{-2} and the improvement of inactivation increases more than 5 logs when the current density is increased from 5 to 50 A m^{-2} regardless the reactor layout tested. The fastest

disinfection rate occurs with the parallel flow since more than 5 log reductions are obtained in 60 min (Q: 0.280 Ah dm^{-3}) whereas only 4 log units are reduced in 60 min (Q: 0.137 Ah dm^{-3}) with the flow-through reactor. After that time, the bacteria depletion is much slower with the parallel flow reactor, attaining less than 6 log decay before 120 min (Q: 0.423 Ah dm^{-3}). The inactivation efficiency is higher when working with the flow-through reactor because complete disinfection (7 log removal) is attained before 120 min (Q: 0.278 Ah dm^{-3}).

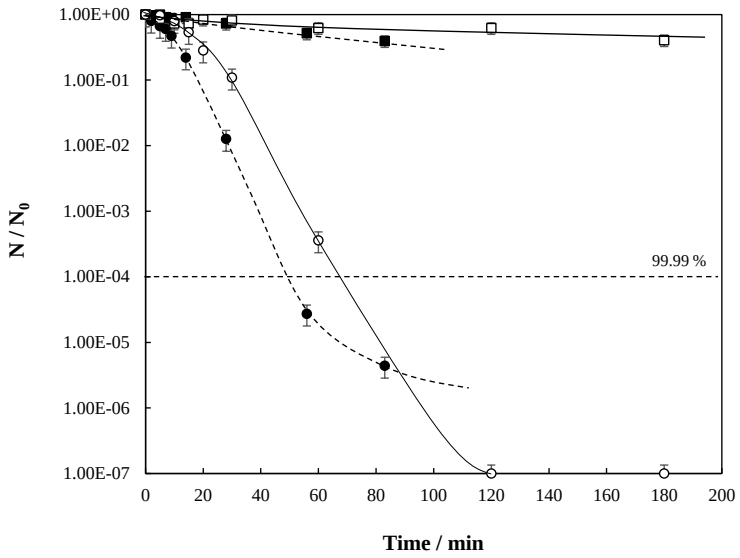

Figure 5.19. Evolution of *K. pneumoniae* as function of the operation time during the electrochemical disinfection of hospital urines. Current density: (■, □) 5 A m^{-2}; (●, ○) 50 A m^{-2}. White symbols: flow-through reactor; black symbols: parallel flow reactor. N_0: 10^6-10^7 CFU ml^{-1}.

Experimental data were fitted to first-order kinetics and the influence of the current density on the calculated kinetic constants are shown in Figure 5.20a. Besides, it is noteworthy that in the electrochemical disinfection process the most relevant parameter is not the time either the current density but the specific current charge passed [129]. Then, the efficiency of the electrochemical disinfection for a specific current charge passed was calculated according to Equation 5.2 (where N_0 and N_i are the bacteria concentration in CFU ml^{-1} at the beginning and at the first third of the experimental time, respectively, and Q_i is the applied electric charge at the first third of

the experimental time in Ah l^{-1}). Q_i values of 0.01 and 0.10 Ah l^{-1} corresponds with current densities of 5 and 50 A m^{-2}, respectively. The efficiency resulting values are plotted in Figure 5.20b.

$$\eta = \frac{N_0 - N_i}{Q_i} \cdot 1000 \qquad (5.2)$$

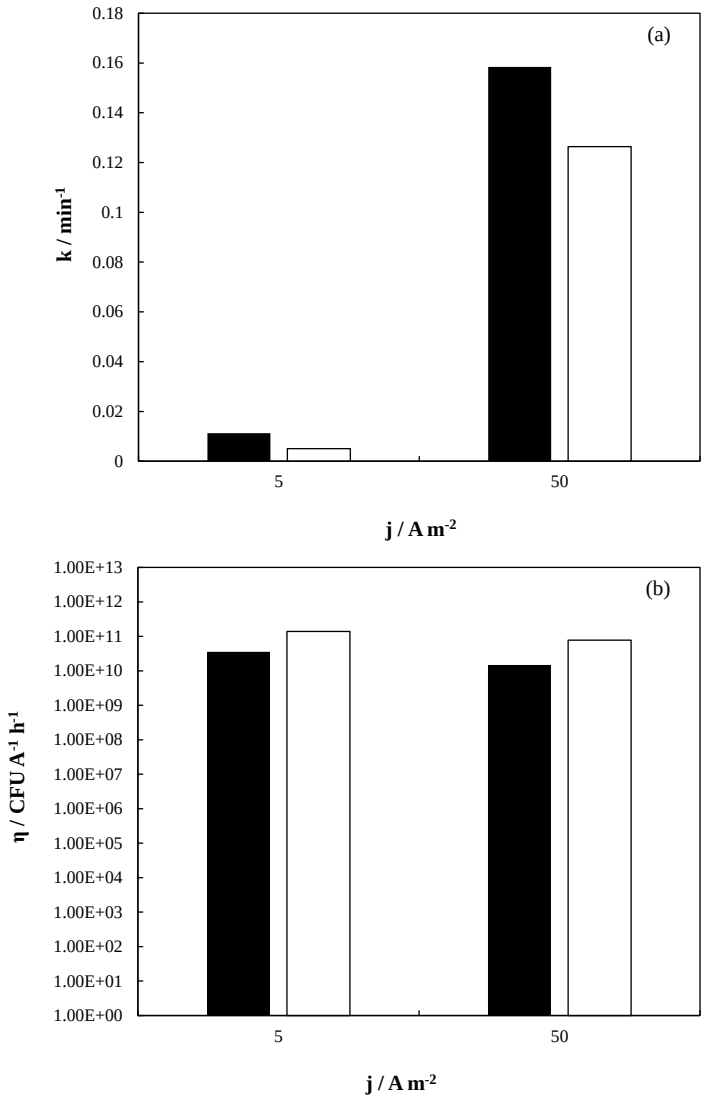

Figure 5.20. Influence of the current density on the kinetic constants (a) and the process efficiency (b) during the electrochemical disinfection of *K. pneumoniae* in synthetic hospital urines. White bars: flow-through reactor; black bars: parallel flow reactor.

As expected, the higher is the current density (directly related to a higher applied electric charge for equal experimental time), the higher is the kinetic constant value. These values are directly related to disinfection rates observed in Figure 5.19 where an almost null inactivation was observed at 5 A m^{-2} and the complete bacteria decay was only attained for 50 A m^{-2}. Furthermore, the kinetic constants also depend on the reactor layout in accordance with the current density studied. Parallel flow conditions attain kinetic constant values up to 1.3-2.2 times higher than flow-through ones during electrochemical disinfection processes at 5 and 50 A m^{-2}. However, an opposite behaviour is observed in the process efficiency, where the flow-through reactor attains higher values (Figure 5.20b). Specifically, values range among $1.48 \cdot 10^{10}$ – $3.55 \cdot 10^{10}$ during electrochemical disinfection with parallel flow conditions whereas they are maintained between $7.80 \cdot 10^{10}$ and $1.40 \cdot 10^{11}$ in the flow-through system. Then, flow-through reactor attains efficiencies around one order of magnitude higher than those obtained in parallel flow cell, regardless of the current density studied. This observation may be related to the hydrodynamic conditions of each configuration (shown in Table 5.10), mainly with the global mass-transfer coefficients (k_m).

Table 5.10. Design parameters of parallel flow and flow-through reactors.

Parameter	Parallel flow reactor	Flow-through reactor
Internal volume (ml)	70	3
τ (s)	135	180
Electrode type	plate	mesh
Electrode area (cm^2)	78	50
Interelectrode gap (mm)	9	0.4

To confirm this, it was evaluated by a standard $Fe(CN)_6^{3+}/Fe(CN)_6^{2+}$ limit current test where the value of the limiting current intensity is given by the mass transport towards the anode [130]. The intensity (I)-voltage (V) curves obtained for different fluid-dynamic conditions at a flow rate of 40 l h^{-1} are plotted in Figure 5.21. The limiting current intensity is higher when the flow-through reactor is tested in

comparison with the parallel flow one (0.61 A *vs.* 0.29 A). Thus, a k_m value of $7.65 \cdot 10^{-6}$ m s^{-1} was calculated under parallel flow conditions whereas $2.55 \cdot 10^{-5}$ m s^{-1} was determined under flow-through conditions. These results may explain the highest efficiencies obtained in the flow-through conditions as a consequence of the enhancement of mass transport due to the local turbulence induced by the three-dimensional electrodes fed in the microfluidic flow-through reactor layout [131, 132].

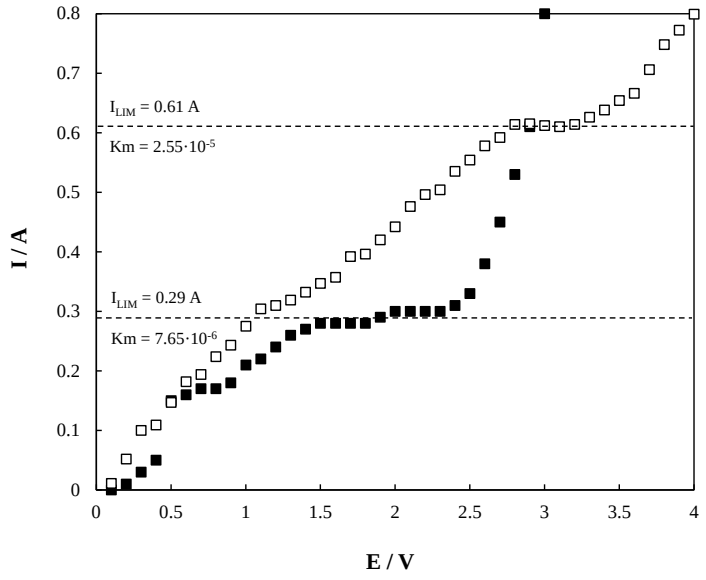

Figure 5.21. I-V curves obtained for 40 l h^{-1} at different fluid-dynamic conditions. Electrochemical reactor layouts: (□) flow-through conditions; (■) parallel flow conditions.

The removal of microorganisms by electrochemical oxidation can take place by two different mechanisms: direct and/or indirect disinfection [133]. In literature, it has been reported that the main mechanism for the inactivation of bacteria is the in-situ production of disinfectants, such as ozone, hydrogen peroxide, and/or chlorine species, which can lead to heavy damage of their cell wall [103, 134]. Hence, the differences observed in the disinfection of hospital urines with both reactors (Figure 5.19) could be also related to the generation of disinfectants during the process. Hypochlorite is the species most widely used as a consequence of its powerful bactericidal effect [135, 136]. The electrogeneration of hypochlorite relies on the natural presence of chlorides in treated effluents since chloride may be electrochemically oxidized to chlorine (Equation

5.3), which disproportionates in water yielding hypochlorous acid (Equation 5.4). Then, hypochlorous acid dissociates to hypochlorite ions depending on the solution pH following an acid-base reaction with pK_a=7.55 (Equation 5.5) [70, 137]. The hospital urine used in this work is a complex water matrix that contains above 10 mmol dm^{-3} of chlorides and then, the evolution of hypochlorite as function of the applied electric charge during the electrochemical disinfection of hospital urines using MMO anodes was monitored and shown in Figure 5.22.

$$2\ Cl^- \rightarrow Cl_2 + 2e^- \quad (5.3)$$

$$Cl_{2(aq)} + H_2O \rightarrow HClO + Cl^- + H^+ \quad (5.4)$$

$$HClO \rightleftharpoons ClO^- + H^+ \quad (5.5)$$

Furthermore, the presence of 1.3 mmol dm^{-3} of ammonium ions (from 83.34 mg dm^{-3} of $(NH_4)_2HPO_4$) in urine generates the well-known breakpoint chlorination, promoting the occurrence of inorganic chloramines (Equations 5.6-5.8) [90]. In this context, inorganic chloramines were also monitored as function of applied electric charge during the electrochemical disinfection process. The evolution of free and combined chlorine species is shown in Figure 5.22.

$$NH_3 + HClO \rightarrow NH_2Cl + H_2O \quad (5.6)$$

$$NH_2Cl + HClO \rightarrow NHCl_2 + H_2O \quad (5.7)$$

$$NHCl_2 + HClO \rightarrow NCl_3 + H_2O \quad (5.8)$$

The concentration of hypochlorite does not follow a clear trend, regardless the current density applied. However, it is important to take in mind that the measured concentration is referred to the free hypochlorite that has not reacted yet. Hence, higher amounts of this species are expected to have been generated during the electrochemical disinfection [99, 138]. Hypochlorite would be further oxidized to other chlorine compounds in high oxidation state (chlorates and perchlorates) or would react not only with bacteria (disinfection) but also with other organic and/or inorganic species contained in the hospital urine. The first hypothesis can be discarded because a null concentration of chlorate or perchlorate was detected during the electrochemical

disinfection of hospital urines with both reactors. On the other hand, it is well known that hypochlorite is very active and can immediately react with organic and/or inorganic species, developing competitive reactions. Specifically, it is noteworthy the high organic load of the urine matrix which contains 3333.33 mg dm^{-3} of urea, 166.67 mg dm^{-3} of creatinine, and 50 mg dm^{-3} of uric acid. In previous works [139], the evolution of these organic species was studied in depth during electrolysis with MMO anodes at similar current densities. A negligible degradation of urea and a percentage removal around 50 % for creatinine was attained whereas the complete decay was reached for uric acid at applied electric charges near 10 Ah dm^{-3}. In the present work, the concentration of urea and creatinine remains constant in the initial value and uric acid achieves removal percentages within the range 50-100 %, depending on the reactor layout (data not shown). These different results are associated to the low electric charges passed during electrochemical disinfection tests performed in this study (0.5 *vs*. 10 Ah dm^{-3}).

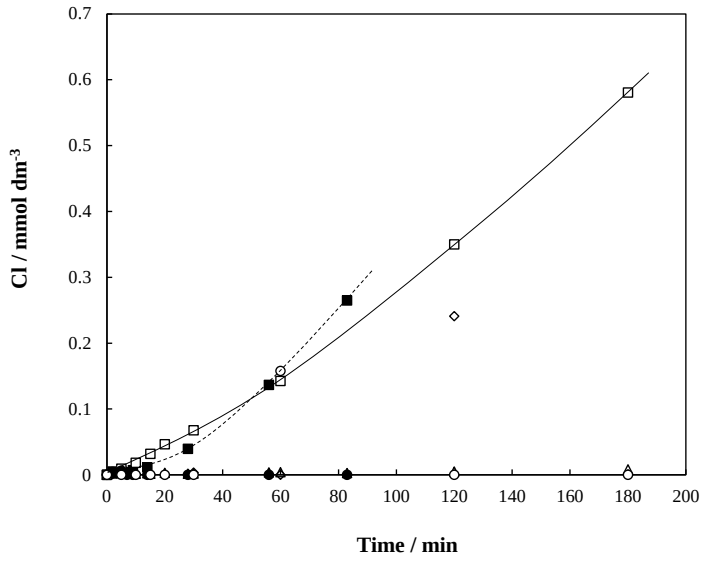

Figure 5.22. Evolution of chlorine disinfectants as function of the operation time during the electrochemical disinfection of hospital urines. (♦) hypochlorite 5 A m^{-2}; (●) hypochlorite 50 A m^{-2}; (▲) chloramines 5 A m^{-2}; (■) chloramines 50 A m^{-2}. White symbols: flow-through reactor; black symbols: parallel flow reactor.

The formation of chloramines is observed to increase with the current density, regardless the flow reactor layout tested. Specifically, 0.003 and 0.265 mmol dm^{-3} of chloramines were obtained during the electrochemical disinfection with a parallel flow reactor at 5 and 50 A m^{-2}, respectively. Likewise, electrolysis with the flow-through reactor at 5 and 50 A m^{-2} attained 0.008 and 0.581 mmol dm^{-3} of chloramines, respectively. These results reveal that the electrogenerated hypochlorite is also wasted in the formation of chloramines during electrochemical disinfection. The influence of the current density on the generation of these species may be explained bearing in mind that their generation by chlorination is mainly related to the molar ratio between Cl_2 and NH_3/NH_4^+ in solution. The increase of Cl_2 concentration up to a molar ratio of 1.0 induces the generation of stable chloramines [90, 140]. Hence, the formation of large amounts of chloramines points out that high concentrations of hypochlorite must have been generated during the electrochemical disinfection.

Furthermore, the generation of these combined chlorine species seems to depend on the reactor layout. At the beginning of the process (operation time < 60 min), the concentration of chloramines is higher when working with the flow-through reactor. This fact can be explained in terms of the different hydraulic retention times which, in turn, depend on the fluid-dynamic conditions tested (as shown in Table 5.10), since the formation of chloramines is a consequence of chemical reactions (Equation 5.6-5.8). A longer contact time among hypochlorite and ammonium ions may induce an increase in the formation of chloramines and this hypothesis may justify the highest efficiency on chloramine formation during electrochemical disinfection under flow-through conditions. However, an opposite behaviour can be seen from operation times higher than 60 min, where the concentration of chloramines is higher with the parallel flow reactor. This can be related to a higher concentration of hypochlorite electrogenerated with this reactor since the electric charge passed at 60 min is higher (0.280 *vs*. 0.137 Ah dm^{-3}). These results are great of importance because reveal that the formation of chloramines during the disinfection of hospital urines could play a key role in the bacteria removal rate. The initial low concentration registered with the parallel flow reactor corresponds to the higher removal rate of *K. pneumoniae* (Figure 5.19). This

suggests that hypochlorite may be wasted to a greater extent on the removal of microorganisms instead of the formation of chloramines and, hence, the disinfection rate is higher. On the other hand, the slow decrease observed in bacteria depletion at operation times higher than 60 min with the parallel flow reactor (corresponding to the high concentration of chloramines) could be due to the accumulation of these species in the system. Free and combined chlorine compounds are the main responsible species for killing microorganisms during electrodisinfection with MMO anodes. Nonetheless, to confirm their contribution on the removal of *K. pneumoniae*, the electrodisinfection of synthetic solutions in absence of chlorides (1000 mg dm^{-3} Na_2SO_4) were carried out with both reactors at 5 and 50 A m^{-2} (Figure 5.23). Results showed that it was not possible to disinfect this synthetic effluent at 5 A m^{-2}, regardless the reactor used. However, 1-log and 2-logs removal were achieved at 50 A m^{-2} when using the flow-through and the parallel flow reactor, respectively. This clearly reveals that the disinfection of hospital urines with both reactors equipped with MMO anodes takes mainly place by the action of electrogenerated disinfectants based on chlorine since it is possible to attain more than 5-logs removal in these complex matrixes.

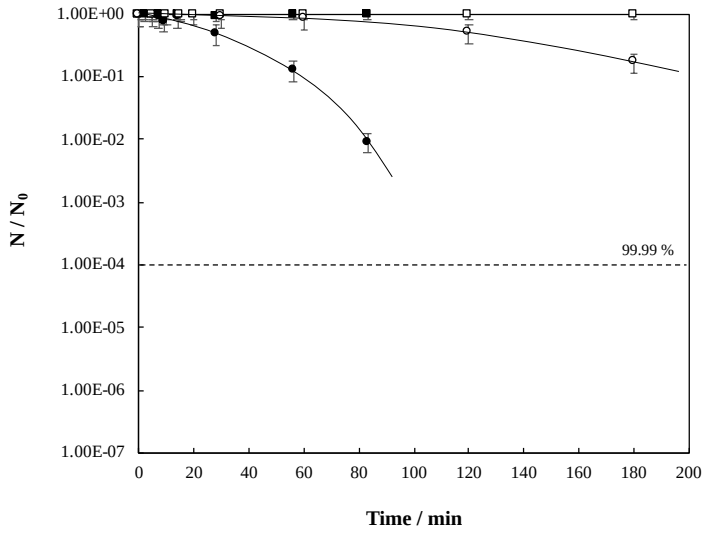

Figure 5.23. Evolution of *K. pneumoniae* as function of the operation time during the electrochemical disinfection of 1000 mg dm^{-3} Na_2SO_4. Current density: (■, □) 5 A m^{-2}; (●, ○) 50 A m^{-2}. White symbols: flow-through reactor; black symbols: parallel flow reactor. N_0: 10^6-10^7 CFU ml^{-1}.

To shed light on the contribution of chloramines during the disinfection of hospital urines, chemical disinfection tests with hypochlorite and chloramines were performed. The concentration of these species used was similar to that generated during the electrochemical disinfection process (0-0.56 mmol dm^{-3} Cl). This study will allow evaluating the bacteria removal rates in hospital urine with both disinfectants and, hence, to elucidate the role of chloramines on the removal of *K. pneumoniae* in this matrix. Figure 5.24 shows the population of bacteria as function of the operation during the chemical disinfection at different chlorine doses.

As can be observed, performance enhancement of the disinfection process is promoted by increasing the chlorine doses and the contact times. Nevertheless, results show that *K. pneumoniae* differs in its inhibitory response to hypochlorite and chloramines. The population of bacteria decreased from 4 to 7 orders of magnitude within the first 5 min at chlorine concentrations between 0.07 and 0.56 mmol dm^{-3}. The complete disinfection is attained before a contact time of 30 min, regardless the hypochlorite dose tested (Figure 5.24a). Conversely, colony-forming units of *K. pneumoniae* decreased only 2-4 orders of magnitude in 30 min using the same doses of chlorine as chloramines. With an increase of contact time up to 60 min, the removal of more than 6 logs is reached for the highest dose of combined chlorine tested (Figure 5.24b). These results support that the inactivation of microorganisms using chloramines requires a longer exposure than hypochlorite since chloramines are weaker oxidants than free chlorine [141, 142].

The presence of free chlorine in a solution can promote the generation of hazardous trihalomethanes (THMs) by its chemical reaction with the organic matter contained in wastewater [143-145]. In literature, it has been widely reported that the use of chloramines as a disinfectant minimizes the formation of THMs and trihalogenated haloacetic acids (THAAs), which are the most prevalent disinfection by-products [146-149]. Specifically, the disinfection of drinking-water supplies using chloramines allows reducing the formation of THMs as much as 40-80 % [150]. Likewise, the THMs formation was only promoted at chloramines dosage upper than 20 mg dm^{-3} and under alkaline pHs during chloramination of reclaimed water [149]. Regarding the treatment

of hospital urines, it has been reported that the formation of chloramines prevents the development of harmful chlorine species such as chlorates and perchlorates [138]. In this work, the presence of these hazardous compounds was not detected by gas chromatography (Figure 5.25).

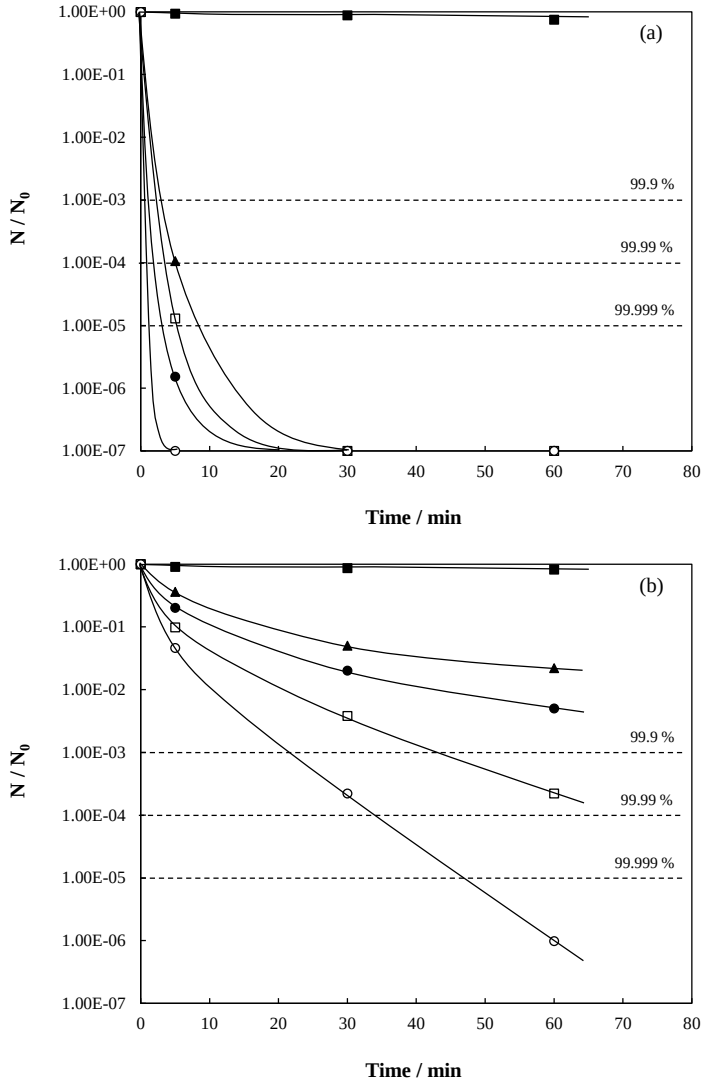

Figure 5.24. Evolution of *Klebsiella pneumoniae* as function of the operation time during the chemical disinfection of hospital urines using hypochlorite (a) and chloramines (b). (■) 0 mmol dm^{-3} Cl, (▲) 0.07 mmol dm^{-3} Cl, (●) 0.14 mmol dm^{-3} Cl, (□) 0.28 mmol dm^{-3} Cl, (○) 0.56 mmol dm^{-3} Cl.

Chloroform, bromodichloromethane, dibromochloromethane and bromoform were analysed in all experiments carried out, although only chloroform is expected to be formed due to the absence of bromide in the initial composition of the synthetic hospital urine used. Results showed that the concentration of THMs was below the detection limit of the equipment used for all the compounds analysed (limit detection < 0.2 ppb) during the electrodisinfection with MMO anodes, regardless the current density applied, and the reactor used. This supports that the presence of chloramines avoids the formation of undesirable disinfection by-products under the operating conditions tested.

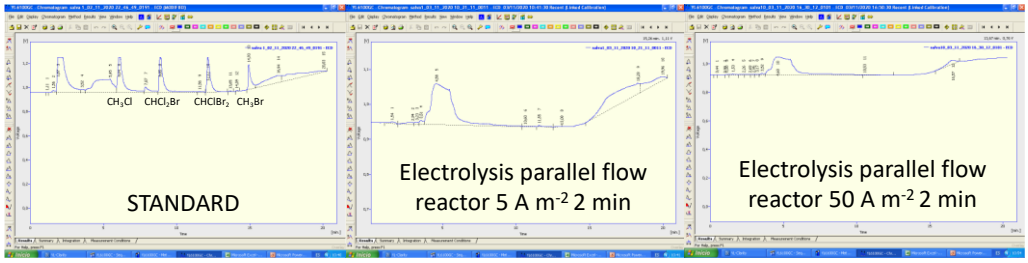

Figure 5.25. Chromatograms of the analysis of trihalomethanes (chloroform, bromodichloromethane, dibromochloromethane and bromoform) from random samples during the electrochemical disinfection of hospital urines.

To clarify the formation and contribution of chloramines during the disinfection of hospital urine by electrochemical oxidation, the removal of *K. pneumoniae* was studied in hospital urine, 1000 mg dm^{-3} KCl, and 1000 mg dm^{-3} KCl with 83.34 mg dm^{-3} $(NH_4)_2HPO_4$. The flow-through reactor was used because complete disinfection was obtained with this device at 50 A m^{-2} (Figure 5.19). These different matrixes have been selected considering the initial composition of the hospital urine. Free chlorine is only expected to be generated as a disinfectant during the electrolysis of KCl solutions meanwhile in KCl with $(NH_4)_2HPO_4$, the presence of both free and combined chlorine species would coexist in solution. This last matrix is more similar than hospital urine although, in this case, the presence of organics can also waste the electrogenerated oxidants in their degradation. Hence, these tests can help to evaluate the role of chloramines during the electrochemical disinfection of hospital urines. Figure 5.26 compares the log removal achieved at the end of the electrochemical disinfection process in different matrixes at 5 and 50 A m^{-2}. Likewise, experimental data were fitted

to a first-order kinetic (Equation 5.9) and the resulting kinetic constants in hospital urine (k_{urine}) were compared with the values obtained in KCl and KCl with $(NH_4)_2HPO_4$ solutions (k_i). Ratios k_i/k_{urine} higher than 1 indicate that the removal of *K. pneumoniae* is faster in synthetic solutions containing KCl than in hospital urine.

$$\text{Ln}\,(N/N_0) = -k \cdot t \qquad (5.9)$$

Results show that, as shown in Figure 5.19, the higher is the current density, the higher is the bacteria log removal (Figure 5.26a). At 5 A m^{-2}, the disinfection performance is higher in KCl media followed by the KCl and $(NH_4)_2HPO_4$ solution and, finally, in hospital urine. Specifically, 6 log removal units are achieved in chloride media, whereas 4 and 1 are obtained in KCl with $(NH_4)_2HPO_4$ and hospital urine, respectively. This fact may be explained bearing in mind the nature of disinfectants electrogenerated in different matrixes [138]. In chloride media, hypochlorite is the only disinfectant produced from the oxidation of chlorides (Equations 5.3-5.5) and cannot react with species other than bacteria. This makes the disinfection performance higher at low current densities. On the other hand, hypochlorite and chloramines are formed during the disinfection of solutions containing KCl and $(NH_4)_2HPO_4$. In this case, all electrogenerated hypochlorite is not only wasted in the bacteria removal but also in the reaction with ammonium to form chloramines. These last species have a lower disinfectant capacity than hypochlorite, as has been previously demonstrated (Figure 5.26), and lead to a lower disinfection efficiency. Finally, the lowest log removal is obtained in hospital urine at 5 A m^{-2}. This complex matrix contains not only inorganic ions that contribute to the formation of chloramines but also organic compounds (urea, creatinine, and uric acid) that can be attacked by the electrogenerated disinfectants, promoting competitive reactions during the treatment. The oxidation of organics releases large amounts of nitrogen to the effluent that is transformed into ammonium during electrolysis, favouring the formation of chloramines [70]. Therefore, the presence of both inorganic and organic compounds in hospital urine causes a low disinfection efficiency under these soft operating conditions.

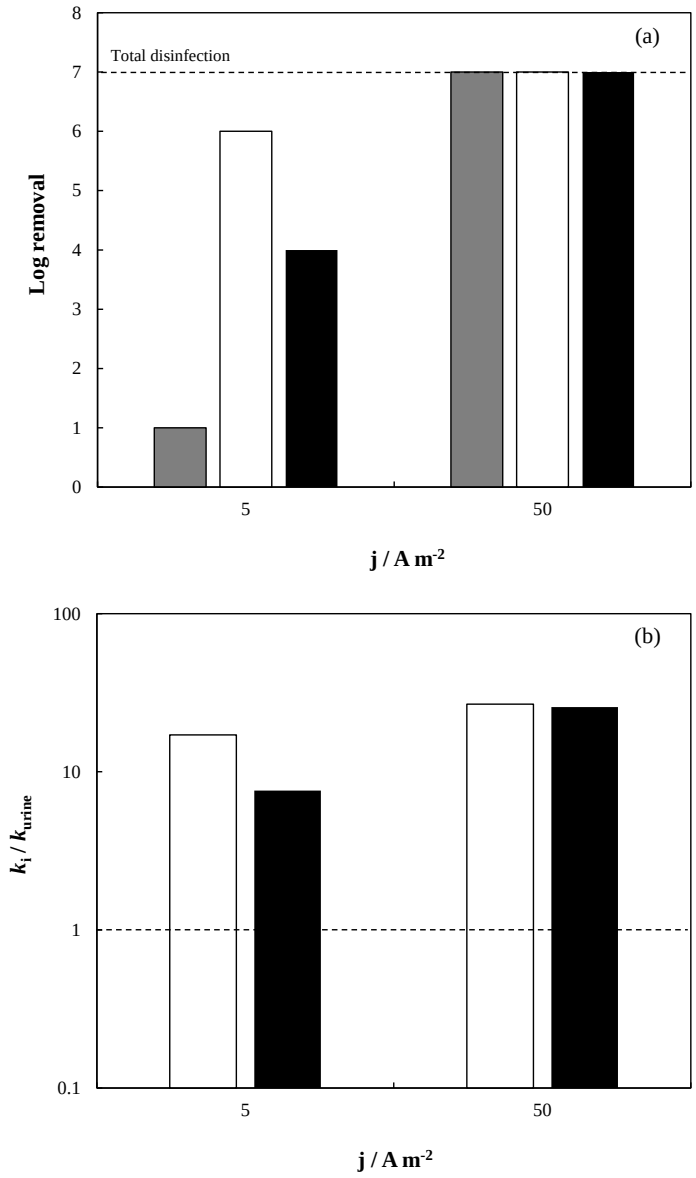

Figure 5.26. Bacteria log inactivation (a) and ratio k_i/k_{urine} (b) as function of the current density during the electrochemical disinfection of *K. pneumoniae* with a flow-through reactor. Grey bars: hospital urine; white bars: 1000 mg dm^{-3} KCl; black bars: 1000 mg dm^{-3} KCl + 83.34 mg dm^{-3} $(NH_4)_2HPO_4$.

At higher current densities, the log removal attained is similar, regardless the water matrix studied. In this case, the production of large amounts of free and combined chlorine species takes place since the applied electric charge is ten times higher than

that passed during the process at 5 A m^{-2} (0.042 *vs*. 0.423 Ah dm^{-3}). Hence, there is enough amount of disinfectants to ensure complete bacteria removal at the end of the treatment in all matrixes.

These results point out that the presence of chloramines generated in the effluents containing ammonium such as hospital urine slows down the removal of *K. pneumoniae* during electrolysis, decreasing the disinfection efficiency. This is also supported by the kinetic constants calculated for all matrixes and the ratio k_i/k_{urine} (Figure 5.26b). This parameter is an indicator of both the selectivity toward the *K. pneumoniae* inactivation and the inhibitory effect of the organic urine components. Results show that the ratio k_i/k_{urine} is higher than 1 despite the current density studied and the matrix compared (KCl or KCl + $(NH_4)_2HPO_4$). The highest values are obtained in KCl media for all the current densities although the difference is more remarkable at 5 A m^{-2}. This demonstrates that the disinfection process occurs slower in hospital urines as a consequence of the side consumption of the most powerful disinfectant (hypochlorite) due to the following reasons: 1) its chemical reaction with ammonium ions to form chloramines which also contribute to the disinfection process although chloramines are weaker disinfectants, 2) its contribution on the mediated oxidation of organic compounds naturally contained in hospital urines that may inhibit its bactericidal effect. Additionally, the kinetic values of disinfection processes generally show an increasing profile as the concentrations of hypochlorite and chloramines were increased at higher current densities. This indicates that the bactericidal effects of both hypochlorite and chloramines are concentration-dependent. In this context, a brief overview of the electrochemical technologies for bacteria removal from urines is summarized in Table 5.12. As can be seen, scarce information has been reported related to disinfection processes from hospital urines since most studies are focused on drinking water or municipal wastewaters. The performance of electrochemical disinfection processes in urines depends on many parameters such as target bacteria, reactor layout, fluid-dynamic conditions, and/or primary operation conditions. Then, a proper selection of the electrochemical working conditions would yield advantages, such as the promotion in the formation of chloramines, which may play a key role in the inactivation

of ARB since they provide the preservation of residual disinfection activity and the non-formation of undesirable chlorine by-products.

Finally, the energy consumption (W, kWh m^{-3}) required for attaining a complete disinfection of hospital urines was calculated according to Equation 5.10, where Q is the applied electric charge to achieve a specific log-removal in kAh m^{-3} and V is the average applied voltage in volts. This parameter has been only calculated for the experiments carried out at 50 A m^{-2} because a negligible disinfection was obtained when working at 5 A m^{-2} (Figure 5.19). The values obtained are shown in Table 5.11.

$$W = Q \cdot V \tag{5.10}$$

Table 5.11. Energy consumption.

Reactor	Parallel flow reactor	Flow-through reactor
Q (kAh dm^{-3})	0.423	0.278
V (V)	4.5	3.9
Operation time (min)	83	120
Log removal	5-6	7
j (A m^{-2})	50	50
W (kWh m^{-3})	1.904	1.083

Results show that the use of the microfluidic flow-through reactor leads to the lowest energy consumption for the disinfection of hospital urines. This is an expected outcome because of its lower interelectrode gap and, consequently its lower ohmic drop and cell voltage (Table 5.10) [131]. Furthermore, the applied electric charge required to attain a complete disinfection is also lower with the microfluidic flow-through reactor due to the high amounts of disinfectants produced with this device, as has been previously described. These results reveal that the application of this novel reactor design for the electrodisinfection of hospital urines does not only improve the process performance but also decreases the energy requirements for the implementation of the process.

Table 5.12. Reported studies on electrochemical disinfection in hospital urines.

Target effluent		Electrochemical technology				Primary operation conditions					
Bacteria	**N_0 (CFU/ml)**	**Type of technology**	**Reactor design**	**Fluid-dynamic conditions**	**Anode material (active surface area / inter-electrode gap)**	**j (A m^{-2})**	**Operation conditions**	**Flow rate**	**Volume treated (dm^3)**	**Operation mode**	**Log unit removal (CFU/ml)**	**Ref.**
E. coli	8.0E+03	Electrochemical Oxidation Photo-electrocatalysis	Single compartment electrochemical cell	Stirrer tank reactor	MMO (42 cm^2 / 2 cm)	303.3	60 min 60 min - 23 ± 2 W m^{-2}	600 rpm	0.4	Discontinuous	3.8 (Total)	[138]
E. coli	1.0E+08	Electrochemical Oxidation	Single compartment electrochemical cell (Advanced Diamond Technology's Diamonox 40 system)	Parallel flow	BDD (42 cm^2 / 2 mm)	880.9	Continuous mode - 30 min Single pulse mode - 100 min	2 l min^{-1}	2	Continuous / Pulsed modes	8 (Total) 6	[116]
E. coli	8.3E+01-8.7E+01	Electrochemical Oxidation	Single compartment electrochemical cell	Parallel flow	Ti/RuO_2 (78 cm^2 / 9 mm)	150	6 Ah dm^{-3}	-	0.6	Discontinuous	1.9 (Total)	[151]
					Ti-Pt (78 cm^2 / 9 mm)		30 Ah dm^{-3}					
					Ti/IrO_2 (78 cm^2 / 9 mm)		10 Ah dm^{-3}					
					BDD (78 cm^2 / 9 mm)		2 Ah dm^{-3}					

Table 5.12. (Cont.) Reported studies on electrochemical disinfection in hospital urines.

Target effluent		Electrochemical technology				Primary operation conditions					Ref.
Bacteria	N_0 (CFU/ml)	Type of technology	Reactor design	Fluid-dynamic conditions	Anode material (active surface area / inter-electrode gap)	j ($A\ m^{-2}$)	Operation conditions	Flow rate	Volume treated (dm^3)	Operation mode	Log unit removal (CFU/ml)	
E. coli	1.0E+04 1.0E+05	Electrochemical Oxidation	Single compartment electrochemical cell	Parallel flow	BDD (78 cm^2 / 9 mm)	5	0.1 kAh m^{-3}	50 l h^{-1}	1	Discontinuous	5 (Total)	[70]
						10	0.2 kAh m^{-3}					
						50	0.4 kAh m^{-3}					
						100	0.8 kAh m^{-3}					
P. aeruginosa	1.0E+04 1.0E+05					5	0.3 kAh m^{-3}				5 (Total)	
						10	0.5 kAh m^{-3}					
						50	1.0 kAh m^{-3}					
						100	2.0 kAh m^{-3}					
E. coli	1.0E+08	Electrochemical Oxidation	Single compartment electrochemical cell	Parallel flow	BDD (42 cm^2 / 2 mm)	-	6 V (30 min) / 8 V (17 min) / 10 V (9 min) / 12 V (6 min)	2 l min^{-1}	2	Discontinuous	8 (Total)	[115]

5.3.2. The role of ozone on the electrodisinfection process

Figure 5.27 shows the evolution of *K. pneumoniae* with the operation time during the electrolysis of urines at different current intensities using the MIKROZON® cell.

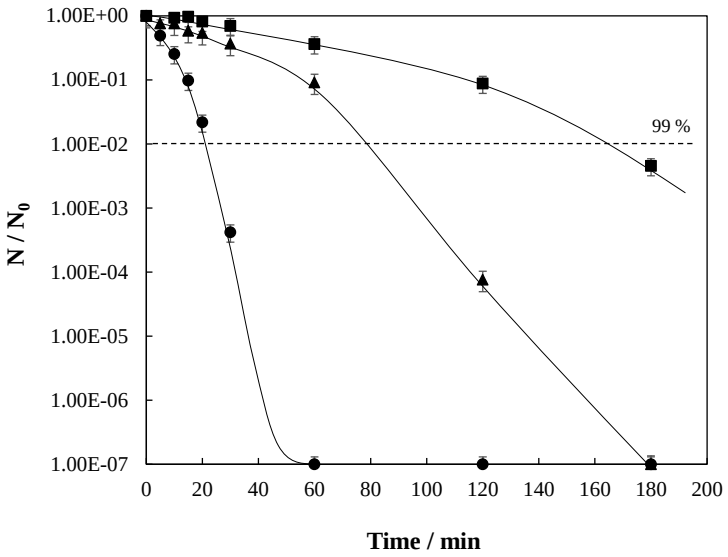

Figure 5.27. Influence of the current intensity on the disinfection of urines using the MIKROZON® reactor. (■) 0.1 A; (▲) 0.5 A; (●) 1.0 A; N_0: 10^7 CFU ml^{-1}.

As can be observed, it is possible to attain a complete disinfection of urines at operation times lower than 180 min when applying current intensities higher than 0.5 A. This reveals that the current intensity clearly influences the process performance because the concentration of *K. pneumoniae* only decreases 2-logs at 0.1 A and the complete disinfection is achieved in 180 and 60 min at 0.5 and 1.0 A, respectively. The higher is the current intensity applied, the higher is the removal rate. Furthermore, the removal efficiency also increases at higher current intensities since the applied electric charge required for killing microorganisms is 1.94 Ah dm^{-3} when working at 0.5 A and 1.21 Ah dm^{-3} at 1.0 A. This is an unexpected behaviour considering the previous results reported in literature, where the use of high current intensities during the electrolysis with diamond anodes leads to lower efficiencies due to the occurrence of undesirable parasitic/competitive reactions [67, 152]. Hence, these results suggest that the nature

and concentration of electrogenerated disinfectants with the MIKROZON® cell could play a key role on the removal of *K. pneumoniae* in urines. The mechanism of direct disinfection has been discarded because it mainly occurs when using porous materials where microorganisms can be retained [153].

Free and combined chlorine species are expected to be generated from the oxidation of chlorides contained in urine and the subsequent reaction with ammonium [154]. In addition, the MIKROZON® cell used in this work is specially designed for the electrochemical production of ozone during the electrolysis which can also contribute to the disinfection process [62, 127]. For this reason, the concentration of hypochlorite, chloramines and ozone were followed during the treatment at different current intensities and the results obtained is shown in Figure 5.28. The concentration plotted in the figure refers to the free disinfectants that have not reacted yet, and it is expected that more disinfectants have been produced during the process but were consumed in the disinfection.

The concentration of hypochlorite increases with the operation time for all the tests carried out, although the maximum concentration is attained at 1.0 A (0.43 mmol dm^{-3} Cl). At low current intensities (0.1 A), hypochlorite concentration shows a typical trend of intermediate compound: there is an initial increase followed by a decrease. On the other hand, hypochlorite increases drastically from 30 min (0.26 mmol dm^{-3} Cl) and then, the production rate is reduced when applying 0.5 A (final concentration: 0.32 mmol dm^{-3} Cl). A similar trend is observed at 1.0 A, but the concentration of hypochlorite increases from the beginning of the experiment.

Hypochlorite is a very reactive species which can react not only with microorganisms (disinfection) but also with other ions contained in the urine such ammonium, favouring the production of chloramines during electrolysis [61]. Furthermore, hypochlorite can also react with organics such as urea, creatinine, and uric acid but the evolution of these compounds will be discussed later.

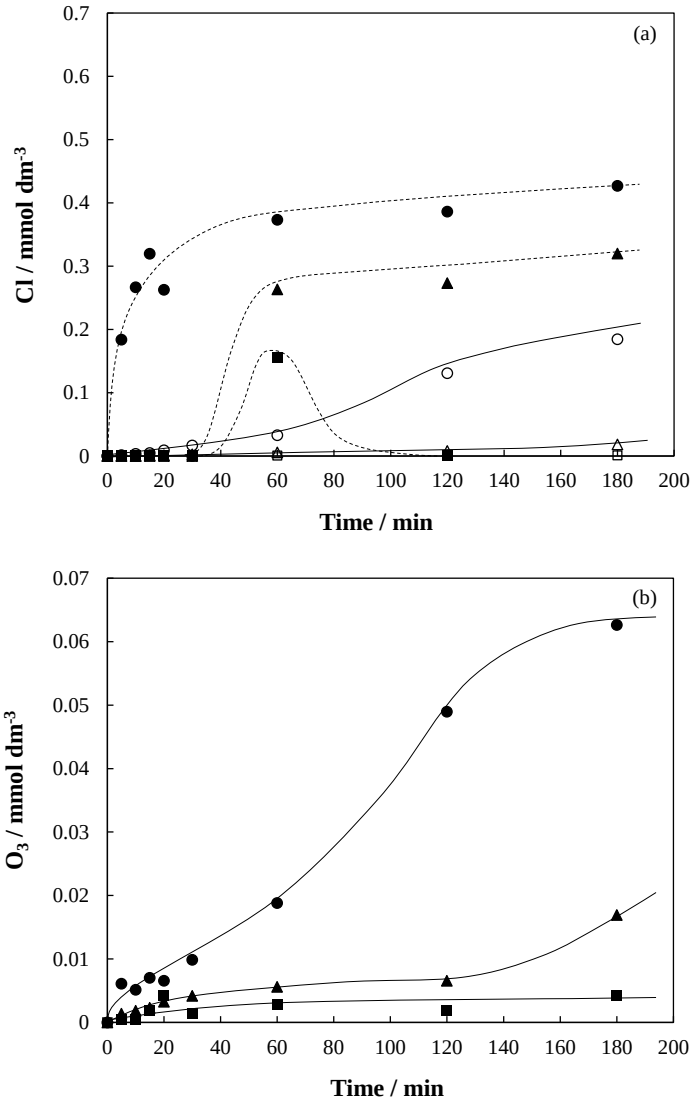

Figure 5.28. Time course of the concentration of chlorine species (a) and ozone (b) electrogenerated during the disinfection of urines using the MIKROZON® reactor. Full symbols: hypochlorite; empty symbols: chloramines; (■) 0.1 A; (▲) 0.5 A; (●) 1.0 A.

The quantity of chloramines is negligible when working at 0.1 A because of the lower concentration of hypochlorite electrogenerated. At current intensities higher than 0.5 A, these combined chlorine species increase with the operation time, reaching final concentrations of 0.02 and 0.18 mmol dm^{-3} Cl at 0.5 and 1.0 A, respectively. These values are lower than those obtained in free chlorine (0.32 and 0.43 mmol dm^{-3} Cl) and

reveal that chloramines could be consumed in the disinfection process or decomposed to chloride ions and nitrogen gas.

Regarding the ozone production during the electrodisinfection of urines (Figure 5.28b), the concentration increases with the operation time and the current intensity applied. The maximum concentration of ozone was obtained when working at 1.0 A, which is in line with the results obtained in chlorine speciation (Figure 5.28a) and the disinfection rate (Figure 5.27). Ozone values are one-fold lower than those obtained for free chlorine, and this could mean that the removal of microorganisms is more affected by the attack of free and combined chlorine species instead ozone. However, the oxidation potential of ozone is higher than hypochlorite or chloramines (E^0: 2.07 V *vs*. 1.49 V; 1.40 V) and it is expected than the disinfection capacity of this oxidant will be higher [109]. Therefore, the lower concentration of ozone measured in the liquid samples can be related to its lower stability in urine and to its higher reactivity.

Ozone and chlorine-based disinfectants seem to be the main responsible species for killing *K. pneumoniae* during the electrolysis of urines with the MIKROZON® cell but their disinfection mechanism can differ: disinfectant species can cause damage on the cell wall [155, 156] or directly penetrate inside the cell [155, 157] and destroy the genetic material. For this reason, to understand the role of disinfectants on the cell damage, the crystal violet assay was carried out. This allows us to check the changes in the cell wall through the uptake of the dye i.e., the cell wall permeability [158-160]. Fresh and treated urines were measured at the different current intensities studied to assess the combined effect of ozone and chlorine disinfectants on the cell damage. Figure 5.29a shows the uptake of crystal violet by *K. pneumoniae* as function of the current intensity before and after the electrolysis of urines. Furthermore, to evaluate the single effect of electrogenerated ozone, the treatment of urines without chlorides were also carried out, where it is expected the production of ozone as main disinfectant. The crystal violet assay was also employed with this different urine matrix and results are presented in Figure 5.29b.

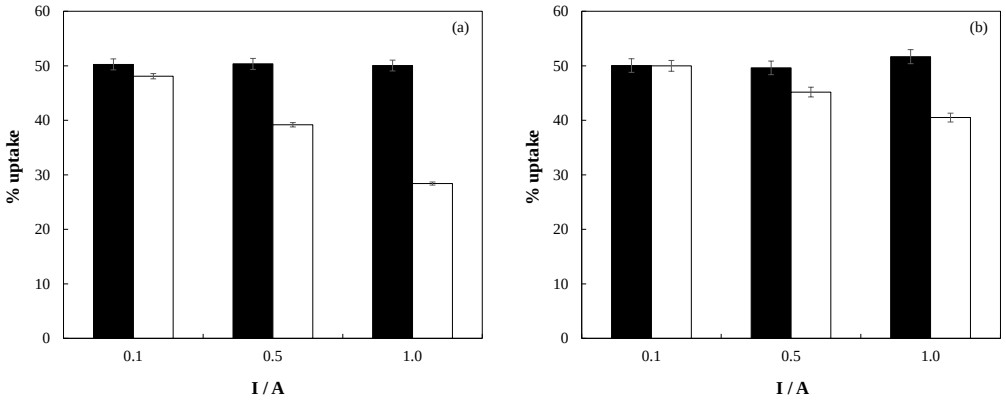

Figure 5.29. Crystal violet uptake as function of the current intensity during the disinfection of urines using the MIKROZON® reactor. (a) Urine; (b) urine without chloride; (■) fresh urine; (□) treated urine.

As can be observed, the uptake of crystal violet decreases with the current intensity in both urine matrixes. This reveals that the cell wall is attacked by the electrogenerated disinfectants during the treatment. Cell changes seem to be more important at higher current intensities, which could be explained by the production of large amounts of disinfectants when increasing the current intensity in both matrixes. Likewise, the damage increases when treating urines containing chlorides for all the current intensities studied since the uptake of crystal violet decreases to a great extent in this urine matrix (Figure 5.29a). Hence, the single effect of ozone on cell damage seems to be smaller than the combined effect with chlorine disinfectants. These results suggest that the main mechanism of the electrogenerated oxidants for killing bacteria could be the damage on the cell wall and, the subsequent attack to the genetic material. This agrees previous works reported in literature where the cell permeability during the electrochemical disinfection is evaluated and changes on cell wall were observed [155, 156, 161, 162].

Proteins and genetic material (DNA) are needed for bacteria survival [163]. During the electrochemical treatment, electrogenerated disinfectants cause damages on cell wall (Figure 5.29) and this could facilitate the pass of disinfectants into the cell, degrading the proteins and DNA [157]. For this reason, to shed light about the contribution of ozone and chlorine species on bacteria removal mechanisms, the

evolution of total proteins and DNA concentrations were measured during the electrolysis of urines with and without chlorides. Figure 5.30 shows the percentage removal of DNA and proteins achieved as function of the current intensity.

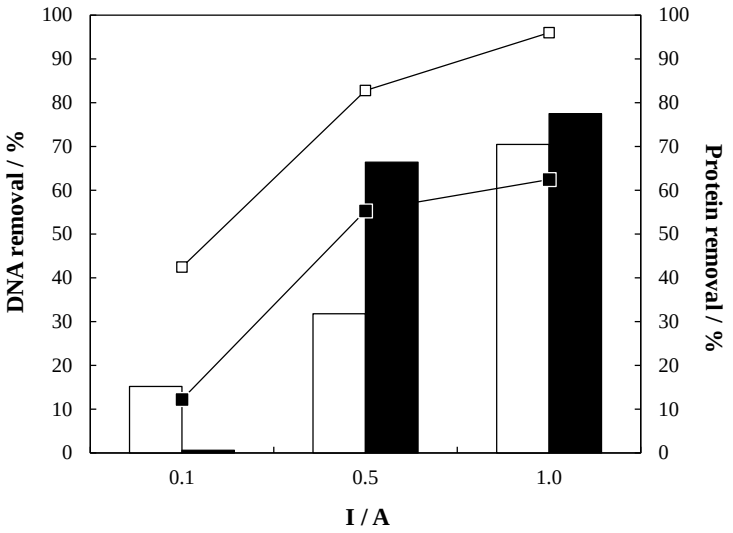

Figure 5.30. DNA (bars) and protein concentration (points) removal as function of the current intensity during the disinfection of urines using the MIKROZON® reactor. (□) Urine; (■) urine without chloride.

As can be observed, the protein removal increases with the current intensity, being higher during the treatment of urine containing chlorides. Specifically, removal percentages higher than 80 % were attained at current intensities above 0.5 A where bacteria had already been completely removed (Figure 5.27) whereas values lower than 70 % were achieved during the electrolysis of chloride-free urines. This reveals that the combined effect of ozone and chlorine-based disinfectants seems to favour the degradation of proteins during the electrolysis of urines using the MIKROZON® electrochemical cell.

Regarding the degradation of DNA, different behaviours can be seen depending on the current intensity applied. At 0.1 A, a negligible DNA removal was obtained during the treatment of urines without chlorides, which could be related to a lower disinfection efficiency reached under these conditions. A DNA removal percentage of 15.18 % was achieved when treating urines containing chlorides at 0.1 A, where the

removal of 2-log disinfection units was reached. Opposite to that, DNA removal is more remarkable during the treatment of chloride-free urines when applying current intensities higher than 0.5 A. Specifically, removal percentages of 66.39 and 77.47 % were obtained at 0.5 and 1.0 A, respectively. The degradation of DNA is slightly higher than 30 % during the electrolysis of urines with chlorides at 0.5 A, which could be an unexpected outcome considering the complete removal of *K. pneumoniae* achieved under these conditions (Figure 5.27). This suggests that DNA degradation seems to be more affected by the single effect of electrogenerated ozone. Finally, DNA removal percentages were quite similar when working at 1.0 A, although the value obtained during the treatment of urines containing chlorides was slightly lower (70.46 *vs*. 77.47 %). This confirms the potential effect of ozone on DNA degradation in comparison with the combined effect of ozone and chlorine-based disinfectants. Therefore, these results reveal that the combined effect of ozone and chlorine disinfectants promotes the degradation of proteins whereas single electrogenerated ozone seems to attack the DNA to a greater extent.

To shed light about the real contribution of ozone on the removal of *K. pneumoniae*, Figure 5.31a compares the log removal units of *K. pneumoniae* during the electrolysis of urines with and without chlorides at different current intensities using the MIKROZON® cell. Likewise, the experimental data were fitted to a first order kinetics model [154] and the resulting rate constants for urine (k_U) and urine without chlorides (k_{UWC}) were also compared throughout the ratio k_U/k_{UWC}. Values higher than 1 indicate that the disinfection process is more efficient by the combination of electrogenerated chlorine and ozone disinfectants whereas ratios lower than 1 suggest a more contribution of ozone on the disinfection process.

As can be observed, a negligible disinfection was obtained during the treatment of urines without chlorides at 0.1 A. This can be related to the low concentration of electrogenerated ozone (Figure 5.31b) under these conditions and the absence of chlorine-based disinfectants. In increasing the current intensity, the disinfection process becomes more efficient, reaching 4-logs removal at 0.5 A and the total disinfection when applying 1.0 A. On the other hand, the ratio k_U/k_{UWC} decreases with the current

intensity which suggests that the electrochemical disinfection based on the ozone production is limited at values lower than 1.0 A and it is required the combination of ozone and chlorine disinfectants to attain a complete removal of microorganisms at 0.5 A. However, the ratio is close to 1 when the electrolysis is carried out at 1.0 A. This means that the disinfection rates are quite similar either by the single effect of ozone or by the combined effect of ozone and chlorine disinfectants. Hence, it is necessary to apply current intensities of 1.0 A to produce large amounts of ozone with the MIKROZON® cell that assure the disinfection process in absence of chlorides.

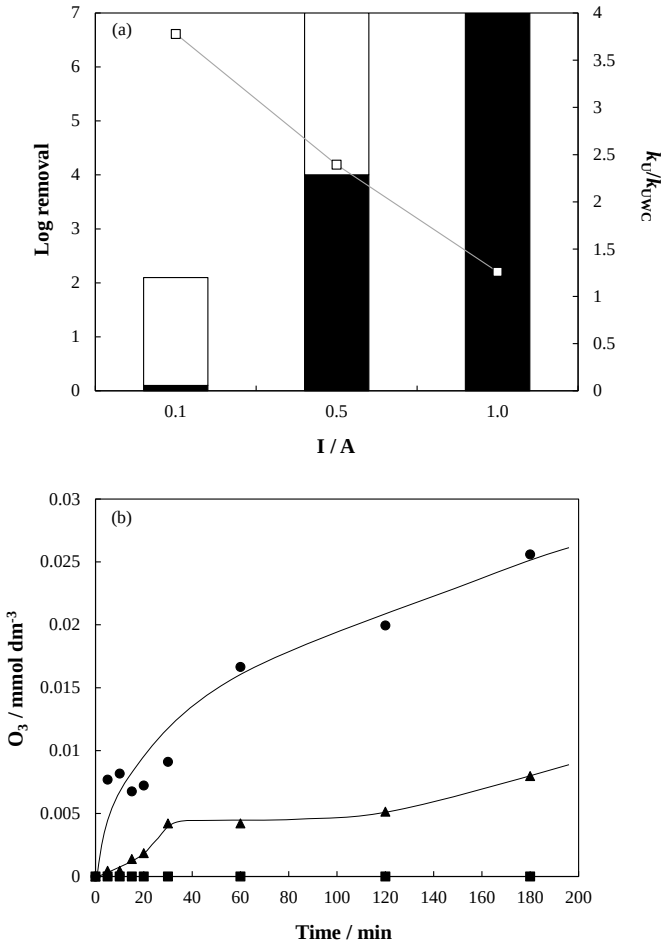

Figure 5.31. (a) Log removal (bars) and ratio k_{HU}/k_{HUWC} (points) as function of the current intensity; (□) urine; (■) urine without chlorides. (b) Time course of the concentration of ozone electrogenerated during the disinfection of urines without chlorides using the MIKROZON® reactor. (■) 0.1 A; (▲) 0.5 A; (●) 1.0 A.

Finally, urine contains organic compounds which can be also oxidized during the electrolysis: urea, creatinine and uric acid [139]. The degradation of these organics can compete with the disinfection process and, for this reason, their concentrations were analysed. Figure 5.32a shows the evolution of urea, creatinine and uric acid as function of the operation time during the electrolysis of urines.

The concentration of urea remains constant for all the tests carried out whereas creatinine slightly decreases, reaching a maximum percentage removal of 25.85 % when working at 1.0 A. Furthermore, uric acid is completely removed from urine at current intensities higher than 0.5 A. The different trends observed in each organic is mainly related to their initial concentration and molecular structure ($[urea]_0$: 3333,34 mg dm^{-3}; $[creatinine]_0$: 166.67 mg dm^{-3}; $[uric\ acid]_0$: 50 mg dm^{-3}) [67]. This reveals that the lower the initial concentration, the higher the removal efficiency. Likewise, the molecular structures of uric acid and creatinine present more functional groups susceptible to be attacked by the disinfectants generated, favouring their degradation. These results point out that there exists a competitive oxidation between organics and components from bacteria during the electrolysis of urines that can be more remarkable at 1.0 A, because the organics removal percentages are higher. This is an expected behaviour considering that higher current intensities lead to higher production of oxidants and, hence, higher organics degradation rates. To overcome the limitations related to competitive oxidation between organics and bacteria, the electrolysis of diluted urines was evaluated with the MIKROZON® cell, where the concentration of organics is ten times lower but the same bacteria concentration. This new formulation could be found in a real hospital effluent, once urine has been mixed with other grey waters from hospital and will allow us to evaluate the efficiency of the solid-electrolyte electro-ozonizer on the removal of *K. pneumoniae* with a small contribution of competitive reactions due to the lower organic load. Figure 5.32b shows changes in bacteria concentration during the disinfection of different urine matrixes at 1.0 A using the MIKROZON® cell.

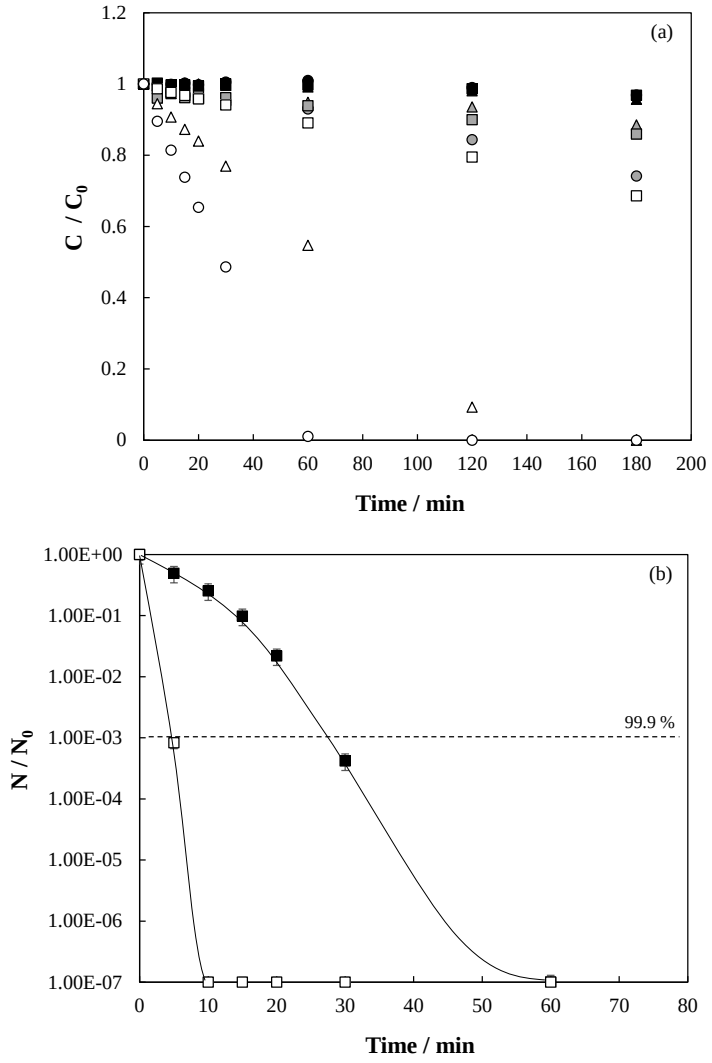

Figure 5.32. (a) Time course of the concentration of organics during the disinfection of urines using the MIKROZON® reactor. Black symbols: urea; grey symbols: creatinine; white symbols: uric acid; (■) 0.1 A; (▲) 0.5 A; (●) 1.0 A. (b) Influence of urine matrix on the disinfection of urines using the MIKROZON® reactor at 1.0 A. (■) hospital urine; (□) diluted (1:10) hospital urine.

As can be observed, a total disinfection of diluted urine is attained in 10 minutes whereas an operation time 6 times higher is required to guarantee the complete removal of *K. pneumoniae* in urines. The low initial concentration of organics in diluted urines ($[urea]_0$: 333,34 mg dm^{-3}; $[creatinine]_0$: 16.67 mg dm^{-3}; $[uric\ acid]_0$: 5 mg dm^{-3}) seems to promote higher disinfection rates (1.4194 *vs*. 0.2194 min^{-1}). This confirms the

occurrence of competitive reactions when treating urines with higher organic load. Likewise, the lower conductivity of diluted urines (300 μS cm^{-1}) could favour the higher disinfection rates with the MIKROZON® cell since this electrochemical device is specially designed for treating low conductivity waters [127]. These outcomes are great of interest because open the possibility of using a solid-electrolyte electro-ozonizer for treating hospital effluents where urine is diluted.

5.3.3. Conclusions

The following conclusions can be drawn from this chapter:

- The disinfection process of *K. pneumoniae* from hospital urines relies on the current density and the reactor layouts. Complete disinfection (7 log unit decay) was attained before 120 min using a flow-through reactor with MMO anode at 50 A m^{-2} and almost 6 log reduction was achieved using a parallel flow cell under the same experimental conditions. The process efficiency also depends on the electrochemical cell tested since the mass-transfer coefficient calculated with the flow-through reactor was one order of magnitude higher than using the parallel flow layout. Furthermore, the presence of chlorides in hospital urines contributes to the electrochemical generation of hypochlorite. Hypochlorite may oxidize the organics naturally contained in urine and/or may react with ammonium ions to form chloramines. The concentration of chloramines increases with the current density and their formation is the highest using the flow-through layout due to its slightly higher hydraulic retention time. Besides, hypochlorite does not evolve to higher chlorine oxidation states such as harmful chlorates and/or perchlorates.
- Chemical disinfection tests of *K. pneumoniae* from hospital urines informed about the dependence on the concentration of chlorine disinfectants. A stronger powerful bactericidal effect of hypochlorite in comparison with chloramines was determined since chloramines require longer exposure to inactive microorganisms. However, chloramines seem to play a key role in

the electrochemical disinfection process in hospital urines since they contribute not only as disinfectants but avoiding the production of chlorine disinfection by-products.

- The use of a commercial electro-ozonizer allows to disinfect urines from current intensities higher than 0.5 A. The disinfection rate is higher when increasing the current intensity due to the higher production of disinfectants. The combined effect of ozone and chlorine disinfectants attains higher disinfection rates than the values obtained when single ozone is the main disinfectant electrogenerated (urine without chlorides) at current intensities lower than 0.5 A. At values of 1.0 A, the disinfection rates are quite similar which reveals that large amounts of ozone have been electrogenerated for the efficient removal of *K. pneumoniae*. The crystal violet assay shows that the combined effect of all disinfectants promotes higher cell damages, increasing the cell wall permeability. DNA and proteins are degraded during the disinfection of urines by electrochemical oxidation. The combined effect of ozone and chlorine disinfectants promotes the degradation of proteins for all the tests carried out. However, single electrogenerated ozone seems to attack the DNA to a greater extent from current intensities higher than 0.5 A, where a remarkable disinfection rate is attained in urine matrixes without chlorides. Higher disinfection rates are obtained during the treatment of diluted urines by a solid-electrolyte electro-ozonizer at 1.0 A. The occurrence of competitive reactions is minimized due to the lower organic load in the effluent. Furthermore, the low conductivity of diluted urines favours the removal of *K. pneumoniae* because the electrochemical cell is specially designed to produce large amounts of ozone in low conductivity water.

5.4. Coupling UV light irradiation with the electrodisinfection process

One of the Advanced Oxidation Processes (AOPs) widely evaluated for the disinfection of urban and hospital wastewater is ultraviolet (UV) disinfection [164-166]. The irradiation of UV light to an effluent containing microorganisms can promote the generation of hydroxyl radicals from water photolysis under vacuum, which are the main responsible species for bacteria removal [167]. Likewise, UV light can penetrate the cell wall, destroying the genetic material. However, the damage caused on bacteria can be repaired after relatively small times, promoting bacteria regrowth [168, 169]. Besides, the presence of suspended solids and colloids in wastewater decreases the process efficiency. At this point, the use of combined treatments appears as a good option to overcome these limitations.

Among the different alternatives, electrochemical oxidation is a potential candidate to be considered. As shown in previous sections, depending on the electrode material and applied current density [76, 170], this technology can promote the formation of hydroxyl radicals from water electrolysis. Additionally, during electrolysis, other oxidants can be generated from the oxidation of the ions naturally contained in the effluents that can also contribute to the disinfection process, preventing the bacteria regrowth. At this point, the role of anode material is critical. Thus, the use of anodes based on Mixed Metal Oxides (MMO) such as RuO_2, IrO_2, or Ta_2O_5 promotes the evolution of chlorine during electrolysis [119-121]. On the other hand, Boron Doped Diamond (BDD) anodes favour the formation of a cocktail of oxidants (e.g., hypochlorite, persulfate, peroxodiphosphate, percarbonate, ozone) which seems to be the main responsible for the good performance of this electrode in the treatment of industrial wastewater [122, 123] and wastewater disinfection [62, 124]. Additionally, the irradiation of UV light also promotes the photoactivation of these oxidants, increasing the quantity of free radicals available for disinfection purposes [171-174].

In this regard, this section comprises the main goal of evaluating the synergies or antagonisms when coupling electrochemical oxidation to UV disinfection for the removal of ARB in hospital urines. The experimental planning to meet this main

objective is summarized in Table 5.13. As observed, electrolysis, phtoelectrolysis and photolysis experiments have been carried out, evaluating also the influence of the current density (5-50 A m^{-2}) and the anode material (BDD and MMO). In all cases, *K. pneumoniae* is selected as target bacterium.

Table 5.13. Experimental planification for evaluating the synergies of the photo-electrochemical disinfection technology to remove *K. pneumoniae* ATCC 4352.

Exp. Nº	Technology	Reactor	Anode / Cathode	Current density (A m^{-2})	Treated effluent
1	Electrolysis	Microfluidic flow-through reactor	BDD / SS	5	Hospital urine
2				50	
3	Electrolysis	Microfluidic flow-through reactor	MMO / SS	5	Hospital urine
4				50	
5	Electrolysis	Microfluidic flow-through reactor	BDD / SS	5	1000 mg dm^{-3} KCl
6				50	
7	Electrolysis	Microfluidic flow-through reactor	MMO / SS	5	1000 mg dm^{-3} KCl
8				50	
9	Photo-Electrolysis	Microfluidic flow-through reactor	BDD / SS	5	Hospital urine
10				50	
11	Photo-Electrolysis	Microfluidic flow-through reactor	MMO / SS	5	Hospital urine
12				50	
13	Photo-Electrolysis	Microfluidic flow-through reactor	BDD / SS	5	1000 mg dm^{-3} KCl
14				50	
15	Photo-Electrolysis	Microfluidic flow-through reactor	MMO / SS	5	1000 mg dm^{-3} KCl
16				50	
17	Photolysis	Microfluidic flow-through reactor	UV lamp / 5 W / λ = 254 nm		Hospital urine

5.4.1. Enhancement of UV disinfection of urine matrixes by electrochemical oxidation

Figure 5.33 shows changes in the concentration of *K. pneumoniae* with the operation time during the UV disinfection, electrodisinfection, and photo-electrodisinfection of hospital urines.

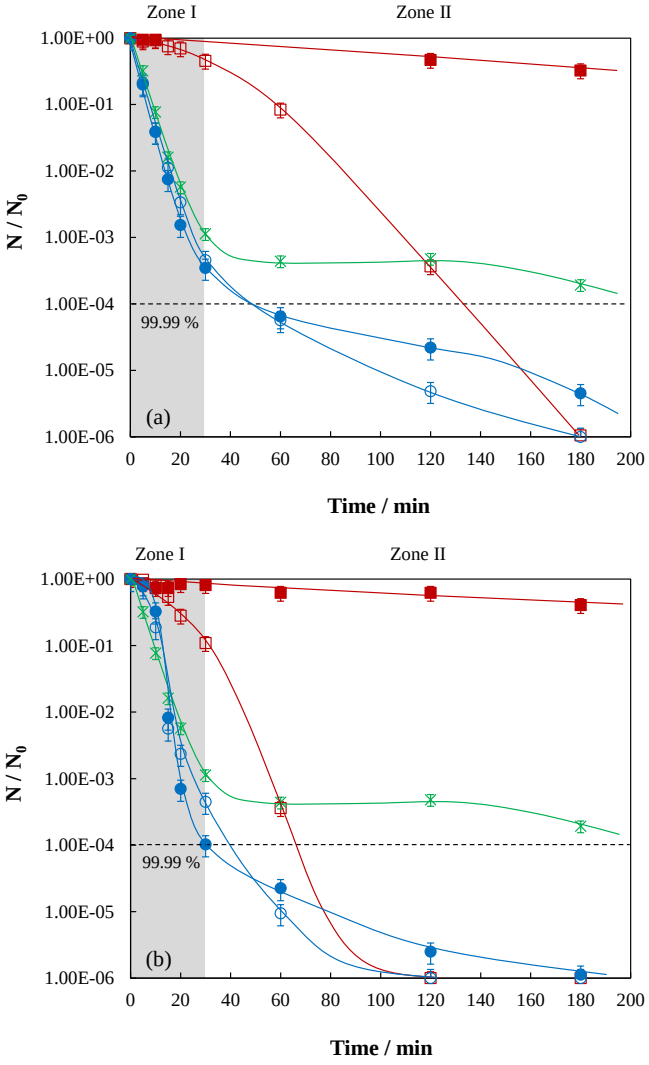

Figure 5.33. Time course of the concentration of *K. pneumoniae* during the treatment of hospital urines. Green symbols (x): UV disinfection; red symbols (■, □): electrolysis; blue symbols (●, ○): photoelectrolysis; full symbols: 5 A m^{-2}; empty symbols: 50 A m^{-2}; (a) BDD anode; (b) MMO anode. *K. pneumoniae*$_0$ (N_0): 10^6 CFU ml^{-1}.

As can be observed, UV disinfection reduces 3 orders of magnitude the concentration of bacteria in hospital urine after 3 hours of treatment. The removal of microorganisms may be due to the penetration of UV light into the cell, destroying the genetic material [175]. Two zones can be distinguished in which the disinfection rate is very different. Initially, the inactivation of *K. pneumoniae* is very fast, reaching the maximum log removal around 30 min (zone I). After that, the disinfection rate decreases drastically (zone II). This behaviour has also been reported in the literature during the application of the UV disinfection process to the treatment of wastewater, although the occurrence of a plateau zone has not yet been clearly explained [176, 177]. Several hypotheses have been proposed such as the aggregation of microorganisms or a resistant subpopulation, but no clear evidences have been reported [168].

On the other hand, complete inactivation of *K. pneumoniae* can be attained in hospital urines using electrolysis with BDD and MMO anodes at 50 A m^{-2}, while at low current densities (5 A m^{-2}) the population of microorganisms slightly decreases without removing 1 order of magnitude, regardless the anode material used. This reveals that a minimum current density (higher than 5 A m^{-2}) should be applied to ensure complete disinfection. However, different trends can be seen during electrolysis at higher current densities with both anodes. Specifically, an operation time of 180 min (which corresponds with 0.42 Ah dm^{-3} of electric charge) is needed for killing bacteria with BDD anodes whereas a total inactivation is achieved in 120 min (which corresponds with 0.28 Ah dm^{-3} of electric charge) using MMO electrodes at 50 A m^{-2}. This is an unexpected behaviour because electrochemical disinfection with BDD is generally more efficient and faster than with MMO anodes [133]. Nonetheless, it should be noted that the properties of diamond anodes significantly influence the performance of an electrochemical process [178-180] and therefore, general conclusions should not be drawn for all diamond electrodes. The electrode used in the work was made over a niobium substrate, which has shown not to promote the production of large amounts of powerful oxidants during electrolysis, as tantalum and silicon substrates [181]. So, this could explain the lower disinfection rate registered in comparison with MMO anodes. Likewise, it is important to point out that the MMO anodes used are based on IrO_2/Ta_2O_5

which favours the evolution of oxygen and chlorine during electrolysis and the subsequent disinfection process [182]. A detailed discussion related to the influence of the anode material on the production of oxidants during electrochemical disinfection is reported later. Nevertheless, at this point, it should be mentioned that the concentration of *K. pneumoniae* was also measured after 24 h to evaluate a possible bacteria regrowth. For this additional test, samples were stored in dark at room temperature when finishing the experiments. The population of microorganisms was similar to that obtained at the end of electrolysis which confirms that the electrochemical process ensures persistent disinfection.

Regarding the photoelectrolysis process, results obtained show the highest disinfection rates, reaching a reduction higher than 5 orders of magnitude for all the current densities and anode materials tested. The removal of *K. pneumoniae* follows the same profile as UV disinfection at the beginning of the treatment (Zone I), reaching 3-4 orders of magnitude reduction for both anodes, regardless the current density applied. Then, unlike behaviour observed during single photolysis, the population of microorganisms continuous to decrease until the total disinfection (Zone II), being the removal rate higher at 50 A m^{-2}. Photoelectrolysis is much better than single processes since improves 2-3 orders of magnitude the UV disinfection process and even 5-6 orders of magnitude the electrochemical process at 5 A m^{-2}. At high current densities, electrochemical and photoelectrochemical processes attain complete disinfection but the last one shows a higher removal rate. Likewise, the use of MMO anodes leads to higher disinfection rates in comparison with BDD anodes due to their different electrocatalytic properties for the production of disinfectants [87]. In this context, the large amounts of disinfectants generated during the electrolysis of hospital urines [70] can be activated by the irradiation of UV light, favouring the production of free radicals which are more reactive than the parent oxidants [183]. Hence, the higher disinfection efficiency can be attributed to the photo-activation of oxidants during the combined treatment. The two different zones observed indicate that the contribution of UV light irradiation is more significant at the beginning of the process (zone I) whereas the combination of photochemical and electrochemical processes leads to remarkable

synergies in the disinfection at the end of the treatment (zone II). Likewise, the low electric charges applied within 30 min of the experiments ($Q < 0.1$ Ah dm^{-3}) may support the almost negligible contribution of electrochemical oxidation at the beginning of the treatment because of the expected low generation and accumulation of disinfectants in the system.

For comparison purposes, experimental data were fitted to a first-order kinetic model and, the resulting kinetic constants, the residual variance (S^2_R), and the correlation coefficient (R^2) are presented in Table 5.14. Two different values have been calculated for photochemical and photoelectrochemical processes that correspond to the different zones observed in the removal of microorganisms and only one value is reported for the single electrochemical process.

Table 5.14. Kinetic constants for the disinfection by UV irradiation, electrolysis, and photoelectrolysis.

Process	**Anode**	**Current density ($A\ m^{-2}$)**	**$k_{Zone\ I}$ (min^{-1})**	**S^2_R (CFU^2/ml^2)**	**R^2**	**$k_{Zone\ II}$ (min^{-1})**	**S^2_R (CFU^2/ml^2)**	**R^2**
Photolysis	-	-	0.2338	0.1327	0.9795	0.0098	0.1498	0.7141
*Electrolysis	BDD	5	0.0062	0.0002	0.9992	0.0062	0.0002	0.9992
		50	0.0770	0.5861	0.9747	0.0770	0.5861	0.9747
	MMO	5	0.0039	0.0125	0.8193	0.0039	0.0125	0.8193
		50	0.1400	0.4833	0.9848	0.1400	0.4833	0.9848
Photoelectrolysis	BDD	5	0.3247	0.0003	0.9999	0.0269	0.1967	0.9411
		50	0.2570	0.1237	0.9842	0.0428	0.2258	0.9726
	MMO	5	0.3491	1.2676	0.9168	0.0301	0.3666	0.9135
		50	0.2926	0.9813	0.9089	0.062	2.2737	0.7498

*only one zone

Comparing the combined process with UV disinfection, the kinetic constants are a little higher in the zone I during photoelectrolysis, which confirms that there exists a small contribution of the electrochemical process to the removal of microorganisms at the beginning of the treatment. On the contrary, the values registered in zone II are much higher, being more noticeable at higher current densities where the production of oxidants is expected to be higher by electrolysis and, hence, the disinfection rate. These

results point out the higher contribution of the electrochemical process at the end of the treatment. To quantify the improvement of UV disinfection by electrolysis, the synergy coefficient was calculated according to Equation 5.11 [184]. Figure 5.34 shows the synergy coefficient for the combined process and the logarithmic removal increase between UV disinfection and photoelectrolysis.

$$\text{Synergy coefficient} = \frac{k_{\text{photoelectrolysis}}}{k_{\text{UV disinfection}} + k_{\text{electrolysis}}} \quad (5.11)$$

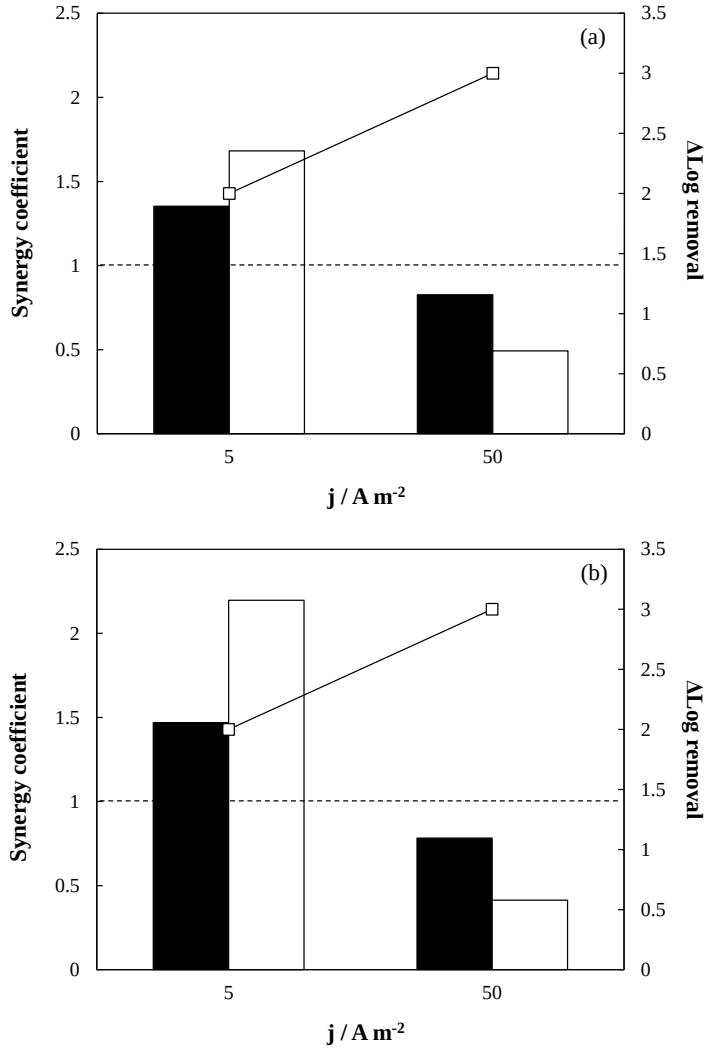

Figure 5.34. Synergistic effect (bars) and ΔLog removal (points) calculated at different current densities. Black bars: zone I; white bars: zone II; (a) BDD anode; (b) MMO anode.

A synergistic effect resulted in the disinfection of urines during photoelectrolysis at 5 A m^{-2}, regardless the anode material used. Under these conditions, there is a marked contribution of UV disinfection at the beginning of the treatment and then, the electrochemical process has a more significant influence on the removal of ARB. The highest synergistic effect was obtained in zone II during photoelectrolysis with MMO anodes where the disinfection by UV irradiation is very limited. These synergies could be explained by the generation and photoactivation of the disinfectant species formed during the combined process. More details about the disinfectants produced during the different processes tested are reported later. At higher current densities, antagonistic effects (synergy coefficient < 1) can be observed during photoelectrolysis with both anodes. This can be due to the competitive oxidation between *K. pneumoniae* and organics contained in the urine matrix (urea, creatinine, and uric acid) under these operating conditions [138]. These results reveal that photoelectrolysis is an efficient technology for the disinfection of hospital urines when working at low current densities since electrolysis can enhance by 2 orders of magnitude the removal of *K. pneumoniae* attained by UV disinfection. The use of current densities of 50 A m^{-2} improves the removal in 3 orders of magnitude but clear antagonistic effects have been obtained.

The removal of ARB from urine by electrochemical processes could take place by the direct oxidation of microorganisms over the anode surface (electroadsorption) or by mediated oxidation via electrogenerated oxidants. The first option mainly occurs when using porous materials such as carbon felt or cloth as the anode, where bacteria can be adsorbed [185]. On the other hand, the in-situ production of disinfectants and the subsequent attack to microorganisms seems to be the main mechanism for killing bacteria during electrolysis with BDD and MMO anodes [70, 186]. Urine matrix used in this work contains large amounts of chloride in its composition (475.52 mg dm^{-3}) whose first oxidation product is hypochlorite (Equations 5.3-5.5).

This species is a well-known disinfectant that is used in conventional disinfection processes [187] and, for this reason, its concentration was monitored during the treatment. Figure 5.35 shows the hypochlorite electrogenerated as a function of the

operation time during the disinfection of hospital urines by electrolysis and photoelectrolysis with BDD and MMO anodes at the current densities tested. Data from UV disinfection is not included in the figure because hypochlorite was not detected during this photochemical process.

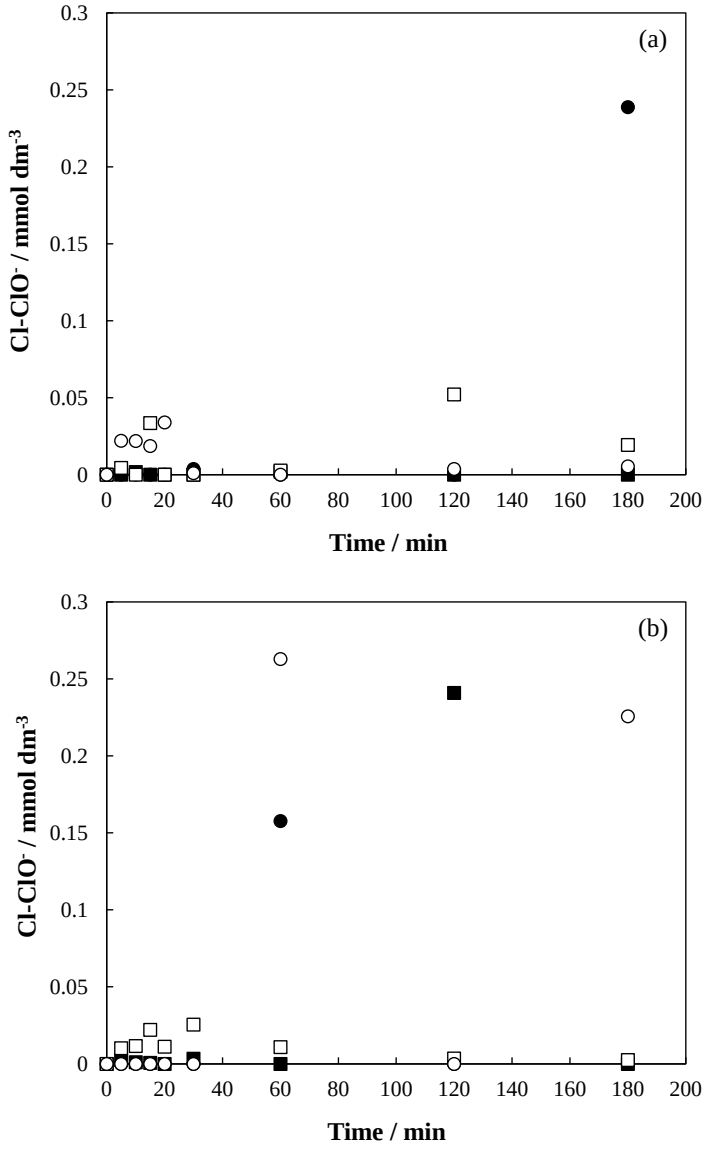

Figure 5.35. Time course of the concentration of hypochlorite during the treatment of hospital urines. Black symbols: electrolysis; white symbols: photoelectrolysis; (■, □) 5 A m^{-2}; (●, ○) 50 A m^{-2}; (a) BDD anode; (b) MMO anode.

The amount of electrogenerated hypochlorite is lower than 0.3 mmol dm^{-3} Cl, regardless the current density and the anode material used. However, it should be pointed out that the hypochlorite measured is referred to the free concentration that has not reacted in the effluent and much higher amounts are expected to have been generated during the treatment. To check this hypothesis, electrolysis of 1000 mg dm^{-3} KCl was carried out (Figure 5.36) since this compound is contained in the urine matrix in the same concentration. In these tests, electrogenerated hypochlorite is expected to be easily accumulated because it cannot react with other species as occur in the urine matrix.

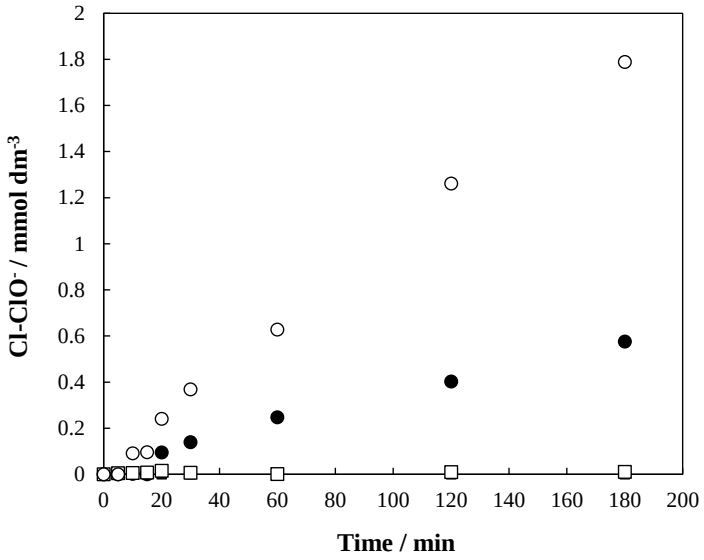

Figure 5.36. Time course of the concentration of hypochlorite during the electrolysis of 1000 mg dm^{-3} KCl. Black symbols: BDD anode; white symbols: MMO anode; (■, □) 5 A m^{-2}; (●, ○) 50 A m^{-2}.

Results confirm that large amounts of hypochlorite are generated at higher current densities (50 A m^{-2}). Nevertheless, the concentration of this species is very low at 5 A m^{-2}, which implies that higher values are required to ensure a significant production of hypochlorite during electrolysis. This also supports the low disinfection rates registered during the treatment of hospital urines under these conditions (5 A m^{-2}) where it is not possible to achieve 1 order of magnitude removal. Furthermore, it can be observed that the electrochemical production of hypochlorite is influenced by the anode material used. Specifically, concentrations around 1.8 mmol dm^{-3} Cl are achieved with

MMO anodes at 50 A m^{-2} whereas the use of BDD anodes leads to the generation of concentrations lower than 0.6 mmol dm^{-3} Cl at the end of the process under the same operating conditions. This confirms the better electrocatalytic properties of the MMO anode tested to produce chlorine disinfectants and the subsequent removal of *K. pneumoniae* from urine.

Hypochlorite concentration does not follow a clear trend during the disinfection tests, and it could be related to the high reactivity of this species in the urine matrix: 1) hypochlorite can promote to other chlorine compounds in high oxidation state (i.e., chlorite, chlorate, and perchlorate) (Equations 5.12-5.14), 2) the photoactivation of hypochlorite can occur by the irradiation of UV light, favouring the production of free chlorine radicals (Equation 5.15), 3) the degradation of organics naturally contained in urine (urea, creatinine and uric acid) can take place by chlorination reaction or 4) hypochlorite can react with ammonium contained in the effluent, favouring the production of combined chlorine species (chloramines) (Equations 5.6-5.8). All these reactions can occur simultaneously during the process.

$$ClO^- + H_2O \rightarrow ClO_2^- + 2\,H^+ + 2\,e^- \quad (E^0 = -1.67\ V) \tag{5.12}$$

$$ClO_2^- + H_2O \rightarrow ClO_3^- + 2\,H^+ + 2\,e^- \quad (E^0 = -1.18\ V) \tag{5.13}$$

$$ClO_3^- + H_2O \rightarrow ClO_4^- + 2\,H^+ + 2\,e^- \quad (E^0 = -1.20\ V) \tag{5.14}$$

$$ClO^- + h\nu \rightarrow Cl^{\bullet} + O^{\bullet -} \quad (E^0 = 2.43\ V) \tag{5.15}$$

The formation of chlorate and perchlorate was not detected by ion chromatography for all the tests carried out with BDD and MMO anodes. The measured concentration was below the detection limit for each species (ClO_3^-: 7 µg dm^{-3}; ClO_4^-: 7 µg dm^{-3}). This data is of great importance because it reveals that the removal of ARB from urine by electrolysis and photoelectrolysis could be carried out under the operating conditions tested without the generation of undesirable chlorine by-products.

On the other hand, the concentration of free chlorine radicals is difficult to measure owing to their short lifetime. Thus, to evaluate the possible formation of these

species during the disinfection of hospital urines by photoelectrolysis, experiments with 1000 mg dm^{-3} were performed (Figure 5.37).

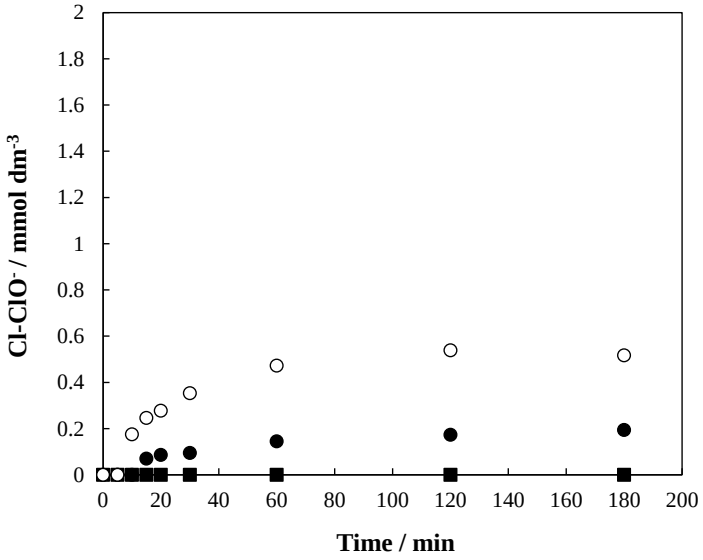

Figure 5.37. Time course of the concentration of hypochlorite during the photoelectrolysis of 1000 mg dm^{-3} KCl. Black symbols: BDD anode; white symbols: MMO anode; (■, □) 5 A m^{-2}; (●, ○) 50 A m^{-2}.

As can be observed, the concentration of hypochlorite increases with the operation time at 50 A m^{-2} whereas a negligible concentration was obtained at 5 A m^{-2} for both anodes. This behaviour is similar to that previously obtained during single electrolysis of KCl solutions (Figure 5.36). However, the concentration achieved is lower during photoelectrolysis which indicates that hypochlorite has been photoactivated, favouring the production of free chlorine radicals (Equation 5.15). Therefore, the occurrence of these radicals can be considered as one way for electrogenerated hypochlorite consumption during photoelectrolysis of hospital urines.

Regarding the chlorination reaction of organics, urine contains large amounts of urea, creatinine, and uric acid which are susceptible to react with hypochlorite during the electrochemical treatment, decreasing their concentration [70]. The concentration of urea remained constant for all the tests carried out with both anodes. Creatinine concentration decreased between 10 and 25 % at 5 A m^{-2} and, up to 40 % at 50 A m^{-2} with BDD anodes whereas its concentration remained constant when using MMO

anodes, regardless the current density applied. Finally, a percentage removal of uric acid around 50 % was achieved during electrolysis and photoelectrolysis with BDD and MMO anodes at 5 and 50 A m^{-2} (data not shown). These reactions could promote the formation of organochlorinated compounds in hospital urines which may increase the toxicity of the resulting effluents. Nonetheless, their generation and accumulation are not expected to be very high due to the low applied electric charges required for killing microorganisms. The degradation of urea, creatinine and uric acid releases a higher nitrogen load to the effluent which can be transformed into other inorganic species [188]. Specifically, nitrite is formed from the oxidation of organic nitrogen released (Equation 5.16, which is rapidly oxidized to nitrate (Equations 5.17-5.18). Besides, this last species can be electrochemically reduced, favouring the generation of ammonium (Equations 5.19-5.20) [189]. Hence, the concentration of ammonium could be considered as an indirect measurement of the degradation of organics during the disinfection of urines. Figure 5.38 shows the time course of the ammonium concentration during the disinfection of hospital urines by electrolysis and photoelectrolysis with BDD and MMO anodes at different current densities. The initial amount in the urine matrix is around 1.26 mmol dm^{-3} N.

$$N_{org} + O_{2(aq)} + e^- \rightarrow NO_2^- \quad (5.16)$$

$$3\ NO_2^- + 2\ H^+ \leftrightarrows 2\ NO_{(aq)} + NO_3^- + H_2O \quad (5.17)$$

$$NO_2^- + ½\ O_{2(aq)} \rightarrow NO_3^- \quad (5.18)$$

$$NO_3^- + 6\ H_2O + 8\ e^- \rightarrow NH_{3(aq)} + 9\ OH^- \quad (5.19)$$

$$NH_{3(aq)} + H_2O \rightleftharpoons NH_4^+ + OH^- \quad (5.20)$$

As can be observed, the concentration of ammonium remains constant at 5 A m^{-2} for both anodes. This suggests that the organics removal rate is very low, and the chlorination of organics does not lead to the release of nitro groups but the formation of organochlorinated compounds. Likewise, this low current density does not favor the production of other oxidants that could be generated and contribute to the removal of organics contained in urine. On the contrary, ammonium concentration continuously

increases with the operation time at 50 A m^{-2}, being higher when working with BDD anodes.

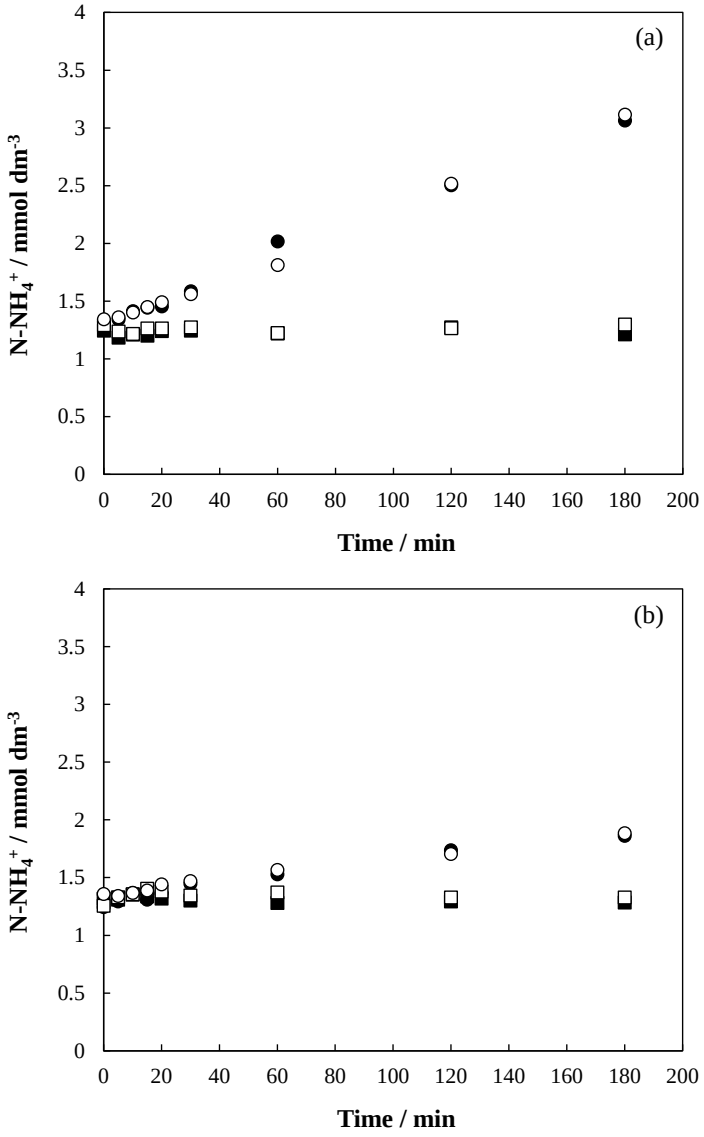

Figure 5.38. Time course of the concentration of ammonium during the treatment of hospital urines. Black symbols: electrolysis; white symbols: photoelectrolysis; (■, □) 5 A m^{-2}; (●, ○) 50 A m^{-2}; (a) BDD anode; (b) MMO anode.

These results suggest that the electrogenerated hypochlorite could also be consumed in the degradation of organics contained in the urine matrix together with other oxidants generated during electrolysis and photoelectrolysis under these

conditions. However, the irradiation of UV light does not influence the removal of organics since similar results are observed in both processes, regardless the anode material tested. The use of MMO anodes seems to be less effective for the removal of organics than BDD. This is an unexpected behaviour considering the previous disinfection data where BDD anode showed lower rates for killing bacteria. At this point, it is important to remark that the removal of organics can also take place by direct oxidation over the anode surface and hydroxyl radical-mediated oxidation [78] and these mechanisms seem to be more relevant when using BDD anodes at 50 A m^{-2}. Hence, there could be a marked competitive reaction between the disinfection and the oxidation of organics with this anode.

Nonetheless, ammonium released could also be consumed together with the electrogenerated hypochlorite to form chloramines (Equations 5.6-5.8) during the disinfection of urines. This could explain the low concentration registered with MMO anodes since the electrogeneration of hypochlorite is also expected to be higher with this anode (Figure 5.36). For this reason, the concentration of chloramines was also monitored during the disinfection of urines by electrolysis and photoelectrolysis and, the results obtained as function of the operation time for both anodes at different current densities are plotted in Figure 5.39.

The concentration of chloramines increases with the operation time, being one order of magnitude higher when using MMO anodes. This can be due to the large amounts of hypochlorite generated with this anode and, it also seems to confirm that the formation of chloramines is the main way of consumption of hypochlorite with MMO anodes whereas the use of BDD anodes promotes the oxidation of organics. Chloramines also contribute to the disinfection of urine although their disinfectant capacity is lower than hypochlorite. Likewise, the presence of chloramines minimizes the production of trihalomethanes (THMs) and trihalogenated haloacetic acids as disinfection by-products [149, 190] and, hence, decreases the accumulation of hazardous organochlorinated compounds in treated effluents.

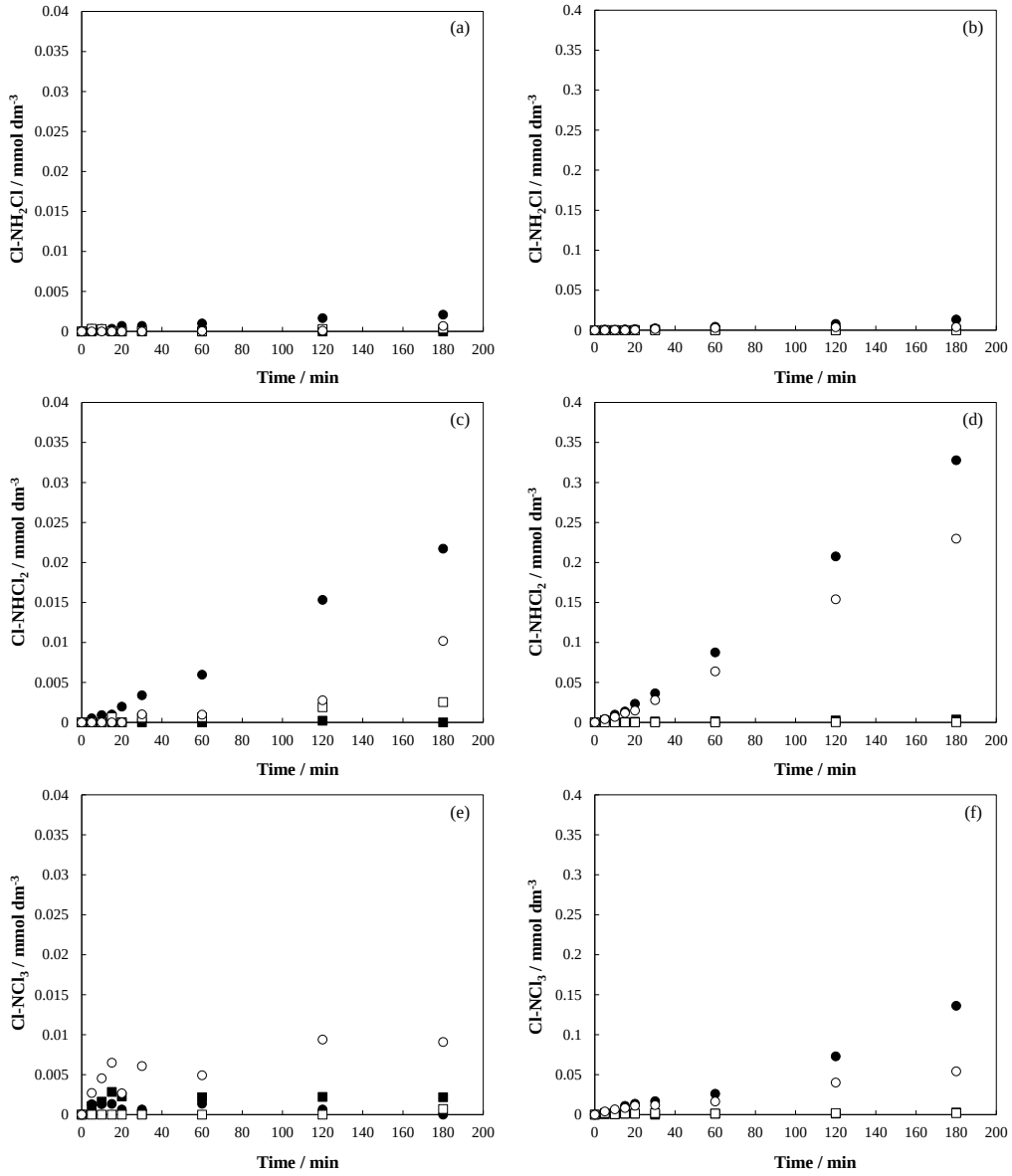

Figure 5.39. Time course of the concentration of chloramines during the treatment of hospital urines. Black symbols: electrolysis; white symbols: photoelectrolysis; (■, □) 5 A m^{-2}; (●, ○) 50 A m^{-2}; (a) Monochloramine-BDD; (b) Monochloramine-MMO; (c) Dichloramine-BDD; (d) Dichloramine-MMO; (e) Trichloramine-BDD; (f) Trichloramine-MMO.

The formation of chloramines follows a sequential reaction that starts with the generation of monochloramine (Equation 5.6). This species is the most reactive chloramine and it has been widely used for the disinfection of wastewater [191, 192].

Then, monochloramine can be continuous to react with hypochlorite, favouring the formation of dichloramine (Equation 5.7), and, finally, trichloramine is formed by the reaction between dichloramine and hypochlorite (Equation 5.8). The presence of one or another chloramine will depend mainly on the ratio Cl/N and the pH of the effluent [193]. In this context, hospital urines used in this work present a pH value around 6, and, according to literature, it favours the presence of dichloramine. This agrees with the results obtained during electrolysis and photoelectrolysis at 50 A m^{-2} where dichloramine is the predominant species followed by trichloramine and, finally, monochloramine. At low current densities, the concentration of chloramines is negligible owing to the low concentration of hypochlorite electrogenerated.

Overall, the concentration of chloramines is lower during photoelectrolysis and it can be related to the photoactivation of hypochlorite (Equation 5.15) that decreases its free concentration to form chloramines. Likewise, the low concentration of monochloramine (Figures 5.39a, 5.39b) registered for both anodes can be explained by the photoactivation of this species (Equation 5.21) [194]. In this context, monochloramine can be decomposed in free amine and chlorine radicals by the irradiation of UV light. This also helps to remove ARB from urine since chlorine radical significantly contributes to the disinfection process. The higher the concentration of hypochlorite, the higher the concentration of chloramines and, hence, the higher the concentration of free chlorine radicals during photoelectrolysis. This supports the disinfection results from Figure 5.33 because the concentration of hypochlorite is expected to be higher with MMO anodes and the removal rates are also higher with this anode.

$$NH_2Cl + h\nu \rightarrow NH_2\cdot + Cl\cdot \quad (5.21)$$

Finally, to evaluate the energy requirements of the combined process in comparison with UV disinfection, the specific electric energy (E_{EO}) was calculated by Equations 5.22 and 5.23, where E_{cell} is the cell voltage (V), I the current intensity (kA), t the operation time (h), V the volume (m^3), C_0 and C_f the initial and final bacteria concentration after 1 order of magnitude removal (CFU ml^{-1}), respectively and W_{lamp} the power of the lamp used (kW). This parameter determines the electric energy required

to decrease the population of *K. pneumoniae* by one order of magnitude in a unit volume [195]. The results obtained are plotted in Figure 5.40.

$$E_{EO} = \frac{E_{cell} \cdot I \cdot t}{V \cdot Log\frac{C_0}{C_f}} \quad (5.22)$$

$$E_{EO} = \frac{W_{lamp} \cdot t}{V \cdot Log\frac{C_0}{C_f}} \quad (5.23)$$

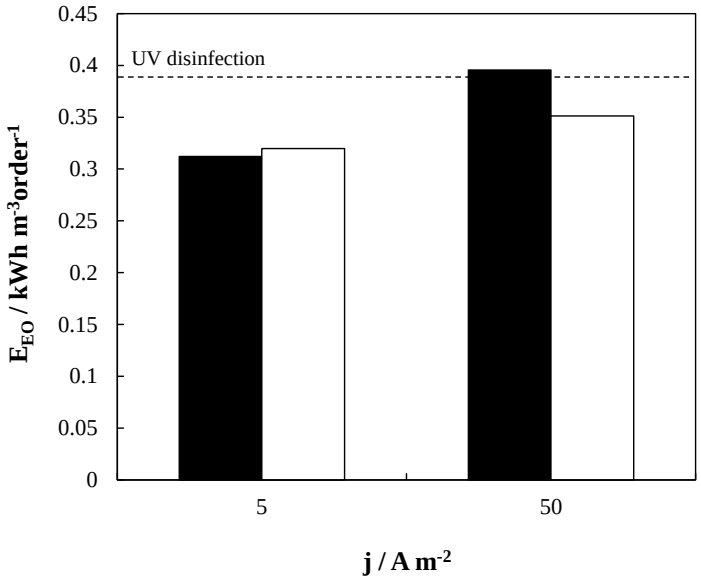

Figure 5.40. Specific electric energy during UV disinfection and photoelectrolysis of hospital urines. Line: UV disinfection; black bars: BDD anode; white bars: MMO anode.

As can be observed, the lowest electric energy resulted in the combined process at low current densities using both BDD and MMO anodes. These results are in line with the synergistic effects found previously, where the highest values resulted when applying 5 A m^{-2}. At 50 A m^{-2}, the electric energy for the process with BDD anodes is slightly higher than that required for the UV disinfection process (0.395 *vs*. 0.389 kWh m^{-3} $order^{-1}$). Nevertheless, the use of MMO anodes at higher current densities leads to lower electric energy.

This reveals that electrolysis improves the efficiencies obtained during the UV disinfection process, decreasing, in turn, the energy requirements. This good performance of the combined process could be explained in terms of the promotion of

free chlorine radicals. However, the use of BDD anodes is limited to their application at lower current densities, whereas MMO anodes can be used for all the current densities studied.

5.4.2. Conclusions

UV disinfection allows to decrease the population of ARB in synthetic hospital urine, but it cannot reach complete disinfection. The irradiation of UV light to urine polluted with *K. pneumoniae* could be limited by the occurrence of bacteria agglomeration or a resistant subpopulation. On the other hand, electrochemical oxidation with BDD and MMO anodes leads to complete removal of ARB from urine when applying 50 A m^{-2}. At 5 A m^{-2}, bacteria removal is negligible because the concentration of disinfectants produced is rather low. The disinfection rate is higher when working with MMO anodes and it can be related to competitive oxidation between bacteria and the organics contained in urine, which seems to be favoured using BDD anodes. Finally, photoelectrolysis enhances single UV disinfection and electrolysis performances for all the current densities tested with BDD and MMO anodes. A more remarkable contribution of UV disinfection is observed at the beginning of the process whereas the electrochemical process has more influence at the end of the treatment. A marked synergistic effect was found when UV disinfection was enhanced by electrolysis at 5 A m^{-2} with BDD and MMO anodes. The use of BDD anodes at 50 A m^{-2} led to antagonistic effects due to the possible competitive degradation between bacteria and organics under these conditions. Regarding energy requirements for single and combined processes, the specific electric energy required for photoelectrolysis at low current densities is lower than that required for UV disinfection. At high current densities, MMO shows lower electric energy whereas the use of BDD anodes leads to a slightly higher value than UV disinfection.

5.5. Electrochemical disinfection of polymicrobial urines

The quick spread of ARB and the exchange of ARGs by pathogenic and opportunistic bacteria have increased hospitalisation lengths and have intensified mortality rates [196]. Disinfection technologies should assure not only the complete removal of microorganisms but also the denaturation of genetic material to avoid HTPs. To the authors' knowledge, research studies are still missing on developing technologies for the treatment of complex hospital effluents with the main aim of preventing the antibiotic resistance spread, removing ARB and ensuring the abatement of ARGs [197].

In this context, this section is focused on testing the microfluidic flow-through reactor and the MIKROZON® cell, working under the optimal operating conditions studied in previous sections, for the disinfection of complex synthetic urines contaminated with several ARB (polymicrobial urines). To reach this global aim, the following partial objectives were stablished:

- A prevalence study to identify the pairs of pathogens causing UTIs in hospitalized patients.
- To evaluate the influence of the reactor employed on the abatement of ARB pairs in hospital urines.
- To evaluate the influence of the reactor employed on the denaturation of DNA and ARGs in polymicrobial hospital urines.

The experimental planification is summarized in Table 5.15.

Table 5.15. Experimental planification for the disinfection of polymicrobial urines.

Exp. Nº	Technology	Reactor	Anode / Cathode	Current density / intensity	Bacterial strains
1	Electrolysis	Microfluidic flow-through reactor	MMO / SS	50 A m^{-2}	*E. faecalis* ATCC 51299 + *K. pneumoniae* ATCC BAA-1705
2					*E. coli* ATCC 35218 + *E. faecalis* ATCC 51299
3					*K. pneumoniae* ATCC BAA-1705 + *E. coli* ATCC 35218

Table 5.15. (Cont.) Experimental planification for the disinfection of polymicrobial urines.

Exp. Nº	Technology	Reactor	Anode / Cathode	Current density / intensity	Bacterial strains
4	Electrolysis	MIKROZON® cell	BDD / BDD	1 A	*E. faecalis* ATCC 51299 + *K. pneumoniae* ATCC BAA-1705
5					*E. coli* ATCC 35218 + *E. faecalis* ATCC 51299
6					*K. pneumoniae* ATCC BAA-1705 + *E. coli* ATCC 35218

To simulate real polymicrobial hospital urines, synthetic urine is intensified with combinations of different ARB. Complex urine 1 (CU1) was intensified with *E. faecalis* and *K. pneumoniae*, complex urine 2 (CU2) was intensified with *E. coli* and *E. faecalis* and, finally, complex urine 3 (CU3) was intensified with *K. pneumoniae* and *E. coli*. To carried out the electrodisinfection experiments, both electrochemical cells are tested under the most suitable operating conditions previously reported in literature [154, 198, 199]. Table 5.16 shows the main design and operational parameters of both reactors tested, considering manufacturer's limitations. The microfluidic flow-through reactor promotes the electrochemical production of chlorine-based disinfectants (mainly chloramines) whereas the MIKROZON® cell is especially designed to produce large amounts of ozone in water with low salinity.

Table 5.16. Design and operational parameters of both reactors tested.

	Microfluidic flow-through	MIKROZON®
Effluent volume	2 dm^3	1 dm^3
Flow rate	160 $dm^3 h^{-1}$	30 $dm^3 h^{-1}$
Current intensity	0.25 A	1 A
Operation time	180 min	180 min
Electric charge	0.42 Ah dm^{-3}	3.87 Ah dm^{-3}
Anode	70/30 IrO_2/Ta_2O_5	BDD
Cathode	SS	BDD

Bacteria counts were performed by an indirect impedance method using a μ-Trac® 4200 system as described in section 4.4.6.2. (i), using a selective nutrient media for each bacterium. However, there is no selective nutrient media for *K. pneumoniae* in which the growth of *E. coli* and *E. faecalis* is prevented. For this reason, the count of *K. pneumoniae* ATCC BAA-1705 is carried out using the membrane filtration technique described in section 4.4.6.2. (ii).

5.5.1. Occurrence of pairs of pathogens in real hospital urines from CHUA

The occurrence of pathogens in a real environment has been firstly analysed based on data supplied by the Microbiology and Parasitology Service from the University Hospital Complex of Albacete, Spain (CHUA) as model of sanitary facility. A previous study about the prevalence of a unique pathogen causing UTIs has been previously commented in section 5.1 to describe the influence of hospital units, patients' gender and kind of pathogens, including UTIs caused by carbapenem-resistant Enterobacteriaceae and methicillin-resistant *S. aureus* [200]. Additionally, 581 (13.05 %) were positive urines within two or more pathogens from the total 4453 positive urines registered. Hence, Figure 5.41 shows the most representative pairs among bacteria and/or bacteria and yeasts found in the monitored positive urines since the presence of two pathogens at the same time represented the 96.73 % within the total 13.05 %.

As can be observed, the most prevalent pairs of pathogens contained the gram-negative, facultative anaerobic, uropathogenic *Escherichia coli (E. coli)* since this bacterium has been widely reported in literature to cause UTIs [22, 31]. The highest presence of pairs corresponds to *E. coli* and *Enterococcus faecalis (E. faecalis)* found in 57 of the total 581 real hospital urines with a prevalence percentage of 9.8 %, *E. coli* and *Klebsiella pneumoniae (K. pneumoniae)* found in 41 complex positive urines (7.1 %), and *E. coli* and *Proteus mirabilis (P. mirabilis)*, positive in 24 complex urines, which represent a prevalence percentage of 4.1 %. Regarding other important pairs of pathogens, *Pseudomonas aeruginosa (P. aeruginosa)* and *E. faecalis* are observed to

represent a prevalence percentage of 3.1 %. Likewise, not only *E. faecalis* but also *K. pneumoniae* are also recognized for causing UTIs although in a lesser presence ratio than *E. coli* and their combination with other bacteria are observed in prevalence percentages ranging from 0.3-0.5 % [32]. Finally, the combination of different yeasts from genus of unicellular fungi as *Candida* with other gram-positive bacteria from genus of lactic acid bacteria (LAB) as *Enterococcus* are also common causes of UTIs, with prevalence presence percentages in the range of 0.3-0.9 %.

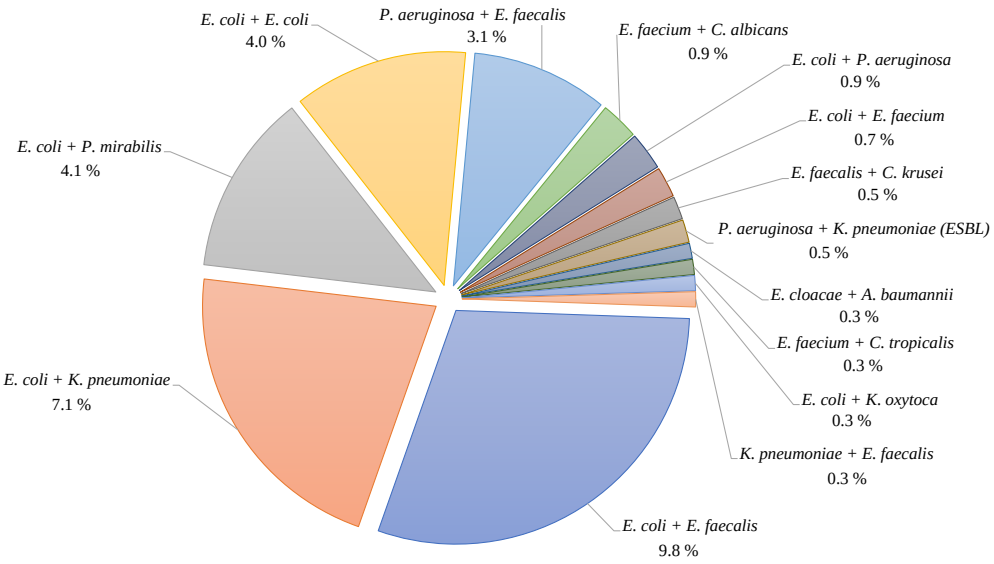

Figure 5.41. Most prevalent pairs of microorganisms presented in patients suffering from urinary tract infections at CHUA within the period 2014-2018.

5.5.2. Electrochemical disinfection of complex synthetic hospital urines

The most prevalent pairs of bacteria depicted from Figure 5.41, *E. coli* and *E. faecalis* and *K. pneumoniae* and *E. coli* were selected as models of pairs of pathogens, including *E. faecalis* and *K. pneumoniae* due to their high environmental and sanitary risks [20, 201, 202]. The electrochemical disinfection of synthetic urines intensified with the previous mentioned models of bacteria pairs was studied. A microfluidic flow-

through reactor and a MIKROZON® cell were tested in this study, and their operational characteristics were properly detailed in Table 5.16. The evolution of ARB as function of the experimental time and the applied electric charge during the electrochemical disinfection of complex synthetic urines is shown in Figure 5.42. Different grey background colours are shown, corresponding to the different disinfection kinetic zones (I, II, and III) which will be discussed below.

Results show that it was possible to attain removal ratios higher than 99.99 % (4-logs) after the 180 min treatment process using the microfluidic flow-through reactor by applying 50 A m^{-2} (Figure 5.42a). Specifically, the treatment of CU1 showed a *K. pneumoniae* removal of almost 5-logs while the process reached 6.5-logs ARB removal for *E. faecalis*. The combination of *E. coli* and *E. faecalis* is represented by CU2. *E. coli* concentration was decreased in almost 6-logs whereas *E. faecalis* showed a similar profile than the one observed in CU1, reducing its concentration in 6.4-logs. Finally, CU3 comprises the intensification of synthetic urine with *K. pneumoniae* and *E. coli*. These both ARB showed a similar behaviour, achieving 5.7 and 5.4-logs reductions for *K. pneumoniae* and *E. coli*, respectively. Hence, the treatment of complex urines led to ARB depletion logarithmic ranges from 6.4 to 6.5, 4.8 to 5.7 and 5.4 to 5.8 for *E. faecalis, K. pneumoniae* and *E. coli*, respectively. Conversely, a complete disinfection (7-logs) was reached for every ARB pair tested within the different matrixes studied when working with the MIKROZON® cell at 1 A (Figure 5.42b). Although a complete disinfection was attained for every ARB tested, different trends can be observed at an initial stage of the experiments up to 30 min. At this time, the processes reached removal ratios in the range of 1.4 to 2.2 logs for *E. faecalis*, while *E. coli* and *K. pneumoniae* exhibited smaller decreases, ranging from 1.1 to 0.6 logs for *E. coli* and 0.5-logs for *K. pneumoniae*.

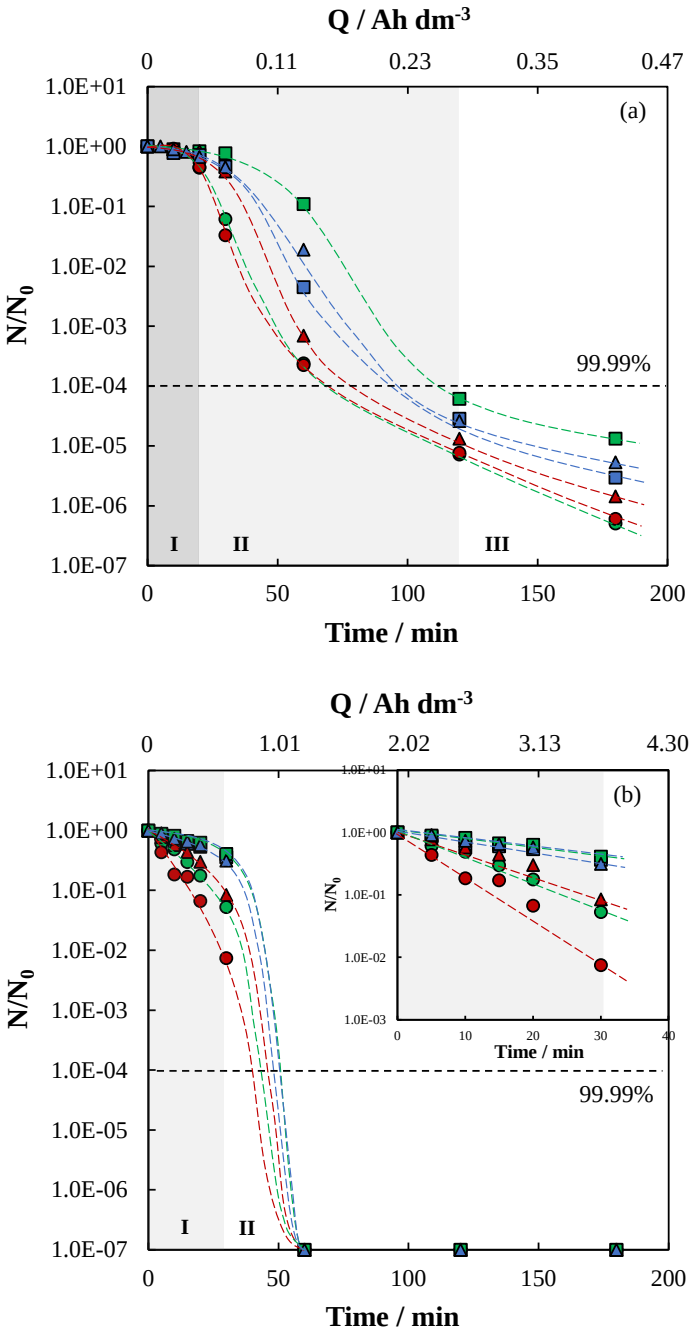

Figure 5.42. Evolution of ARB as function of the experimental time and the applied electric charge during the electrochemical disinfection of complex synthetic hospital urines. (a) microfluidic flow-through reactor; (b) MIKROZON® cell. (●) *E. faecalis*; (■) *K. pneumoniae*; (▲) *E. coli*; green symbols: CU1; red symbols: CU2; blue symbols: CU3. N_0: 10^7 CFU mL^{-1}.

Nevertheless, disinfection efficiencies were observed to significantly vary depending on the electrochemical reactor used due to the individual operating conditions tested. MIKROZON® cell exhibited a complete disinfection after passing an applied electric charge of 1 Ah dm^{-3} whereas an almost complete disinfection (6-logs) was only attained during the treatment of CU2 using the microfluidic flow-through reactor for 0.4 Ah dm^{-3}. These results reveal that the use of microfluidic flow-through reactor leads to higher disinfection efficiencies since the removal of microorganisms with the MIKROZON® reactor at applied electric charges around 0.4 Ah dm^{-3} is negligible. Nonetheless, it is important to bear in mind that the operating conditions tested (current intensity and electrode material) are different for each device.

A more efficient electrochemical disinfection process does not necessarily mean that it is faster because there can exist mass transfer limitations of the microorganisms to the electrode surfaces [67]. Regarding the disinfection kinetics of the process, different grey background-colored zones can be appreciated in Figure 5.42 using both reactors. Experiments carried out with the microfluidic flow-through reactor exhibited three different zones: 1) an initial phase (Zone I), from 0 to 20 min, where the concentration of ARB did not undergo significant changes; 2) a subsequent intermediate step (Zone II), from 20 to 120 min, where the decrease in the concentration of ARB was noteworthy; 3) a final zone (Zone III), from 120 to 180 min, where the concentration of ARB decreased with a marked smoother velocity. On the other hand, only two zones can be observed when working with the MIKROZON® cell: 1) Zone I from 0 to 30 min, where ARB concentration barely varied or slightly decreased, 2) Zone II from 30 to 60 min, where the disinfection rate for every ARB tested increased drastically. For comparison purposes, experimental data were fitted to a first order kinetic model and the resulting kinetic constants of every ARB tested in the different zones observed are presented in Table 5.17.

As can be observed, the same ARB showed quite similar kinetics constants using the same electrochemical reactor despite the complex urine treated (CU1, CU2, or CU3). Results showed mean values for *E. faecalis* of 0.0340 min^{-1} (Zone I), 0.1060 min^{-1} (Zone II) and 0.0433 min^{-1} (Zone III) with the microfluidic flow-through reactor

whereas these values significantly increased up to 0.1212 min^{-1} (Zone I) and 0.4066 min^{-1} (Zone II) when using the MIKROZON® cell. On the other hand, *K. pneumoniae* and *E. coli* showed similar kinetics constants under the same operational conditions which could be due to these ARB are gram-negative bacteria and are classified within the same bacterial family (Enterobacteriaceae). Overall, both reactors exhibit the highest disinfection kinetics for *E. faecalis* in Zone I, which corresponds with the highest disinfection rate of this ARB in the entire disinfection process. This could be justified by the differences of gram-positive (*E. faecalis*) and gram-negative (*K. pneumoniae* and *E. coli*) bacteria related to the structure and organo-chemical composition of their cell membranes [203]. Particularly, gram-positive bacteria are more affected by chemical treatments, while gram-negative bacteria are more susceptible to physical disinfection technologies [204, 205]. These results suggest that the disinfectant species electrogenerated could have a significant influence on the removal of ARB during the electrochemical processes.

Table 5.17. Kinetic constants for the disinfection tests with the microfluidic flow-through reactor and the MIKROZON® cell.

	ARB	$k_{Zone\ I}$ 0-20 min (min^{-1})	R^2	$k_{Zone\ II}$ 20-120 min (min^{-1})	R^2	$k_{Zone\ III}$ 120-180 min (min^{-1})	R^2
Microfluidic flow-through reactor	*E. faecalis* (CU1)	0.0348	0.9014	0.1076	0.9159	0.0443	1
	E. faecalis (CU2)	0.0332	0.8741	0.1043	0.9056	0.0423	1
	K. pneumoniae (CU1)	0.0092	0.9963	0.0985	0.9655	0.0254	1
	K. pneumoniae (CU3)	0.0182	0.9645	0.1044	0.9810	0.0337	1
	E. coli (CU2)	0.0087	0.9935	0.1132	0.9299	0.0370	1
	E. coli (CU3)	0.0163	0.9229	0.1042	0.9958	0.0265	1
	ARB	$k_{Zone\ I}$ 0-30 min (min^{-1})	R^2	$k_{Zone\ II}$ 30-60 min (min^{-1})			R^2
MIKROZON® cell	*E. faecalis* (CU1)	0.0915	0.9918	0.4392			1
	E. faecalis (CU2)	0.1508	0.9864	0.3739			1
	K. pneumoniae (CU1)	0.0337	0.9943	0.5034			1
	K. pneumoniae (CU3)	0.0272	0.9853	0.5073			1
	E. coli (CU2)	0.0713	0.9702	0.4547			1
	E. coli (CU3)	0.0338	0.9748	0.4987			1

Previous works have demonstrated the generation of hypochlorite and inorganic chloramines as the main disinfectant species during the electrochemical disinfection of synthetic hospital urines with the microfluidic flow-through reactor at 50 A m^{-2} [199]. This work demonstrated that the microfluidic flow-through reactor enhanced the generation of chloramines over hypochlorite under the conditions tested. Likewise, the MIKROZON® cell is a commercial solid-electrolyte electrolyzer which has been specially designed for promoting the production of ozone during water electrolysis [62]. Our previous works reported to maximize the generation of ozone during the electrochemical disinfection of synthetic hospital urines at 1 A [198].

In this context, Figure 5.43 shows the evolution of the main disinfectant species (hypochlorite, chloramines and ozone) electrogenerated with the operation time using a microfluidic flow-through reactor (Figure 5.43a) and a MIKROZON® cell (Figure 5.43b).

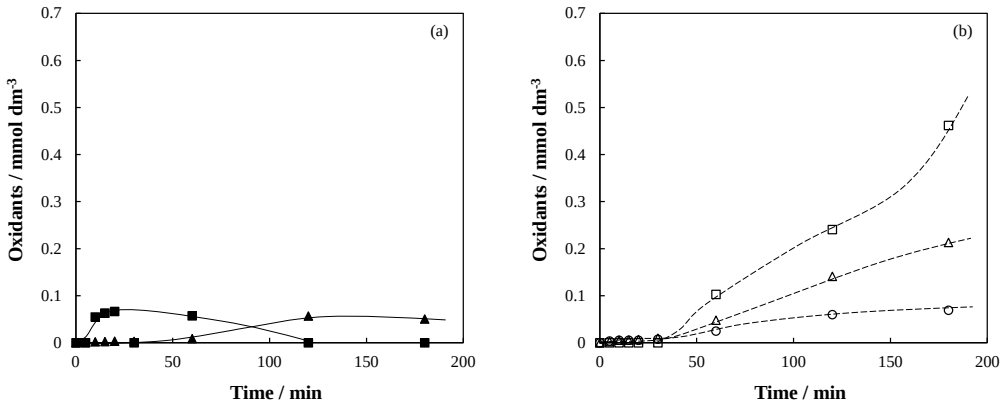

Figure 5.43. Time course of the molar concentration of disinfectant species electrogenerated during the electrochemical disinfection of complex synthetic hospital urines, using a microfluidic flow-through reactor (a) or a MIKROZON® cell (b). (■, □) Cl-Hypochlorite; (▲, Δ) Cl-Chloramines; (●, ○) Ozone.

It is important to highlight that the monitored concentration of oxidants is referred to those that have not reacted yet since higher amounts of these species are expected to have been generated during the electrochemical disinfection [99, 138].

As can be observed, the remained concentration in the bulk of hypochlorite increased sharply to 0.07 mmol dm^{-3} from the beginning of the experiment until 20 min

(0.04 Ah dm^{-3}), using the microfluidic flow-through reactor. After this time, hypochlorite concentration started to decrease gently towards its non-detection from 120 min (0.28 Ah dm^{-3}) until the end of the experiment. Hence, hypochlorite showed a typical profile of an intermediate compound that has been generated and consumed along the experiments. Opposite, the monitored hypochlorite concentration was lower than 0.1 mmol dm^{-3} below 60 min (1.21 Ah dm^{-3}) when the complete disinfection process was achieved (Figure 5.42b) and after that experimental time, hypochlorite concentration continuously increased up to 0.46 mmol dm^{-3} at 180 min (3.87 Ah dm^{-3}) when working with the MIKROZON® cell. The maximum values of hypochlorite were about 6.5 times higher than those reached with the microfluidic flow-through reactor. Hypochlorite is a very reactive species that can compete for the killing of microorganisms, the degradation of urine natural organic compounds or the evolution of other chlorine-based species, such as chloramines [186]. Chloramines are well known to be generated from the chemical reaction between hypochlorite and ammonium ions which are naturally contained in the urine matrix and/or coming from the electrochemical oxidation of urine natural organic compounds [154]. Hence, the remained concentration of chloramines was almost negligible during the beginning of the treatment (30 min (0.07 Ah dm^{-3})) using the microfluidic flow-through reactor and after that, their concentration increased smoothly to a constant value of 0.06 mmol dm^{-3} from 120 min (0.28 Ah dm^{-3}). This fact supports the decrease in the hypochlorite concentration from 20 min (0.04 Ah dm^{-3}), promoting the generation of chloramines with the microfluidic flow-through reactor [199]. Likewise, the same profile was observed for chloramines using the MIKROZON® cell although the concentration of chloramines did not remain constant but increased from 60 min (1.21 Ah dm^{-3}) (complete disinfection) up to 3.5 times higher (0.21 mmol dm^{-3} at 180 min (3.87 Ah dm^{-3})) than with the microfluidic flow-through reactor. Regarding the monitorization of ozone in the bulk solution, null concentrations were detected when working with the microfluidic flow-through reactor. Likewise, the concentration of ozone was almost negligible when working with the MIKROZON® cell at an early stage of 30 min. However, the concentration of ozone monitored increases from 30 to 180 min, reaching

maximum values of 0.069 mmol dm^{-3}. Furthermore, it is important to remark that ozone is a very reactive species (E^0: 2.07 V), and the measured concentration is not referred to total ozone electrogenerated but to free ozone that has not reacted in the effluent yet. Additionally, the composition and pH of the supporting electrolyte has a paramount importance on the efficiency of ozone production. Acidic media favours ozone production, but the presence of species which can become scavengers decreases the overall efficiency of the process. Hence, it is expected that higher concentrations of ozone had been generated and wasted in the disinfection process [206, 207].

5.5.3. Electrochemical denaturation of DNA and ARGs

The production of disinfectant species such as hypochlorite, chloramines or ozone may contribute to the removal of ARB by different mechanisms such as damages to membrane cells and DNA, inhibition of enzyme activity essential for the growth or injuries to membrane transport capacity [208, 209]. To shed light about the disinfection mechanisms that may take place depending on the electrochemical reactor configuration and operational conditions tested, the logarithmic reduction values of DNA were calculated using the Equation 5.24. $DNA_{initial}$ corresponds to the total amount of DNA measured in ng μL^{-1} for total ARB present in each experiment before the treatment, whereas DNA_{final} is the total amount of DNA after the treatment (180 min). The closer the results of Equation 5.24 are to 0, the lower the DNA reduction. Results of the logarithmic reduction of DNA for each complex urine tested are summarized in Table 5.18.

$$\text{Log reduction of DNA} = \log_{10}\left(\frac{DNA_{initial}}{DNA_{final}}\right) \quad (5.24)$$

Results of the microfluidic flow-through reactor showed a high variability in the calculated values of DNA reduction, ranging from 0.65 for the CU2 (*E. coli* + *E. faecalis*) to 0.15 for the CU3 (*K. pneumoniae* + *E. coli*). This fact may reflect that the DNA from *K. pneumoniae* is less easy to be degraded than DNA from *E. faecalis* or *E. coli*. Conversely, the MIKROZON® cell exhibited the highest DNA depletion capacity

with a mean DNA reduction of 0.79-logs for the three experiments. Likewise, this cell offered a similar behaviour in the removal of DNA with an average error rate with respect to the mean value of 7.1 %. Specifically, 0.85, 0.82 and 0.70-logs were obtained for CU2 (*E. coli* + *E. faecalis*), CU1 (*E. faecalis* + *K. pneumoniae*) and CU3 (*K. pneumoniae* + *E. coli*), respectively. Previous studies have investigated the effects of different disinfectant species (based on chlorine or ozone) on the removal of DNA, proving the major capacity of the combination of ozone and chlorine derived species [198]. This fact may explain the differences observed in the DNA reduction between both electrochemical reactors which can be attributed to the distinct disinfectant species involved (Figure 5.43). These results agree the previous findings reported by Long et al. [162] during the electrochemical disinfection of synthetic solutions with BDD anodes where the DNA remained constant during the elimination of *E. coli*.

Table 5.18. Logarithmic reduction of DNA in the electrochemical disinfection of complex synthetic hospital urines, using a microfluidic flow-through reactor or a MIKROZON® cell.

	ARB pairs in the complex synthetic hospital urine	**Microfluidic flow-through reactor**	**MIKROZON® cell**
CU1	*E. faecalis* + *K. pneumoniae*	0.41	0.82
CU2	*E. coli* + *E. faecalis*	0.65	0.85
CU3	*K. pneumoniae* + *E. coli*	0.15	0.70

Furthermore, the analysis of ARGs is necessary to control the antibiotic resistance spread into the aquatic environment. Infections caused by *E. faecalis* strains are alternatively treated with erythromycin, from the class of macrolide antibiotics [210]. The gene *erm*B, contained in the *E. faecalis* ATCC 51299 strain, encodes a ribosomal methylase that confers resistance to macrolides [211]. Conversely, *K. pneumoniae* isolates producing carbapenemase are able to hydrolyze carbapenems and represent the most common cause of carbapenem resistance in *Enterobacteriaceae* [212, 213]. *The* bla_{KPC} *gene, harbored in the K. pneumoniae* ATCC BAA-1705 strain, plays a crucial role in the dissemination of antibiotic resistant strains [214]. Similarly, one of the most common producers of extended spectrum beta lactamases (ESBLs) is *E. coli* [215]. There are several types of ESBL such as TEM, SHV or CTX genes that

encodes resistance against beta lactam antibiotics [216]. Specifically, *bla*$_{TEM}$ gene is present in the *E. coli* ATCC 35218 strain. Hence, the performance of the electrochemical reactors on the removal of *erm*B, *bla*$_{KPC}$ and *bla*$_{TEM}$ genes will be studied during the disinfection process.

Standard curves of the ARGs tested were determined based on the methodology reported by Polo-López et al. to correlate the cycle threshold (C_T) with the concentration of ARGs [217]. These standard curves were calculated by relating the cycle thresholds (C_T) obtained in the qPCR with the ARGs concentration used. The different concentration points were prepared through 10-fold serial dilutions of the corresponding genes. Figure 5.44 shows the linear standard curves for *erm*B, *bla*$_{KPC}$ and *bla*$_{TEM}$ genes.

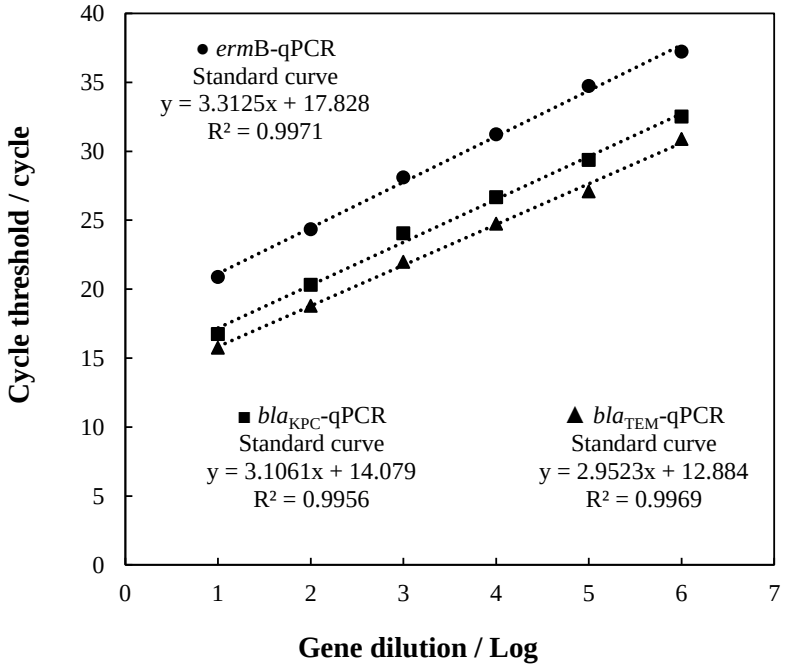

Figure 5.44. Standard curves of the relationship between cycle threshold (C_T) and the concentration of *erm*B, *bla*$_{KPC}$ and *bla*$_{TEM}$ genes for qPCR.

As can be observed, the C_T values can be related to the relative logarithmic reduction of ARGs. Results show linear profiles for every ARG tested. Specifically, the standard curves y = 3.3125·x + 17.828, y = 3.1061·x + 14.079 and y = 2.9523·x +

12.884, with high correlation coefficients, 0.9971, 0.9956 and 0.9969 were obtained for *erm*B, bla_{KPC} and bla_{TEM} genes, respectively. This implies that every increment in the cycle threshold of 3.3125, 3.1061 and 2.9523 correspond to one logarithmic reduction in the concentration of *erm*B, bla_{KPC} and bla_{TEM} genes, respectively.

In this context, Figure 5.45 plots the initial (0 min) and final (180 min) cycle threshold (C_T) values obtained for each ARG analyzed depending on the experimental test carried out and the electrochemical reactor used. Consequently, two ARGs were analyzed in each experiment related to the ARB pairs tested: CU1 (*erm*B and bla_{KPC} genes), CU2 (bla_{TEM} and *erm*B genes) and CU3 (bla_{KPC} and bla_{TEM} genes). It is important to remark that the qPCR was employed to quantify the removal efficiency of ARGs in complex synthetic hospital urines. The qPCR assay measures the number of cycles required for the fluorescent signal to cross the selected threshold, although the amount of the target ARG is inversely proportional to the cycle threshold (C_T).

Results show that the degradation of ARGs was not influenced by the ARB pairs studied since for the *erm*B, bla_{KPC} and bla_{TEM} genes their cycles varied below 1.52, 3.27 and 4.05, respectively. However, it is observed that the configuration and operational conditions of the electrochemical reactors employed have a significant influence on the degradation of ARGs. The amount of *erm*B, bla_{KPC} and bla_{TEM} genes was mostly increased using the microfluidic flow-through reactor since the mean number of cycles slightly decreased from 23.09 to 21.77, from 20.53 to 19.37 and from 14.02 to 13.39, respectively. Conversely, the use of the MIKROZON® cell clearly increased the cycle threshold values of the final samples (180 min) for each gene tested, which implies a decrease in the amount of ARGs. Specifically, mean cycle threshold increments of 10.70, 12.96 and 11.68 were obtained for *erm*B, bla_{KPC} and bla_{TEM} genes, respectively.

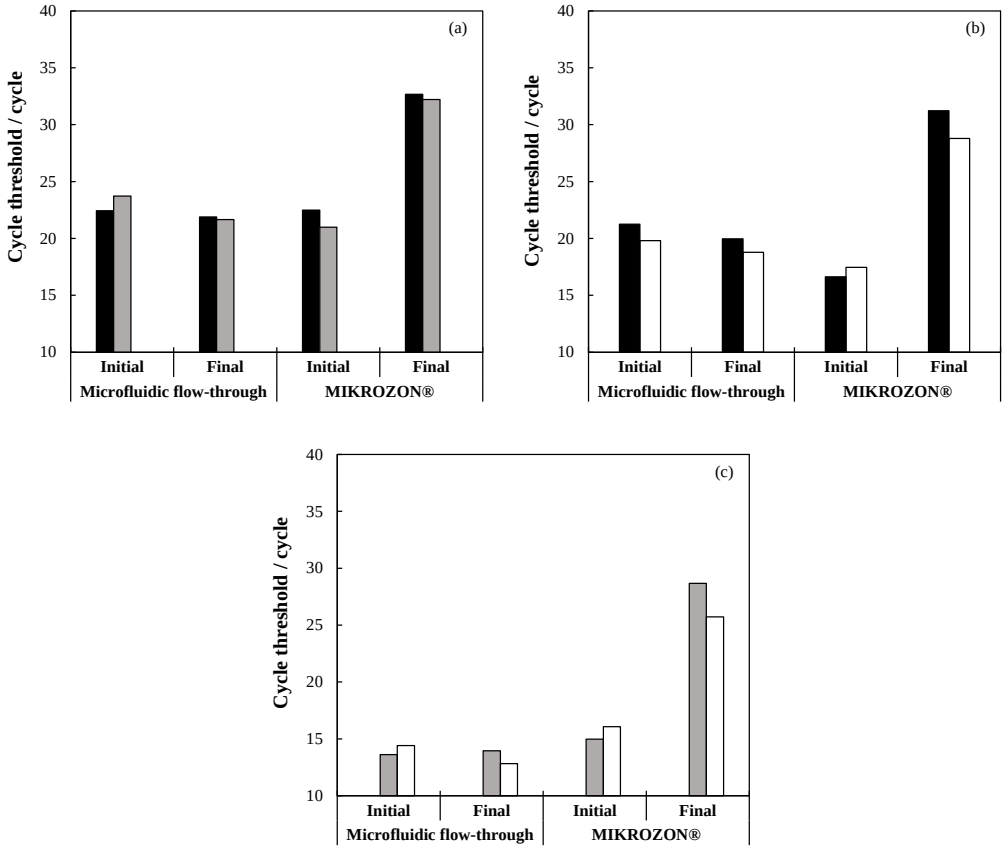

Figure 5.45. Cycle threshold detection of ARGs during the disinfection of complex synthetic hospital urines, using a microfluidic flow-through reactor or a MIKROZON® cell. ARGs: *erm*B gene (a); bla_{KPC} gene (b); bla_{TEM} gene (c). (■) CU1: *E. faecalis* + *K. pneumoniae*; (■) CU2: *E. coli* + *E. faecalis*; (□) CU3: *K. pneumoniae* + *E. coli*.

To correlate the C_T values obtained in Figure 5.45 with the logarithmic removal of ARGs, it was proposed the Equation 5.25. $C_{T,\,final}$ and $C_{T,\,initial}$ represents the final and initial C_T values (cycles) of every ARG tested, respectively, and the $Gradient_{standard\ curve}$ is the slope (cycles/log) that has been previously determined for every ARG in Figure 5.43. Negative values obtained from Equation 5.25 would correspond to an increment in the concentration of ARGs, meanwhile, the further the positive values move away from zero, the greater the reduction in ARGs concentration.

$$\text{Log removal of ARGs} = \frac{C_{T,\,final} - C_{T,\,initial}}{Gradient_{standard\ curve}} \qquad (5.25)$$

According to Equation 5.25, Table 5.19 summarizes the results obtained for ARGs abatement after the electrochemical disinfection at 180 min, depending on the electrochemical reactor tested.

Table 5.19. Logarithmic removal of ARGs after 180 min of electrochemical disinfection of complex synthetic hospital urines.

Complex hospital urines	Electrochemical reactor configuration	*erm*B	bla_{KPC}	bla_{TEM}
CU1: *E. Faecalis* + *K. pneumoniae*	Microfluidic flow-through	-0.17	-0.41	-
CU2: *E. coli* + E. faecalis		-0.63	-	0.11
CU3: *K. pneumoniae* + *E. coli*		-	-0.33	-0.53
CU1: *E. Faecalis* + *K. pneumoniae*	MIKROZON®	3.07	4.70	-
CU2: *E. coli* + E. faecalis		3.39	-	4.64
CU3: *K. pneumoniae* + *E. coli*		-	3.65	3.27

Despite the experiment tested, the microfluidic flow-through reactor showed a mean increase in the ARGs concentration in the following order: *erm*B (-0.40-log) > bla_{KPC} (-0.37-log) > bla_{TEM} (-0.21-log), promoting a mean increment of -0.33-log for all ARGs tested. This fact may be supported by previous studies that have demonstrated that an insufficient chlorine dosage can increase the amount of ARGs [218, 219]. Specifically, Wang et al. studied the effects of chlorine in bacterial inactivation and ARGs removal on phosphate buffer saline (PBS) [220]. They concluded that low chlorine dosages (< 0.0141 mmol dm^{-3}) could enhance the conjugation transfer frequency, promoting the increment in the amount of ARGs. Hence, it was previously described in Figure 5.42a that the maximum chlorine concentration that remained in the bulk solution were below 0.1 mmol dm^{-3}, using the microfluidic flow-through reactor. Conversely, the MIKROZON® cell reached a mean decrease ranked as follows: bla_{KPC} (4.18-logs) > bla_{TEM} (3.96-logs) > *erm*B (3.23-logs), offering a mean depletion of 3.77-logs for all ARGs tested. In literature, chlorine has been reported that may lead to initially attack proteins and peptidoglycan bound to the cell wall and the cell membrane and, subsequently, penetrate into the cell wall to reach cytoplasm and react with nucleic acids [221, 222]. Additionally, not only chlorine but also ozone has been recently

reported for its ability to destroy ARGs [223-225]. Ozone reacts with bacterial functional groups, such as amines or amino acids, and also attacks proteins, peptidoglycan and liposaccharides in the cell envelope [226, 227]. Stange et al. studied a comparative removal of ARB (*E. coli* and *Enterococcus faecium*) and ARGs (*tet*A, *amp*C, *van*A and *erm*B) during chlorination and ozonation [222]. They observed similar inactivation rates for ARB (5-logs) and ARGs (4.3-4.6 logs) when using 0.02 mmol dm^{-3} of ozone for 5 min. However, dosages of 0.014 mmol dm^{-3} of chorine for a contact time of 30 min resulted in an ARB depletion in the range of 3.8-5.6 logs and an incomplete degradation of ARGs (0.8-2.8 logs). Hence, the cocktail of oxidants not only of chlorine species (with maximum remained concentrations of 0.46 mmol dm^{-3} Cl-ClO^- and 0.21 mmol dm^{-3} Cl-NH_xCl_y) but also ozone (with maximum remained concentrations of 0.08 mmol dm^{-3}) generated when using the MIKROZON® cell as detailed in Figure 5.42b, may contribute to the significant ARGs depletion.

To gain insight into the mechanisms for ARB and ARGs destruction during the disinfection of complex urines with different electrochemical reactors, the evolution of microorganisms' morphology was examined by scanning electron micrographs (SEM). Figure 5.46 shows images of the bacteria studied at the beginning and the end of the electrochemical treatment of complex urines with the different reactors employed.

Initial samples images (Figures 5.46a, 5.46b, 5.46c) exhibited smooth and intact cell membranes of the three bacteria. As can be observed, *E. coli* and *K. pneumoniae* are rod-shaped bacteria, while *E. faecalis* presents a coccus-shaped morphology. Final samples images obtained after the treatment with the microfluidic flow-through reactor (Figures 5.46d, 5.46e, 5.46f) showed that cell walls wrinkled with small pits and bulges since this reactor did not achieve a complete disinfection in any of the three ARB combinations studied. Furthermore, it could be seen some intracellular materials that may come from the release of cell lysis, although, there was apparently no cell membrane rupture observed.

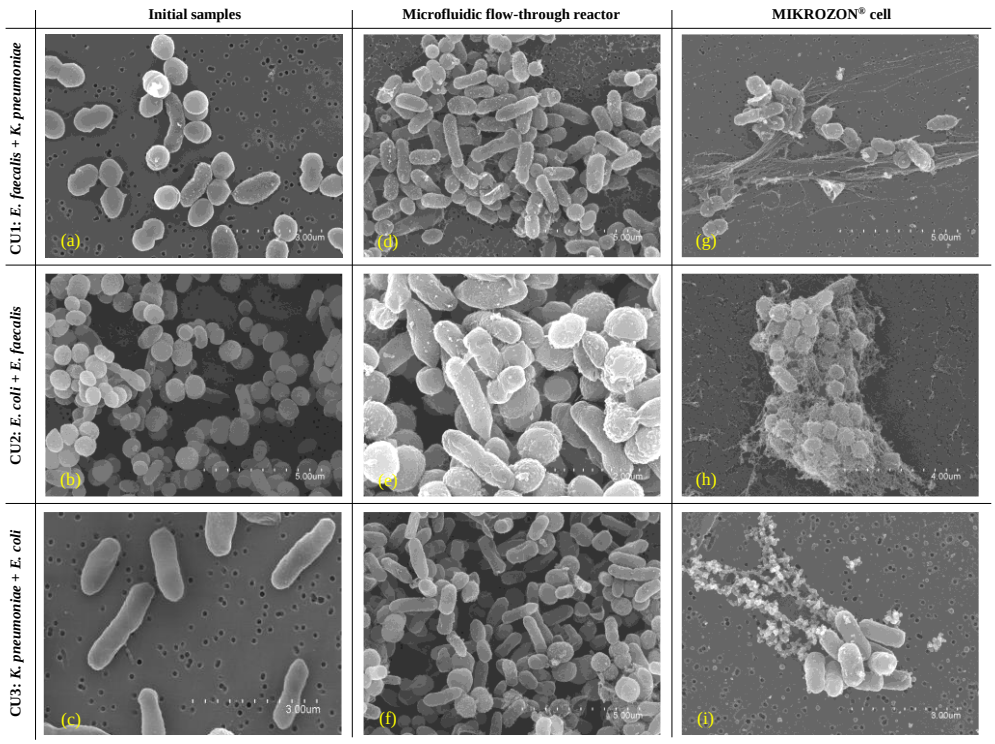

Figure 5.46. Scanning electron micrographs of ARB presented in the disinfection tests carried out with different electrochemical reactors.

Opposite to that, the MIKROZON® cell induced more severe damages in the cell walls, resulting in the integrity loss of bacterial structures. Subsequently, it affected the membrane permeability, intracellular chemical environment and the physiological function, leading to the leakage of cytoplasm [228]. The leakage of cytoplasm may lead to bond cells as it was previously reported by Li et al., where they explained the morphological changes observed in cell structures after ozonation, chlorination and monochloramination disinfection [155]. This fact may be observed in figures 5.46g, 5.46h, 5.46i where cells were bonded to each other after the treatment using the MIKROZON® cell. Thereby, the SEM analyses demonstrate that the treatment of complex hospital urines with the MIKROZON® cell under the operation conditions recommended by the manufacturer has a major capacity than the microfluidic flow-through reactor to cause the cell membrane rupture, resulting in faster killing of ARB and higher both DNA damage and ARGs abatement. This can be directly attributed to

the nature and amount of the electrogenerated disinfectants during the treatment since the microfluidic flow-through reactor promotes the generation of chlorine-based species whereas the MIKROZON® also favours the electrochemical production of large amounts of ozone [198].

5.5.4. Conclusions

The following conclusions can be drawn from this work:

- The most prevalent pairs of bacteria which causes complex Urinary Tract Infections in patients from the University Hospital Complex of Albacete (Spain) were *E. coli* and *E. faecalis* within a 9.8 %, followed by *E. coli* and *K. pneumoniae* with 7.1 %.
- During the disinfection of complex hospital urines, the microfluidic flow-through reactor achieved removal rates between 5 and 6 logs after 180 min whereas the MIKROZON® cell reached the total disinfection (7 logs) after 60 min. However, the microfluidic flow-through reactor could be said to achieve up to one order of magnitude higher disinfection efficiencies than the MIKROZON® cell, attending to the applied electric charge needed to reach a similar disinfection removal.
- The electrogeneration of hypochlorite and chloramines as the main disinfectant species was observed when working with the microfluidic flow-through reactor, reaching maximum values in the bulk solution of 0.07 mmol dm^{-3} and 0.06 mmol dm^{-3}, respectively. The MIKROZON® cell, which was designed to promote the generation of ozone, achieved maximum concentrations remained in the solution of 0.46 mmol dm^{-3}, 0.21 mmol dm^{-3} and 0.07 mmol dm^{-3} for hypochlorite, chloramines and ozone, respectively.
- The microfluidic flow-through reactor showed a slight increment in the quantity of all ARGs tested which could be explained by the lowest chlorine dosages remained in solution. Further research should be done to study the

efficiency of the microfluidic flow-through reactor on the removal of ARB and ARGs using harsher operational conditions. Conversely, the MIKROZON® cell reached a mean decrease in ARGs ranked as follows: bla_{KPC} (4.18-logs) > bla_{TEM} (3.96-logs) > *erm*B (3.23-logs), offering a mean depletion of 3.77-logs for all ARGs tested.

- SEM images confirmed the complete disinfection attained using the MIKROZON® cell, where severe damages were induced in the cell walls, resulting in the integrity loss of bacterial structures. Hence, this electro-ozonizer could be consider as a promising cell to attain significant reductions in the concentration of ARB and ARGs, avoiding HTPs in sanitary effluents.

5.6. Bibliography

[1] K.K.-W. To, I.F.-N. Hung, J.D. Ip, A.W.-H. Chu, W.-M. Chan, A.R. Tam, C.H.-Y. Fong, S. Yuan, H.-W. Tsoi, A.C.-K. Ng, COVID-19 re-infection by a phylogenetically distinct SARS-coronavirus-2 strain confirmed by whole genome sequencing, Clin. Infect. Dis., (2020).

[2] E. Mahase, Covid-19: What have we learnt about the new variant in the UK?, British Medical Journal Publishing Group, 2020.

[3] R.J. Fair, Y. Tor, Antibiotics and bacterial resistance in the 21st century, Perspect Medicin Chem, 6 (2014) 25-64.

[4] A.A. Medeiros, Evolution and dissemination of β-lactamases accelerated by generations of β-lactam antibiotics, Clin. Infect. Dis., 24 (1997) S19-S45.

[5] W. Sneader, Drug discovery: a history, John Wiley & Sons2005.

[6] A.M. Queenan, K. Bush, Carbapenemases: The versatile β-lactamases, Clinical Microbiology Reviews, 20 (2007) 440-458.

[7] G. Patel, R.A. Bonomo, Status report on carbapenemases: challenges and prospects, Expert review of anti-infective therapy, 9 (2011) 555-570.

[8] M. Delgado-Valverde, J. Sojo-Dorado, Á. Pascual, J. Rodríguez-Baño, Clinical management of infections caused by multidrug-resistant Enterobacteriaceae, Therapeutic advances in infectious disease, 1 (2013) 49-69.

[9] R. Cantón, M. Akóva, Y. Carmeli, C.G. Giske, Y. Glupczynski, M. Gniadkowski, D.M. Livermore, V. Miriagou, T. Naas, G.M. Rossolini, Ø. Samuelsen, H. Seifert, N. Woodford, P. Nordmann, L. Poirel, P. Bogaerts, S. Navon-Venezia, G. Cornaglia, Rapid evolution and spread of carbapenemases among Enterobacteriaceae in Europe, Clin. Microbiol. Infect., 18 (2012) 413-431.

[10] O. Tenaillon, D. Skurnik, B. Picard, E. Denamur, The population genetics of commensal Escherichia coli, Nat. Rev. Microbiol., 8 (2010) 207-217.

[11] J.M. Rangel, P.H. Sparling, C. Crowe, P.M. Griffin, D.L. Swerdlow, Epidemiology of Escherichia coli O157:H7 outbreaks, United States, 1982-2002, Emerg. Infect. Dis., 11 (2005) 603-609.

[12] F. Cruz-López, L. Villarreal-Treviño, A. Camacho-Ortiz, R. Morfín-Otero, S. Flores-Treviño, E. Garza-González, Acquired Genetic Elements that Contribute to Antimicrobial Resistance in Frequent Gram-Negative Causative Agents of Healthcare-Associated Infections, Am. J. Med. Sci., 360 (2020) 631-640.

[13] C. Troeger, M. Forouzanfar, P.C. Rao, I. Khalil, A. Brown, R.C. Reiner Jr, N. Fullman, R.L. Thompson, A. Abajobir, M. Ahmed, Estimates of global, regional, and national morbidity, mortality, and aetiologies of diarrhoeal diseases: a systematic analysis for the Global Burden of Disease Study 2015, The Lancet Infectious Diseases, 17 (2017) 909-948.

[14] R. Bala, V.A. Singh, N. Gupta, P. Rakshit, Prevalence, multidrug-resistance and risk factors for AmpC β-lactamases producing Escherichia coli from hospitalized patients, J. Infect. Dev. Ctries., 14 (2020) 1466-1469.

[15] K.J. Ryan, C.G. Ray, Medical microbiology, McGraw Hill, 4 (2004) 370.

[16] R. Podschun, U. Ullmann, Klebsiella spp. as nosocomial pathogens: Epidemiology, taxonomy, typing methods, and pathogenicity factors, Clinical Microbiology Reviews, 11 (1998) 589-603.

[17] D.J. Farrell, I. Morrissey, D. de Rubeis, M. Robbins, D. Felmingham, A UK multicentre study of the antimicrobial susceptibility of bacterial pathogens causing urinary tract infection, J. Infect., 46 (2003) 94-100.

[18] K.M. Papp-Wallace, C.R. Bethel, A.M. Distler, C. Kasuboski, M. Taracila, R.A. Bonomo, Inhibitor resistance in the KPC-2 β-lactamase, a preeminent property of this class A β-lactamase, Antimicrobial agents and chemotherapy, 54 (2010) 890-897.

[19] L.S. Munoz-Price, L. Poirel, R.A. Bonomo, M.J. Schwaber, G.L. Daikos, M. Cormican, G. Cornaglia, J. Garau, M. Gniadkowski, M.K. Hayden, K. Kumarasamy, D.M. Livermore, J.J. Maya, P. Nordmann, J.B. Patel, D.L. Paterson, J. Pitout, M.V. Villegas, H. Wang, N. Woodford, J.P. Quinn, Clinical epidemiology of the global expansion of Klebsiella pneumoniae carbapenemases, Lancet Infect. Dis., 13 (2013) 785-796.

[20] A. Cassini, L.D. Högberg, D. Plachouras, A. Quattrocchi, A. Hoxha, G.S. Simonsen, M. Colomb-Cotinat, M.E. Kretzschmar, B. Devleesschauwer, M. Cecchini, Attributable deaths and disability-adjusted life-years caused by infections with antibiotic-resistant bacteria in the EU and the European Economic Area in 2015: a population-level modelling analysis, Lancet Infect. Dis., 19 (2019) 56-66.

[21] W.E. Stamm, S.R. Norrby, Urinary tract infections: disease panorama and challenges, The Journal of infectious diseases, 183 (2001) S1-S4.

[22] A.L. Flores-Mireles, J.N. Walker, M. Caparon, S.J. Hultgren, Urinary tract infections: Epidemiology, mechanisms of infection and treatment options, Nat. Rev. Microbiol., 13 (2015) 269-284.

[23] B. Foxman, Urinary tract infection syndromes: occurrence, recurrence, bacteriology, risk factors, and disease burden, Infectious disease clinics of North America, 28 (2013) 1-13.

[24] B. Foxman, Epidemiology of urinary tract infections: incidence, morbidity, and economic costs, The American Journal of Medicine, 113 (2002) 5-13.

[25] G. Schmiemann, E. Kniehl, K. Gebhardt, M.M. Matejczyk, E. Hummers-Pradier, The diagnosis of urinary tract infection: A systematic review, Dtsch. Arztebl., 107 (2010) 361-367.

[26] C.E. Chenoweth, C.V. Gould, S. Saint, Diagnosis, management, and prevention of catheter-associated urinary tract infections, Infectious Disease Clinics, 28 (2014) 105-119.

[27] N. Samaras, T. Chevalley, D. Samaras, G. Gold, Older patients in the emergency department: A review, Ann. Emerg. Med., 56 (2010) 261-269.

[28] A. Ronald, The etiology of urinary tract infection: traditional and emerging pathogens, The American journal of medicine, 113 (2002) 14-19.

[29] Y.-H. Chen, W.-C. Ko, P.-R. Hsueh, Emerging resistance problems and future perspectives in pharmacotherapy for complicated urinary tract infections, Expert opinion on pharmacotherapy, 14 (2013) 587-596.

[30] S. Jacobsen, D. Stickler, H. Mobley, M. Shirtliff, Complicated catheter-associated urinary tract infections due to Escherichia coli and Proteus mirabilis, Clinical microbiology reviews, 21 (2008) 26-59.

[31] L.M. Weiner, A.K. Webb, B. Limbago, M.A. Dudeck, J. Patel, A.J. Kallen, J.R. Edwards, D.M. Sievert, Antimicrobial-Resistant Pathogens Associated With Healthcare-Associated Infections: Summary of Data Reported to the National Healthcare Safety Network at the Centers for Disease Control and Prevention, 2011–2014, Infection Control & Hospital Epidemiology, 37 (2016) 1288-1301.

[32] R.F. Leihof, S. Ethelberg, K.L. Nielsen, S.C. Rasmussen, N. Frimodt-Møller, Nosocomial urinary tract infection and risk of bacteraemia in elderly patients: urinary catheter, clinical factors and bacterial species, Infect. Dis., 51 (2019) 547-549.

[33] S.K. Fridkin, S.F. Welbel, R.A. Weinstein, Magnitude and prevention of nosocomial infections in the intensive care unit, Infectious disease clinics of North America, 11 (1997) 479-496.

[34] R. Gaynes, J.R. Edwards, Overview of nosocomial infections caused by gram-negative bacilli, Clin. Infect. Dis., 41 (2005) 848-854.

[35] A.Y. Peleg, D.C. Hooper, Hospital-acquired infections due to gram-negative bacteria, New Engl. J. Med., 362 (2010) 1804-1813.

[36] N.T. Mutters, V. Mersch-Sundermann, R. Mutters, C. Brandt, W. Schneider-Brachert, U. Frank, Control of the spread of vancomycin-resistant enterococci in hospitals: Epidemiology and clinical relevance, Dtsch. Arztebl. Inter., 110 (2013) 725-731 and 721.

[37] F. Álvarez-Lerma, J. Nolla-Salas, C. León, M. Palomar, R. Jordá, N. Carrasco, F. Bobillo, Candiduria in critically ill patients admitted to intensive care medical units, Intensive care medicine, 29 (2003) 1069-1076.

[38] J.L. Vincent, J. Rello, J. Marshall, E. Silva, A. Anzueto, C.D. Martin, R. Moreno, J. Lipman, C. Gomersall, Y. Sakr, K. Reinhart, International study of the prevalence and outcomes of infection in intensive care units, J. Am. Med. Assoc., 302 (2009) 2323-2329.

[39] J.C.O. Sardi, L. Scorzoni, T. Bernardi, A.M. Fusco-Almeida, M.J.S. Mendes Giannini, Candida species: Current epidemiology, pathogenicity, biofilm formation, natural antifungal products and new therapeutic options, J. Med. Microbiol., 62 (2013) 10-24.

[40] G. Ece, Distribution of fungi at a University Hospital in Turkey, Jundishapur J. Microbiol., 7 (2014).

[41] S.K. Fridkin, W.R. Jarvis, Epidemiology of nosocomial fungal infections, Clinical microbiology reviews, 9 (1996) 499-511.

[42] P.E. Greenwood, M.S. Nikulin, A guide to chi-squared testing, John Wiley & Sons1996.

[43] S.B. Levy, M. Bonnie, Antibacterial resistance worldwide: Causes, challenges and responses, Nat. Med., 10 (2004) S122-S129.

[44] D.L. Paterson, R.A. Bonomo, Extended-spectrum β-lactamases: A clinical update, Clinical Microbiology Reviews, 18 (2005) 657-686.

[45] A.r.s.i. Europe, Annual report of the European Antimicrobial Resistance Surveillance Network (EARS-Net), European Centre for Disease Prevention and Control Stockholm, 2014.

[46] A. Mazzariol, A. Bazaj, G. Cornaglia, Multi-drug-resistant Gram-negative bacteria causing urinary tract infections: a review, J. Chemother., 29 (2017) 2-9.

[47] K. Bush, P.A. Bradford, Epidemiology of β-lactamase-producing pathogens, Clinical Microbiology Reviews, 33 (2020).

[48] N. Woodford, P.M. Tierno, Jr., K. Young, L. Tysall, M.F. Palepou, E. Ward, R.E. Painter, D.F. Suber, D. Shungu, L.L. Silver, K. Inglima, J. Kornblum, D.M. Livermore, Outbreak of Klebsiella pneumoniae producing a new carbapenem-hydrolyzing class A β-lactamase, KPC-3, in a New York Medical Center, Antimicrob. Agents Chemother., 48 (2004) 4793.

[49] W. Ke, C.R. Bethel, J.M. Thomson, R.A. Bonomo, F. van den Akker, Crystal Structure of KPC-2: Insights into Carbapenemase Activity in Class A β-Lactamases, Biochemistry, 46 (2007) 5732-5740.

[50] J.D.D. Pitout, P. Nordmann, L. Poirel, Carbapenemase-Producing Klebsiella pneumoniae, a Key Pathogen Set for Global Nosocomial Dominance, Antimicrobial Agents and Chemotherapy, 59 (2015) 5873.

[51] A.I. Hidron, J.R. Edwards, J. Patel, T.C. Horan, D.M. Sievert, D.A. Pollock, S.K. Fridkin, Antimicrobial-resistant pathogens associated with healthcare-associated infections: Annual summary of data reported to the National Healthcare Safety Network at the Centers for Disease Control and Prevention, 2006-2007, Infect. Control Hosp. Epidemiol., 29 (2008) 996-1011.

[52] W.W. Lim, P. Wu, H.S. Bond, J.Y. Wong, K. Ni, W.H. Seto, M. Jit, B.J. Cowling, Determinants of methicillin-resistant Staphylococcus aureus (MRSA) prevalence in the Asia-Pacific region: A systematic review and meta-analysis, Journal of Global Antimicrobial Resistance, 16 (2019) 17-27.

[53] M.G. Sabzehali, A. Mohammadi, H. Goudarzi, M. Fazeli, F. Sabzehali, Genetic variability and integron occurrence in methicillin resistant staphylococcus aureus strains recovered from patients with urinary tract infection, Arch. Pediatr. Infect. Dis., 7 (2019).

[54] T. Schwartz, W. Kohnen, B. Jansen, U. Obst, Detection of antibiotic-resistant bacteria and their resistance genes in wastewater, surface water, and drinking water biofilms, FEMS Microbiol. Ecol., 43 (2003) 325-335.

[55] L. Rizzo, C. Manaia, C. Merlin, T. Schwartz, C. Dagot, M.C. Ploy, I. Michael, D. Fatta-Kassinos, Urban wastewater treatment plants as hotspots for antibiotic resistant bacteria and genes spread into the environment: A review, Science of The Total Environment, 447 (2013) 345-360.

[56] P. Verlicchi, M. Al Aukidy, E. Zambello, What have we learned from worldwide experiences on the management and treatment of hospital effluent? — An overview and a discussion on perspectives, Science of The Total Environment, 514 (2015) 467-491.

[57] S. Rodriguez-Mozaz, S. Chamorro, E. Marti, B. Huerta, M. Gros, A. Sànchez-Melsió, C.M. Borrego, D. Barceló, J.L. Balcázar, Occurrence of antibiotics and antibiotic resistance genes in hospital and urban wastewaters and their impact on the receiving river, Water Research, 69 (2015) 234-242.

[58] L. Proia, A. Adriana, S. Jessica, B. Carles, F. Marinella, L. Marta, B.J. Luis, P. Servais, Antibiotic resistance in urban and hospital wastewaters and their impact on a receiving freshwater ecosystem, Chemosphere, 206 (2018) 70-82.

[59] A. Solanki, T.H. Boyer, Pharmaceutical removal in synthetic human urine using biochar, Environmental Science: Water Research & Technology, 3 (2017) 553-565.

[60] J. Llanos, S. Cotillas, P. Cañizares, M.A. Rodrigo, Conductive diamond sono-electrochemical disinfection (CDSED) for municipal wastewater reclamation, Ultrasonics Sonochemistry, 22 (2015) 493-498.

[61] S. Cotillas, J. Llanos, I. Moraleda, P. Cañizares, M.A. Rodrigo, Scaling-up an integrated electrodisinfection-electrocoagulation process for wastewater reclamation, Chemical Engineering Journal, 380 (2020).

[62] J. Isidro, D. Brackemeyer, C. Sáez, J. Llanos, J. Lobato, P. Cañizares, T. Matthée, M.A. Rodrigo, Testing the use of cells equipped with solid polymer electrolytes for electro-disinfection, Science of the Total Environment, 725 (2020).

[63] N. Gonzalez-Rivas, H. Reyes-Pérez, C.E. Barrera-Díaz, Recent Advances in Water and Wastewater Electrodisinfection, ChemElectroChem, 6 (2019) 1978-1983.

[64] M.A. Rodrigo, P. Cañizares, C. Buitrón, C. Sáez, Electrochemical technologies for the regeneration of urban wastewaters, Electrochimica Acta, 55 (2010) 8160-8164.

[65] J. Radjenovic, D.L. Sedlak, Challenges and Opportunities for Electrochemical Processes as Next-Generation Technologies for the Treatment of Contaminated Water, Environmental Science and Technology, 49 (2015) 11292-11302.

[66] M.A. Rodrigo, P. Cañizares, A. Sánchez-Carretero, C. Sáez, Use of conductive-diamond electrochemical oxidation for wastewater treatment, Catalysis Today, 151 (2010) 173-177.

[67] S. Cotillas, E. Lacasa, C. Sáez, P. Cañizares, M.A. Rodrigo, Removal of pharmaceuticals from the urine of polymedicated patients: A first approach, Chemical Engineering Journal, 331 (2018) 606-614.

[68] G.O.S. Santos, I.M.D. Gonzaga, K.I.B. Eguiluz, G.R. Salazar-Banda, C. Saez, M.A. Rodrigo, Improving biodegradability of clopyralid wastes by photoelectrolysis: The role of the anode material, J Electroanal Chem, 864 (2020).

[69] G.D.O.S. Santos, I.M.D. Gonzaga, A.R. Dória, A. Moratalla, R.S. da Silva, K.I.B. Eguiluz, G.R. Salazar-Banda, C. Saez, M.A. Rodrigo, Testing and scaling-up of a novel

Ti/Ru0.7Ti0.3O2 mesh anode in a microfluidic flow-through reactor, Chemical Engineering Journal, 398 (2020).

[70] S. Cotillas, E. Lacasa, C. Sáez, P. Cañizares, M.A. Rodrigo, Disinfection of urine by conductive-diamond electrochemical oxidation, Applied Catalysis B: Environmental, 229 (2018) 63-70.

[71] P. Verlicchi, A. Galletti, M. Petrovic, D. Barceló, Hospital effluents as a source of emerging pollutants: an overview of micropollutants and sustainable treatment options, Journal of Hydrology, 389 (2010) 416-428.

[72] T. Michael, Brock Biology Of Microorganisms, 14th Edn, (2005).

[73] M.E.H. Bergmann, J. Rollin, Product and by-product formation in laboratory studies on disinfection electrolysis of water using boron-doped diamond anodes, Catalysis Today, 124 (2007) 198-203.

[74] J. Lienert, M. Koller, J. Konrad, C.S. McArdell, N. Schuwirth, Multiple-Criteria Decision Analysis Reveals High Stakeholder Preference to Remove Pharmaceuticals from Hospital Wastewater, Environmental Science & Technology, 45 (2011) 3848-3857.

[75] P. Verlicchi, M. Al Aukidy, E. Zambello, Occurrence of pharmaceutical compounds in urban wastewater: Removal, mass load and environmental risk after a secondary treatment-A review, Science of the Total Environment, 429 (2012) 123-155.

[76] C.A. Martínez-Huitle, M.A. Rodrigo, I. Sirés, O. Scialdone, Single and Coupled Electrochemical Processes and Reactors for the Abatement of Organic Water Pollutants: A Critical Review, Chemical Reviews, 115 (2015) 13362-13407.

[77] A. Karaçali, M. Muñoz-Morales, S. Kalkan, B.K. Körbahti, C. Saez, P. Cañizares, M.A. Rodrigo, A comparison of the electrolysis of soil washing wastes with active and non-active electrodes, Chemosphere, 225 (2019) 19-26.

[78] M. Panizza, G. Cerisola, Direct and mediated anodic oxidation of organic pollutants, Chemical Reviews, 109 (2009) 6541-6569.

[79] C.M. Dominguez, N. Oturan, A. Romero, A. Santos, M.A. Oturan, Removal of organochlorine pesticides from lindane production wastes by electrochemical oxidation, Environmental Science and Pollution Research, 25 (2018) 34985-34994.

[80] P. Cañizares, C. Sáez, J. Lobato, R. Paz, M.A. Rodrigo, Effect of the operating conditions on the oxidation mechanisms in conductive-diamond electrolyses, Journal of the Electrochemical Society, 154 (2007) E37-E44.

[81] S. Dbira, N. Bensalah, A. Bedoui, P. Cañizares, M.A. Rodrigo, Treatment of synthetic urine by electrochemical oxidation using conductive-diamond anodes, Environ. Sci. Pollut. Res., 22 (2015) 6176-6184.

[82] S. Dbira, N. Bensalah, P. Cañizares, M.A. Rodrigo, A. Bedoui, The electrolytic treatment of synthetic urine using DSA electrodes, Journal of Electroanalytical Chemistry, 744 (2015) 62-68.

[83] A. Sánchez-Carretero, C. Sáez, P. Cañizares, M.A. Rodrigo, Production of Strong Oxidizing Substances with BDD Anodes, Synthetic Diamond Films: Preparation, Electrochemistry, Characterization, and Applications, John Wiley and Sons2011, pp. 281-310.

[84] S. Cotillas, E. Lacasa, M. Herraiz, C. Sáez, P. Cañizares, M.A. Rodrigo, The Role of the Anode Material in Selective Penicillin G Oxidation in Urine, ChemElectroChem, 6 (2019) 1376-1384.

[85] E. Lacasa, J. Llanos, P. Cañizares, M.A. Rodrigo, Electrochemical denitrificacion with chlorides using DSA and BDD anodes, Chemical Engineering Journal, 184 (2012) 66-71.

[86] P. Cañizares, C. Sáez, A. Sánchez-Carretero, M.A. Rodrigo, Synthesis of novel oxidants by electrochemical technology, Journal of Applied Electrochemistry, 39 (2009) 2143-2149.

[87] A. Sánchez-Carretero, C. Sáez, P. Cañizares, M.A. Rodrigo, Electrochemical production of perchlorates using conductive diamond electrolyses, Chemical Engineering Journal, 166 (2011) 710-714.

[88] M.A.Q. Alfaro, S. Ferro, C.A. Martínez-Huitle, Y.M. Vong, Boron doped diamond electrode for the wastewater treatment, Journal of the Brazilian Chemical Society, 17 (2006) 227-236.

[89] S. Cotillas, E. Lacasa, C. Sáez, P. Cañizares, M.A. Rodrigo, Electrolytic and electro-irradiated technologies for the removal of chloramphenicol in synthetic urine with diamond anodes, Water Research, 128 (2018) 383-392.

[90] S. Garcia-Segura, E. Mostafa, H. Baltruschat, Electrogeneration of inorganic chloramines on boron-doped diamond anodes during electrochemical oxidation of ammonium chloride, urea and synthetic urine matrix, Water Research, 160 (2019) 107-117.

[91] G. McKay, B. Sjelin, M. Chagnon, K.P. Ishida, S.P. Mezyk, Kinetic study of the reactions between chloramine disinfectants and hydrogen peroxide: temperature dependence and reaction mechanism, Chemosphere, 92 (2013) 1417-1422.

[92] E. Mostafa, P. Reinsberg, S. Garcia-Segura, H. Baltruschat, Chlorine species evolution during electrochlorination on boron-doped diamond anodes: In-situ electrogeneration of Cl2, Cl2O and ClO2, Electrochimica Acta, 281 (2018) 831-840.

[93] S. Garcia-Segura, E.B. Cavalcanti, E. Brillas, Mineralization of the antibiotic chloramphenicol by solar photoelectro-Fenton: From stirred tank reactor to solar pre-pilot plant, Applied Catalysis B: Environmental, 144 (2014) 588-598.

[94] J. Chen, Y. Xia, Q. Dai, Electrochemical degradation of chloramphenicol with a novel Al doped PbO2 electrode: Performance, kinetics and degradation mechanism, Electrochimica Acta, 165 (2015) 277-287.

[95] J. Singla, A. Verma, V.K. Sangal, Applications of doped mixed metal oxide anode for the electro-oxidation treatment and mineralization of urine metabolite, uric acid, J. Water Process Eng., 32 (2019) 100944.

[96] M. Nie, C. Yan, X. Xiong, X. Wen, X. Yang, Z. lv, W. Dong, Degradation of chloramphenicol using a combination system of simulated solar light, Fe2+ and persulfate, Chemical Engineering Journal, 348 (2018) 455-463.

[97] Y. Zhang, Y. Shao, N. Gao, Y. Gao, W. Chu, S. Li, Y. Wang, S. Xu, Kinetics and by-products formation of chloramphenicol (CAP) using chlorination and photocatalytic oxidation, Chemical Engineering Journal, 333 (2018) 85-91.

[98] H.J. Balbi, Chloramphenicol: A review, Pediatr. Rev., 25 (2004) 284-288.

[99] A.M. Polcaro, A. Vacca, M. Mascia, F. Ferrara, Product and by-product formation in electrolysis of dilute chloride solutions, Journal of Applied Electrochemistry, 38 (2008) 979-984.

[100] M.B. Ferreira, M. Muñoz-Morales, C. Sáez, P. Cañizares, C.A. Martínez-Huitle, M.A. Rodrigo, Improving biotreatability of hazardous effluents combining ZVI, electrolysis and photolysis, Science of The Total Environment, 713 (2020) 136647.

[101] M. Zaghdoudi, F. Fourcade, I. Soutrel, D. Floner, A. Amrane, H. Maghraoui-Meherzi, F. Geneste, Direct and indirect electrochemical reduction prior to a biological treatment for dimetridazole removal, Journal of Hazardous Materials, 335 (2017) 10-17.

[102] C. Pulgarin, M. Invernizzi, S. Parra, V. Sarria, R. Polania, P. Péringer, Strategy for the coupling of photochemical and biological flow reactors useful in mineralization of biorecalcitrant industrial pollutants, Catalysis Today, 54 (1999) 341-352.

[103] C. Disinfection, Combined Sewer Overflow Technology Fact Sheet, (1999).

[104] L. Rizzo, C. Manaia, C. Merlin, T. Schwartz, C. Dagot, M.C. Ploy, I. Michael, D. Fatta-Kassinos, Urban wastewater treatment plants as hotspots for antibiotic resistant bacteria and genes spread into the environment: a review, The Science of the total environment, 447 (2013) 345-360.

[105] Q. Tan, W. Li, J. Zhang, W. Zhou, J. Chen, Y. Li, J. Ma, Presence, dissemination and removal of antibiotic resistant bacteria and antibiotic resistance genes in urban drinking water system: A review, Frontiers of Environmental Science & Engineering, 13 (2019) 36.

[106] A.K. Gautam, S. Kumar, P.C. Sabumon, Preliminary study of physico-chemical treatment options for hospital wastewater, J Environ Manage, 83 (2007) 298-306.

[107] E.D. Sunkari, H.M. Korboe, M. Abu, T. Kizildeniz, Sources and routes of SARS-CoV-2 transmission in water systems in Africa: Are there any sustainable remedies?, Science of The Total Environment, 753 (2021) 142298.

[108] S. Kataki, S. Chatterjee, M.G. Vairale, S. Sharma, S.K. Dwivedi, Concerns and strategies for wastewater treatment during COVID-19 pandemic to stop plausible transmission, Resources, Conservation and Recycling, 164 (2021) 105156.

[109] C.P. Huang, C. Dong, Z. Tang, Advanced chemical oxidation: Its present role and potential future in hazardous waste treatment, Waste Management, 13 (1993) 361-377.

[110] J. Oh, D.E. Salcedo, C.A. Medriano, S. Kim, Comparison of different disinfection processes in the effective removal of antibiotic-resistant bacteria and genes, J. Environ. Sci., 26 (2014) 1238-1242.

[111] M. Munoz, P. Garcia-Muñoz, G. Pliego, Z.M.d. Pedro, J.A. Zazo, J.A. Casas, J.J. Rodriguez, Application of intensified Fenton oxidation to the treatment of hospital wastewater: Kinetics, ecotoxicity and disinfection, Journal of Environmental Chemical Engineering, 4 (2016) 4107-4112.

[112] J.A.L. Perini, A.L. Tonetti, C. Vidal, C.C. Montagner, R.F.P. Nogueira, Simultaneous degradation of ciprofloxacin, amoxicillin, sulfathiazole and sulfamethazine, and disinfection of hospital effluent after biological treatment via photo-Fenton process under ultraviolet germicidal irradiation, Appl. Catal. B Environ., 224 (2018) 761-771.

[113] G. Moussavi, E. Fathi, M. Moradi, Advanced disinfecting and post-treating the biologically treated hospital wastewater in the UVC/H2O2 and VUV/H2O2 processes: Performance comparison and detoxification efficiency, Process Safety and Environmental Protection, 126 (2019) 259-268.

[114] C.A. Somensi, A.L.F. Souza, E.L. Simionatto, P. Gaspareto, M. Millet, C.M. Radetski, Genetic material present in hospital wastewaters: Evaluation of the efficiency of DNA denaturation by ozonolysis and ozonolysis/sonolysis treatments, J. Environ. Manage., 162 (2015) 74-80.

[115] A.S. Raut, G.B. Cunningham, C.B. Parker, E.J.D. Klem, B.R. Stoner, M.A. Deshusses, J.T. Glass, Disinfection of E. Coli Contaminated Urine Using Boron-Doped Diamond Electrodes, Journal of The Electrochemical Society, 161 (2014) G81-G85.

[116] A.S. Raut, C.B. Parker, E.J.D. Klem, B.R. Stoner, M.A. Deshusses, J.T. Glass, Reduction in energy for electrochemical disinfection of E. coli in urine simulant, Journal of Applied Electrochemistry, 49 (2019) 443-453.

[117] I. Moraleda, N. Oturan, C. Saez, J. Llanos, M.A. Rodrigo, M.A. Oturan, A comparison between flow-through cathode and mixed tank cells for the electro-Fenton process with conductive diamond anode, Chemosphere, 238 (2020) 124854.

[118] J.F. Pérez, J. Llanos, C. Sáez, C. López, P. Cañizares, M.A. Rodrigo, On the design of a jet-aerated microfluidic flow-through reactor for wastewater treatment by electro-Fenton, Separation and Purification Technology, 208 (2019) 123-129.

[119] A. Kraft, M. Stadelmann, M. Blaschke, D. Kreysig, B. Sandt, F. Schröder, J. Rennau, Electrochemical water disinfection. Part I: Hypochlorite production from very dilute chloride solutions, Journal of Applied Electrochemistry, 29 (1999) 861-868.

[120] J. Jeong, C. Kim, J. Yoon, The effect of electrode material on the generation of oxidants and microbial inactivation in the electrochemical disinfection processes, Water Research, 43 (2009) 895-901.

[121] M.I. Kerwick, S.M. Reddy, A.H.L. Chamberlain, D.M. Holt, Electrochemical disinfection, an environmentally acceptable method of drinking water disinfection?, Electrochimica Acta, 50 (2005) 5270-5277.

[122] I. Sirés, E. Brillas, M.A. Oturan, M.A. Rodrigo, M. Panizza, Electrochemical advanced oxidation processes: Today and tomorrow. A review, Environmental Science and Pollution Research, 21 (2014) 8336-8367.

[123] C. Sáez, P. Cañizares, J. Llanos, M.A. Rodrigo, The Treatment of Actual Industrial Wastewaters Using Electrochemical Techniques, Electrocatalysis, 4 (2013) 252-258.

[124] H. Bergmann, A discussion on diamond electrodes for water disinfection electrolysis, Zur Bewertung von Diamantelektroden für die Wasserdesinfektionselektrolyse, 151 (2010) 604-613.

[125] J.A. Lara-Ramos, C. Saez, F. Machuca-Martínez, M.A. Rodrigo, Electro-ozonizers: A new approach for an old problem, Separation and Purification Technology, 241 (2020) 116701.

[126] J.A. Lara-Ramos, J. Diaz-Angulo, F. Machuca-Martínez, Use of modified flotation cell as ozonation reactor to minimize mass transfer limitations, Chemical Engineering Journal, 405 (2021) 126978.

[127] J. Isidro, D. Brackemeyer, C. Sáez, J. Llanos, J. Lobato, P. Cañizares, T. Matthée, M.A. Rodrigo, Electro-disinfection with BDD-electrodes featuring PEM technology, Separation and Purification Technology, 248 (2020) 117081.

[128] S. Cotillas, D. Clematis, P. Cañizares, M.P. Carpanese, M.A. Rodrigo, M. Panizza, Degradation of dye Procion Red MX-5B by electrolytic and electro-irradiated technologies using diamond electrodes, Chemosphere, 199 (2018) 445-452.

[129] J. Isidro, D. Brackemeyer, C. Sáez, J. Llanos, J. Lobato, P. Cañizares, T. Matthee, M.A. Rodrigo, Operating the CabECO® membrane electrolytic technology in continuous mode for the direct disinfection of highly fecal-polluted water, Separation and Purification Technology, 208 (2019) 110-115.

[130] P. Cañizares, J. García-Gómez, I. Fernández de Marcos, M.A. Rodrigo, J. Lobato, Measurement of Mass-Transfer Coefficients by an Electrochemical Technique, Journal of Chemical Education, 83 (2006) 1204.

[131] J.F. Pérez, J. Llanos, C. Sáez, C. López, P. Cañizares, M.A. Rodrigo, Development of an innovative approach for low-impact wastewater treatment: A microfluidic flow-through electrochemical reactor, Chemical Engineering Journal, 351 (2018) 766-772.

[132] J. Kristal, R. Kodym, K. Bouzek, V. Jiricny, J. Hanika, Electrochemical Microreactor Design for Alkoxylation Reactions—Experiments and Simulations, Industrial & Engineering Chemistry Research, 51 (2012) 1515-1524.

[133] S. Cotillas, J. Llanos, M.A. Rodrigo, P. Cañizares, Use of carbon felt cathodes for the electrochemical reclamation of urban treated wastewaters, Applied Catalysis B: Environmental, 162 (2015) 252-259.

[134] S. Giannakis, S. Rtimi, C. Pulgarin, Light-Assisted Advanced Oxidation Processes for the Elimination of Chemical and Microbiological Pollution of Wastewaters in Developed and Developing Countries, Molecules (Basel, Switzerland), 22 (2017).

[135] M.C. Collivignarelli, A. Abbà, I. Benigna, S. Sorlini, V. Torretta, Overview of the Main Disinfection Processes for Wastewater and Drinking Water Treatment Plants, Sustainability, 10 (2018) 86.

[136] T. Kohn, L. Decrey, B. Vinneras, Chemical disinfectants, Michigan State University, UNESCO, 2017.

[137] M. Deborde, U. von Gunten, Reactions of chlorine with inorganic and organic compounds during water treatment-Kinetics and mechanisms: a critical review, Water Res, 42 (2008) 13-51.

[138] M. Herraiz-Carboné, S. Cotillas, E. Lacasa, P. Cañizares, M.A. Rodrigo, C. Sáez, Removal of antibiotic resistant bacteria by electrolysis with diamond anodes: A pretreatment or a tertiary treatment?, J. Water Process Eng., 38 (2020) 101557.

[139] M. Herraiz-Carboné, S. Cotillas, E. Lacasa, Á. Moratalla, P. Cañizares, M.A. Rodrigo, C. Sáez, Improving the biodegradability of hospital urines polluted with chloramphenicol by the application of electrochemical oxidation, Science of The Total Environment, 725 (2020) 138430.

[140] J.C. Crittenden, R.R. Trussell, D.W. Hand, K.J. Howe, G. Tchobanoglous, MWH's Water Treatment: Principles and Design, Wiley2012.

[141] J.D. Johnson, J.N. Jensen, THM and TOX Formation: Routes, Rates, and Precursors, Journal - AWWA, 78 (1986) 156-162.

[142] S. Chen, X. Li, Y. Wang, J. Zeng, C. Ye, X. Li, L. Guo, S. Zhang, X. Yu, Induction of Escherichia coli into a VBNC state through chlorination/chloramination and differences in characteristics of the bacterium between states, Water Research, 142 (2018) 279-288.

[143] B.A. Lyon, A.D. Dotson, K.G. Linden, H.S. Weinberg, The effect of inorganic precursors on disinfection byproduct formation during UV-chlorine/chloramine drinking water treatment, Water Research, 46 (2012) 4653-4664.

[144] X. Zhang, W. Li, E.R. Blatchley, 3rd, X. Wang, P. Ren, UV/chlorine process for ammonia removal and disinfection by-product reduction: comparison with chlorination, Water Res, 68 (2015) 804-811.

[145] Y. Du, X.-T. Lv, Q.-Y. Wu, D.-Y. Zhang, Y.-T. Zhou, L. Peng, H.-Y. Hu, Formation and control of disinfection byproducts and toxicity during reclaimed water chlorination: A review, Journal of Environmental Sciences, 58 (2017) 51-63.

[146] G. Hua, D.A. Reckhow, Comparison of disinfection byproduct formation from chlorine and alternative disinfectants, Water Research, 41 (2007) 1667-1678.

[147] A.C. Diehl, G.E. Speitel Jr., J.M. Symons, S.W. Krasner, C.J. Hwang, S.E. Barrett, DBP formation during chloramination, Journal - AWWA, 92 (2000) 76-90.

[148] E.H. Goslan, S.W. Krasner, M. Bower, S.A. Rocks, P. Holmes, L.S. Levy, S.A. Parsons, A comparison of disinfection by-products found in chlorinated and chloraminated drinking waters in Scotland, Water Research, 43 (2009) 4698-4706.

[149] F. Wang, B. Gao, D. Ma, R. Li, S. Sun, Q. Yue, Y. Wang, Q. Li, Effects of operating conditions on trihalomethanes formation and speciation during chloramination in reclaimed water, Environmental Science and Pollution Research, 23 (2016) 1576-1583.

[150] G.J. Kirmeyer, A.R. Foundation, Optimizing chloramine treatment, American Water Works Association, Denver, Colo., 2004.

[151] S. Dbira, N. Bensalah, M.I. Ahmad, A. Bedoui, Electrochemical Oxidation/Disinfection of Urine Wastewaters with Different Anode Materials, Materials (Basel), 12 (2019) 1254.

[152] M. Panizza, G. Cerisola, Application of diamond electrodes to electrochemical processes, Electrochimica Acta, 51 (2005) 191-199.

[153] H. Liu, X.-Y. Ni, Z.-Y. Huo, L. Peng, G.-Q. Li, C. Wang, Y.-H. Wu, H.-Y. Hu, Carbon Fiber-Based Flow-Through Electrode System (FES) for Water Disinfection via Direct Oxidation Mechanism with a Sequential Reduction–Oxidation Process, Environmental Science & Technology, 53 (2019) 3238-3249.

[154] M. Herraiz-Carboné, S. Cotillas, E. Lacasa, P. Cañizares, M.A. Rodrigo, C. Sáez, Enhancement of UV disinfection of urine matrixes by electrochemical oxidation, Journal of Hazardous Materials, 410 (2021).

[155] H. Li, X. Zhu, J. Ni, Comparison of electrochemical method with ozonation, chlorination and monochloramination in drinking water disinfection, Electrochimica Acta, 56 (2011) 9789-9796.

[156] H.F. Diao, X.Y. Li, J.D. Gu, H.C. Shi, Z.M. Xie, Electron microscopic investigation of the bactericidal action of electrochemical disinfection in comparison with chlorination, ozonation and Fenton reaction, Process Biochemistry, 39 (2004) 1421-1426.

[157] H. Li, Z. Zhang, J. Duan, N. Li, B. Li, T. Song, M.F. Sardar, X. Lv, C. Zhu, Electrochemical disinfection of secondary effluent from a wastewater treatment plant: Removal efficiency of ARGs and variation of antibiotic resistance in surviving bacteria, Chemical Engineering Journal, 392 (2020) 123674.

[158] S.J. Ahmad, H.H. Lian, D.F. Basri, N.M. Zin, Mode of action of endophytic Streptomyces sp., SUK 25 extracts against MRSA; microscopic, biochemical and time-kill analysis, Int. J. Pharm. Sci. Rev. Res, 30 (2015) 11-17.

[159] K.P. Devi, S.A. Nisha, R. Sakthivel, S.K. Pandian, Eugenol (an essential oil of clove) acts as an antibacterial agent against Salmonella typhi by disrupting the cellular membrane, Journal of Ethnopharmacology, 130 (2010) 107-115.

[160] M. Vaara, T. Vaara, Outer Membrane Permeability Barrier Disruption by Polymyxin in Polymyxin-Susceptible and -Resistant Salmonella typhimurium, Antimicrobial Agents and Chemotherapy, 19 (1981) 578-583.

[161] C. Bruguera-Casamada, I. Sirés, M.J. Prieto, E. Brillas, R.M. Araujo, The ability of electrochemical oxidation with a BDD anode to inactivate Gram-negative and Gram-positive bacteria in low conductivity sulfate medium, Chemosphere, 163 (2016) 516-524.

[162] Y. Long, J. Ni, Z. Wang, Subcellular mechanism of Escherichia coli inactivation during electrochemical disinfection with boron-doped diamond anode: a comparative study of three electrolytes, Water Res., 84 (2015) 198-206.

[163] T.D. Brock, M.T. Madigan, J.M. Martinko, J. Parker, Brock biology of microorganisms, Upper Saddle River (NJ): Prentice-Hall, 2003.2003.

[164] B.R. Kim, J.E. Anderson, S.A. Mueller, W.A. Gaines, A.M. Kendall, Literature review - Efficacy of various disinfectants against Legionella in water systems, Water Res., 36 (2002) 4433-4444.

[165] Y. Luo, L. Feng, Y. Liu, L. Zhang, Disinfection by-products formation and acute toxicity variation of hospital wastewater under different disinfection processes, Sep. Purif. Technol., 238 (2020).

[166] J.R. Bolton, K.G. Linden, Standardization of methods for fluence (UV Dose) determination in bench-scale UV experiments, J. Environ. Eng., 129 (2003) 209-215.

[167] C. Von Sonntag, Advanced oxidation processes: Mechanistic aspects, Water Sci. Technol., 2008, pp. 1015-1021.

[168] W.A.M. Hijnen, E.F. Beerendonk, G.J. Medema, Inactivation credit of UV radiation for viruses, bacteria and protozoan (oo)cysts in water: A review, Water Research, 40 (2006) 3-22.

[169] G. Wen, Q. Wan, X. Deng, R. Cao, X. Xu, Z. Chen, J. Wang, T. Huang, Reactivation of fungal spores in water following UV disinfection: Effect of temperature, dark delay, and real water matrices, Chemosphere, 237 (2019).

[170] E. Lacasa, S. Cotillas, C. Saez, J. Lobato, P. Cañizares, M.A. Rodrigo, Environmental applications of electrochemical technology. What is needed to enable full-scale applications?, Current Opinion in Electrochemistry, 16 (2019) 149-156.

[171] J. Rodríguez-Chueca, S. Giannakis, M. Marjanovic, M. Kohantorabi, M.R. Gholami, D. Grandjean, L.F. de Alencastro, C. Pulgarín, Solar-assisted bacterial disinfection and removal of contaminants of emerging concern by Fe2+-activated HSO5- vs. S2O82- in drinking water, Appl. Catal. B Environ., 248 (2019) 62-72.

[172] L.C. Ferreira, M. Castro-Alférez, S. Nahim-Granados, M.I. Polo-López, M.S. Lucas, G. Li Puma, P. Fernández-Ibáñez, Inactivation of water pathogens with solar photo-activated persulfate oxidation, Chemical Engineering Journal, 381 (2020).

[173] E.A. Serna-Galvis, L. Salazar-Ospina, J.N. Jiménez, N.J. Pino, R.A. Torres-Palma, Elimination of carbapenem resistant Klebsiella pneumoniae in water by UV-C, UV-C/persulfate and UV-C/H2O2. Evaluation of response to antibiotic, residual effect of the processes and removal of resistance gene, J. Environ. Chem. Eng., 8 (2020).

[174] T. Zhang, Y. Hu, L. Jiang, S. Yao, K. Lin, Y. Zhou, C. Cui, Removal of antibiotic resistance genes and control of horizontal transfer risk by UV, chlorination and UV/chlorination treatments of drinking water, Chemical Engineering Journal, 358 (2019) 589-597.

[175] K. Oguma, H. Katayama, H. Mitani, S. Morita, T. Hirata, S. Ohgaki, Determination of Pyrimidine Dimers in Escherichia coli and Cryptosporidium parvum during UV Light Inactivation, Photoreactivation, and Dark Repair, APPL. ENVIRON. MICROBIOL., 67 (2001) 4630-4637.

[176] S. Vilhunen, H. Särkkä, M. Sillanpää, Ultraviolet light-emitting diodes in water disinfection, Environmental Science and Pollution Research, 16 (2009) 439-442.

[177] M. Guo, H. Hu, J.R. Bolton, M.G. El-Din, Comparison of low- and medium-pressure ultraviolet lamps: Photoreactivation of Escherichia coli and total coliforms in secondary effluents of municipal wastewater treatment plants, Water Research, 43 (2009) 815-821.

[178] C.D.N. Brito, D.M. De Araújo, C.A. Martínez-Huitle, M.A. Rodrigo, Understanding active chlorine species production using boron doped diamond films with lower and higher sp3/sp2 ratio, Electrochemistry Communications, 55 (2015) 34-38.

[179] P. Canizares, C. Sáez, F. Martínez, M.A. Rodrigo, The role of the characteristics of p-Si BDD anodes on the efficiency of wastewater electro-oxidation processes, Electrochemical and Solid-State Letters, 11 (2008) E15-E19.

[180] J.P. De Paiva Barreto, K.C. De Freitas Aráujo, D.M. De Aráujo, C.A. Martínez-Huitle, Effect of sp3/sp2 ratio on boron doped diamond films for producing persulfate, ECS Electrochemistry Letters, 4 (2015) E9-E11.

[181] I. Moraleda, S. Cotillas, J. Llanos, C. Sáez, P. Cañizares, L. Pupunat, M.A. Rodrigo, Can the substrate of the diamond anodes influence on the performance of the electrosynthesis of oxidants?, Journal of Electroanalytical Chemistry, 850 (2019) 113416.

[182] W. Feng, A. Deletic, Z. Wang, X. Zhang, T. Gengenbach, D.T. McCarthy, Electrochemical oxidation disinfects urban stormwater: Major disinfection mechanisms and longevity tests, Science of The Total Environment, 646 (2019) 1440-1447.

[183] S. Cotillas, M.J.M. de Vidales, J. Llanos, C. Sáez, P. Cañizares, M.A. Rodrigo, Electrolytic and electro-irradiated processes with diamond anodes for the oxidation of persistent pollutants and disinfection of urban treated wastewater, Journal of Hazardous Materials, 319 (2016) 93-101.

[184] F.L. Souza, C. Sáez, P. Cañizares, M.A. Rodrigo, Improving photolytic treatments with electrochemical technology, Separation and Purification Technology, 235 (2020).

[185] D. Golub, E. Ben-Hur, Y. Oren, A. Soffer, Electroadsorption of bacteria on porous carbon and graphite electrodes, Bioelectrochemistry and Bioenergetics, 17 (1987) 175-182.

[186] S. Cotillas, J. Llanos, P. Cañizares, S. Mateo, M.A. Rodrigo, Optimization of an integrated electrodisinfection/electrocoagulation process with Al bipolar electrodes for urban wastewater reclamation, Water Res., 47 (2013) 1741-1750.

[187] D. Ghernaout, B. Ghernaout, From chemical disinfection to electrodisinfection: The obligatory itinerary?, Desalination and Water Treatment, 16 (2010) 156-175.

[188] M.J. Martin De Vidales, M. Millán, C. Sáez, P. Cañizares, M.A. Rodrigo, What happens to inorganic nitrogen species during conductive diamond electrochemical oxidation of real wastewater?, Electrochemistry Communications, 67 (2016) 65-68.

[189] E. Lacasa, P. Cañizares, J. Llanos, M.A. Rodrigo, Effect of the cathode material on the removal of nitrates by electrolysis in non-chloride media, Journal of Hazardous Materials, 213-214 (2012) 478-484.

[190] A.C. Diehl, G.E. Speitel Jr., J.M. Symons, S.W. Krasner, C.J. Hwang, S.E. Barrett, DBP formation during chloramination, Journal AWWA, 92 (2000) 76-90.

[191] K. Doederer, W. Gernjak, H.S. Weinberg, M.J. Farré, Factors affecting the formation of disinfection by-products during chlorination and chloramination of secondary effluent for the production of high quality recycled water, Water Research, 48 (2014) 218-228.

[192] J. Le Roux, M.J. Plewa, E.D. Wagner, M. Nihemaiti, A. Dad, J.P. Croué, Chloramination of wastewater effluent: Toxicity and formation of disinfection byproducts, J. Environ. Sci., 58 (2017) 135-145.

[193] A.T. Palin, The determination of free chlorine and of chloramine in water using p-aminodimethylaniline, Analyst, 70 (1945) 203-207.

[194] B. Jiang, Y. Tian, Z. Zhang, Z. Yin, L. Feng, Y. Liu, L. Zhang, Degradation behaviors of Isopropylphenazone and Aminopyrine and their genetic toxicity variations during UV/chloramine treatment, Water Research, 170 (2020) 115339.

[195] J.R. Bolton, K.G. Bircher, W. Tumas, C.A. Tolman, Figures-of-merit for the technical development and application of advanced oxidation technologies for both electric- and solar-driven systems (IUPAC Technical Report), 73 (2001) 627.

[196] W.H. Organization, Antimicrobial resistance: global report on surveillance, World Health Organization2014.

[197] M. Herraiz-Carboné, S. Cotillas, E. Lacasa, C. Sainz de Baranda, E. Riquelme, P. Cañizares, M.A. Rodrigo, C. Sáez, A review on disinfection technologies for controlling the antibiotic resistance spread, Science of The Total Environment, 797 (2021) 149150.

[198] M. Herraiz-Carboné, S. Cotillas, E. Lacasa, P. Cañizares, M.A. Rodrigo, C. Sáez, Disinfection of urines using an electro-ozonizer, Electrochimica Acta, 382 (2021).

[199] M. Herraiz-Carboné, E. Lacasa, S. Cotillas, M. Vasileva, P. Cañizares, M.A. Rodrigo, C. Sáez, The role of chloramines on the electrodisinfection of Klebsiella pneumoniae in hospital urines, Chemical Engineering Journal, 409 (2021).

[200] M. Herraiz-Carboné, S. Cotillas, E. Lacasa, C. Sainz de Baranda, E. Riquelme, P. Cañizares, M.A. Rodrigo, C. Sáez, Are we correctly targeting the research on disinfection of antibiotic-resistant bacteria (ARB)?, Journal of Cleaner Production, 320 (2021).

[201] E. Tacconelli, E. Carrara, A. Savoldi, S. Harbarth, M. Mendelson, D.L. Monnet, C. Pulcini, G. Kahlmeter, J. Kluytmans, Y. Carmeli, Discovery, research, and development of new antibiotics: the WHO priority list of antibiotic-resistant bacteria and tuberculosis, Lancet Infect. Dis., 18 (2018) 318-327.

[202] L.K. Logan, R.A. Weinstein, The epidemiology of Carbapenem-resistant enterobacteriaceae: The impact and evolution of a global menace, J. Infect. Dis., 215 (2017) S28-S36.

[203] J. Racyte, S. Bernard, A.H. Paulitsch-Fuchs, D.R. Yntema, H. Bruning, H.H.M. Rijnaarts, Alternating electric fields combined with activated carbon for disinfection of Gram negative and Gram positive bacteria in fluidized bed electrode system, Water Res., 47 (2013) 6395-6405.

[204] S.P. Denyer, J.-Y. Maillard, Cellular impermeability and uptake of biocides and antibiotics in Gram-negative bacteria, Journal of applied microbiology, 92 (2002) 35S-45S.

[205] P. Lambert, Cellular impermeability and uptake of biocides and antibiotics in Gram-positive bacteria and mycobacteria, Journal of applied microbiology, 92 (2002) 46S-54S.

[206] C. Huang, C. Dong, Z. Tang, Advanced chemical oxidation: its present role and potential future in hazardous waste treatment, Waste management, 13 (1993) 361-377.

[207] M. Rodríguez-Peña, J.A.B. Pérez, J. Llanos, C. Saez, C.E. Barrera-Díaz, M.A. Rodrigo, Understanding ozone generation in electrochemical cells at mild pHs, Electrochimica Acta, 376 (2021).

[208] S. Fukuzaki, Mechanisms of actions of sodium hypochlorite in cleaning and disinfection processes, Biocontrol Sci., 11 (2006) 147-157.

[209] J. Jeong, J.Y. Kim, J. Yoon, The role of reactive oxygen species in the electrochemical inactivation of microorganisms, Environmental Science and Technology, 40 (2006) 6117-6122.

[210] B. Zheng, H. Tomita, T. Inoue, Y. Ike, Isolation of VanB-type Enterococcus faecalis strains from nosocomial infections: First report of the isolation and identification of the pheromone-responsive plasmids pMG2200, encoding VanB-type vancomycin resistance and a Bac41-type bacteriocin, and pMG2201, encoding erythromycin resistance and cytolysin (Hly/Bac), Antimicrobial Agents and Chemotherapy, 53 (2009) 735-747.

[211] M.N. Mosleh, M. Gharibi, M.Y. Alikhani, M. Saidijam, F. Vakhshiteh, Antimicrobial susceptibility and analysis of macrolide resistance genes in Streptococcus pneumoniae isolated in Hamadan, Iranian journal of basic medical sciences, 17 (2014) 595.

[212] A. Ghasemnejad, M. Doudi, N. Amirmozafari, The role of the bla (KPC) gene in antimicrobial resistance of Klebsiella pneumoniae, Iran J Microbiol, 11 (2019) 288-293.

[213] A.M.L. Scavuzzi, M.A.V. Maciel, H.R.L. de Melo, L.C. Alves, F.A. Brayner, A.C.S. Lopes, Occurrence of qnrB1 and qnrB12 genes, mutation in gyrA and ramR, and expression of efflux pumps in isolates of Klebsiella pneumoniae carriers of blaKPC-2, J. Med. Microbiol., 66 (2017) 477-484.

[214] G. Cornaglia, G. Rossolini, The emerging threat of acquired carbapenemases in Gram-negative bacteria, Clin. Microbiol. Infect., 16 (2010) 99-101.

[215] P. Savard, T.M. Perl, A call for action: managing the emergence of multidrug-resistant Enterobacteriaceae in the acute care settings, Current opinion in infectious diseases, 25 (2012) 371-377.

[216] A.A. Alsultan, E. Aboulmagd, T.T. Amin, ESBL-producing E. coli and K. pneumoniae in Al-Ahsa, Saudi Arabia: Antibiotic susceptibility and prevalence of blaSHV and blaTEM, J. Infect. Dev. Ctries., 7 (2013) 1016-1019.

[217] M.I. Polo-López, M. Castro-Alférez, S. Nahim-Granados, S. Malato, P. Fernández-Ibáñez, Legionella jordanis inactivation in water by solar driven processes: EMA-qPCR versus culture-based analyses for new mechanistic insights, Catal Today, 287 (2017) 15-21.

[218] Y. Hu, T. Zhang, L. Jiang, Y. Luo, S. Yao, D. Zhang, K. Lin, C. Cui, Occurrence and reduction of antibiotic resistance genes in conventional and advanced drinking water treatment processes, Science of the Total Environment, 669 (2019) 777-784.

[219] M.-T. Guo, Q.-B. Yuan, J. Yang, Distinguishing effects of ultraviolet exposure and chlorination on the horizontal transfer of antibiotic resistance genes in municipal wastewater, Environmental science & technology, 49 (2015) 5771-5778.

[220] H. Wang, J. Wang, S. Li, G. Ding, K. Wang, T. Zhuang, X. Huang, X. Wang, Synergistic effect of UV/chlorine in bacterial inactivation, resistance gene removal, and gene conjugative transfer blocking, Water Res., 185 (2020) 116290.

[221] M.C. Dodd, Potential impacts of disinfection processes on elimination and deactivation of antibiotic resistance genes during water and wastewater treatment, Journal of Environmental Monitoring, 14 (2012) 1754-1771.

[222] C. Stange, J.P.S. Sidhu, S. Toze, A. Tiehm, Comparative removal of antibiotic resistance genes during chlorination, ozonation, and UV treatment, International Journal of Hygiene and Environmental Health, 222 (2019) 541-548.

[223] J. Xia, H. Sun, X. Ma, K. Huang, L. Ye, Ozone pretreatment of wastewater containing aromatics reduces antibiotic resistance genes in bioreactors: The example of p-aminophenol, Environment International, 142 (2020) 105864.

[224] Y. Choi, H. He, M.C. Dodd, Y. Lee, Degradation Kinetics of Antibiotic Resistance Gene mecA of Methicillin-Resistant Staphylococcus aureus (MRSA) during Water Disinfection with Chlorine, Ozone, and Ultraviolet Light, Environmental Science & Technology, 55 (2021) 2541-2552.

[225] L. Lan, Y. Xie, X. Kong, C. Li, D. Liu, Investigation of reduction in risk from antibiotic resistance genes in laboratory wastewater by using O3, ultrasound, and autoclaving, Water Environ. Res., 93 (2021) 479-486.

[226] U. von Gunten, Ozonation of drinking water: Part I. Oxidation kinetics and product formation, Water Res., 37 (2003) 1443-1467.

[227] D.M. Scott, E.C. Lesher, Effect of ozone on survival and permeability of Escherichia coli, Journal of bacteriology, 85 (1963) 567-576.

[228] R. Xiao, L. Bai, K. Liu, Y. Shi, D. Minakata, C.-H. Huang, R. Spinney, R. Seth, D.D. Dionysiou, Z. Wei, Elucidating sulfate radical-mediated disinfection profiles and mechanisms of Escherichia coli and Enterococcus faecalis in municipal wastewater, Water Res., 173 (2020) 115552.

CHAPTER 6:

CONCLUSIONS AND PERSPECTIVES

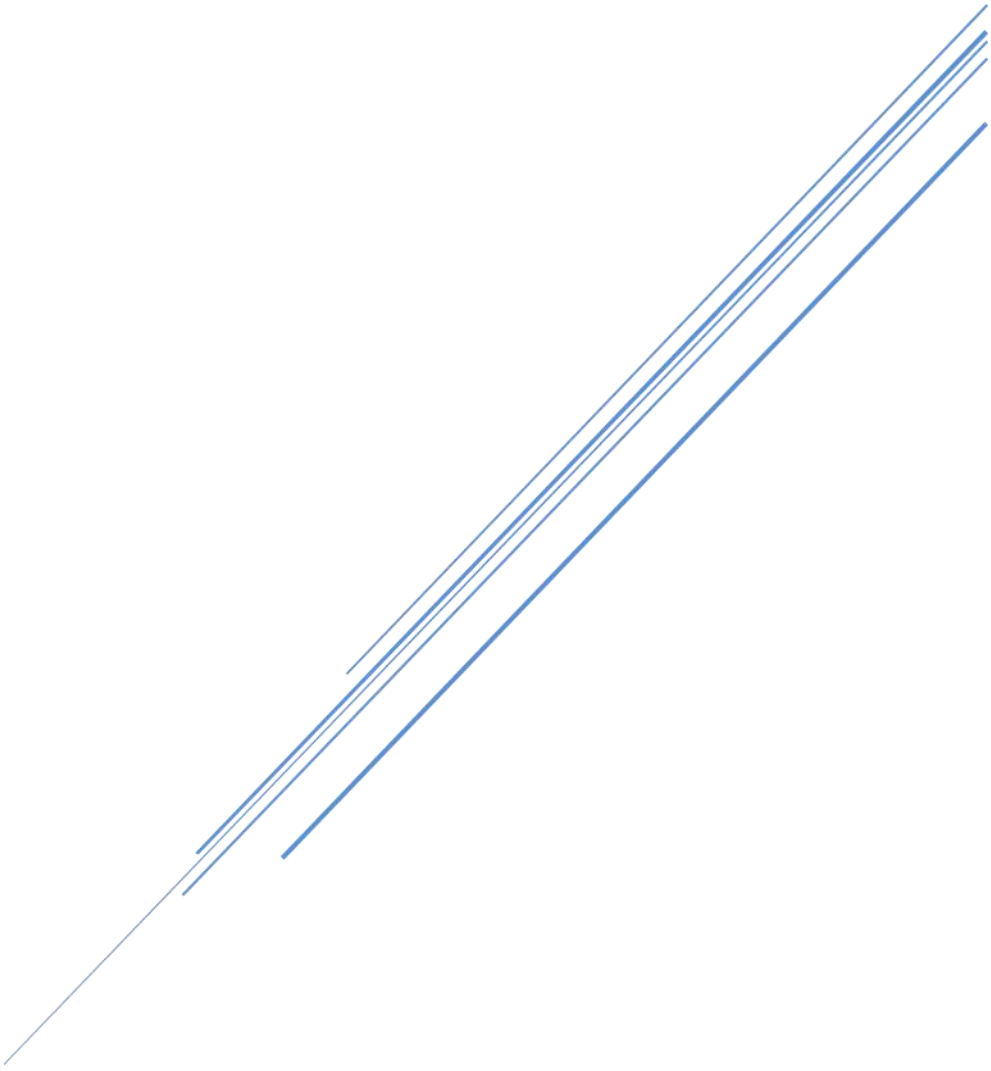

From the results detailed and discussed in this PhD Thesis, the following most important conclusions for each partial objective are established:

1) The prospective study of pathogens causing UTIs based on data provided by the Microbiology and Parasitology Service from CHUA showed, as expected, that *E. coli* was the most significant bacteria found in PUs. Additionally, other more specific conclusions were extracted:

- Gram-negative bacteria (*E. coli*, *K. pneumoniae*, *P. aeruginosa* and *P. mirabilis*) predominate over gram-positive bacteria (*E. faecalis*) and yeasts (*C. albicans*). However, *K. pneumoniae* showed the highest percentages of ARB_{ESBL} and ARB_{CPB}.
- The importance given to *K. pneumoniae* as ARB from a sanitary viewpoint does not correspond to the research carried out on the disinfection of ARB by the scientific community.

2) The evaluation of electrolysis for the treatment of hospital urines showed the advantages of treating isolated hospital urines before its merge with other hospital effluents or even with municipal wastewater and its technical feasibility to reduce the biological and chemical risk of hospital urines. The following conclusions were depicted from this study:

- The bacterial removal efficiency was lower in hospital urines compared to urban wastewater due to the existence of other competitive oxidation reactions during electrolysis. Nevertheless, the occurrence of hazardous disinfection by-product was avoided when the removal of bacteria was carried out in hospital urines.
- A complete removal of CAP at 12.5 A m^{-2} (below 8 Ah dm^{-3}) was achieved during electrolysis with BDD anodes, allowing to decrease the hazardousness of hospital urines. The acute toxicity evolution towards *Vibrio fischeri* luminescence inhibition showed EC_{50} percentages up to 23 %. Likewise, the rapid biodegradability percentage increased in a range

from 22 to 36 % and the final standard biodegradability (Zahn-Wellens method) was higher than 40 %.

3) The study of the contribution of disinfectant species showed that the electrochemical disinfection of hospital urines infected with *K. pneumoniae* was significantly influenced by the reactor layout due to the different promotion of electrogenerated oxidants. A microfluidic flow-through reactor with MMO anodes promotes the formation of chloramines which allows to avoid the production of chlorine-based disinfection by-products such as THMs, whereas a solid-electrolyte electro-ozonizer (MIKROZON®) boost the production of ozone which leads the degradation of bacterial DNA. Likewise, the following specific conclusions has been also highlighted:

- A complete disinfection (7 log) was attained before 120 min using a microfluidic flow-through reactor with MMO anode at 50 A m^{-2} and almost 6 log reduction was achieved using a parallel flow cell under the same experimental conditions. The presence of chlorides in hospital urines contributed to the generation of hypochlorite, which may oxidize the organics and/or may react with ammonium ions to form chloramines. The formation of chloramines was enhanced when using the microfluidic flow-through reactor due to its slightly higher hydraulic retention time. Additionally, chemical disinfection tests proved the stronger bactericidal effect of hypochlorite than chloramines. However, chloramines played a key role in the electrochemical disinfection process since they contribute not only as disinfectants but avoiding the production of chlorine disinfection by-products.
- A solid-electrolyte electro-ozonizer allowed to disinfect urines from current intensities higher than 0.5 A. The crystal violet assay showed that the combined effect of all disinfectants promoted higher cell damages, increasing the cell wall permeability. Likewise, DNA and proteins were degraded during the electrochemical disinfection of urines under the combined effect of ozone and chlorine disinfectants. However, single

electrogenerated ozone seemed to attack the DNA to a greater extent than chlorine disinfectants. On the other hand, diluted (1:10) urines (low conductivity water) promoted the production of large amounts of ozone which led to higher disinfection rates than undiluted urines.

4) The evaluation of the synergies and/or antagonisms when coupling electrochemical oxidation to UV disinfection for the removal of ARB in hospital urines allowed to gain insight into the most suitable operating conditions for an efficient photoelectrolytic disinfection process. From this study, the following conclusion has been highlighted:

- The photoelectrolysis enhanced single UV disinfection and electrolysis performances with a marked synergistic effect when working at 5 A m^{-2} with BDD and MMO anodes using a microfluidic flow-through reactor. A more remarkable contribution of UV disinfection was observed at the beginning of the process, until 30 min ($Q < 0.1$ Ah dm^{-3}), whereas the electrochemical process had more influence at the end of the treatment. The specific electric energy required for photoelectrolysis at low current densities was lower than that for UV disinfection.

5) The electrochemical technology validated to disinfect monomicrobial hospital urines was tested to check its robustness in the treatment of polymicrobial hospital urines intensified with pairs of ARB. The polymicrobial hospital urines simulate real hospital urines since the pandemic caused by the coronavirus SARS-CoV-2 did not allow us to validate the electrochemical technology in a real environment due to the sanitary restrictions. The tested combinations of bacteria were: 1) *E. faecalis* and *K. pneumoniae*, 2) *E. coli* and *E. faecalis*, and 3) *K. pneumoniae* and *E. coli*. From this study, the following conclusions has been highlighted:

- In polymicrobial hospital urines, the most prevalent pairs of bacteria causing complex UTIs in patients were *E. coli* and *E. faecalis* (9.8 %) followed by *E. coli* and *K. pneumoniae* (7.1 %).

- The microfluidic flow-through reactor achieved removal rates between 5 and 6 logs after 180 min, whereas the MIKROZON® cell reached the total disinfection (7 logs) after 60 min under their most suitable operational conditions for each electrochemical cell. The microfluidic flow-through reactor promoted the generation of hypochlorite and chloramines as the main disinfectant species and the MIKROZON® cell promoted the additional electrogeneration of ozone as disinfectant. SEM images confirmed the complete disinfection attained using the MIKROZON® cell where severe damages were induced in the cell walls, resulting in the integrity loss of bacterial structures.
- The MIKROZON® cell reached a mean decrease in ARGs ranked as follows: bla_{KPC} (4.18-logs) > bla_{TEM} (3.96-logs) > *erm*B (3.23-logs), offering a mean depletion of 3.77-logs for all ARGs tested. However, further research should be done to attain the removal of ARGs when working with the microfluidic flow-through reactor.

Unfortunately, due to causes supervening by the COVID-19 pandemic, the CHUA has not been able to supply real urine for the verification of the technology, as was initially proposed. Nevertheless, considering these conclusions, it is clear that the electrochemical technology may be a promising technological alternative to be tested in the disinfection of real hospital urines to contribute to minimising the spread of ARB and ARGs into other water bodies. Bearing in mind the whole experimental results, it could be particularly exciting the building of a compact design of an electrochemical set-up to be coupled to a toilet where just hospital urines were collected inside. This coupled electrochemical system allows to disinfect hospital urines before their merge with other hospital effluents which would decrease not only the environmental but also the sanitary risk of hospital urines. These actions would increase the technology readiness levels (TRLs) from TRL 4 – Technology validated in lab to even TRL 6 – Technology demonstrated in relevant environment (industrially relevant environment in the case of key enabling technologies).

CAPÍTULO 6:

CONCLUSIONES Y PERSPECTIVAS FUTURAS

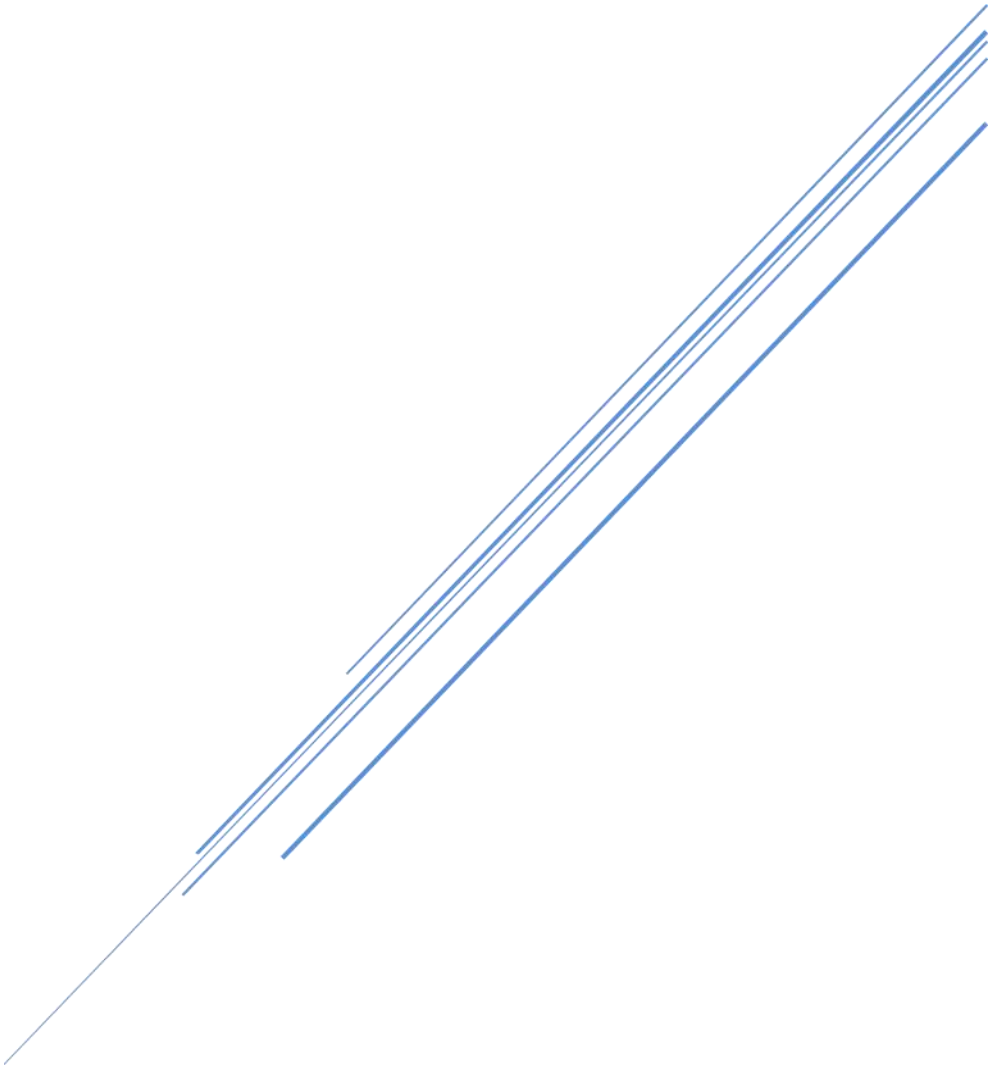

A continuación, se establecen las conclusiones más relevantes de cada objetivo parcial a partir de los resultados obtenidos en esta Tesis Doctoral:

1) El estudio de prevalencia de los patógenos causantes de infecciones del tracto urinario (ITUs) a partir de los datos aportados por el Servicio de Microbiología y Parasitología del CHUA en el período 2014 - 2018 mostró, como era de esperar, que *E. coli* era la bacteria más significativa encontrada en las orinas positivas. Además, se extrajeron otras conclusiones más específicas:

- Las bacterias gram-negativas (*E. coli*, *K. pneumoniae*, *P. aeruginosa* y *P. mirabilis*) predominan sobre las gram-positivas (*E. faecalis*) y los hongos (*C. albicans*). Sin embargo, *K. pneumoniae* mostró los mayores porcentajes de resistencia antibiótica a betalactámicos y carbapenémicos.
- La importancia dada a *K. pneumoniae* como bacteria resistente a los antibióticos desde el punto de vista sanitario, no se corresponde con las investigaciones realizadas sobre la desinfección de estas super-bacterias por la comunidad científica.

2) La evaluación de la electrólisis para el tratamiento de desinfección de orinas hospitalarias mostró las ventajas de tratar estas orinas directamente en el punto de generación, antes incluso de su contacto con otros efluentes hospitalarios o municipales, así como su viabilidad técnica para reducir el riesgo biológico y químico de estas orinas.

- La eficiencia en la eliminación de bacterias fue menor en las orinas hospitalarias en comparación con las aguas residuales urbanas, debido a las reacciones de oxidación competitivas durante la electrólisis. Sin embargo, se evita la aparición de subproductos de desinfección peligrosos cuando la eliminación de las bacterias se lleva a cabo directamente en orinas hospitalarias.
- La completa eliminación de cloranfenicol (antibiótico modelo) se alcanzó a 12,5 A m^{-2} (por debajo de 8 Ah dm^{-3}) durante la electrólisis con ánodos BDD, lo que permitió disminuir la peligrosidad de las orinas hospitalarias. La evolución de la toxicidad teniendo en cuenta la inhibición de la

luminiscencia en *Vibrio fischeri* mostró porcentajes de EC_{50} de hasta el 23 %. Asimismo, el porcentaje de biodegradabilidad rápida aumentó en el intervalo del 22 al 36 % y la biodegradabilidad estándar final a través del método Zahn-Wellens fue superior al 40 %.

3) La desinfección electroquímica de las orinas hospitalarias infectadas con *K. pneumoniae* está significativamente influenciada por el diseño del reactor, puesto que repercute en la generación de diferentes especies oxidantes. El reactor microfluídico de flujo a través de los electrodos utilizando ánodos de mezcla de óxidos metálicos promueve la formación de cloraminas, lo que permite evitar la producción de subproductos de desinfección basados en el cloro como los THMs. Por otro lado, el electroozonizador de electrolito sólido denominado MIKROZON® potencia la producción de ozono, que conduce a la degradación del ADN bacteriano.

- El reactor microfluídico de flujo a través de los electrodos con un ánodo de mezcla de óxidos metálicos a 50 A m^{-2} alcanzó una desinfección completa (7 log) antes de 120 min y se logró una reducción de casi 6 log con un reactor convencional de flujo paralelo, bajo las mismas condiciones experimentales. La presencia de cloruros en las orinas de los hospitales contribuyó a la generación de hipoclorito, que puede oxidar los compuestos orgánicos y/o reaccionar con los iones de amonio para formar cloraminas. La formación de cloraminas fue mayor cuando se utilizó el reactor microfluídico de flujo a través de los electrodos gracias a su mayor tiempo de retención hidráulica. Además, las pruebas de desinfección química demostraron el mayor efecto bactericida del hipoclorito con respecto a las cloraminas. Sin embargo, las cloraminas desempeñan un papel clave en el proceso de desinfección electroquímica, ya que contribuyen no sólo como agentes desinfectantes sino también evitando la producción de subproductos de desinfección clorados.
- La celda MIKROZON® permitió desinfectar las orinas a partir de intensidades de corriente superiores a 0,5 A. El ensayo de cristal violeta mostró que el efecto combinado de todos los desinfectantes promovió

mayores daños celulares, aumentando la permeabilidad de la pared celular. Asimismo, el ADN y las proteínas se degradaron durante la desinfección electroquímica de las orinas bajo el efecto combinado de los desinfectantes ozono y cloro. Sin embargo, el ozono electrogenerado ataca el ADN en mayor medida que los desinfectantes basados en cloro. Por otro lado, las orinas diluidas (1:10) (efluente de baja conductividad) promovieron la producción de grandes cantidades de ozono, lo que condujo a tasas de desinfección más altas que las orinas sin diluir.

4) La evaluación las sinergias y/o antagonismos que surgen del acoplamiento de la oxidación electroquímica y la desinfección UV para la eliminación de bacterias en orinas hospitalarias permitió conocer las condiciones de operación más adecuadas para lograr un proceso de desinfección fotoelectrolítica eficiente.

- La fotoelectrolisis mejoró el rendimiento de la desinfección UV y de la electrólisis con un marcado efecto sinérgico cuando se trabaja a 5 A m^{-2} con ánodos BDD y MMO utilizando un reactor microfluídico de flujo a través de los electrodos. Se observó una contribución más notable de la desinfección UV al principio del proceso, hasta los 30 minutos ($Q < 0,1$ Ah dm^{-3}), mientras que el proceso electroquímico tuvo más influencia al final del tratamiento. La energía eléctrica específica requerida para la fotoelectrolisis a bajas densidades de corriente fue menor que la de la desinfección UV.

5) La tecnología electroquímica validada para la desinfección de orinas hospitalarias monomicrobianas se probó para comprobar la robustez de la tecnología en el tratamiento de orinas hospitalarias polimicrobianas intensificadas con pares de ARB. Las orinas hospitalarias polimicrobianas simulan las orinas hospitalarias reales ya que la pandemia causada por el coronavirus SARS-CoV-2 no nos permitió validar la tecnología electroquímica en un entorno real, debido a las restricciones sanitarias. Las combinaciones de bacterias probadas fueron 1) *E. faecalis* y *K. pneumoniae*, 2) *E. coli* y *E. faecalis*, y 3) *K. pneumoniae* y *E. coli*.

- En las orinas hospitalarias polimicrobianas, los pares de bacterias causantes de ITUs complejas más frecuentes en los pacientes fueron *E. coli* y *E. faecalis* (9,8 %), seguidos de *E. coli* y *K. pneumoniae* (7,1 %).
- El reactor microfluídico de flujo a través de los electrodos alcanzó tasas de eliminación de entre 5 y 6 logs después de 180 minutos, mientras que la celda MIKROZON® alcanzó la desinfección total (7 logs) después de 60 minutos. El reactor microfluídico de flujo a través promueve la generación de hipoclorito y cloraminas como principales especies desinfectantes, mientras que la celda MIKROZON® favorece la electrogeneración de ozono como desinfectante. Las imágenes SEM confirmaron la completa desinfección lograda con la celda MIKROZON®, donde se indujeron graves daños en las paredes celulares que provocan la pérdida de integridad de las estructuras bacterianas.
- La celda MIKROZON® alcanzó una disminución de genes resistentes a los antibióticos según el orden: bla_{KPC} (4,18-logs) > bla_{TEM} (3,96-logs) > *erm*B (3,23-logs), ofreciendo una disminución media de 3,77-logs para todos los genes estudiados. Sin embargo, sería necesario seguir investigando para lograr la eliminación de genes de resistencia bacteriana cuando se trabaja con el reactor microfluídico de flujo a través de los electrodos.

Desafortunadamente, por causas sobrevenidas por la pandemia por COVID-19 el CHUA no ha podido suministrar orinas reales para la verificación de la tecnología, tal y como estaba inicialmente planteado. No obstante, teniendo en cuenta estas conclusiones, la tecnología electroquímica se postula como una alternativa tecnológica prometedora para ser probada en la desinfección de orinas hospitalarias reales, contribuyendo a minimizar la propagación tanto de bacterias resistentes a los antibióticos como sus genes de resistencia hacia otros medios acuáticos.

Teniendo en cuenta todos los resultados experimentales, podría ser particularmente interesante la construcción de un prototipo de diseño compacto de un sistema electroquímico que fuese acoplado a un inodoro donde sólo se recogiesen las orinas hospitalarias. Este sistema electroquímico acoplado al inodoro permitiría

desinfectar las orinas del hospital antes de que se mezclen con otros efluentes, lo que disminuiría no sólo el riesgo ambiental sino también el sanitario de las orinas hospitalarias. Estas acciones aumentarían los niveles de preparación de la tecnología (TRLs) desde TRL 4 - Tecnología validada en laboratorio hasta incluso TRL 6 - Tecnología demostrada en un entorno relevante (entorno industrial relevante en el caso de las tecnologías facilitadoras clave).